A Volume-Limited Sample of Ultracool Dwarfs. I. Construction, Space Density, and a Gap in the L/T Transition

Accepted by *The Astronomical Journal*, October 27, 2020
Draft version December 1, 2020
Typeset using LaTeX **twocolumn** style in AASTeX62

A Volume-Limited Sample of Ultracool Dwarfs. I. Construction, Space Density, and a Gap in the L/T Transition

William M. J. Best,[1,2] Michael C. Liu,[2] Eugene A. Magnier,[2] and Trent J. Dupuy[3,4]

[1] *University of Texas at Austin, Department of Astronomy, 2515 Speedway C1400, Austin, TX 78712, USA*
[2] *Institute for Astronomy, University of Hawaii, 2680 Woodlawn Drive, Honolulu, HI 96822, USA*
[3] *Gemini Observatory, 670 N. A'ohoku Place, Hilo, HI, 96720, USA*
[4] *Institute for Astronomy, University of Edinburgh, Blackford Hill, Edinburgh, EH9 3HJ, United Kingdom*

(Received October 30, 2019; Revised August 28, 2020; Accepted October 27, 2020)

ABSTRACT

We present a new volume-limited sample of L0–T8 dwarfs out to 25 pc defined entirely by parallaxes, using our recent measurements from UKIRT/WFCAM along with Gaia DR2 and literature parallaxes. With 369 members, our sample is the largest parallax-defined volume-limited sample of L and T dwarfs to date, yielding the most precise space densities for such objects. We find the local L0–T8 dwarf population includes $5.5\% \pm 1.2\%$ young objects ($\lesssim$200 Myr) and $2.6\% \pm 1.6\%$ subdwarfs, as expected from recent studies favoring representative ages $\lesssim$4 Gyr for the ultracool field population. This is also the first volume-limited sample to comprehensively map the transition from L to T dwarfs (spectral types ≈L8–T4). After removing binaries, we identify a previously unrecognized, statistically significant ($> 4.4\sigma$) gap ≈0.5 mag wide in $(J-K)_{\rm MKO}$ colors in the L/T transition, i.e., a lack of such objects in our volume-limited sample, implying a rapid phase of atmospheric evolution. In contrast, the most successful models of the L/T transition to date — the "hybrid" models of Saumon & Marley — predict a pileup of objects at the same colors where we find a deficit, demonstrating the challenge of modeling the atmospheres of cooling brown dwarfs. Our sample illustrates the insights to come from even larger parallax-selected samples from the upcoming Legacy Survey of Space and Time (LSST) by the Vera Rubin Obsevatory.

Keywords: Brown dwarfs (185), L dwarfs (894), T dwarfs (1679), Stellar atmospheres (1584), Stellar evolution (1599), Stellar evolutionary models (2046), Close binary stars (254), Wide binary stars (1801), Stellar colors (1590), Infrared photometry (792)

1. INTRODUCTION

Brown dwarfs have masses $\lesssim$70 $M_{\rm Jup}$ (e.g., Chabrier et al. 2000; Dupuy & Liu 2017), insufficient to sustain hydrogen fusion and achieve the steady-state luminosity that defines main-sequence stars. Brown dwarfs therefore cool as they age, causing their atmospheres to undergo complex chemical transformations over time. This is particularly true in the L/T transition (spectral types ≈L8–T4), where evolutionary and atmospheric models have difficulty reproducing observed magnitudes, luminosities, and effective temperatures for L/T objects with known masses and/or ages (e.g., Barman et al. 2011; Bowler et al. 2010b; Dupuy et al. 2009a, 2015; Leggett et al. 2008; Naud et al. 2014). Likewise, a fully physical model that matches observations of the L/T transition in color-magnitude diagrams has yet to be developed (e.g., Burrows et al. 2006; Saumon & Marley 2008; Marley et al. 2010; Tremblin et al. 2016). Up to this point, the small number of accurate parallax-based luminosities measured for L/T transition dwarfs (<30; Best et al. 2018) has hindered the development of an accurate map for this distinctive evolutionary phase.

Volume-limited samples are ideal for population studies, as they minimize the selection biases intrinsic to the more common magnitude-limited samples. Parallaxes provide the most direct measures of distance to nearby objects and are therefore preferred for establishing volume-limited samples in the solar neigh-

Corresponding author: William M. J. Best
wbest@utexas.edu

borhood. Parallax-defined volume-limited samples of nearby brown dwarfs enable the best estimates of the underlying mass and age distributions of the local substellar population. The most complete previous sample encompassing all brown dwarf spectral types is the full-sky 8 pc sample of Kirkpatrick et al. (2012), which contains only 33 L, T, and Y dwarfs. Kirkpatrick et al. (2019, hereinafter K19) have recently assembled a volume-limited sample of 278 objects out to 20 pc, defined using K19's Spitzer parallaxes along with Gaia DR2 and literature values. However, their sample comprises L0–L5 dwarfs (complete at 20 pc) and T6 and later-type dwarfs (complete at <20 pc due to the faintness of these objects), entirely skipping L6–T5 dwarfs, and therefore cannot be used to study the L/T transition. The largest volume-limited samples of ultracool dwarfs (spectral types M6 and later) published to date are those of Reid et al. (2008b, 196 M7–T2.5 dwarfs out to 20 pc, but incomplete for types >L6 and selected primarily using photometric distances) and Bardalez Gagliuffi et al. (2019, hereinafter BG19; 410 M7–L5 dwarfs out to 25 pc). The latter study presents the most comprehensive analysis to date of the warmest ultracool dwarfs down to the hydrogen-burning limit (spectral type ≈L4; Dupuy & Liu 2017), but does not include the L/T transition or cooler T dwarfs.

In this paper, we present a new volume-limited sample of L and T dwarfs out to 25 pc containing 369 members, spanning spectral types L0–T8 and chosen entirely by parallaxes, the largest such sample to date. Using a near-infrared (NIR) color-magnitude diagram for this sample, we identify a gap in $J-K$ color in the L/T transition that is ≈0.5 mag wide. We describe our volume-limited sample in Section 2, present the L/T gap in Section 3, and discuss its implications in Section 4. We summarize our findings in Section 5.

2. VOLUME-LIMITED SAMPLE

2.1. *Construction*

Best et al. (2020, hereinafter Best20) used UKIRT/WFCAM to obtain parallaxes for 348 L0–T8 dwarfs with declinations $-30° \leq \delta \leq 60°$ and photometric distances $d_{\rm phot} \leq 25 + 1\sigma_{\rm dist}$ pc (i.e., no further beyond 25 pc than the distance uncertainty) based on AllWISE $W2$-band photometry (Cutri et al. 2014), with the goal of completing a volume-limited 25 pc sample for this portion of the sky (68.3% of the full sky). Additionally, we searched the literature for all spectroscopically confirmed objects in Best20's spectral type and declination ranges that had parallax measurements with errors < 20%, including parallaxes from Gaia DR2 (Gaia Collaboration et al. 2018). As in Best20, in all instances where an object has both an optical and an NIR spectral type, we adopted the optical types for L dwarfs and the NIR types for T dwarfs. After merging the Best20 and literature parallax lists and choosing the most precise parallax available for each object, we removed objects with parallaxes < 40 mas (i.e., distances > 25 pc) to define our volume-limited sample.

2.2. *The Sample*

We present our volume-limited sample in Table 1. The sample includes 369 L0–T8 dwarfs and is constructed from 128 Best20 parallaxes, 121 from Gaia DR2, and 120 from other literature sources. Figure 1 shows the spectral type distribution of our sample, featuring a clear deficit at early-T spectral types. This deficit was predicted by evolutionary models (e.g., Saumon & Marley 2008, hereinafter SM08) and seen in previous photometrically selected samples (Burgasser 2007a; Metchev et al. 2008; Reid et al. 2008b; Marocco et al. 2015; Best et al. 2018), and is now confirmed in our volume-limited sample, indicating that brown dwarfs cool through these spectral types ($T_{\rm eff} \approx 1400 - 1100$; Luhman et al. 2007; Cushing et al. 2008; Stephens et al. 2009; King et al. 2010; Deacon et al. 2012a,b, 2017a; Reylé et al. 2014; Filippazzo et al. 2015; Dupuy & Liu 2017) in a relatively short time. We also note an uneven distribution of L0–L5 dwarfs whose origin is unclear given that our sample is ≳90% complete at these types (Section 2.3). One possible contributing factor is that the spectral types are a mixture of optical and NIR assignments by many different astronomers using several methods. At the L0 boundary of our sample in particular, this lack of consistency in typing could potentially have impacted the choice of objects we included in our sample (we included L0 and later types, but not M9.5 and earlier types). However, the relative lack of L0 dwarfs compared with L1 dwarfs was seen previously in the more homogenously typed 20 pc samples of Cruz et al. (2007), Reid et al. (2008b), and BG19, which also included late-M dwarfs, suggesting that the L0 deficit is not a selection effect at the spectral type boundary of our sample.

Table 1. Our Volume-limited 25 pc Sample of L0–T8 Dwarfs

Object	Distance	Parallax	Spectral Type[a]	Flag[b]	Y_{MKO}	J_{MKO}	H_{MKO}	K_{MKO}	References
	(pc)	(mas)	(Optical/NIR)		(mag)	(mag)	(mag)	(mag)	(Disc; ϖ; SpT; Flag; Phot)
SDSS J000013.54+255418.6	14.1 ± 0.4	70.8 ± 1.9	T5/T4.5	···	15.80 ± 0.06	14.73 ± 0.03	14.74 ± 0.03	14.82 ± 0.03	108; 64; 153,29; –; 64,108
2MASS J00132229−1143006	24.8 ± 1.9	40.3 ± 3.1	.../T3pec	···	···	16.05 ± 0.02	[[15.74 ± 0.22]]	[[15.76 ± 0.22]]	97; 9; 97; –; 1,9,51
2MASSW J0015447+351603	17.06 ± 0.11	58.6 ± 0.4	L2/L1.0	···	[14.95 ± 0.05]	13.74 ± 0.02	[12.96 ± 0.02]	[12.25 ± 0.02]	101; 77; 101,5; –; 1,9
PSO J004.6359+56.8370	21.5 ± 1.8	46.5 ± 3.9	.../T4.5	···	···	16.22 ± 0.02	···	···	125; 9; 125; –; 9
2MASS J00282091+2249050	24.2 ± 1.2	41.3 ± 2.0	.../L7:	···	[16.82 ± 0.05]	15.49 ± 0.02	[14.55 ± 0.06]	[13.77 ± 0.06]	37; 77; 37; –; 1,9
WISE J003110.04+574936.3	14.1 ± 1.0	71.0 ± 5.0	.../L9	B	[15.92 ± 0.05]	14.796 ± 0.012	13.862 ± 0.014	[13.21 ± 0.03]	185; 9; 10; 12; 1,10
PSO J007.9194+33.5961	22.0 ± 1.8	45.4 ± 3.8	.../L9	···	[17.48 ± 0.06]	16.38 ± 0.02	[15.46 ± 0.05]	[14.67 ± 0.05]	11; 9; 11; –; 1,9
2MASS J00320509+0219017	24.4 ± 0.3	41.0 ± 0.4	L1.5/M9	···	15.443 ± 0.004	14.220 ± 0.002	13.446 ± 0.002	12.797 ± 0.002	164; 77; 164,193; –; 111
2MASS J00332386−1521309	22.9 ± 0.5	43.6 ± 0.9	L4 β/L1: FLD-G	Y	[16.38 ± 0.08]	[15.22 ± 0.06]	[14.26 ± 0.04]	[13.39 ± 0.04]	84; 77; 48,3; 48,3; 1
2MASS J00345157+0523050	8.3 ± 0.2	120.1 ± 3.0	.../T6.5	···	16.213 ± 0.007	15.140 ± 0.004	15.576 ± 0.010	16.07 ± 0.03	26; 107; 29; –; 111
2MASSW J0036159+182110	8.74 ± 0.02	114.4 ± 0.2	L3.5/L4:	B	13.58 ± 0.06	12.30 ± 0.03	11.64 ± 0.03	11.04 ± 0.03	160; 77; 101,108; 8,156; 64,108
HD 3651B	11.137 ± 0.007	89.79 ± 0.06	.../T7.5	C	[17.12 ± 0.06]	16.16 ± 0.03	16.68 ± 0.04	16.87 ± 0.05	147; 77; 132; 147,132; 1,132
WISE J004024.88+090054.8	14.3 ± 0.3	69.8 ± 1.5	.../T7	···	17.15 ± 0.02	16.131 ± 0.011	16.56 ± 0.02	16.55 ± 0.05	135; 107; 135; –; 111
2MASSW J0045214+163445	15.38 ± 0.05	65.0 ± 0.2	L2 β/L2: VL-G	BY	[14.22 ± 0.05]	[12.98 ± 0.02]	[12.12 ± 0.02]	[11.33 ± 0.02]	193; 77; 48,3; 156,48,3; 1
WISE J004542.56+361139.1	18.7 ± 1.8	53.4 ± 5.2	.../T5	···	[16.81 ± 0.05]	15.91 ± 0.02	[16.13 ± 0.05]	[16.07 ± 0.05]	135; 9; 135; –; 1,9
WISEPC J004928.48+044100.1	16.0 ± 0.7	62.6 ± 2.9	.../L9	···	16.903 ± 0.012	15.767 ± 0.008	14.802 ± 0.006	14.131 ± 0.006	105; 9; 105; –; 111
SIPS J0050−1538	24.80 ± 0.15	40.3 ± 0.2	L1:/L0.5	···	[14.68 ± 0.05]	13.69 ± 0.02	[13.15 ± 0.03]	[12.62 ± 0.03]	54; 77; 47,5; –; 1,9
WISEA J010202.11+035541.4	24.9 ± 1.7	40.2 ± 2.8	.../L9	···	17.82 ± 0.03	16.67 ± 0.02	15.753 ± 0.012	15.066 ± 0.012	172; 9; 172; –; 111
2MASSI J0103320+193536	21.3 ± 3.5	46.9 ± 7.6	L6 β/L6: INT-G	BY	[17.45 ± 0.09]	16.16 ± 0.08	14.94 ± 0.06	14.09 ± 0.06	101; 69; 69,3; 67,69,3; 1,69
SDSSp J010752.33+004156.1	15.6 ± 1.1	64.1 ± 4.5	L8/L7pec	···	16.91 ± 0.03	15.75 ± 0.03	14.56 ± 0.03	13.58 ± 0.03	79; 191; 95,73; –; 113
2MASS J01311838+3801554	24.9 ± 0.5	40.2 ± 0.8	L4:/L1.5	···	[15.91 ± 0.05]	14.63 ± 0.02	[13.77 ± 0.03]	[13.03 ± 0.03]	47; 77; 47,37; –; 1,9
WISE J013525.64+171503.4	21.4 ± 1.6	46.7 ± 3.5	.../T6	···	[18.03 ± 0.06]	17.07 ± 0.02	[17.43 ± 0.06]	[17.74 ± 0.07]	135; 9; 135; –; 1,9
SIMP J013656.5+093347.3	6.17 ± 0.02	162.1 ± 0.6	T2/T2.5	Y	14.392 ± 0.003	13.252 ± 0.002	12.809 ± 0.002	12.585 ± 0.002	4; 53; 153,4; 75; 110,111
WISEPC J013836.59−032221.2	22.8 ± 1.5	43.9 ± 2.9	.../T3	···	[17.16 ± 0.05]	16.13 ± 0.02	[15.68 ± 0.05]	[15.27 ± 0.05]	105; 9; 105; –; 1,9
2MASSW J0141032+180450	23.6 ± 0.2	42.3 ± 0.3	L1/L4.5	···	[15.01 ± 0.06]	[13.83 ± 0.03]	[13.10 ± 0.03]	[12.48 ± 0.03]	193; 77; 47,193; –; 1
2MASS J01443536−0716142	12.65 ± 0.10	79.0 ± 0.6	L5/L5	···	[15.52 ± 0.05]	14.15 ± 0.02	[13.09 ± 0.02]	[12.26 ± 0.02]	117; 77; 117,140; –; 1,9
SDSS J015141.69+124429.6	21.4 ± 1.5	46.7 ± 3.4	.../T1	···	17.40 ± 0.02	16.388 ± 0.012	15.597 ± 0.012	15.288 ± 0.013	79; 191; 29; –; 111
2MASS J01550354+0950003	22.4 ± 0.3	44.7 ± 0.7	L5/L3.2 INT-G	Y	16.109 ± 0.007	14.731 ± 0.004	13.884 ± 0.003	[13.11 ± 0.04]	164; 77; 164,73; 73; 111,1
HIP 9269B	24.76 ± 0.02	40.38 ± 0.04	.../L6	C	[17.30 ± 0.05]	16.13 ± 0.02	15.082 ± 0.014	14.30 ± 0.02	58; 77; 58; 58; 1,58
2MASSW J0205034+125142	23.5 ± 1.7	42.5 ± 3.0	L5/L5.5	···	17.018 ± 0.013	15.561 ± 0.006	14.513 ± 0.004	13.637 ± 0.004	101; 9; 101,37; –; 111
DENIS J020529.0−115925	18.6 ± 0.4	53.7 ± 1.1	L7/L5.5::	B	15.55 ± 0.03	14.43 ± 0.05	13.61 ± 0.05	12.99 ± 0.05	61; 53; 100,108; 109,16; 113
WISEPA J020625.26+264023.6	19.2 ± 0.5	52.1 ± 1.4	.../L8 (red)	···	[17.60 ± 0.12]	[16.42 ± 0.11]	[15.16 ± 0.08]	[14.50 ± 0.08]	105; 124; 124; –; 1
2MASSW J0208183+254253	23.7 ± 0.4	42.3 ± 0.6	L1/...	···	[15.06 ± 0.05]	13.91 ± 0.02	[13.18 ± 0.03]	[12.57 ± 0.03]	101; 77; 101; –; 1,9
2MASS J02132062+3648506C	14.28 ± 0.04	70.0 ± 0.2	.../T3	C	16.28 ± 0.02	15.158 ± 0.013	14.89 ± 0.02	14.93 ± 0.02	60; 77; 60; 60; 60
2MASSI J0213288+444445	19.35 ± 0.14	51.7 ± 0.4	L1.5/...	···	···	13.41 ± 0.02	[[12.81 ± 0.02]]	[[12.19 ± 0.02]]	45; 77; 45; –; 1,9,51
WISEPC J022322.39−293258.1	12.4 ± 0.4	80.7 ± 2.6	.../T7.5	···	[18.08 ± 0.07]	17.10 ± 0.05	17.30 ± 0.11	[17.59 ± 0.08]	105; 107; 105; –; 1,105
WISEPA J022623.98−021142.8	19.6 ± 0.9	51.1 ± 2.3	.../T7	B	···	18.41 ± 0.02	18.88 ± 0.10	···	105; 9; 105; 107; 9,107

Table 1 continued

Table 1 *(continued)*

Object	Distance	Parallax	Spectral Type[a]	Flag[b]	Y_{MKO}	J_{MKO}	H_{MKO}	K_{MKO}	References
	(pc)	(mas)	(Optical/NIR)		(mag)	(mag)	(mag)	(mag)	(Disc; ϖ; SpT; Flag; Phot)
2MASS J02271036−1624479	20.50 ± 0.14	48.8 ± 0.3	L1/L0.5:	···	[14.66 ± 0.05]	13.53 ± 0.02	[12.70 ± 0.03]	[12.13 ± 0.03]	164; 77; 164,140; –; 1,9
2MASS J02284243+1639329	21.7 ± 0.2	46.0 ± 0.4	L0:/M8.7	···	[14.05 ± 0.05]	13.09 ± 0.02	[12.38 ± 0.02]	[11.80 ± 0.02]	164; 77; 164,5; –; 1,9
GJ 1048B	21.47 ± 0.13	46.6 ± 0.3	L1/L1	C	[13.82 ± 0.50]	12.66 ± 0.50	[12.80 ± 0.08]	12.17 ± 0.08	82; 77; 82,82; 82; 1,69
2MASSI J0243137−245329	10.7 ± 0.4	93.6 ± 3.6	T5.5/T6	···	16.13 ± 0.06	15.13 ± 0.03	15.39 ± 0.03	15.34 ± 0.03	21; 191; 153,29; –; 64,108
WISE J024714.52+372523.5	15.4 ± 0.5	64.8 ± 2.0	.../T8	···	···	18.02 ± 0.02	···	···	135; 9; 135; –; 9
2MASSI J0251148−035245	12.8 ± 0.6	78.0 ± 3.5	L3/L1	···	···	12.94 ± 0.02	[[12.30 ± 0.02]]	[[11.64 ± 0.02]]	45; 9; 45,193; –; 1,9,51
PSO J043.5395+02.3995	6.84 ± 0.07	146.1 ± 1.5	.../T8	···	17.000 ± 0.014	15.916 ± 0.009	16.29 ± 0.02	16.73 ± 0.05	121,176; 107; 121; –; 111
CFBDS J030135.11−161418.0	20.4 ± 1.6	49.1 ± 3.8	.../T7	···	19.38 ± 0.05	18.34 ± 0.07	18.99 ± 0.10	18.07 ± 0.06	2; 67; 2; –; 2
2MASS J03140344+1603056	13.62 ± 0.05	73.4 ± 0.3	L0/L0: FLD-G	···	[13.51 ± 0.05]	[12.47 ± 0.02]	[11.87 ± 0.02]	[11.21 ± 0.02]	164; 77; 164,3; –; 1
WISE J031624.35+430709.1	13.6 ± 0.5	73.3 ± 2.8	.../T8	···	···	19.47 ± 0.04	19.70 ± 0.09	···	135; 107; 135; –; 135
WISEA J032301.86+562558.0	16.4 ± 1.5	60.8 ± 5.6	.../L7	···	[17.06 ± 0.05]	15.78 ± 0.02	[14.70 ± 0.05]	[13.75 ± 0.05]	134; 9; 134; –; 1,9
WISE J032547.72+083118.2	12.7 ± 0.5	78.5 ± 3.0	.../T7	···	[17.14 ± 0.09]	[16.29 ± 0.07]	[16.19 ± 0.08]	[16.39 ± 0.09]	135; 107; 135; –; 1
SDSS J032553.17+042540.1	22.7 ± 1.6	44.0 ± 3.2	.../T5.5	···	17.168 ± 0.014	15.996 ± 0.009	16.26 ± 0.02	16.52 ± 0.04	44; 9; 44; –; 111
PSO J052.2746+13.3754	22.5 ± 1.5	44.3 ± 3.0	.../T3.5	···	[17.34 ± 0.05]	16.23 ± 0.02	[15.93 ± 0.05]	[15.73 ± 0.05]	125; 9; 125; –; 1,9
PSO J052.7214−03.8409	17.5 ± 1.1	57.1 ± 3.5	.../L9:	···	[17.36 ± 0.05]	16.27 ± 0.02	15.24 ± 0.02	[14.58 ± 0.05]	11; 9; 11; –; 1,11
2MASS J03552337+1133437	9.12 ± 0.06	109.7 ± 0.7	L5 γ/L3: VL-G	BY	[15.46 ± 0.06]	[13.95 ± 0.02]	[12.60 ± 0.02]	11.502 ± 0.001	163; 77; 48,3; 8,48,3; 1,110
WISE J040137.21+284951.7	12.45 ± 0.04	80.3 ± 0.3	L3/L2.5	···	[14.61 ± 0.05]	13.34 ± 0.02	[12.50 ± 0.02]	[11.80 ± 0.02]	43; 77; 43,43; –; 1,9
WISE J040418.01+412735.6	16.19 ± 0.11	61.8 ± 0.4	L2/L2pec	···	[15.37 ± 0.05]	14.08 ± 0.02	[13.17 ± 0.02]	12.343 ± 0.002	43; 77; 43,43; –; 1,9,131
2MASS J04070885+1514565	18.1 ± 0.9	55.4 ± 2.7	.../T5	···	[16.88 ± 0.05]	15.67 ± 0.02	[15.84 ± 0.05]	15.88 ± 0.03	26; 9; 29; –; 1,9,111
2MASSI J0408290−145033	22.0 ± 0.2	45.4 ± 0.3	L2/L4.5	···	[15.33 ± 0.05]	14.15 ± 0.02	[13.41 ± 0.02]	[12.80 ± 0.02]	193; 77; 45,193; –; 1,9
PSO J062.3459+11.1794	21.9 ± 1.3	45.7 ± 2.7	.../T3.5	···	···	16.17 ± 0.02	[[15.73 ± 0.15]]	15.88 ± 0.02	125; 9; 125; –; 1,9,51,111
2MASSI J0415195−093506	5.71 ± 0.06	175.2 ± 1.7	T8/T8	···	[16.39 ± 0.06]	15.32 ± 0.03	15.70 ± 0.03	15.83 ± 0.03	21; 64; 22,29; –; 1,108
SDSSp J042348.57−041403.5	14.1 ± 0.2	71.1 ± 0.8	L7.5/T0	B	15.41 ± 0.03	14.30 ± 0.03	13.51 ± 0.03	12.96 ± 0.03	79; 65; 45,29; 27; 113
WISE J042417.94+072744.1	22.9 ± 0.8	43.7 ± 1.5	.../T7.5	···	···	18.32 ± 0.02	···	···	135; 9; 135; –; 9
WISE J043052.92+463331.6	12.3 ± 0.5	81.4 ± 3.5	.../T8	···	···	19.06 ± 0.02	19.25 ± 0.13	···	135; 9; 135; –; 9,135
2MASSI J0439010−235308	12.38 ± 0.08	80.8 ± 0.5	L6.5/L6	···	[15.51 ± 0.06]	14.31 ± 0.03	13.44 ± 0.03	12.77 ± 0.02	45; 77; 45,37; –; 1,69
WISEPA J044853.29−193548.5	18.1 ± 1.1	55.3 ± 3.4	.../T5pec	···	[17.51 ± 0.06]	16.63 ± 0.02	[16.94 ± 0.06]	[17.30 ± 0.08]	105; 9; 105; –; 1,9
WISE J045746.08−020719.2	12.2 ± 0.4	82.0 ± 2.9	.../T2	···	···	14.64 ± 0.02	14.187 ± 0.004	13.986 ± 0.004	13; 9; 13; –; 9,111
WISEPA J050003.05−122343.2	11.8 ± 0.3	84.6 ± 2.2	.../T8	···	[18.69 ± 0.06]	17.88 ± 0.02	18.13 ± 0.12	[18.06 ± 0.08]	105; 9; 105; –; 1,9,111
2MASS J05002100+0330501	13.12 ± 0.06	76.2 ± 0.4	L4/L4.2 FLD-G	···	[14.93 ± 0.05]	[13.60 ± 0.02]	[12.76 ± 0.02]	[12.04 ± 0.02]	164; 77; 164,73; –; 1
2MASS J05012406−0010452	21.2 ± 0.4	47.1 ± 0.9	L4 γ/L3: VL-G	Y	[16.26 ± 0.06]	[14.89 ± 0.04]	[13.78 ± 0.04]	[12.92 ± 0.04]	164; 77; 48,3; 48,3; 1
PSO J076.7092+52.6087	16.8 ± 1.5	59.6 ± 5.4	.../T4.5	···	[16.61 ± 0.05]	15.44 ± 0.02	15.47 ± 0.02	15.60 ± 0.03	11; 9; 11; –; 1,11
2MASSI J0512063−294954	20.2 ± 1.1	49.6 ± 2.8	L5 γ/L3.8 INT-G	Y	[16.86 ± 0.08]	[15.38 ± 0.06]	[14.26 ± 0.04]	[13.25 ± 0.04]	45; 67; 70,73; 70,73; 1
WISEPA J051317.28+060814.7	14.1 ± 0.3	70.8 ± 1.5	.../T6.5	···	···	[[15.97 ± 0.06]]	[[16.19 ± 0.08]]	[[16.17 ± 0.11]]	105; 107; 105; –; 1,105
2MASS J05160945−0445499	18.4 ± 1.5	54.2 ± 4.3	.../T5.5	···	16.813 ± 0.013	15.545 ± 0.008	15.773 ± 0.011	15.79 ± 0.02	25; 9; 29; –; 110,111
2MASS J05185995−2828372	22.9 ± 0.4	43.7 ± 0.8	L7/T1pec	B	[17.12 ± 0.11]	15.87 ± 0.10	14.86 ± 0.07	14.11 ± 0.07	46; 64; 103,29; 30; 1,69
WISE J052126.29+102528.4	7.1 ± 0.2	141.2 ± 4.8	.../T7.5	···	[15.71 ± 0.05]	14.87 ± 0.02	[15.27 ± 0.05]	[15.00 ± 0.05]	13; 9; 13; –; 1,9
2MASSI J0523382−140302	12.76 ± 0.03	78.4 ± 0.2	L2.5/L5	···	···	[[13.02 ± 0.03]]	[[12.27 ± 0.03]]	[[11.62 ± 0.03]]	45; 77; 45,193; –; 1,51
SDSSp J053951.99−005902.0	12.73 ± 0.09	78.5 ± 0.6	L5/L5	···	15.02 ± 0.03	13.85 ± 0.03	13.04 ± 0.03	12.40 ± 0.03	71; 77; 71,108; –; 112

Table 1 continued

Table 1 *(continued)*

Object	Distance	Parallax	Spectral Type[a]	Flag[b]	Y_{MKO}	J_{MKO}	H_{MKO}	K_{MKO}	References
	(pc)	(mas)	(Optical/NIR)		(mag)	(mag)	(mag)	(mag)	(Disc; ϖ; SpT; Flag; Phot)
PSO J085.1080−18.0445	16.9 ± 1.2	59.2 ± 4.0	.../T5	···	···	15.99 ± 0.02	···	···	125; 9; 125; –; 9
WISEPA J054231.26−162829.1	16.3 ± 0.7	61.3 ± 2.6	.../T6.5	···	···	16.28 ± 0.02	[[16.63 ± 0.10]]	[[16.76 ± 0.14]]	105; 9; 105; –; 1,9,105
WISE J054601.19−095947.5	19.9 ± 1.4	50.4 ± 3.6	.../T5	···	[17.04 ± 0.05]	15.98 ± 0.02	[16.24 ± 0.05]	[16.43 ± 0.06]	135; 9; 135; –; 1,9
WISEA J055007.94+161051.9	20.4 ± 0.4	49.1 ± 0.9	.../L2	···	[15.64 ± 0.05]	14.36 ± 0.02	[13.56 ± 0.03]	[12.81 ± 0.03]	106; 77; 106; –; 1,9
PSO J089.1751−09.4513	22.6 ± 1.2	44.3 ± 2.5	.../T5.5	···	[17.66 ± 0.06]	16.46 ± 0.02	[16.58 ± 0.06]	[16.66 ± 0.07]	125; 9; 125; –; 1,9
2MASS J05591914−1404488	10.28 ± 0.06	97.3 ± 0.6	T5/T4.5	···	14.69 ± 0.02	13.57 ± 0.03	13.64 ± 0.03	13.73 ± 0.03	20; 53; 22,29; –; 113
2MASS J06020638+4043588	15.4 ± 1.0	65.1 ± 4.2	.../T4.5	···	[16.38 ± 0.05]	15.28 ± 0.02	[15.39 ± 0.05]	[15.41 ± 0.05]	129; 9; 129; –; 1,9
LSR J0602+3910	11.68 ± 0.02	85.6 ± 0.2	L1/L2: INT-G	Y	[13.35 ± 0.05]	[12.23 ± 0.02]	[11.51 ± 0.02]	[10.83 ± 0.02]	168; 77; 168,3; 3; 1
WISEP J060738.65+242953.4	7.30 ± 0.04	136.9 ± 0.7	L8/L9	···	[15.35 ± 0.06]	[14.12 ± 0.03]	[13.12 ± 0.03]	[12.46 ± 0.02]	42; 77; 43,43; –; 1
Gl 229B	5.757 ± 0.002	173.70 ± 0.05	.../T7pec	C	15.17 ± 0.10	14.01 ± 0.05	14.36 ± 0.05	14.36 ± 0.05	150; 77; 29; 150; 114
WISEPA J061135.13−041024.0	21.2 ± 1.4	47.2 ± 3.2	.../T0	B	16.614 ± 0.010	15.398 ± 0.006	14.743 ± 0.005	14.292 ± 0.005	105; 80; 105; 80; 110,80,111
WISEPA J061407.49+391236.4	18.6 ± 0.6	53.7 ± 1.7	.../T6	B	···	[[16.70 ± 0.16]]	[[16.42 ± 0.25]]	···	105; 107; 105; 107,67; 1,105
WISE J061437.73+095135.0	17.6 ± 0.6	56.7 ± 2.0	.../T7	···	[17.54 ± 0.05]	16.44 ± 0.02	[16.66 ± 0.05]	[16.51 ± 0.05]	135; 9; 135; –; 1,9
2MASS J06143818+3950357	22.7 ± 1.3	44.0 ± 2.6	.../L9:	···	[17.63 ± 0.05]	16.54 ± 0.02	[15.67 ± 0.05]	[15.04 ± 0.05]	149; 9; 149; –; 1,9
DENIS-P J0615493−010041	21.88 ± 0.05	45.70 ± 0.11	L2:/L1.0	···	[14.75 ± 0.06]	[13.70 ± 0.03]	[13.05 ± 0.03]	[12.52 ± 0.03]	152; 166; 152,5; –; 1
WISEPA J062309.94−045624.6	11.6 ± 0.2	86.5 ± 1.7	.../T8	···	[18.04 ± 0.06]	17.10 ± 0.02	[17.34 ± 0.07]	[17.26 ± 0.09]	105; 9; 105; –; 1,9
WISEPA J062542.21+564625.5	20.2 ± 0.8	49.5 ± 2.0	.../T6	···	···	16.73 ± 0.02	[[16.96 ± 0.10]]	[[16.96 ± 0.15]]	105; 107; 105; –; 1,9,105
WISEPA J062720.07−111428.8	13.4 ± 0.6	74.8 ± 3.6	.../T6	···	[16.37 ± 0.07]	[15.25 ± 0.05]	[15.50 ± 0.18]	[15.51 ± 0.18]	105; 107; 105; –; 1
WISE J064205.58+410155.5	16.0 ± 0.2	62.6 ± 0.9	.../L9 (red)	···	[17.30 ± 0.05]	16.15 ± 0.02	15.113 ± 0.014	14.306 ± 0.012	135; 67; 11; –; 1,11
WISE J064336.71−022315.4	13.9 ± 0.3	71.9 ± 1.4	.../L8	···	···	[[15.35 ± 0.05]]	[[14.44 ± 0.05]]	[[13.60 ± 0.06]]	137; 77; 137; –; 1,51
WISE J064528.38−030248.2	19.7 ± 1.6	50.7 ± 4.2	.../T6	···	···	16.934 ± 0.011	17.33 ± 0.03	17.34 ± 0.09	189; 107; 189; –; 110
WISEA J064750.85−154616.4	21.0 ± 1.7	47.6 ± 3.9	.../L9.5	B	···	15.15 ± 0.02	[[14.35 ± 0.06]]	[[13.72 ± 0.06]]	178; 9; 178; 12; 1,9,51
DENIS-P J0652197−253450	16.12 ± 0.02	62.02 ± 0.07	L0/M9.2	···	[13.67 ± 0.05]	[12.72 ± 0.02]	[12.09 ± 0.02]	[11.49 ± 0.02]	152; 166; 152,5; –; 1
PSO J103.0927+41.4601	22.2 ± 1.8	45.1 ± 3.7	.../T0	B	[16.47 ± 0.05]	15.361 ± 0.014	14.51 ± 0.03	13.95 ± 0.03	10; 9; 10; 12; 1,10
2MASSI J0652307+471034	9.07 ± 0.02	110.3 ± 0.3	L4.5/L6.5	···	[14.74 ± 0.05]	13.38 ± 0.02	[12.47 ± 0.02]	[11.67 ± 0.02]	45; 53; 45,37; –; 1,9
WISEPA J065609.60+420531.0	15.9 ± 1.0	63.0 ± 4.1	T2/T3	···	[16.19 ± 0.05]	15.27 ± 0.02	[14.98 ± 0.05]	[14.99 ± 0.05]	105; 9; 153,105; –; 1,9
WISEA J065958.55+171710.9	23.8 ± 0.5	42.1 ± 0.9	.../L2	···	···	14.74 ± 0.02	[[13.82 ± 0.03]]	[[13.00 ± 0.03]]	106; 77; 106; –; 1,9,51
2MASS J07003664+3157266	11.33 ± 0.04	88.3 ± 0.3	L3.5/...	B	···	12.82 ± 0.02	12.00 ± 0.02	11.29 ± 0.02	186; 77; 186; 163; 69
WISEA J071552.38−114532.9	17.99 ± 0.11	55.6 ± 0.3	.../L4pec	···	[15.41 ± 0.05]	14.18 ± 0.02	[13.58 ± 0.05]	[12.78 ± 0.04]	106; 77; 106; –; 1,9
DENIS-P J0716478−063037	24.44 ± 0.08	40.92 ± 0.14	L1:/L1.1	···	[14.85 ± 0.05]	13.799 ± 0.002	13.131 ± 0.001	12.556 ± 0.002	152; 166; 152,5; –; 1,131
2MASSI J0727182+171001	8.89 ± 0.07	112.5 ± 0.9	T8/T7	···	16.16 ± 0.06	15.19 ± 0.03	15.67 ± 0.03	15.69 ± 0.03	21; 64; 22,29; –; 64,108
SDSS J074149.15+235127.5	18.9 ± 1.3	53.0 ± 3.7	.../T5	···	17.129 ± 0.013	15.886 ± 0.005	16.10 ± 0.02	16.28 ± 0.04	108; 9; 29; –; 111
SDSS J074201.41+205520.5	17.1 ± 1.0	58.4 ± 3.3	.../T5	···	[16.98 ± 0.06]	15.78 ± 0.02	15.95 ± 0.03	16.06 ± 0.03	108; 9; 29; –; 1,108
WISEPA J074457.15+562821.8	14.8 ± 0.5	67.6 ± 2.1	.../T8	···	···	17.27 ± 0.02	[[17.65 ± 0.12]]	[[17.70 ± 0.20]]	105; 9; 105; –; 1,9,105
2MASSI J0746425+200032	12.31 ± 0.04	81.2 ± 0.2	L0.5/L1	B	12.71 ± 0.02	11.64 ± 0.03	11.01 ± 0.03	10.43 ± 0.03	160; 94; 101,108; 161; 113
PSO J117.0600−01.6779	23.5 ± 2.0	42.6 ± 3.7	.../T5.5	···	[17.50 ± 0.05]	16.34 ± 0.02	[16.57 ± 0.06]	[16.44 ± 0.06]	125; 9; 125; –; 1,9
DENIS-P J0751164−253043	17.76 ± 0.03	56.30 ± 0.09	L1.5/L1.1	···	[14.15 ± 0.05]	[13.10 ± 0.02]	[12.57 ± 0.02]	[11.97 ± 0.02]	152; 166; 152,5; –; 1
2MASSI J0755480+221218	17.0 ± 1.0	58.9 ± 3.3	T6/T5	···	16.811 ± 0.011	15.484 ± 0.004	15.784 ± 0.011	15.93 ± 0.02	21; 9; 22,29; –; 111
HIP 38939B	18.484 ± 0.014	54.10 ± 0.04	.../T4.5	C	[16.84 ± 0.05]	15.78 ± 0.02	[15.87 ± 0.05]	[15.98 ± 0.05]	56; 77; 56; 56; 1,9

Table 1 continued

Table 1 *(continued)*

Object	Distance	Parallax	Spectral Type[a]	Flag[b]	Y_{MKO}	J_{MKO}	H_{MKO}	K_{MKO}	References
	(pc)	(mas)	(Optical/NIR)		(mag)	(mag)	(mag)	(mag)	(Disc; ϖ; SpT; Flag; Phot)
SDSS J075840.33+324723.4	10.7 ± 0.5	93.7 ± 4.4	T3/T2	···	[15.82 ± 0.05]	14.73 ± 0.02	14.21 ± 0.04	[13.90 ± 0.06]	108; 9; 153,29; –; 1,9,151
SDSS J080531.84+481233.0	21.4 ± 0.4	46.8 ± 1.0	L4/L9:	B	[15.81 ± 0.06]	14.61 ± 0.03	14.01 ± 0.03	13.51 ± 0.03	95; 77; 95,108; 32,64; 1,108
WISE J080700.23+413026.8	19.6 ± 1.5	51.1 ± 3.8	.../L8pec	···	[17.08 ± 0.05]	15.93 ± 0.02	[15.00 ± 0.05]	[14.25 ± 0.05]	185; 9; 185; –; 1,9
SDSS J080959.01+443422.2	23.6 ± 2.0	42.4 ± 3.6	.../L5.4 INT-G	Y	[17.69 ± 0.05]	16.42 ± 0.02	[15.34 ± 0.05]	[14.39 ± 0.05]	108; 9; 73; 73; 1,9
DENIS-P J0812316−244442	21.15 ± 0.04	47.28 ± 0.09	L2.5:/L0.9	···	[14.94 ± 0.06]	[13.78 ± 0.03]	[13.00 ± 0.02]	[12.38 ± 0.02]	152; 166; 152,5; –; 1
WISEPA J081958.05−033529.0	13.9 ± 0.6	71.7 ± 3.3	T4/T4	···	[15.94 ± 0.05]	14.78 ± 0.02	[14.60 ± 0.05]	[14.64 ± 0.05]	105; 9; 153,105; –; 1,9
WISEPA J082131.63+144319.3	22.9 ± 2.0	43.7 ± 3.9	.../T5.5	···	[17.49 ± 0.06]	16.40 ± 0.02	[16.61 ± 0.05]	[16.33 ± 0.06]	105; 9; 105; –; 1,9
2MASSI J0825196+211552	10.73 ± 0.07	93.2 ± 0.6	L7.5/L7pec	···	16.03 ± 0.03	14.89 ± 0.03	13.81 ± 0.03	12.93 ± 0.03	101; 53; 101,108; –; 113
WISEA J082640.45−164031.8	18.5 ± 1.5	54.0 ± 4.3	.../L9	···	···	15.60 ± 0.02	[[14.66 ± 0.07]]	[[14.09 ± 0.07]]	106; 9; 106; –; 1,9,51
SSSPM J0829−1309	11.65 ± 0.02	85.8 ± 0.2	L2/L2:	···	[13.91 ± 0.06]	[12.76 ± 0.03]	[11.92 ± 0.02]	[11.28 ± 0.02]	173; 166; 126,140; –; 1
SDSSp J083008.12+482847.4	13.1 ± 0.6	76.4 ± 3.4	L8/L9:	···	16.25 ± 0.03	15.22 ± 0.03	14.40 ± 0.03	13.68 ± 0.03	79; 191; 103,79; –; 113
PSO J127.5648−11.1861	23.3 ± 2.0	42.9 ± 3.7	.../T3	···	[16.89 ± 0.05]	15.71 ± 0.02	[15.40 ± 0.05]	[15.48 ± 0.05]	125; 9; 125; –; 1,9
SDSS J083048.80+012831.1	23.4 ± 2.6	42.7 ± 4.7	.../T4.5	···	17.203 ± 0.013	16.049 ± 0.009	16.25 ± 0.02	16.35 ± 0.04	108; 9; 29; –; 111
2MASSW J0832045−012835	23.7 ± 0.2	42.2 ± 0.4	L1.5/L1:	···	[15.24 ± 0.05]	14.08 ± 0.02	[13.39 ± 0.03]	[12.69 ± 0.03]	101; 77; 101,140; –; 1,9
2MASSI J0835425−081923	7.214 ± 0.015	138.6 ± 0.3	L5/L4pec	···	[14.37 ± 0.05]	13.04 ± 0.02	11.99 ± 0.02	11.08 ± 0.02	45; 77; 45,73; –; 1,69
WISEPC J083641.12−185947.2	24.5 ± 2.2	40.8 ± 3.6	.../T8pec	···	···	[[18.71 ± 0.22]]	19.49 ± 0.24	···	105; 107; 105; –; 1,135,7
2MASSI J0847287−153237	17.57 ± 0.10	56.9 ± 0.3	L2/...	···	[14.62 ± 0.06]	13.42 ± 0.03	12.66 ± 0.03	12.02 ± 0.02	45; 77; 45; –; 1,69
SDSS J085234.90+472035.0	23.7 ± 1.9	42.2 ± 3.4	.../L9.5:	···	[17.23 ± 0.05]	16.16 ± 0.02	[15.31 ± 0.05]	[14.65 ± 0.05]	108; 9; 108; –; 1,9
WISEPA J085716.25+560407.6	13.1 ± 0.4	76.3 ± 2.4	.../T8	···	···	17.35 ± 0.02	···	···	105; 9; 105; –; 9
SDSSp J085758.45+570851.4	14.0 ± 0.2	71.2 ± 1.0	L8/L8:	···	[16.09 ± 0.05]	14.86 ± 0.02	[13.89 ± 0.03]	[12.94 ± 0.03]	79; 77; 103,79; –; 1,9
SDSS J085834.42+325627.7	24.4 ± 2.1	40.9 ± 3.6	.../T1	···	[17.42 ± 0.06]	16.36 ± 0.02	[15.50 ± 0.05]	[14.74 ± 0.05]	44; 9; 44; –; 1,9
ULAS J085910.69+101017.1	19.9 ± 0.7	50.3 ± 1.7	.../T7	···	19.02 ± 0.07	17.88 ± 0.02	18.30 ± 0.09	18.28 ± 0.16	154; 107; 154; –; 111,9
2MASSI J0859254−194926	14.0 ± 0.7	71.2 ± 3.5	L6::/L8	···	[16.66 ± 0.07]	15.42 ± 0.05	14.47 ± 0.04	13.70 ± 0.06	45; 181; 45,185; –; 1,69
ULAS J090116.23−030635.0	16.0 ± 0.7	62.6 ± 2.6	.../T7.5	···	18.90 ± 0.05	17.89 ± 0.04	18.49 ± 0.13	···	127; 139; 127; –; 111
2MASS J09054654+5623117	24.8 ± 0.8	40.4 ± 1.2	L5/L6	···	[16.67 ± 0.06]	15.33 ± 0.02	[14.37 ± 0.04]	[13.71 ± 0.04]	164; 77; 164,37; –; 1,9
WISEPA J090649.36+473538.6	20.7 ± 1.5	48.4 ± 3.4	.../T8	B	···	[[17.87 ± 0.16]]	[[17.87 ± 0.16]]	[[18.67 ± 0.34]]	105; 107; 105; 67; 1,105
2MASSI J0908380+503208	10.44 ± 0.08	95.8 ± 0.7	L5/L9:	···	[15.52 ± 0.05]	14.43 ± 0.02	[13.56 ± 0.03]	[12.93 ± 0.03]	45; 77; 45,108; –; 1,9
DENIS-P J090957.1−065806	24.9 ± 0.2	40.1 ± 0.3	L0/L0:	···	[14.90 ± 0.05]	13.81 ± 0.02	13.12 ± 0.02	12.50 ± 0.03	62; 77; 103,140; –; 1,69
Gl 337CD	20.35 ± 0.14	49.2 ± 0.3	L8/T0	BC	[16.68 ± 0.05]	15.53 ± 0.02	14.65 ± 0.08	14.00 ± 0.06	192; 77; 192,29; 28,192; 1,9,69
2MASS J09153413+0422045	18.2 ± 0.4	54.8 ± 1.1	L6/...	B	15.770 ± 0.005	14.518 ± 0.003	13.632 ± 0.003	12.887 ± 0.002	164; 77; 164; 163; 111
WISE J092055.40+453856.3	12.6 ± 0.6	79.4 ± 3.9	.../L9.5	···	[16.14 ± 0.05]	15.04 ± 0.01	14.19 ± 0.02	13.766 ± 0.011	135; 9; 10; –; 1,10
2MASS J09211410−2104446	12.61 ± 0.04	79.3 ± 0.2	L1.5/L4:	···	[13.77 ± 0.05]	12.71 ± 0.02	[12.23 ± 0.02]	[11.66 ± 0.02]	164; 77; 164,34; –; 1,9
SDSS J092308.70+234013.7	22.8 ± 1.9	43.8 ± 3.7	L1/L2.3	···	[14.82 ± 0.05]	13.79 ± 0.02	[13.23 ± 0.02]	[12.78 ± 0.02]	171; 9; 171,5; –; 1,9
SDSSp J092615.38+584720.9	23.0 ± 0.5	43.4 ± 1.0	T5/T4.5	B	[16.90 ± 0.08]	[15.71 ± 0.06]	[15.38 ± 0.19]	[15.53 ± 0.19]	79; 65; 153,29; 30; 1
WISEPC J092906.77+040957.9	24.4 ± 1.3	41.0 ± 2.2	.../T6.5	···	17.890 ± 0.010	16.870 ± 0.010	17.240 ± 0.010	17.61 ± 0.02	105; 107; 105; –; 41
2MASSI J0937347+293142	6.12 ± 0.07	163.4 ± 1.8	T7/T6pec	···	15.18 ± 0.06	14.29 ± 0.03	14.67 ± 0.03	15.39 ± 0.06	21; 169; 22,29; –; 64,108
2MASS J09393548−2448279	5.34 ± 0.13	187.3 ± 4.6	T8/T8	···	16.47 ± 0.09	15.61 ± 0.09	15.96 ± 0.09	16.83 ± 0.09	188; 35; 153,29; –; 115
ULAS J095047.28+011734.3	19.69 ± 0.03	50.80 ± 0.08	.../T8	C	18.90 ± 0.03	18.02 ± 0.03	18.40 ± 0.03	18.85 ± 0.07	41; 77; 135; 133; 41
WISEPC J095259.29+195507.3	24.3 ± 2.3	41.1 ± 3.9	.../T6	B	[17.88 ± 0.08]	[16.89 ± 0.06]	[17.28 ± 0.10]	[17.51 ± 0.08]	105; 107; 105; 67; 1

Table 1 continued

Table 1 *(continued)*

Object	Distance	Parallax	Spectral Type[a]	Flag[b]	Y_{MKO}	J_{MKO}	H_{MKO}	K_{MKO}	References
	(pc)	(mas)	(Optical/NIR)		(mag)	(mag)	(mag)	(mag)	(Disc; ϖ; SpT; Flag; Phot)
ULAS J095429.90+062309.6	24.5 ± 1.9	40.9 ± 3.2	.../T5	···	17.730 ± 0.010	16.600 ± 0.010	16.870 ± 0.010	17.050 ± 0.010	177,41; 9; 41; –; 41
PSO J149.0341−14.7857	15.3 ± 0.8	65.4 ± 3.4	.../L9	···	17.18 ± 0.05	15.99 ± 0.02	15.073 ± 0.013	14.46 ± 0.02	11; 9; 11; –; 9,11
G 196-3B	22.5 ± 0.4	44.3 ± 0.8	L3 β/L3: VL-G	CY	[16.23 ± 0.07]	[14.73 ± 0.05]	[13.72 ± 0.03]	[12.73 ± 0.03]	159; 77; 48,3; 159,48,3; 1
DENIS J1004403−131818	24.6 ± 0.4	40.7 ± 0.7	.../L1:	···	···	[[14.62 ± 0.04]]	[[13.93 ± 0.04]]	[[13.34 ± 0.04]]	143; 77; 140; –; 1,51
SDSS J100711.74+193056.2	21.9 ± 0.9	45.6 ± 2.0	.../L8:	···	[17.78 ± 0.06]	16.70 ± 0.02	[15.88 ± 0.05]	[15.24 ± 0.05]	44; 9; 44; –; 1,9
2MASSI J1010148−040649	18.2 ± 1.3	55.0 ± 4.0	L6/L6	···	[16.67 ± 0.05]	15.40 ± 0.02	14.43 ± 0.04	13.57 ± 0.05	45; 9; 45,104; –; 1,9,69
ULAS J101243.54+102101.7	16.8 ± 0.5	59.7 ± 1.8	.../T5.5	···	18.02 ± 0.03	16.880 ± 0.014	17.25 ± 0.05	17.45 ± 0.08	174; 9; 39; –; 111
WISEPC J101808.05−244557.7	12.0 ± 0.5	83.6 ± 3.6	.../T8	···	···	···	···	···	105; 107; 105; –; 0
DENIS J1019245−270717	23.34 ± 0.13	42.8 ± 0.2	L0.5/M9.5	···	[14.42 ± 0.05]	13.50 ± 0.02	[12.97 ± 0.02]	[12.45 ± 0.02]	143; 77; 143,99; –; 1,9
2MASS J10224821+5825453	18.41 ± 0.11	54.3 ± 0.3	L1 β/L1: FLD-G	Y	[14.55 ± 0.06]	[13.43 ± 0.03]	[12.69 ± 0.03]	[12.13 ± 0.03]	164; 77; 48,3; 48,3; 1
CFBDS J102841.01+565401.9	22.2 ± 1.4	45.0 ± 2.9	.../T8	···	18.85 ± 0.02	17.98 ± 0.04	18.38 ± 0.08	18.85 ± 0.09	2; 107; 2; –; 2
2MASSI J1029216+162652	19.1 ± 0.3	52.3 ± 0.7	L2.5/L2.8	···	[15.52 ± 0.05]	14.23 ± 0.02	[13.41 ± 0.02]	[12.60 ± 0.02]	101; 77; 101,5; –; 1,9
ULAS J102940.52+093514.6	14.6 ± 0.4	68.6 ± 1.7	.../T8	···	18.24 ± 0.02	17.280 ± 0.010	17.630 ± 0.010	17.64 ± 0.02	41; 9; 41; –; 41
WISE J103907.73−160002.9	22.1 ± 0.9	45.3 ± 2.0	.../T7.5	···	18.19 ± 0.03	16.89 ± 0.02	17.19 ± 0.04	[17.09 ± 0.07]	135; 9; 135; –; 145,1
2MASS J10430758+2225236	19.1 ± 1.1	52.4 ± 2.9	L8/L9:	···	[17.03 ± 0.06]	15.85 ± 0.02	[14.82 ± 0.04]	[13.98 ± 0.04]	47; 9; 47,37; –; 1,9
SDSS J104335.08+121314.1	16.7 ± 0.9	59.9 ± 3.1	.../L9	···	17.049 ± 0.012	15.865 ± 0.007	14.910 ± 0.005	14.212 ± 0.005	44; 9; 104; –; 111
2MASSI J1045240−014957	17.05 ± 0.07	58.7 ± 0.2	L1/L1: FLD-G	···	14.231 ± 0.002	13.084 ± 0.001	12.402 ± 0.001	11.780 ± 0.001	83; 77; 83,3; –; 111
2MASSI J1047538+212423	10.6 ± 0.4	94.7 ± 3.8	T7/T6.5	···	16.44 ± 0.03	15.46 ± 0.03	15.83 ± 0.03	16.20 ± 0.03	18; 191; 22,29; –; 113
SDSS J104842.84+011158.5	15.05 ± 0.05	66.5 ± 0.2	L1/L4	···	13.945 ± 0.002	12.797 ± 0.001	12.157 ± 0.001	11.579 ± 0.001	95; 77; 95,98; –; 111
WISE J105047.90+505606.2	22.1 ± 1.1	45.3 ± 2.2	.../T8	···	···	17.94 ± 0.02	18.31 ± 0.03	···	135; 9; 135; –; 135
2MASS J10511900+5613086	15.62 ± 0.05	64.0 ± 0.2	L2/L0.8	···	[14.31 ± 0.05]	13.18 ± 0.02	[12.49 ± 0.02]	[11.88 ± 0.02]	164; 77; 164,5; –; 1,9
WISE J105257.95−194250.2	14.7 ± 0.5	67.8 ± 2.2	.../T7.5	···	[17.72 ± 0.05]	16.83 ± 0.02	[17.08 ± 0.05]	[17.00 ± 0.05]	185; 9; 185; –; 1,9
DENIS-P J1058.7−1548	18.3 ± 0.2	54.7 ± 0.5	L3/L2.2 FLD-G	···	15.31 ± 0.04	14.12 ± 0.05	13.29 ± 0.05	12.55 ± 0.05	61; 77; 100,73; –; 113
2MASSI J1104012+195921	17.88 ± 0.14	55.9 ± 0.4	L4/L5.5	···	[15.64 ± 0.05]	14.34 ± 0.02	[13.56 ± 0.03]	[12.93 ± 0.03]	45; 77; 45,37; –; 1,9
2MASS J11061197+2754225	20.8 ± 1.3	48.0 ± 3.0	.../T2.5	B	[16.10 ± 0.06]	14.96 ± 0.04	14.20 ± 0.05	13.84 ± 0.05	129; 138; 129; 37,138; 1,138
SDSSp J111010.01+011613.1	19.2 ± 0.4	52.1 ± 1.2	.../T5.5	Y	17.338 ± 0.012	16.161 ± 0.008	16.20 ± 0.02	16.05 ± 0.03	79; 64; 29; 74; 111
Gl 417BC	21.9 ± 0.2	45.6 ± 0.4	L4.5/L5: FLD-G	BC	[15.83 ± 0.05]	14.47 ± 0.02	13.55 ± 0.03	12.67 ± 0.03	101; 195; 101,3; 15,102,15; 1,9,69
2MASS J11145133−2618235	5.58 ± 0.04	179.2 ± 1.4	T8/T7.5	···	16.36 ± 0.05	15.52 ± 0.05	15.82 ± 0.05	16.54 ± 0.05	188; 64; 153,29; –; 116
WISEPC J112254.73+255021.5	15.1 ± 0.5	66.3 ± 2.3	.../T6	C	[17.29 ± 0.06]	16.29 ± 0.02	[16.67 ± 0.06]	[16.67 ± 0.06]	105; 107; 105; 105; 1,9
WISE J112438.12−042149.7	16.2 ± 0.8	61.6 ± 3.1	.../T7	···	[17.35 ± 0.05]	16.37 ± 0.02	[16.77 ± 0.05]	[16.64 ± 0.06]	135; 107; 135; –; 1,9
ULAS J115508.39+044502.3	20.3 ± 1.0	49.1 ± 2.3	.../T7	···	19.35 ± 0.07	18.31 ± 0.02	···	···	41; 9; 41; –; 111,9
SDSS J115553.86+055957.5	21.5 ± 1.8	46.5 ± 3.9	.../L6.8 FLD-G	···	16.928 ± 0.011	15.720 ± 0.006	14.749 ± 0.006	14.109 ± 0.006	108; 9; 73; –; 111
PSO J180.1475−28.6160	24.6 ± 3.3	40.7 ± 5.4	.../T0	···	[17.06 ± 0.05]	15.96 ± 0.02	15.15 ± 0.01	[14.75 ± 0.05]	11; 9; 11; –; 1,11
SDSSp J120358.19+001550.3	14.87 ± 0.12	67.2 ± 0.6	L3/L5.0	···	15.257 ± 0.005	13.931 ± 0.002	13.114 ± 0.002	12.440 ± 0.002	71; 77; 71,5; –; 111
2MASSI J1204303+321259	24.3 ± 0.2	41.2 ± 0.3	L0/M9	···	[14.84 ± 0.05]	13.80 ± 0.02	[13.16 ± 0.03]	[12.49 ± 0.03]	45; 77; 45,193; –; 1,9
SDSS J120747.17+024424.8	22.3 ± 1.8	44.8 ± 3.6	L8/T0	···	16.616 ± 0.009	15.455 ± 0.006	14.710 ± 0.005	14.187 ± 0.007	95; 9; 95,29; –; 111
2MASS J12095613−1004008	21.8 ± 0.5	45.8 ± 1.0	T3.5/T3	B	16.56 ± 0.03	15.55 ± 0.03	15.24 ± 0.03	15.17 ± 0.03	26; 64; 103,29; 120; 44
2MASSI J1213033−043243	16.8 ± 0.3	59.5 ± 1.0	L5/L4.2	Y	[15.85 ± 0.05]	14.58 ± 0.02	[13.73 ± 0.03]	[13.00 ± 0.03]	45; 77; 45,5; 76; 1,9
2MASSI J1217110−031113	10.9 ± 0.3	91.7 ± 2.2	T7/T7.5	···	16.58 ± 0.03	15.56 ± 0.03	15.98 ± 0.03	15.92 ± 0.03	18; 187,107; 22,29; –; 113

Table 1 continued

Table 1 *(continued)*

Object	Distance	Parallax	Spectral Type[a]	Flag[b]	Y_{MKO}	J_{MKO}	H_{MKO}	K_{MKO}	References
	(pc)	(mas)	(Optical/NIR)		(mag)	(mag)	(mag)	(mag)	(Disc; ϖ; SpT; Flag; Phot)
SDSS J121951.45+312849.4	19.2 ± 1.4	52.0 ± 3.8	.../L8	···	17.146 ± 0.014	15.951 ± 0.009	15.025 ± 0.007	14.348 ± 0.006	44; 9; 44; –; 110,111
2MASS J12212770+0257198	18.54 ± 0.09	54.0 ± 0.2	L0/M9.7 FLD-G	···	14.121 ± 0.002	13.072 ± 0.001	12.438 ± 0.001	11.912 ± 0.001	164; 77; 164,73; –; 111
2MASS J12255432−2739466	13.2 ± 0.4	76.0 ± 2.5	T6/T6	B	15.84 ± 0.03	14.88 ± 0.03	15.17 ± 0.03	15.28 ± 0.03	18; 187,107; 22,29; 23; 113
WISE J122558.86−101345.0	24.3 ± 1.7	41.1 ± 2.9	.../T6	···	17.33 ± 0.02	16.120 ± 0.009	16.49 ± 0.03	[16.49 ± 0.06]	135; 9; 135; –; 145,1
DENIS-P J122813.8−154711	20.8 ± 0.7	48.1 ± 1.7	L5/L6::	B	15.53 ± 0.03	14.28 ± 0.05	13.40 ± 0.05	12.71 ± 0.05	61; 65; 100,108; 142; 113
2MASS J12314753+0847331	14.3 ± 0.7	70.2 ± 3.6	T6/T5.5	···	16.340 ± 0.008	15.153 ± 0.004	15.456 ± 0.008	15.55 ± 0.02	26; 9; 153,29; –; 111
2MASSW J1239272+551537	23.6 ± 1.2	42.4 ± 2.1	L5/...	B	15.94 ± 0.03	14.62 ± 0.03	13.63 ± 0.03	12.76 ± 0.03	101; 64; 101; 84; 64
2MASSW J1246467+402715	22.6 ± 0.4	44.2 ± 0.8	L4/L4.0	···	[16.29 ± 0.05]	14.90 ± 0.02	[14.04 ± 0.04]	[13.25 ± 0.04]	101; 77; 101,5; –; 1,9
SDSS J125011.65+392553.9	23.4 ± 1.7	42.8 ± 3.2	.../T4	···	···	16.14 ± 0.02	[[16.24 ± 0.25]]	[[16.18 ± 0.25]]	44; 9; 44; –; 1,9,51
WISE J125015.56+262846.9	17.4 ± 1.1	57.5 ± 3.7	.../T6	···	17.75 ± 0.02	16.404 ± 0.012	16.74 ± 0.02	16.79 ± 0.05	135; 9; 11; –; 111
WISE J125448.52−072828.4	24.3 ± 1.6	41.1 ± 2.7	.../T7	···	[18.41 ± 0.05]	17.300 ± 0.010	17.63 ± 0.03	[17.40 ± 0.07]	185; 9; 185; –; 1,185
SDSSp J125453.90−012247.4	12.8 ± 0.2	78.3 ± 1.1	T2/T2	···	15.858 ± 0.006	14.667 ± 0.003	14.136 ± 0.003	13.886 ± 0.005	112; 53; 22,29; –; 111
VHS J125601.92−125723.9 b	22.2 ± 1.2	45.0 ± 2.4	L8::/L7:: VL-G	CY	18.56 ± 0.05	17.14 ± 0.02	15.78 ± 0.02	[[14.55 ± 0.12]]	78; 66; 78,78; 78,78; 1,145,51
WISE J125715.90+400854.2	17.6 ± 0.6	57.0 ± 1.8	.../T7	···	[18.14 ± 0.06]	16.89 ± 0.02	[17.14 ± 0.06]	[17.18 ± 0.06]	135; 9; 135; –; 1,9
Ross 458C	11.51 ± 0.02	86.9 ± 0.2	.../T8	C	17.72 ± 0.03	16.69 ± 0.01	17.01 ± 0.04	16.90 ± 0.06	89; 77; 49; 89; 111
2MASSW J1300425+191235	13.95 ± 0.04	71.7 ± 0.2	L1/L3	···	[13.65 ± 0.05]	12.63 ± 0.02	[12.16 ± 0.02]	[11.60 ± 0.02]	81; 77; 81,34; –; 1,9
Kelu-1	18.6 ± 0.2	53.8 ± 0.7	L2/L0.5pec	B	14.52 ± 0.03	13.23 ± 0.05	12.45 ± 0.05	11.78 ± 0.05	165; 77; 100,184; 119; 116
2MASSI J1305410+204639	19.8 ± 0.3	50.4 ± 0.8	L5/L6.5	C	[16.45 ± 0.07]	[15.12 ± 0.05]	[14.13 ± 0.04]	[13.35 ± 0.04]	45; 77; 90,5; 90; 1
ULAS J131508.42+082627.4	19.8 ± 2.2	50.5 ± 5.7	.../T7.5	···	20.00 ± 0.08	18.86 ± 0.04	19.50 ± 0.10	19.60 ± 0.12	154; 107; 154; –; 154
2MASSI J1315309−264951	18.6 ± 0.4	53.9 ± 1.1	L5.5/L6.7	BY	[16.28 ± 0.07]	[15.11 ± 0.05]	[14.14 ± 0.04]	[13.45 ± 0.04]	93; 77; 103,5; 38,92,83; 1
WISE J131833.98−175826.5	17.3 ± 0.8	57.8 ± 2.7	.../T8	···	···	[[18.15 ± 0.19]]	[[17.76 ± 0.23]]	···	135; 107; 144; –; 1,135
WISEPA J132233.66−234017.1	12.9 ± 0.7	77.5 ± 4.2	.../T8	···	[17.74 ± 0.12]	[16.75 ± 0.10]	[16.65 ± 0.14]	[17.02 ± 0.40]	105; 107; 105; –; 1
2MASSW J1326201−272937	18.3 ± 2.0	54.7 ± 5.9	L5/L6.6:	B	[17.02 ± 0.05]	15.74 ± 0.02	[14.83 ± 0.05]	[13.83 ± 0.05]	83; 9; 83,5; 12; 1,9
SDSSp J132629.82−003831.5	20.9 ± 1.3	47.9 ± 2.9	L8:/L7	···	17.59 ± 0.02	16.221 ± 0.011	15.111 ± 0.007	14.171 ± 0.006	71; 9; 71,141; –; 111
SDSS J133148.92−011651.4	20.0 ± 1.8	50.0 ± 4.6	L6/L6:	···	16.498 ± 0.009	15.330 ± 0.006	14.671 ± 0.004	14.051 ± 0.005	95; 181; 95,141; –; 111
WISEA J133300.03−160754.4	20.8 ± 2.0	48.0 ± 4.7	.../T7.5	···	···	···	18.37 ± 0.13	···	107; 107; 107; –; 107
WISE J133750.46+263648.6	24.8 ± 1.3	40.4 ± 2.1	.../T5	···	17.72 ± 0.02	16.56 ± 0.01	16.81 ± 0.03	17.02 ± 0.06	135; 9; 135; –; 111
2MASSW J1338261+414034	21.13 ± 0.12	47.3 ± 0.3	L2.5/L2.4	···	[15.33 ± 0.05]	14.13 ± 0.02	[13.38 ± 0.02]	[12.75 ± 0.02]	101; 77; 101,5; –; 1,9
SDSSp J134646.45−003150.4	14.5 ± 0.5	69.2 ± 2.3	T7/T6.5	···	16.795 ± 0.010	15.641 ± 0.006	15.973 ± 0.011	15.96 ± 0.02	190; 187,107; 22,29; –; 111
LHS 2803B	18.18 ± 0.03	55.00 ± 0.08	.../T5.5	C	17.49 ± 0.05	16.39 ± 0.02	16.57 ± 0.04	16.90 ± 0.08	57; 77; 57; 57; 57
SDSS J135852.68+374711.9	20.1 ± 1.3	49.6 ± 3.1	.../T4.5:	···	[17.32 ± 0.05]	16.24 ± 0.02	[16.50 ± 0.05]	[16.70 ± 0.06]	44; 9; 44; –; 1,9
SDSS J140023.12+433822.3	24.5 ± 1.9	40.8 ± 3.2	.../L7:	···	[17.33 ± 0.05]	16.20 ± 0.02	[15.21 ± 0.05]	[14.45 ± 0.05]	44; 9; 44; –; 1,9
ULAS J141623.94+134836.3	9.30 ± 0.03	107.6 ± 0.3	.../(sd)T7.5	CS	18.16 ± 0.03	17.26 ± 0.02	17.58 ± 0.03	[18.42 ± 0.09]	175,40; 77; 36; 175,40,36; 111,1
SDSS J141624.08+134826.7	9.30 ± 0.03	107.6 ± 0.3	sdL7/sdL7	CS	14.352 ± 0.003	13.066 ± 0.001	12.503 ± 0.001	12.107 ± 0.002	17,170; 77; 104,194; 175,40,104,194; 111
2MASSW J1421314+182740	18.99 ± 0.09	52.7 ± 0.3	L0/M8.9	···	[14.16 ± 0.05]	13.14 ± 0.02	[12.49 ± 0.02]	[11.92 ± 0.02]	81; 77; 164,5; –; 1,9
BD +01 2920B	17.2 ± 0.2	58.2 ± 0.5	.../T8	C	19.51 ± 0.14	18.55 ± 0.03	18.96 ± 0.07	19.89 ± 0.33	155; 195; 135; 155; 111,135,155
2MASS J14283132+5923354	22.0 ± 0.2	45.4 ± 0.5	L4/L4.4	···	[16.03 ± 0.05]	14.73 ± 0.02	[13.95 ± 0.03]	[13.25 ± 0.03]	164; 77; 164,5; –; 1,9
VHS J143311.46−083736.3	16.1 ± 0.9	62.2 ± 3.6	.../T8	···	20.14 ± 0.25	19.01 ± 0.02	19.22 ± 0.14	···	128; 9; 128; –; 128,9
WISEPA J143602.19−181421.8	20.7 ± 1.0	48.3 ± 2.4	.../T8pec	···	···	17.40 ± 0.02	···	···	105; 107; 105; –; 9

Table 1 continued

Table 1 *(continued)*

Object	Distance	Parallax	Spectral Type[a]	Flag[b]	Y_{MKO}	J_{MKO}	H_{MKO}	K_{MKO}	References
	(pc)	(mas)	(Optical/NIR)		(mag)	(mag)	(mag)	(mag)	(Disc; ϖ; SpT; Flag; Phot)
2MASSW J1439284+192915	14.33 ± 0.09	69.8 ± 0.4	L1/...	···	13.67 ± 0.02	12.66 ± 0.03	12.05 ± 0.03	11.47 ± 0.03	100; 53; 100; –; 113
SDSSp J144600.60+002452.0	22.0 ± 1.6	45.5 ± 3.2	L6/L5	···	16.895 ± 0.014	15.584 ± 0.007	14.657 ± 0.005	13.921 ± 0.005	79; 191; 95,108; –; 111
WISE J144806.48−253420.3	19.0 ± 0.9	52.5 ± 2.5	.../T8	···	···	18.90 ± 0.02	18.91 ± 0.12	···	185; 107; 185; –; 9,107
2MASSW J1448256+103159	14.04 ± 0.14	71.2 ± 0.7	L4:/L4.7 FLD-G	···	15.804 ± 0.006	14.420 ± 0.002	13.510 ± 0.003	12.674 ± 0.002	193; 77; 164,70; –; 111
HD 130948BC	18.21 ± 0.02	54.91 ± 0.07	.../L4:	BC	···	13.20 ± 0.08	12.42 ± 0.15	11.69 ± 0.04	157; 77; 91; 157,157; 63
WISEPC J145715.03+581510.2	18.2 ± 0.8	55.0 ± 2.3	T8/T7	···	[17.81 ± 0.05]	16.79 ± 0.02	[17.14 ± 0.06]	[17.21 ± 0.06]	105; 107; 105,105; –; 1,9
Gliese 570D	5.882 ± 0.003	170.01 ± 0.09	T7/T7.5	C	15.78 ± 0.10	14.82 ± 0.05	15.28 ± 0.05	15.52 ± 0.05	19; 77; 22,29; 19; 116
PSO J224.3820+47.4057	20.2 ± 1.2	49.5 ± 2.9	.../T7	···	[18.01 ± 0.05]	17.11 ± 0.02	17.43 ± 0.06	[17.08 ± 0.06]	11; 9; 11; –; 1,9,11
2MASS J15031961+2525196	6.45 ± 0.05	154.9 ± 1.1	T6/T5	···	14.76 ± 0.06	13.55 ± 0.03	13.90 ± 0.03	13.99 ± 0.03	24; 77; 22,29; –; 108
SDSS J150411.63+102718.4	21.7 ± 0.7	46.1 ± 1.5	.../T7	···	17.63 ± 0.02	16.506 ± 0.011	16.99 ± 0.05	17.12 ± 0.08	44; 64; 44; –; 111
HIP 73786B	19.02 ± 0.03	52.59 ± 0.07	.../T6:pec	C	17.65 ± 0.02	16.59 ± 0.02	17.05 ± 0.04	17.41 ± 0.09	174,148; 77; 148; 174; 111
2MASSW J1506544+132106	11.68 ± 0.04	85.6 ± 0.3	L3/L4	···	[14.52 ± 0.05]	13.23 ± 0.02	[12.46 ± 0.02]	[11.72 ± 0.02]	81; 77; 81,37; –; 1,9
2MASSW J1507476−162738	7.32 ± 0.02	136.6 ± 0.3	L5/L5.5	···	13.91 ± 0.03	12.70 ± 0.03	11.90 ± 0.03	11.29 ± 0.03	160; 53; 101,108; –; 113
2MASSW J1515008+484742	9.75 ± 0.06	102.6 ± 0.6	L6/L6	···	[15.14 ± 0.05]	13.97 ± 0.02	[13.18 ± 0.02]	[12.48 ± 0.02]	193; 53; 47,193; –; 1,9
SDSS J151643.01+305344.4	20.7 ± 1.2	48.2 ± 2.7	.../T0.5:	···	17.96 ± 0.03	16.77 ± 0.01	16.00 ± 0.02	15.160 ± 0.013	44; 9; 44; –; 111
WISE J151721.13+052929.3	21.7 ± 1.0	46.1 ± 2.1	.../T8	···	19.57 ± 0.07	18.52 ± 0.02	18.85 ± 0.04	···	135; 9; 135; –; 111,9,107
SDSS J152039.82+354619.8	17.4 ± 1.5	57.4 ± 4.8	.../T0:	···	[16.61 ± 0.05]	15.49 ± 0.02	14.58 ± 0.05	[14.01 ± 0.05]	44; 9; 44; –; 1,9,151
SDSS J152103.24+013142.7	23.1 ± 3.3	43.3 ± 6.2	.../T3	···	17.34 ± 0.02	16.097 ± 0.010	15.679 ± 0.009	15.57 ± 0.01	108; 9; 141; –; 111
WISE J152305.10+312537.6	16.3 ± 1.0	61.4 ± 3.8	.../T6.5pec	···	···	18.27 ± 0.07	18.69 ± 0.18	···	135; 107; 135; –; 135
Gl 584C	17.9 ± 0.2	56.0 ± 0.8	L8/L8	C	17.27 ± 0.01	16.052 ± 0.007	15.084 ± 0.006	14.376 ± 0.007	101; 195; 101,79; 101,102; 111
2MASSI J1526140+204341	20.0 ± 0.6	50.0 ± 1.5	L7/L5.5	···	[16.57 ± 0.05]	15.41 ± 0.02	14.52 ± 0.04	13.88 ± 0.05	101; 77; 101,37; –; 1,9,69
2MASSI J1534498−295227	15.9 ± 0.3	63.0 ± 1.1	T6/T5.5	B	[15.68 ± 0.06]	14.60 ± 0.03	14.74 ± 0.03	14.91 ± 0.03	21; 65; 22,29; 23; 1,108
SDSS J153453.33+121949.2	20.0 ± 0.7	49.9 ± 1.7	.../L4:	···	[16.56 ± 0.06]	15.30 ± 0.02	[14.38 ± 0.04]	[13.80 ± 0.04]	44; 77; 44; –; 1,9
DENIS-P J153941.96−052042.4	17.00 ± 0.12	58.8 ± 0.4	L4:/L2	···	[15.11 ± 0.06]	13.84 ± 0.03	13.08 ± 0.03	12.54 ± 0.03	98; 77; 103,98; –; 1,69
SDSS J154009.36+374230.3	24.5 ± 2.8	40.8 ± 4.7	.../L9:	···	[17.44 ± 0.06]	16.35 ± 0.02	[15.40 ± 0.05]	[14.63 ± 0.05]	44; 9; 44; –; 1,9
WISE J154459.27+584204.5	20.4 ± 0.8	49.1 ± 1.9	.../T7.5	···	···	18.09 ± 0.02	[[18.39 ± 0.29]]	···	135; 9; 135; –; 1,9,135
2MASS J15461461+4932114	21.5 ± 2.5	46.5 ± 5.4	.../T2.5:	···	[16.78 ± 0.05]	15.64 ± 0.02	15.35 ± 0.12	[15.08 ± 0.05]	146; 9; 146; –; 1,9,151
2MASSW J1552591+294849	20.41 ± 0.08	49.0 ± 0.2	L0 β/L0: INT-G	Y	[14.55 ± 0.06]	[13.41 ± 0.03]	[12.66 ± 0.03]	[11.98 ± 0.03]	193; 77; 48,3; 48,3; 1
2MASSI J1553022+153236	13.3 ± 0.2	75.1 ± 0.9	.../T7	B	16.37 ± 0.06	15.34 ± 0.03	15.76 ± 0.03	15.94 ± 0.03	21; 64; 29; 30; 108
2MASSW J1555157−095605	13.58 ± 0.04	73.7 ± 0.2	L1/L1.6	···	[13.55 ± 0.05]	[12.50 ± 0.02]	[12.06 ± 0.02]	[11.42 ± 0.02]	83; 77; 83,5; –; 1
2MASS J16150413+1340079	17.1 ± 0.7	58.4 ± 2.5	.../T6	···	[17.35 ± 0.10]	16.32 ± 0.09	[16.73 ± 0.10]	[16.70 ± 0.10]	129; 107; 129; –; 1,69
2MASSW J1615441+355900	19.98 ± 0.15	50.1 ± 0.4	L3/L3.6	···	[15.73 ± 0.05]	14.43 ± 0.02	[13.60 ± 0.03]	[12.91 ± 0.03]	101; 77; 101,5; –; 1,9
WISEPA J161705.75+180714.3	12.8 ± 0.5	78.0 ± 3.1	T8/T8	···	···	17.57 ± 0.02	18.23 ± 0.08	···	105; 9; 105,105; –; 9,105
WISEPA J162208.94−095934.6	24.9 ± 2.2	40.2 ± 3.5	.../T6	B	[17.28 ± 0.05]	16.194 ± 0.011	[16.46 ± 0.05]	[16.51 ± 0.05]	105; 107; 105; 67; 1,145
SDSSp J162414.37+002915.6	10.89 ± 0.14	91.8 ± 1.2	T6/T6	···	16.28 ± 0.05	15.20 ± 0.05	15.48 ± 0.05	15.61 ± 0.05	183; 187,107; 153,29; –; 183
PSO J246.1033−19.6194	23.0 ± 1.6	43.5 ± 3.0	.../T2	···	···	16.35 ± 0.02	15.87 ± 0.02	15.82 ± 0.02	125; 9; 125; –; 9,111
WISEPA J162725.64+325525.5	18.4 ± 0.6	54.4 ± 1.9	.../T6	···	[17.33 ± 0.05]	16.23 ± 0.02	[16.56 ± 0.05]	[16.87 ± 0.05]	105; 107; 105; –; 1,9
SDSS J162838.77+230821.1	13.3 ± 0.2	75.1 ± 0.9	.../T7	···	17.27 ± 0.03	16.25 ± 0.03	16.63 ± 0.03	16.72 ± 0.03	44; 64; 44; –; 44
PSO J247.3273+03.5932	13.1 ± 0.6	76.5 ± 3.5	T3/T2	···	16.19 ± 0.02	15.100 ± 0.010	14.530 ± 0.010	14.28 ± 0.02	55; 9; 153,55; –; 55

Table 1 continued

Table 1 *(continued)*

Object	Distance	Parallax	Spectral Type[a]	Flag[b]	Y_{MKO}	J_{MKO}	H_{MKO}	K_{MKO}	References
	(pc)	(mas)	(Optical/NIR)		(mag)	(mag)	(mag)	(mag)	(Disc; ϖ; SpT; Flag; Phot)
SDSS J163022.92+081822.0	22.2 ± 2.3	45.1 ± 4.7	.../T5.5	···	···	16.16 ± 0.02	16.35 ± 0.03	16.41 ± 0.03	44; 9; 44; –; 44
SDSS J163030.53+434404.0	22.4 ± 1.3	44.7 ± 2.6	.../L7:	···	[17.66 ± 0.05]	16.53 ± 0.02	[15.56 ± 0.05]	[14.77 ± 0.05]	108; 9; 108; –; 1,9
2MASSW J1632291+190441	15.1 ± 0.4	66.3 ± 1.6	L8/L8	···	16.86 ± 0.05	15.77 ± 0.05	14.68 ± 0.05	13.97 ± 0.05	100; 53; 100,29; –; 113
2MASSW J1645221−131951	11.26 ± 0.02	88.82 ± 0.14	L1.5/...	···	[13.47 ± 0.06]	12.37 ± 0.03	11.71 ± 0.03	11.11 ± 0.03	83; 77; 83; –; 1,69
WISEPA J164715.59+563208.2	23.4 ± 1.1	42.7 ± 2.1	L7/L9pec	···	[17.71 ± 0.05]	16.49 ± 0.02	[15.41 ± 0.05]	[14.48 ± 0.05]	105; 9; 153,105; –; 1,9
WISEPA J165311.05+444423.9	13.2 ± 0.3	75.7 ± 1.9	T8/T8	···	[18.11 ± 0.06]	17.08 ± 0.02	[17.59 ± 0.05]	[17.07 ± 0.06]	105; 9; 105,105; –; 1,9
2MASS J16573454+1054233	23.9 ± 0.2	41.9 ± 0.3	L2/L1.4	B	[15.23 ± 0.05]	14.09 ± 0.02	[13.40 ± 0.03]	[12.78 ± 0.03]	164; 77; 164,5; 12; 1,9
DENIS-P J170548.38−051645.7	18.99 ± 0.13	52.7 ± 0.3	L0.5/L1: FLD-G	···	[14.32 ± 0.06]	[13.24 ± 0.03]	[12.60 ± 0.02]	[12.00 ± 0.02]	98; 77; 164,3; –; 1
2MASS J17065487−1314396	19.4 ± 0.2	51.5 ± 0.5	.../L5.0 FLD-G	···	···	[[14.44 ± 0.04]]	[[13.68 ± 0.03]]	[[13.08 ± 0.03]]	73; 77; 73; –; 1,51
WISE J170745.85−174452.5	12.6 ± 0.5	79.2 ± 3.2	.../T5:	···	···	16.35 ± 0.02	17.11 ± 0.03	···	135; 9; 135; –; 135
WISEPA J171104.60+350036.8	24.8 ± 1.5	40.3 ± 2.4	.../T8	B	[18.55 ± 0.14]	[17.63 ± 0.13]	[18.06 ± 0.14]	[18.09 ± 0.14]	105; 107; 105; 122; 1
2MASS J17114559+4028578	21.1 ± 0.3	47.4 ± 0.6	.../L5.0	C	[16.17 ± 0.05]	14.96 ± 0.02	[14.38 ± 0.05]	[13.78 ± 0.05]	158; 77; 5; 158; 1,9
2MASSI J1721039+334415	16.31 ± 0.06	61.3 ± 0.2	L3/L5:	···	[14.63 ± 0.05]	[13.54 ± 0.02]	[13.03 ± 0.03]	[12.46 ± 0.02]	45; 77; 45,34; –; 1
WISE J172134.46+111739.4	23.8 ± 2.3	42.0 ± 4.0	.../T6	···	[17.45 ± 0.06]	16.42 ± 0.02	[16.69 ± 0.06]	[16.50 ± 0.06]	135; 107; 135; –; 1,9
VVV BD001	18.52 ± 0.12	54.0 ± 0.4	.../L5: blue	···	14.290 ± 0.012	13.200 ± 0.010	12.670 ± 0.010	[[12.21 ± 0.03]]	6; 77; 6; –; 1,182,51
2MASS J17312974+2721233	11.94 ± 0.02	83.74 ± 0.12	L0/L0: FLD-G	···	[13.06 ± 0.06]	[12.05 ± 0.03]	[11.45 ± 0.02]	[10.89 ± 0.02]	164; 77; 164,3; –; 1
DENIS-P J1733423−165449	18.09 ± 0.02	55.27 ± 0.07	L0.5:/L0.9	···	[14.59 ± 0.07]	[13.48 ± 0.05]	[12.87 ± 0.03]	[12.33 ± 0.03]	152; 166; 152,5; –; 1
2MASS J17392515+2454421	24.0 ± 0.5	41.7 ± 0.9	.../L4	···	[16.92 ± 0.09]	[15.73 ± 0.07]	[14.73 ± 0.05]	[13.93 ± 0.05]	104; 77; 104; –; 1
WISE J174303.71+421150.0	18.3 ± 1.4	54.8 ± 4.2	.../T4.5	···	[16.82 ± 0.05]	15.62 ± 0.02	[15.64 ± 0.05]	[15.66 ± 0.06]	135; 9; 135; –; 1,9
DENIS-P J1745346−164053	19.66 ± 0.04	50.87 ± 0.10	L1.5:/L1.3	···	[14.63 ± 0.06]	[13.59 ± 0.03]	[12.95 ± 0.02]	[12.38 ± 0.02]	152; 166; 152,5; –; 1
2MASS J17461199+5034036	20.7 ± 0.2	48.3 ± 0.6	L5/L5.7	···	[16.23 ± 0.05]	14.95 ± 0.02	[14.12 ± 0.04]	[13.51 ± 0.04]	164; 77; 164,5; –; 1,9
2MASS J17502484−0016151	9.24 ± 0.02	108.3 ± 0.3	L5/L5.5	···	[14.40 ± 0.05]	13.21 ± 0.02	12.44 ± 0.02	11.81 ± 0.02	99; 77; 153,99; –; 1,69
SDSSp J175032.96+175903.9	22.5 ± 1.5	44.5 ± 3.0	T4/T3.5	···	17.19 ± 0.05	16.16 ± 0.02	15.94 ± 0.05	16.02 ± 0.05	79; 9; 153,29; –; 113,9
2MASS J17545447+1649196	15.6 ± 0.8	64.3 ± 3.4	T5/T5.5	···	[16.53 ± 0.05]	15.49 ± 0.02	15.64 ± 0.13	[15.61 ± 0.05]	69,33; 9; 153,69; –; 1,9,69
WISE J175510.28+180320.2	19.4 ± 1.8	51.5 ± 4.8	.../T2.5	···	[16.87 ± 0.05]	15.82 ± 0.02	15.32 ± 0.02	15.24 ± 0.02	135; 9; 11; –; 1,11
SDSS J175805.46+463311.9	13.990 ± 0.008	71.48 ± 0.04	.../T6.5	C	16.91 ± 0.06	15.86 ± 0.03	16.20 ± 0.03	16.12 ± 0.03	108; 77; 29; 68; 64,108
2MASS J18000116−1559235	12.36 ± 0.05	80.9 ± 0.3	.../L4.3	···	[14.67 ± 0.05]	13.34 ± 0.02	[12.60 ± 0.03]	[11.96 ± 0.03]	72,5; 77; 5; –; 1,9
WISEP J180026.60+013453.1	7.85 ± 0.04	127.4 ± 0.7	L7.5/L7.5	···	[15.30 ± 0.05]	14.17 ± 0.02	[13.20 ± 0.03]	[12.41 ± 0.03]	86; 77; 88,86; –; 1,9
2MASSI J1807159+501531	14.63 ± 0.03	68.33 ± 0.13	L1.5/L1	···	[14.02 ± 0.06]	[12.88 ± 0.02]	[12.20 ± 0.03]	[11.58 ± 0.03]	45; 77; 45,193; –; 1
PSO J272.0887−04.9943	23.4 ± 1.1	42.8 ± 2.0	.../T1.5pec	···	[17.99 ± 0.05]	16.98 ± 0.02	16.27 ± 0.04	[15.82 ± 0.05]	11; 9; 11; –; 1,9,11
WISE J180901.07+383805.4	19.1 ± 0.8	52.4 ± 2.3	.../T7.5	···	[18.23 ± 0.06]	17.39 ± 0.02	[17.70 ± 0.06]	[17.32 ± 0.06]	133; 9; 135; –; 1,9
WISE J180952.53−044812.5	20.3 ± 1.4	49.3 ± 3.4	.../T1	B	[16.21 ± 0.05]	15.147 ± 0.007	[14.44 ± 0.05]	13.977 ± 0.006	135; 9; 10; 59; 1,10
WISE J181329.40+283533.3	13.6 ± 0.4	73.6 ± 2.0	.../T8	···	[17.86 ± 0.05]	16.91 ± 0.02	[17.11 ± 0.05]	[16.93 ± 0.06]	135; 9; 135; –; 1,9
2MASS J18212815+1414010	9.38 ± 0.02	106.7 ± 0.2	L4.5pec/L5: FLD-G	···	[14.63 ± 0.06]	[13.33 ± 0.02]	[12.46 ± 0.02]	[11.62 ± 0.02]	130; 167; 130,124; –; 1
WISE J185101.83+593508.6	20.5 ± 0.3	48.8 ± 0.6	.../L9	···	[16.04 ± 0.05]	14.846 ± 0.013	14.03 ± 0.02	[13.45 ± 0.05]	185; 77; 11; –; 1,10
WISEPA J185215.78+353716.3	13.9 ± 0.4	72.0 ± 1.9	.../T7	···	[17.41 ± 0.05]	16.32 ± 0.02	[16.73 ± 0.05]	[16.51 ± 0.05]	105; 107; 105; –; 1,9
2MASS J19010601+4718136	18.3 ± 1.4	54.5 ± 4.3	.../T5	···	[16.58 ± 0.05]	15.53 ± 0.02	[15.66 ± 0.05]	[15.72 ± 0.05]	26; 9; 29; –; 1,9
WISEPA J190624.75+450808.2	15.6 ± 0.4	64.1 ± 1.6	.../T6	···	17.03 ± 0.05	15.98 ± 0.02	16.37 ± 0.08	[16.40 ± 0.05]	105; 107; 105; –; 125,9,1
WISEP J190648.47+401106.8	16.79 ± 0.04	59.57 ± 0.14	L1/L1	···	[14.13 ± 0.05]	[13.04 ± 0.02]	[12.33 ± 0.02]	[11.75 ± 0.02]	85; 77; 87,85; –; 1

Table 1 continued

Table 1 *(continued)*

Object	Distance	Parallax	Spectral Type[a]	Flag[b]	Y_{MKO}	J_{MKO}	H_{MKO}	K_{MKO}	References
	(pc)	(mas)	(Optical/NIR)		(mag)	(mag)	(mag)	(mag)	(Disc; ϖ; SpT; Flag; Phot)
DENIS-P J1909081−193748	22.1 ± 0.3	45.2 ± 0.5	L1:/...	···	···	14.46 ± 0.02	[[13.59 ± 0.03]]	[[12.90 ± 0.03]]	152; 77; 152; –; 1,9,51
WISE J191915.54+304558.4	21.6 ± 1.9	46.3 ± 4.1	.../L9	···	[16.68 ± 0.05]	15.52 ± 0.02	14.557 ± 0.014	[13.96 ± 0.05]	185; 9; 11; –; 1,11
WISE J192841.35+235604.9	6.67 ± 0.11	149.9 ± 2.4	.../T6	···	[15.09 ± 0.05]	13.98 ± 0.02	[14.24 ± 0.05]	[14.18 ± 0.05]	135; 107; 135; –; 1,9
WISE J200050.19+362950.1	7.51 ± 0.14	133.1 ± 2.5	.../T8	···	[16.31 ± 0.05]	15.440 ± 0.010	15.850 ± 0.010	16.13 ± 0.04	50; 107; 50; –; 1,50,131
2MASS J20025073−0521524	17.6 ± 0.5	56.7 ± 1.5	L5 β/L7	Y	[16.52 ± 0.05]	15.22 ± 0.02	[14.38 ± 0.04]	[13.39 ± 0.04]	47; 77; 70,140; 70,73; 1,9
HR 7672B	17.72 ± 0.02	56.43 ± 0.07	.../L4.5:	C	···	···	[[14.10 ± 0.14]]	[[13.02 ± 0.10]]	118; 77; 118; 118; 1,14
WISE J200520.38+542433.9	16.559 ± 0.008	60.39 ± 0.03	.../sdT8	CS	···	19.64 ± 0.09	19.57 ± 0.08	···	136; 77; 136; 136,136; 136
WISE J200804.71−083428.5	18.4 ± 1.3	54.2 ± 3.8	.../T5.5	···	[17.16 ± 0.05]	16.03 ± 0.02	[16.31 ± 0.05]	[16.36 ± 0.05]	135; 9; 135; –; 1,9
WISE J201404.13+042408.5	22.0 ± 1.2	45.5 ± 2.4	.../T6.5pec	···	···	18.01 ± 0.02	[[18.71 ± 0.30]]	[[17.97 ± 0.29]]	135; 9; 135; –; 1,9,135
WISE J201920.76−114807.5	12.9 ± 0.6	77.5 ± 3.5	.../T8:	···	···	18.09 ± 0.06	18.23 ± 0.07	···	135; 107; 135; –; 135
WISE J203042.79+074934.7	9.62 ± 0.09	104.0 ± 1.0	.../T1.5	···	15.220 ± 0.012	14.046 ± 0.011	[13.51 ± 0.04]	[13.36 ± 0.04]	135; 77; 135; –; 9,10,1
2MASS J20360316+1051295	23.6 ± 0.2	42.4 ± 0.4	L3/L3.5	B	[15.12 ± 0.06]	[13.89 ± 0.03]	[13.09 ± 0.03]	[12.42 ± 0.03]	164; 77; 164,37; 67; 1
2MASSI J2057540−025230	15.51 ± 0.06	64.5 ± 0.2	L1.5/L2: FLD-G	Y	[14.19 ± 0.05]	[13.05 ± 0.02]	[12.32 ± 0.03]	[11.69 ± 0.03]	45; 77; 45,3; 45,103,179; 1
2MASSI J2104149−103736	17.19 ± 0.12	58.2 ± 0.4	L2.5/L2	···	[14.99 ± 0.06]	[13.78 ± 0.03]	[13.05 ± 0.02]	[12.35 ± 0.02]	45; 77; 103,37; –; 1
PSO J318.5338−22.8603	22.2 ± 0.8	45.1 ± 1.7	.../L7: VL-G	Y	18.81 ± 0.10	17.15 ± 0.04	15.68 ± 0.02	14.41 ± 0.02	123; 124; 123; 123; 123
PSO J319.3102−29.6682	19.1 ± 2.5	52.4 ± 6.8	.../T0:	···	16.59 ± 0.02	15.45 ± 0.02	14.655 ± 0.012	[14.17 ± 0.05]	11; 9; 11; –; 9,11,1
WISE J212321.92−261405.1	24.8 ± 2.9	40.3 ± 4.7	.../T5.5	···	[18.07 ± 0.06]	17.03 ± 0.02	[17.52 ± 0.06]	[17.69 ± 0.07]	135; 9; 135; –; 1,9
SDSS J212413.89+010000.3	17.5 ± 1.0	57.0 ± 3.2	.../T5	···	17.21 ± 0.02	15.829 ± 0.008	16.05 ± 0.02	16.09 ± 0.03	108; 9; 29; –; 111
2MASS J21371044+1450475	23.6 ± 0.2	42.4 ± 0.3	L2/L0.8	···	[15.21 ± 0.05]	14.07 ± 0.02	[13.37 ± 0.03]	[12.80 ± 0.03]	164; 77; 164,5; –; 1,9
2MASS J21373742+0808463	15.1 ± 0.2	66.1 ± 0.9	L5:/L5	···	···	14.64 ± 0.02	[[13.67 ± 0.03]]	[[13.00 ± 0.03]]	164; 77; 164,37; –; 1,9,51
2MASS J21392676+0220226	9.9 ± 0.2	101.5 ± 2.0	T2/T1.5	···	[16.23 ± 0.07]	[15.10 ± 0.05]	[14.27 ± 0.05]	[13.60 ± 0.05]	164,31; 180; 153,29; –; 1
HN Peg B	18.13 ± 0.02	55.16 ± 0.06	.../T2.5	CY	[16.91 ± 0.06]	15.86 ± 0.03	15.40 ± 0.03	15.12 ± 0.03	132; 77; 132; 132,132; 1,132
WISE J214706.78−102924.0	22.5 ± 1.9	44.4 ± 3.8	.../T7.5	···	···	17.37 ± 0.02	17.73 ± 0.09	···	135; 9; 135; –; 9,107
2MASS J21481628+4003593	8.11 ± 0.03	123.3 ± 0.5	L6/L6 FLD-G	···	[15.52 ± 0.06]	[14.04 ± 0.03]	[12.86 ± 0.02]	[11.72 ± 0.02]	130; 77; 130,123; –; 1
2MASS J21522609+0937575	24.4 ± 4.1	40.9 ± 6.9	L6:/...	B	···	15.09 ± 0.02	[[14.13 ± 0.03]]	[[13.32 ± 0.03]]	163; 9; 164; 163; 1,9,51
2MASS J21543318+5942187	15.5 ± 0.4	64.7 ± 1.5	.../T5	···	[16.54 ± 0.09]	[15.44 ± 0.07]	[15.70 ± 0.09]	[15.70 ± 0.09]	129; 67; 129; –; 1
WISEPC J215751.38+265931.4	16.8 ± 0.6	59.7 ± 2.2	.../T7	···	[18.00 ± 0.05]	17.04 ± 0.02	[17.49 ± 0.04]	[17.35 ± 0.06]	105; 107; 105; –; 1,9
2MASS J21580457−1550098	21.7 ± 2.6	46.1 ± 5.6	L4:/L5	···	[16.13 ± 0.05]	14.84 ± 0.02	[13.95 ± 0.04]	[13.16 ± 0.04]	103; 9; 103,140; –; 1,9
WISEA J220304.18+461923.4	15.2 ± 1.0	66.0 ± 4.2	.../T8	···	···	18.57 ± 0.02	···	···	144; 107; 144; –; 144
2MASS J22092183−2711329	24.6 ± 2.3	40.7 ± 3.9	.../T2.5	B	···	15.53 ± 0.02	[[15.20 ± 0.15]]	[[15.11 ± 0.15]]	140; 9; 140; 67; 1,9,51
WISEPC J220922.10−273439.5	13.8 ± 0.7	72.3 ± 3.8	.../T7	···	[17.53 ± 0.05]	16.55 ± 0.02	[16.91 ± 0.05]	[17.31 ± 0.06]	105; 9; 105; –; 1,9
WISEPC J221354.69+091139.4	18.3 ± 0.8	54.5 ± 2.5	.../T7	···	[17.81 ± 0.05]	16.76 ± 0.02	[17.11 ± 0.05]	[17.12 ± 0.06]	105; 107; 105; –; 1,9
2MASS J22153705+2110554	17.9 ± 1.4	55.9 ± 4.4	.../T1pec	···	···	15.90 ± 0.02	[[15.51 ± 0.06]]	[[15.17 ± 0.06]]	96; 9; 96; –; 1,9,96
2MASSW J2224438−015852	11.43 ± 0.07	87.5 ± 0.5	L4.5/L3: FLD-G	B	15.32 ± 0.06	13.89 ± 0.03	12.84 ± 0.03	11.98 ± 0.03	101; 53; 101,124; 67; 64,108
WISEPC J222623.05+044003.9	18.4 ± 2.0	54.4 ± 5.9	.../T8	···	18.04 ± 0.03	16.90 ± 0.02	17.45 ± 0.07	17.24 ± 0.09	105; 107; 105; –; 111
WISE J223617.59+510551.9	9.7 ± 0.2	102.8 ± 1.9	.../T5	···	15.655 ± 0.014	14.457 ± 0.011	14.61 ± 0.02	[14.57 ± 0.05]	135; 9; 10; –; 9,10,1
2MASSI J2238074+435317	22.70 ± 0.13	44.1 ± 0.2	L1.5/L0.6	B	[14.64 ± 0.06]	[13.81 ± 0.03]	[13.12 ± 0.03]	[12.53 ± 0.03]	45; 77; 45,5; 8; 1
WISEPC J223937.55+161716.2	23.3 ± 1.6	42.9 ± 3.0	.../T3	B	[17.00 ± 0.05]	15.96 ± 0.02	[15.57 ± 0.05]	[15.37 ± 0.05]	105; 9; 105; 67; 1,9
2MASS J22425317+2542573	21.3 ± 0.3	47.0 ± 0.7	L3/...	···	[16.03 ± 0.06]	[14.76 ± 0.04]	[13.82 ± 0.03]	[13.03 ± 0.03]	84; 77; 47; –; 1

Table 1 continued

Table 1 *(continued)*

Object	Distance	Parallax	Spectral Type[a]	Flag[b]	Y_{MKO}	J_{MKO}	H_{MKO}	K_{MKO}	References
	(pc)	(mas)	(Optical/NIR)		(mag)	(mag)	(mag)	(mag)	(Disc; ϖ; SpT; Flag; Phot)
2MASSW J2244316+204343	17.0 ± 0.3	58.7 ± 0.9	L6.5/L6: VL-G	Y	17.53 ± 0.05	16.33 ± 0.03	15.06 ± 0.03	13.90 ± 0.03	52; 124; 103,3; 3; 64,108
2MASS J22490917+3205489	20.1 ± 1.3	49.7 ± 3.2	L5/...	···	···	15.54 ± 0.02	[[14.41 ± 0.05]]	[[13.57 ± 0.05]]	47; 9; 47; –; 1,9,51
DENIS-P J225210.73−173013.4	16.9 ± 0.2	59.2 ± 0.8	.../L7.5	B	15.26 ± 0.03	14.20 ± 0.03	13.41 ± 0.03	12.90 ± 0.02	98; 77; 98; 162; 64
2MASSI J2254188+312349	13.9 ± 0.6	72.0 ± 3.0	T5/T4	···	[16.54 ± 0.07]	15.32 ± 0.05	15.06 ± 0.08	14.99 ± 0.15	21; 138; 153,29; –; 1,138
WISE J230133.32+021635.0	18.9 ± 1.0	53.0 ± 2.8	.../T6.5	···	17.62 ± 0.02	16.358 ± 0.010	16.70 ± 0.03	16.87 ± 0.05	135; 107; 135; –; 111
WISEA J230329.45+315022.7	21.5 ± 1.5	46.5 ± 3.3	.../T2 (blue)	···	···	15.92 ± 0.02	[[15.53 ± 0.16]]	[[15.52 ± 0.16]]	172; 9; 172; –; 1,9,51
2MASS J23185497−1301106	15.0 ± 0.7	66.5 ± 3.2	.../T5	···	···	15.30 ± 0.02	[[15.30 ± 0.13]]	[[15.13 ± 0.13]]	140; 9; 140; –; 1,9,51
WISEPC J231939.13−184404.3	12.6 ± 0.5	79.2 ± 3.1	.../T7.5	···	[18.56 ± 0.06]	17.56 ± 0.02	17.95 ± 0.05	[18.27 ± 0.08]	105; 107; 105; –; 1,105
ULAS J232035.28+144829.8	21.3 ± 1.8	47.0 ± 4.0	.../T5	···	18.14 ± 0.02	16.79 ± 0.02	17.14 ± 0.02	17.40 ± 0.02	174; 138; 39; –; 39
ULAS J232123.79+135454.9	12.0 ± 0.3	83.6 ± 2.4	.../T7.5	···	17.92 ± 0.03	16.72 ± 0.03	17.15 ± 0.03	17.160 ± 0.010	174; 107; 39; –; 39
2MASS J23254530+4251488	14.8 ± 0.5	67.6 ± 2.1	L8/L7.5:	···	[16.58 ± 0.05]	15.42 ± 0.02	[14.53 ± 0.05]	[13.76 ± 0.05]	47; 77; 47,37; –; 1,9
ULAS J232600.40+020139.2	20.2 ± 1.9	49.5 ± 4.6	.../T8	···	19.40 ± 0.08	17.98 ± 0.04	18.46 ± 0.12	18.41 ± 0.20	41; 107; 41; –; 111
WISEPC J232728.75−273056.5	18.0 ± 2.0	55.6 ± 6.1	.../L9	···	[17.58 ± 0.05]	16.47 ± 0.02	[15.55 ± 0.05]	[14.87 ± 0.05]	105; 9; 105; –; 1,9
WISE J233527.07+451140.9	22.7 ± 0.7	44.0 ± 1.4	.../L7pec	···	[18.02 ± 0.06]	16.83 ± 0.03	15.63 ± 0.02	14.65 ± 0.06	185; 124; 124; –; 1,11
2MASSI J2339101+135230	16.0 ± 1.1	62.7 ± 4.4	.../T5	···	16.955 ± 0.014	15.846 ± 0.010	16.06 ± 0.02	16.20 ± 0.04	21; 9; 29; –; 111
WISEPC J234026.62−074507.2	20.9 ± 1.4	47.8 ± 3.1	T7/T7	···	[17.20 ± 0.06]	16.08 ± 0.03	16.41 ± 0.04	[16.51 ± 0.06]	105; 107; 105,105; –; 1,125
WISEPC J234841.10−102844.4	17.1 ± 1.0	58.4 ± 3.5	.../T7	···	[17.69 ± 0.05]	16.62 ± 0.02	[16.99 ± 0.05]	[16.84 ± 0.06]	105; 107; 105; –; 1,9
2MASS J23512200+3010540	24.3 ± 0.8	41.2 ± 1.4	L5.5/L5: FLD-G	···	[17.05 ± 0.11]	[15.76 ± 0.10]	[14.64 ± 0.06]	[13.99 ± 0.06]	104; 124; 104,124; –; 1
2MASSI J2356547−155310	14.5 ± 0.7	69.0 ± 3.4	.../T5.5	···	16.64 ± 0.06	15.48 ± 0.03	15.70 ± 0.03	15.73 ± 0.03	21; 191; 29; –; 64,108
WISE J235716.49+122741.8	16.8 ± 1.2	59.5 ± 4.1	.../T6	···	17.34 ± 0.02	16.100 ± 0.010	16.49 ± 0.03	16.52 ± 0.04	135; 107; 135; –; 111

Table 1 continued

Table 1 *(continued)*

Object	Distance	Parallax	Spectral Type[a]	Flag[b]	Y_{MKO}	J_{MKO}	H_{MKO}	K_{MKO}	References
	(pc)	(mas)	(Optical/NIR)		(mag)	(mag)	(mag)	(mag)	(Disc; ϖ; SpT; Flag; Phot)

NOTE—This table lists all spectroscopically confirmed L0–T8 dwarfs having declinations between $-30°$ and $+60°$ and parallax-determined distances less than 25 pc. Y_{MKO}, J_{MKO}, H_{MKO}, and K_{MKO} photometry enclosed in single brackets indicates synthetic photometry (Section 2.5); double brackets indicates photometry converted from 2MASS into the MKO system using $M_{Ks,2MASS}$ and the polynomials of Dupuy & Liu (2017).

[a] β, γ, and δ indicate classes of increasingly low gravity based on optical (Kirkpatrick 2005; Cruz et al. 2009) or near-infrared (Gagné et al. 2015b; Cruz et al. 2018) spectra. FLD-G indicates near-infrared spectral signatures of field-age gravity, INT-G indicates intermediate gravity, and VL-G indicates very low gravity (Allers & Liu 2013).

[b] B = binary (presented here as a single unresolved source); C = companion (resolved) to another star or brown dwarf; Y = young ($\lesssim$200 Myr); S = subdwarf.

References—(1) This work, (2) Albert et al. (2011), (3) Allers & Liu (2013), (4) Artigau et al. (2006), (5) Bardalez Gagliuffi et al. (2014), (6) Beamín et al. (2013), (7) Beichman et al. (2014), (8) Bernat et al. (2010), (9) Best20, (10) Best et al. (2013), (11) Best et al. (2015), (12) W. Best et al. (in prep), (13) Bihain et al. (2013), (14) Boccaletti et al. (2003), (15) Bouy et al. (2003), (16) Bouy et al. (2005), (17) Bowler et al. (2010a), (18) Burgasser et al. (1999), (19) Burgasser et al. (2000a), (20) Burgasser et al. (2000b), (21) Burgasser et al. (2002), (22) Burgasser et al. (2003a), (23) Burgasser et al. (2003c), (24) Burgasser et al. (2003b), (25) Burgasser et al. (2003d), (26) Burgasser et al. (2004), (27) Burgasser et al. (2005b), (28) Burgasser et al. (2005a), (29) Burgasser et al. (2006a), (30) Burgasser et al. (2006b), (31) Burgasser & McElwain (2006), (32) Burgasser (2007b), (33) Burgasser et al. (2008a), (34) Burgasser et al. (2008b), (35) Burgasser et al. (2008c), (36) Burgasser et al. (2010b), (37) Burgasser et al. (2010a), (38) Burgasser et al. (2011), (39) Burningham et al. (2010a), (40) Burningham et al. (2010b), (41) Burningham et al. (2013), (42) Castro & Gizis (2012), (43) Castro et al. (2013), (44) Chiu et al. (2006), (45) Cruz et al. (2003), (46) Cruz et al. (2004), (47) Cruz et al. (2007), (48) Cruz et al. (2009), (49) Cushing et al. (2011), (50) Cushing et al. (2014), (51) Cutri et al. (2003), (52) Dahn et al. (2002), (53) Dahn et al. (2017), (54) Deacon et al. (2005), (55) Deacon et al. (2011), (56) Deacon et al. (2012a), (57) Deacon et al. (2012b), (58) Deacon et al. (2014), (59) Deacon et al. (2017b), (60) Deacon et al. (2017a), (61) Delfosse et al. (1997), (62) Delfosse et al. (1999), (63) Dupuy et al. (2009b), (64) Dupuy & Liu (2012), (65) Dupuy & Liu (2017), (66) Dupuy et al. (2020), (67) T. Dupuy (private communication), (68) Faherty et al. (2010), (69) Faherty et al. (2012), (70) Faherty et al. (2016), (71) Fan et al. (2000), (72) Folkes et al. (2012), (73) Gagné et al. (2015b), (74) Gagné et al. (2015a), (75) Gagné et al. (2017), (76) Gagné & Faherty (2018), (77) Gaia Collaboration et al. (2018), (78) Gauza et al. (2015), (79) Geballe et al. (2002), (80) Gelino et al. (2014), (81) Gizis et al. (2000b), (82) Gizis et al. (2001), (83) Gizis (2002), (84) Gizis et al. (2003), (85) Gizis et al. (2011b), (86) Gizis et al. (2011a), (87) Gizis et al. (2013), (88) Gizis et al. (2015b), (89) Goldman et al. (2010), (90) Gomes et al. (2013), (91) Goto et al. (2002), (92) Hall (2002a), (93) Hall (2002b), (94) Harris et al. (2015), (95) Hawley et al. (2002), (96) Kellogg et al. (2015), (97) Kellogg et al. (2017), (98) Kendall et al. (2004), (99) Kendall et al. (2007), (100) Kirkpatrick et al. (1999), (101) Kirkpatrick et al. (2000), (102) Kirkpatrick et al. (2001), (103) Kirkpatrick et al. (2008), (104) Kirkpatrick et al. (2010), (105) Kirkpatrick et al. (2011), (106) Kirkpatrick et al. (2014), (107) Kirkpatrick et al. (2019), (108) Knapp et al. (2004), (109) Koerner et al. (1999), (110) Lawrence et al. (2007), (111) Lawrence et al. (2012), (112) Leggett et al. (2000), (113) Leggett et al. (2002b), (114) Leggett et al. (2002a), (115) Leggett et al. (2009), (116) Leggett et al. (2010), (117) Liebert et al. (2003), (118) Liu et al. (2002), (119) Liu & Leggett (2005), (120) Liu et al. (2010), (121) Liu et al. (2011), (122) Liu et al. (2012), (123) Liu et al. (2013), (124) Liu et al. (2016), (125) M. Liu et al. (in prep), (126) Lodieu et al. (2005), (127) Lodieu et al. (2007), (128) Lodieu et al. (2012), (129) Looper et al. (2007b), (130) Looper et al. (2008b), (131) Lucas et al. (2012), (132) Luhman et al. (2007), (133) Luhman et al. (2012), (134) Luhman & Sheppard (2014), (135) Mace et al. (2013a), (136) Mace et al. (2013b), (137) Mamajek et al. (2018), (138) Manjavacas et al. (2013), (139) Marocco et al. (2010), (140) Marocco et al. (2013), (141) Marocco et al. (2015), (142) Martín et al. (1999a), (143) Martín et al. (2010), (144) Martin et al. (2018), (145) McMahon et al. (2013), (146) Metchev et al. (2008), (147) Mugrauer et al. (2006), (148) Murray et al. (2011), (149) Muzic et al. (2012), (150) Nakajima et al. (1995), (151) Peña Ramírez et al. (2015), (152) Phan-Bao et al. (2008), (153) Pineda et al. (2016), (154) Pinfield et al. (2008), (155) Pinfield et al. (2012), (156) Pope et al. (2013), (157) Potter et al. (2002), (158) Radigan et al. (2008), (159) Rebolo et al. (1998), (160) Reid et al. (2000), (161) Reid et al. (2001), (162) Reid et al. (2006b), (163) Reid et al. (2006a), (164) Reid et al. (2008b), (165) Ruiz et al. (1997), (166) Sahlmann et al. (2014), (167) Sahlmann et al. (2016), (168) Salim et al. (2003), (169) Schilbach et al. (2009), (170) Schmidt et al. (2010a), (171) Schmidt et al. (2010b), (172) Schneider et al. (2016a), (173) Scholz & Meusinger (2002), (174) Scholz (2010a), (175) Scholz (2010b), (176) Scholz et al. (2011), (177) Scholz et al. (2012), (178) Scholz et al. (2014), (179) Seifahrt et al. (2010), (180) Smart et al. (2013), (181) Smart et al. (2018), (182) Smith et al. (2018), (183) Strauss et al. (1999), (184) Stumpf et al. (2009), (185) Thompson et al. (2013), (186) Thorstensen & Kirkpatrick (2003), (187) Tinney et al. (2003), (188) Tinney et al. (2005), (189) Tinney et al. (2018), (190) Tsvetanov et al. (2000), (191) Vrba et al. (2004), (192) Wilson et al. (2001), (193) Wilson et al. (2003), (194) Zhang et al. (2017), (195) van Leeuwen (2007).

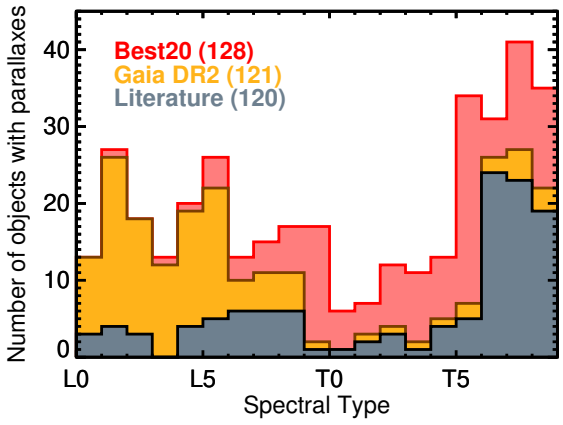

Figure 1. Distribution of spectral types for our volume-limited sample, indicating the sources of the parallaxes for sample members: Best20 (red), Gaia DR2 (orange), and other literature sources (gray). For objects with more than one parallax, we use the most precise measurement. (Most of the T dwarf parallaxes from Gaia DR2 are actually parallaxes for main-sequence stars with T dwarf companions.) The relative scarcity of L/T transition objects (especially types T0–T4) reflects the shorter timescale for this phase of brown dwarf cooling.

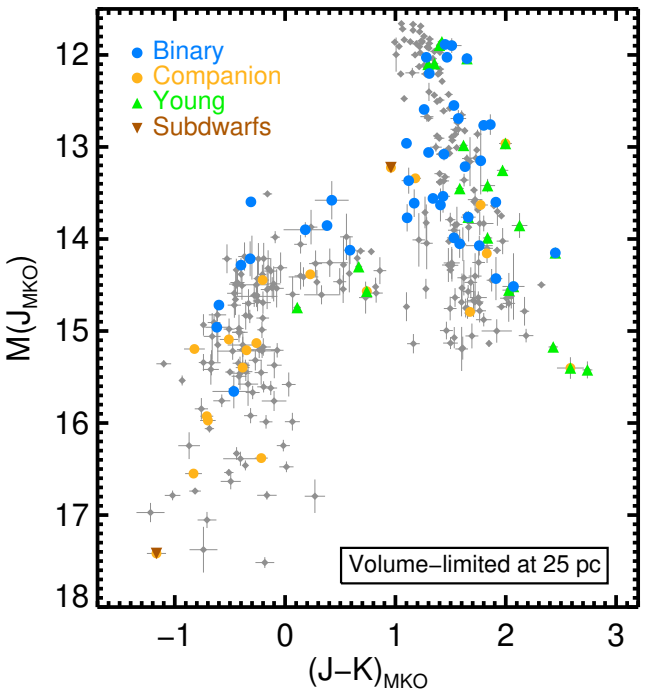

Figure 2. M_J vs. $J-K$ (Maunakea Observatories system) color-magnitude diagram (CMD) for our volume-limited sample of L0–T8 dwarfs, highlighting binaries (blue circles), companions (orange circles), young objects ($\lesssim$200 Myr; green triangles), and subdwarfs (brown triangles), with other members plotted as gray diamonds. As previously noted (e.g., Liu et al. 2013, 2016; Faherty et al. 2016), young L dwarfs ($J-K>1$ mag) typically have redder colors than field-age L dwarfs. Binaries (shown here with integrated-light photometry) tend to sit higher on the CMD than single brown dwarfs, as expected for intrinsically brighter objects. The companions are not distinguishable from single objects in this CMD. The gap in the L/T transition at $(J-K, M_J) \approx (1, 14.5)$ mag has not been identified previously and is discussed in Sections 3 and 4.

Figure 2 shows our volume-limited sample in an NIR color-magnitude diagram (CMD), highlighting the young ($\lesssim$200 Myr) objects and binary systems (Sections 2.6 and 2.7 respectively). We have removed objects with parallax uncertainties $\geq$20% of the parallax and objects with $(J-K)_{\rm MKO}$ uncertainties $\geq$0.2 mag from the figure. The CMD clearly shows the established evolutionary sequence for brown dwarfs (e.g., Dahn et al. 2002; Knapp et al. 2004; Dupuy & Liu 2012, hereinafter DL12): L dwarfs ($J-K>1$ mag) moving down the right-hand sequence as they cool and their luminosities decline; the L/T transition (types $\approx$L8–T4) where brown dwarfs become $\approx$2 mag bluer in $J-K$, moving right to left on the CMD, while brightening by $\approx$0.5 mag in J band; followed by a drop in NIR absolute magnitudes and widening spread of $J-K$ colors for cooling late-T dwarfs. We note that types $\lesssim$L4 are mostly hydrogen-burning stars (Dupuy & Liu 2017) that will remain at $M_J \lesssim 12.5$ mag throughout their main-sequence liftetimes. Our volume-limited CMD exhibits a clear, previously unidentified gap in the L/T transition at $(J-K)_{\rm MKO} \approx 0.9$–$1.4$ mag which we discuss in detail in Sections 3 and 4.

2.3. *Completeness*

We assessed the completeness of our volume-limited sample using the $V/V_{\rm max}$ statistic (Schmidt 1968). Here V is the volume of space enclosed at the distance to a given object in the sample, and $V_{\rm max}$ is the volume of space enclosed by the outer boundary of the sample. $V/V_{\rm max}$ thus quantifies the position of a given object within the sample with a value between 0 and 1; objects in the inner half of the sample's volume have $V/V_{\rm max} < 0.5$, while objects in the outer half have $V/V_{\rm max} > 0.5$. For a sample with uniform spatial distribution, the expectation value is therefore $\langle V/V_{\rm max}\rangle = 0.5$. Significant differences from $\langle V/V_{\rm max}\rangle = 0.5$ indicate that a sample is not uniformly distributed in its volume. Our 25 pc volume resides near the midplane of the Galaxy and contains no clusters, so uniform spatial distribution is a reasonable assumption for our sample, and thus deviations from $\langle V/V_{\rm max}\rangle = 0.5$ would imply incompleteness.

Because more distant objects in samples are fainter and more difficult to observe, samples centered on the Sun tend to be less complete in their outer portions. Determining $\langle V/V_{\rm max}\rangle$ for a sample over a series of distances can reveal the extent to which a sample becomes incomplete approaching its outer boundary.

Figure 3 shows $\langle V/V_{\rm max}\rangle$ as a function of boundary distance for our volume-limited sample. We estimated uncertainties for our $\langle V/V_{\rm max}\rangle$ calculations using the method described in Appendix A. Our full volume-limited sample has $\langle V/V_{\rm max}\rangle = 0.50 \pm 0.05$ at 16 pc (132 objects), indicating completeness at this distance. $\langle V/V_{\rm max}\rangle$ is within 1σ of 0.5 (implying consistency with completeness) out to 20 pc, and the steady decrease of $\langle V/V_{\rm max}\rangle$ beyond 16 pc implies that the sample is becoming less complete. At 25 pc, $\langle V/V_{\rm max}\rangle = 0.41 \pm 0.03$, indicating $83\% \pm 5\%$ completeness for our full sample.

Figure 3 also breaks our sample into four spectral type bins. The $\langle V/V_{\rm max}\rangle$ trends imply completeness out to ≈22 pc for L dwarfs and the full 25 pc for T0–T4.5 dwarfs, suggesting that our sample is complete at 22 pc through the L/T transition. The sample is complete at ≈16 pc for T5-T8 dwarfs. At the 25 pc limit of our sample, it is $90\% \pm 8\%$ complete for L dwarfs and $69\% \pm 8\%$ for T5–T8 dwarfs. We expected our sample to be less complete for spectral types later than T6 due to the limiting magnitude of the WISE survey (Wright et al. 2010), the primary source of late-T dwarf discoveries in our sample. We present our $\langle V/V_{\rm max}\rangle$ values for our sample and several subsets thereof, including the four spectral type bins shown in Figure 3 as well as individual spectral subtypes, in Table 2.

The fact that the L dwarfs in our sample appear to be complete out to a smaller distance than the T0–T4.5 dwarfs is somewhat surprising, since later-type objects are overall less luminous and should in principle be more difficult to detect. Given that the $\langle V/V_{\rm max}\rangle$ values for the L0–L4 dwarfs (0.46 ± 0.05), L5–L9 dwarfs (0.43 ± 0.05), and T0–T4 dwarfs (0.50 ± 0.07) are all within 1σ of each other out to 25 pc, the greater completeness of the early-Ts could simply be a random statistical feature arising from our smaller spectral type subsamples. However, it could also arise from selection effects that may have impacted our volume-limited sample, which we consider briefly here. The objects in our sample were discovered by multiple searches using different telescopes and methods, but nearly all relied on photometry from large sky surveys, in particular 2MASS (Skrutskie et al. 2006), the Pan-STARRS1 3π Survey (PS1; Chambers et al. 2020), WISE, SDSS (York et al. 2000), and UKIDSS (Lawrence et al. 2007). Searches using PS1 (optical; e.g., Best et al. 2015), 2MASS (NIR; e.g., Kirkpatrick et al. 2000; Reid et al. 2008b), and WISE (mid-infrared (MIR); e.g., Mace et al. 2013a; Thompson et al. 2013) cover the entire area of our volume-limited sample in 12 bands spanning the full spectral energy distribution of L0–T8 dwarfs, and each alone is sensitive enough to detect all of the spectral types in our sample out to 25 pc, except for the more distant T6–T8 dwarfs (detected only by WISE). SDSS (optical; e.g., Chiu et al. 2006; Schmidt et al. 2010b) and UKIDSS (NIR; e.g., Burningham et al. 2013; Marocco et al. 2015) discovered many objects in smaller regions of the sky, with the depth of UKIDSS also contributing to the discovery of numerous late-T dwarfs. While each search used different surveys and criteria, in aggregate they have enabled detection of all late-L and early-T spectral types to well beyond 25 pc. In particular, the targeted search for L6–T4.5 dwarfs by Best et al. (2015), which discovered 24% of the objects with those spectral types in our volume-limited sample, also discovered objects beyond 30 pc. Many of the searches avoided the Galactic plane ($|b| \lesssim 20°$), and many looked only for objects with clear proper motion, so it is possible that the majority of the undiscovered objects are concentrated in the Galactic plane and/or are slow-moving, although there is no reason why these factors would lead to the discovery of T dwarfs at greater distances than L dwarfs. We therefore conclude that if the early-T dwarfs in our volume-limited sample are truly complete to a greater depth than the L dwarfs, it is most likely a statistical fluctuation arising from the smaller sizes (<100 objects) of these spectral type bins.

2.3.1. *Anisotropy*

Our primary tool for analyzing the completeness of our sample, the $V/V_{\rm max}$ statistic, is unable to account for anisotropies over the sky. We consider two possible cases of anisotropy by other means. One is the claim by Bihain & Scholz (2016) of a highly non-uniform distribution of brown dwarfs within 6.5 pc, whereby 21 out of 26 objects lie ahead of the Sun in its Galactic orbit. K19 found no such anisotropy in their complete samples of early-L dwarfs (out to 20 pc) and late-T dwarfs (out to 12.5 pc), describing the distribution of the smaller Bihain & Scholz (2016) sample as a random statistical effect. Our larger 25 pc volume-limited sample spanning L0–T8 spectral types can provide a robust assessment of this claim, but we must account for the declination limits in our sample that exclude more of the space trailing the Sun than leading. In a model population of isotropically distributed objects filling our sample's volume, we find 59% of the objects are ahead of the Sun and 41% are behind. For our volume-limited sample, 60% of the

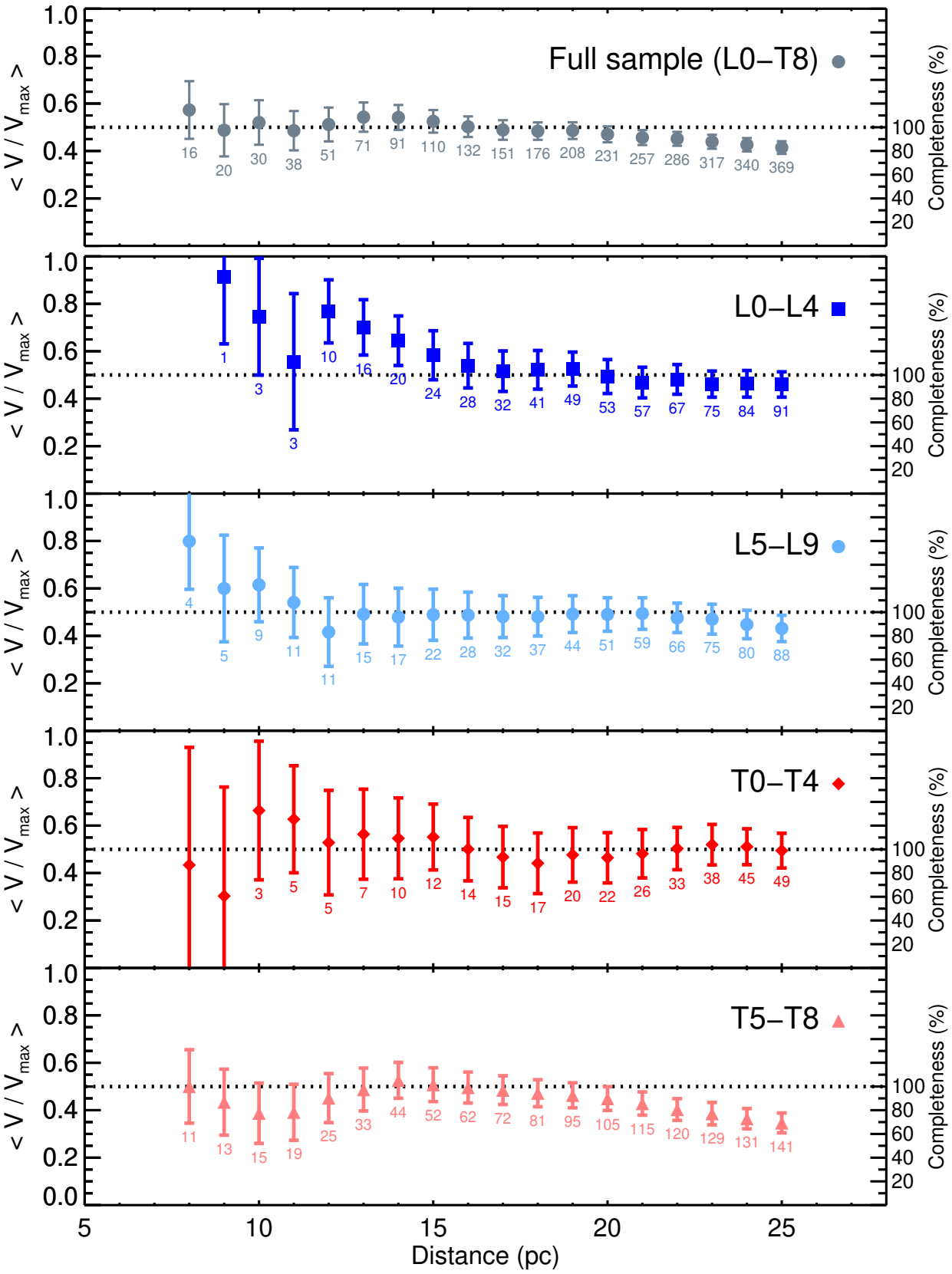

Figure 3. $\langle V/V_{\rm max}\rangle$ as a function of limiting distance for our volume-limited sample, for all spectral types in our full sample (L0–T8, top panel) and for four spectral type bins (*other panels*). The right-hand axes indicate the completeness values corresponding to $\langle V/V_{\rm max}\rangle$ values less than 0.5. Our full sample is consistent with completeness (i.e., $\langle V/V_{\rm max}\rangle$ is within 1σ of 0.5) out to 20 pc, with the declining trend of $\langle V/V_{\rm max}\rangle$ implying that the sample starts to become incomplete beyond 16 pc. Our sample is complete at 22 pc for L0–T4.5 dwarfs, i.e., through the L/T transition. The completeness at 25 pc is $92\% \pm 7\%$ for L0–T4.5 dwarfs, and $69\% \pm 8\%$ for T5–T8 dwarfs. The lower completeness for later-T dwarfs is expected because T7–T8 dwarfs near 25 pc are too faint to be discovered by most large sky surveys.

Table 2. Space Density and $\langle V/V_{\rm max}\rangle$ for Our 25 pc Sample of L0–T8 Dwarfs

				Space Density (10^{-3} objects pc^{-3})		
Objects	Number	$\langle V/V_{\rm max}\rangle$[a]	Corrected Number[a]	Value	$\sigma_{\rm binomial}$	$\sigma_{\rm Poisson}$
L0 ≤ SpT < L1	13	0.47 ± 0.14	14.2 ± 2.1	0.32	0.05	0.09
L1 ≤ SpT < L2	27	0.50 ± 0.10	28.0 ± 3.0	0.63	0.07	0.12
L2 ≤ SpT < L3	18	0.49 ± 0.12	19.6 ± 2.5	0.44	0.06	0.10
L3 ≤ SpT < L4	13	0.34 ± 0.13	20.4 ± 3.1	0.46	0.07	0.13
L4 ≤ SpT < L5	20	0.46 ± 0.12	21.8 ± 2.7	0.49	0.06	0.11
L5 ≤ SpT < L6	26	0.42 ± 0.10	30.7 ± 3.5	0.69	0.08	0.14
L6 ≤ SpT < L7	13	0.42 ± 0.15	15.4 ± 2.6	0.34	0.06	0.10
L7 ≤ SpT < L8	15	0.47 ± 0.14	15.8 ± 2.3	0.35	0.05	0.09
L8 ≤ SpT < L9	17	0.40 ± 0.12	22.2 ± 3.0	0.50	0.07	0.12
L9 ≤ SpT < T0	17	0.45 ± 0.13	17.9 ± 2.6	0.40	0.06	0.10
T0 ≤ SpT < T1	6	0.60 ± 0.22	5.8 ± 1.4	0.13	0.03	0.05
T1 ≤ SpT < T2	7	0.45 ± 0.21	8.2 ± 1.8	0.18	0.04	0.07
T2 ≤ SpT < T3	12	0.41 ± 0.15	15.7 ± 2.6	0.35	0.06	0.10
T3 ≤ SpT < T4	11	0.62 ± 0.17	8.4 ± 1.6	0.19	0.04	0.06
T4 ≤ SpT < T5	13	0.45 ± 0.14	16.2 ± 2.5	0.36	0.06	0.10
T5 ≤ SpT < T6	34	0.41 ± 0.09	40.7 ± 4.2	0.91	0.09	0.16
T6 ≤ SpT < T7	31	0.35 ± 0.09	43.4 ± 4.6	0.97	0.10	0.18
T7 ≤ SpT < T8	41	0.33 ± 0.07	62.4 ± 5.8	1.40	0.13	0.22
T8 ≤ SpT < T8.5	35	0.29 ± 0.08	60.0 ± 6.3	1.34	0.14	0.23
L0 ≤ SpT < L5	91	0.46 ± 0.05	99 ± 6	2.22	0.13	0.23
L5 ≤ SpT < T0	88	0.43 ± 0.05	98 ± 6	2.20	0.14	0.24
T0 ≤ SpT < T5	49	0.50 ± 0.07	50 ± 4	1.12	0.10	0.16
T5 ≤ SpT ≤ T8	141	0.35 ± 0.04	200 ± 10	4.48	0.23	0.39
L0 ≤ SpT < T0	179	0.45 ± 0.04	197 ± 9	4.41	0.19	0.33
T0 ≤ SpT ≤ T8	190	0.39 ± 0.04	243 ± 11	5.45	0.24	0.40
Single	301	0.41 ± 0.03	363 ± 13	8.13	0.28	0.48
Binary/triple[b]	44	0.50 ± 0.08	43 ± 4	0.97	0.09	0.15
Companion[c]	27	0.37 ± 0.03	36 ± 4	0.81	0.09	0.16
Young	22	0.45 ± 0.11	24 ± 3	0.54	0.07	0.12
All	369	0.42 ± 0.03	438 ± 13	9.80	0.30	0.52

Note— *Number*: number of objects in our volume-limited sample. $\langle V/V_{\rm max}\rangle$: calculated for our volume-limited sample. A sample with uniform spatial distribution will have $\langle V/V_{\rm max}\rangle = 0.5$. Twice the $\langle V/V_{\rm max}\rangle$ gives an estimate of the volume-completeness of each sample bin (1 = complete). *Corrected Number*: number of objects in each bin, corrected for incompleteness (i.e., divided by $2 \times \langle V/V_{\rm max}\rangle$). The numbers in smaller bins may not add up to the numbers in larger bins because the Monte Carlo trials were run separately for each bin. *Space Density*: corrected number for each bin divided by the volume of our sample (44703.031 pc^3). $\sigma_{\rm binomial}$ describes how precisely our space density measurements represent the full 25 pc volume around the Sun. $\sigma_{\rm Poisson}$ describes how precisely our space density measurements represent brown dwarfs in our general neighborhood of the Galaxy. The calculation of $\sigma_{\rm binomial}$ and $\sigma_{\rm Poisson}$ is described in Appendix B.

[a] Mean and standard deviation from Monte Carlo trials that resample the parallaxes from their errors and incorporate binomial uncertainties to account for statistical fluctuations in our sample (Appendix B).

[b] Close binaries and triples are counted as single objects with unresolved spectral types.

[c] Three companions are themselves binaries (see the text for details) and are also included in the binary/triple bin.

objects are ahead of the Sun and 40% behind. We thus find no evidence for anisotropy in our sample relative to the Sun's Galactic orbit other than the cuts imposed by our declination limits, supporting K19's explanation.

The other anisotropy to consider is motivated by the fact that many searches for ultracool dwarfs eschewed the Galactic plane ($|b| \lesssim 20°$), and by K19's finding that their own 20 pc sample was deficient at low Galactic latitudes. To assess whether our volume-limited sample is similarly deficient, we take the same approach as K19, dividing the sky into eight equal-area slices at Galactic latitudes $b = 0°$, $\pm 14.47°$, $\pm 30.00°$, and $\pm 48.49°$, except that we combine slices that have the same absolute Galactic latitudes to obtain four bins, each covering 25% of the sky. We then count the number of objects in each bin, calculating uncertainties from the binomial distribution as described in Appendix B (Equation B5). Since our sample does not cover the full sky, we must also account for the fact that the declination limits of our sample include different fractions of the Galactic latitude bins. Specifically, our sample covers 62.4% of the $0° \leq |b| < 14.47°$ slices, 62.8% of the $14.47° \leq |b| < 30.00°$ slices, 70.0% of the $30.00° \leq |b| < 48.49°$ slices, and 77.2% of the $48.49° \leq |b| \leq 90°$ slices. We use the coverage fractions to convert the number of objects in each bin into a number of objects per square degree. We show the resulting distribution of objects as a function of absolute Galactic latitude in Figure 4. There is a clear deficit at low Galactic latitudes, echoing what K19 saw in their 20 pc sample, and confirming the combined impact of many brown dwarf searches that avoided the Galactic plane. If we assume the sample is complete for $|b| \geq 14.47°$, then the deficit seen at lower Galactic latitudes would comprise ≈13% of a complete sample, consistent with our $83\% \pm 5\%$ completeness estimate. This indicates that most objects missing from our volume-limited sample reside at $|b| < 14.47°$.

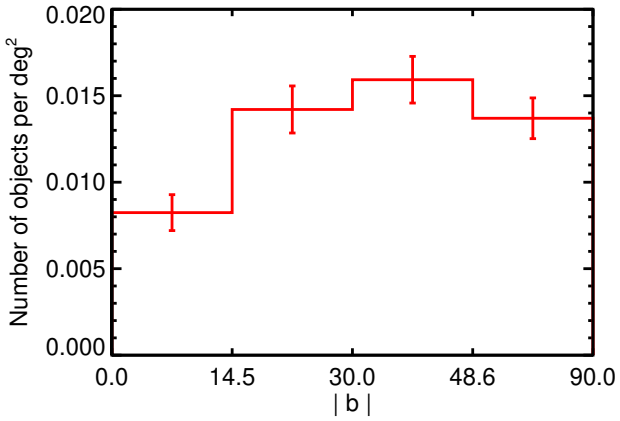

Figure 4. Distribution of objects in our volume-limited sample as a function of Galactic latitude, divided into four bins of $|b|$ each corresponding to a quarter of the full sky. To account for the differing fractions of each bin that are actually within the declination limits of our sample, we normalized the number of objects in each bin to the area of sky it covers. There is a clear deficit of objects near the Galactic plane, likely an artifact of the choice to avoid low Galactic latitudes made by many searches for brown dwarfs. Objects missing from our volume-limited sample mostly reside at these low Galactic latitudes.

2.4. *Space Density*

We calculated the space density of our 25 pc volume-limited sample and several subsets thereof, including young objects (Section 2.6); binaries, triples, and companions (Section 2.7); and single objects. We divided the number of objects in each sample or subset by twice the corresponding $\langle V/V_{\rm max} \rangle$ value to obtain an estimate of the true number of objects in our 25 pc volume, including objects missing from our sample. We then divided these corrected numbers of objects by our sample volume (44703.031 pc^3) to obtain space densities. We present our results in Table 2, including two different sets of uncertainties ($\sigma_{\rm binomial}$ and $\sigma_{\rm Poisson}$) for the space densities whose calculation and purpose we describe in Appendix B. Briefly, the binomial uncertainties $\sigma_{\rm binomial}$ are appropriate for estimating how well our volume-limited sample's space density represents the full 25 pc volume, of which our sample covers 68.3%. The Poisson uncertainties $\sigma_{\rm Poisson}$ are appropriate for estimating how well our volume-limited sample represents L0–T8 dwarfs in the much larger local neighborhood of our Galaxy. Both of these uncertainties also incorporate the parallax uncertainties of individual objects in our sample, whose impact is small compared to the statistical fluctuations described by $\sigma_{\rm binomial}$ and $\sigma_{\rm Poisson}$. For our discussion here, we adopt the Poisson uncertainties in order to comment on the space density of L0–T8 dwarfs in general and compare with previous estimates (which adopt Poisson uncertainties). Like previous studies, we do not account in this work for uncertainties in the spectral types themselves.

The uncertainties on our space densities for L and T0–T8 dwarfs are <10%, making ours the most precise estimates to date spanning these spectral type ranges. (BG19 quote a similar precision for their M7–L5 sample.) Our $(4.41 \pm 0.33) \times 10^{-3}$ pc^{-3} space density for L dwarfs and subsets thereof are consistent with most previous estimates (Cruz et al. 2007; Reylé et al. 2010; Marocco et al. 2015; K19), but are a factor of 1.8 smaller for L0–L5 dwarfs than the estimate of BG19. The latter work attempts to correct for sample selection effects

as well as incompleteness in their sample. BG19 identify their completeness correction as larger than their correction for selection effects, so the most straightforward explantion for their much larger space density is that their adopted sample completeness is underestimated.

For T dwarfs, our space densities are consistent with most previous estimates (Kirkpatrick et al. 2012; Burningham et al. 2013; Marocco et al. 2015). Our overall T0–T8 dwarf space density of $(5.45 \pm 0.40) \times 10^{-3}$ pc^{-3} is lower than the $\approx (7 \pm 3) \times 10^{-3}$ pc^{-3} estimates of Metchev et al. (2008) and Reylé et al. (2010), with much of the discrepancy coming at later T6–T8 dwarfs, although our estimate differs by less than 1σ due to the large uncertainties presented in those studies. K19 present their space densities using bins of $T_{\rm eff}$, which do not necessarily map to specific spectral types, but assuming that their bins spanning 600–1050 K correspond approximately to spectral types T6–T8, their estimate for those types appears also to be ≈40% higher than ours. If this discrepancy is real, its source is unclear, as our sample includes all of the T6 ≤ SpT ≤ T8 dwarfs in K19's 20 pc sample, and the incompleteness of our sample beyond 20 pc for these spectral types is addressed by our $\langle V/V_{\rm max} \rangle$ analysis (Figure 3) and consequent correction for completeness.

2.5. *Photometry*

Table 1 reports $YJHK$ photometry on the Maunakea Observatories system (MKO; Simons & Tokunaga 2002; Tokunaga et al. 2002) for our volume-limited sample. Best20 used the J band for parallax observations, providing us with $J_{\rm MKO}$ photometry for those objects. For other objects, we use $J_{\rm MKO}$ photometry from the literature where available, and for all objects we use $Y_{\rm MKO}$, $H_{\rm MKO}$, and $K_{\rm MKO}$ photometry from the literature where available.

When MKO photometry was not available, we calculated synthetic MKO photometry using SpeX prism spectra (Rayner et al. 2003) from the SpeX Prism Library (Burgasser et al. 2014) or from the literature. We calibrated our synthetic photometry with 2MASS photometry in the same band when available, or MKO photometry from another NIR bandpass. We calculated uncertainties in a Monte Carlo fashion using the measurement uncertainties of the spectrum, adding in quadrature the uncertainties from the calibrating photometry. Following the analysis of DL12, we added an additional 0.05 mag uncertainty in quadrature for all synthesized colors between bands within a photometry system (e.g., $(J-H)_{\rm MKO}$), but added no additional uncertainty for conversions between systems in a single band (e.g., $J_{\rm MKO} - J_{\rm 2MASS}$).

When no prism spectra were available, we converted 2MASS magnitudes into the MKO system using $M_{Ks,{\rm 2MASS}}$ and the polynomials of Dupuy & Liu (2017, Appendix A.2).

2.6. *Young and Old Objects*

Our volume-limited sample contains 22 young objects ($\lesssim$200 Myr), identified as such via spectroscopic indications of low surface gravity, lithium absorption, or Hα emission, and/or kinematic association with a young moving group. With completeness corrections, our sample implies a population that is 5.5% ± 1.2% young (assuming Poisson statistics), more than the expected ≈2% (7 ± 3 objects in our sample) for a commonly assumed uniform age distribution in a 10 Gyr old galaxy. This suggests that the local population of brown dwarfs is not uniform and skews toward younger ages. BG19 similarly identify 33 out of 410 (8%) of the M7–L5 dwarfs in their sample as young, and Kirkpatrick et al. (2008) found that 7.6% ± 1.6% of a sample of 303 L dwarfs are younger than 100 Myr. These young-leaning samples echo the 0.4–4 Gyr distribution (median age 1.3 Gyr) derived by Dupuy & Liu (2017) from evolutionary models using individual luminosities and dynamical masses of 20 resolved L and T dwarfs in binaries, as well as the 0.5–2 Gyr age distribution found by Zapatero Osorio et al. (2007) in the kinematics of nearby 21 L and T dwarfs, but are less consistent with the statistical 3–8 Gyr kinematic age found by Faherty et al. (2009) from the proper motions of 184 L0–T8 dwarfs. Dupuy & Liu (2017) point out that a young-leaning age distribution such as ours is consistent with a constant star formation rate coupled with dynamical heating, which tends to scatter older objects out of the Galactic plane where our Sun resides. Congruently, our volume-limited sample contains only three likely old objects (completeness-corrected 2.6% ± 1.6%): the T8 subdwarf WISE J200520.38+542433.9 (Mace et al. 2013b), and the two components of the comoving brown dwarf pair SDSS J141624.08+134826.7 (sdL6; Bowler et al. 2010a; Kirkpatrick et al. 2010; Schmidt et al. 2010a) and ULAS J141623.94+134836.3 ((sd)T7.5; Burgasser et al. 2010b; Burningham et al. 2010b; Scholz 2010b). More analysis of our volume-limited sample, including its kinematics and comparison to synthetic populations of differing ages, will yield better constraints on its age distribution.

Figure 2 shows the positions of the young objects in the M_J versus $J-K$ CMD of our volume-limited sample. All but three of these young objects are L dwarfs, which display the previously observed trends (e.g., Liu et al. 2013, 2016; Faherty et al. 2016) of redder colors

and (for late-L types) lower J-band luminosities than field-age L dwarfs. In general we would expect T dwarfs to be older than L dwarfs because brown dwarfs cool as they age, but since there are currently no clear spectroscopic identifiers of youth for ≥L8 dwarfs, it is possible that our sample contains T dwarfs with unrecognized young ages, which would make the fraction of young objects in our sample even higher. The three identified young T dwarfs in our sample are the T2.5 dwarf companion HN Peg B, age 300 ± 200 Myr (Luhman et al. 2007), the T2.5 dwarf SIMP J013656.5+093347.3 (Artigau et al. 2006) in the 200 ± 50 Myr old Carina-Near Moving Group (Zuckerman et al. 2006; Gagné et al. 2017), and the T5.5 dwarf SDSS J111010.01+011613.1 (hereinafter SDSS J1110+0116; Geballe et al. 2002) in the 149^{+51}_{-19} Myr old AB Doradus Moving Group (Bell et al. 2015; Gagné et al. 2015a). Atmospheric models predict a wide range of J-band luminosities for the L/T transition as a function of gravity (e.g., SM08; Charnay et al. 2018), though Liu et al. (2016) do not find such a wide range in their parallax sample. Consistently with Liu et al. (2016), we see an ≈1 mag spread of $M_{J_{\rm MKO}}$ in the L/T transition of our volume-limited sample, which could be an indication of a variety of gravities. All three of the young T dwarfs in our sample are part of the group of young benchmark T dwarfs that Zhang et al. (2020) describe as marginally ($\lesssim$0.5 mag) fainter in $J_{\rm MKO}$ than older objects of the same spectral type. We note that none of these T dwarfs has ages less than 100 Myr, so they are not as young as many of the young L dwarfs in our sample.

Figure 2 also shows the positions of two of the subdwarfs (SDSS J141624.08+134826.7 and ULAS J141623.94+134836.3) on our volume-limited CMD, both of which are among the bluest objects in their respective regions of the brown dwarf evolutionary sequence. The third subdwarf in our sample, WISE J200520.38+542433.9, does not appear on our CMD plot because it lacks $K_{\rm MKO}$ photometry.

2.7. *Binaries and Companions*

Binaries and multiples require special consideration in population studies. These systems can be considered separately from single objects, or the components can be treated as individual objects; both of these approaches require identification of the binaries and multiples in the sample. Alternatively, the impact of unresolved binaries on the photometry, luminosity, and mass of the sample can be accounted for statistically (e.g., Metchev et al. 2008; Day-Jones et al. 2013). We searched the literature to identify binaries in our volume-limited sample detected via high-angular resolution imaging, radial velocity measurements, or astrometric signatures. Contemporaneously with observations for the Best20 parallaxes, we also conducted our own high-angular resolution imaging survey of candidate members of the volume-limited sample lacking previous such observations across all spectral types, using laser guide star adaptive optics (LGSAO) on Keck II/NIRC2 at ≈0.″05–0.″10 resolution (W. Best et al., in preparation). The overwhelming majority of our sample (88%) has now been observed with high-angular resolution, without preference for particular spectral types, meaning that our full L0–T8 evolutionary sequence has been explored for binaries. (The remaining objects were largely not observed due to the lack of tip-tilt guide stars needed for LGSAO, which is also independent of spectral type.)

We identified 44 binaries in our volume-limited sample, from which we calculate a 9.9% ± 1.6% binary fraction for L0–T8 dwarfs, correcting for spatial incompleteness (Section 2.3) and assuming Poisson statistics.[1] (Two-thirds of these binaries have resolved J- and K-band photometry.) This includes two systems that are thought to include a third component: DENIS J020529.0−115925 (Bouy et al. 2005) and 2MASS J07003664+3157266 (Dupuy & Liu 2017); for simplicity, we include these systems in the category of "binaries" for this work. Figure 2 highlights the binaries (with unresolved photometry) in the M_J versus $J-K$ CMD of our volume-limited sample. Unresolved binaries combine the light of two objects and are therefore more luminous than single objects, so their tendency to sit higher (brighter M_J) than single objects on the CMD is expected.

A total of 27 of the binaries have L-dwarf primaries in our volume-limited sample. After correcting for spatial incompleteness (Section 2.3), we find a 15.1% ± 3.2% L-dwarf binary fraction, consistent with previous estimates (Gizis et al. 2003; Reid et al. 2008a) for binaries resolvable with high-angular resolution imaging ($\gtrsim$1.5 au), but somewhat lower than the ≈24% fraction estimate of Reid et al. (2006a) that includes L-dwarf binaries with smaller separations (see also Bardalez Gagliuffi et al. 2015). It is therefore reasonable to expect that our volume-limited sample contains ≈10 unresolved bi-

[1] We do not treat the components of L and T dwarf binaries as separate objects in this discussion. We also do not include L and T dwarfs that are in close binaries with earlier-type primaries in our sample. Known L and T dwarf secondaries not included in our sample are LHS 1070C (Leinert et al. 1994; Rajpurohit et al. 2012), 2MASSW J0320284-044636B (Blake et al. 2008; Burgasser et al. 2008a), WISE J072003.20-084651.2B (Burgasser et al. 2015), LHS 2397aB (Freed et al. 2003), 2MASS J17072343-0558249B (McElwain & Burgasser 2006), and LSPM J1735+2634 (Law et al. 2006).

naries with L-dwarf primaries. For T dwarfs, 17 (corrected 5.9%±1.6%) in our sample are binaries, a fraction consistent with the recent comprehensive assessment of Fontanive et al. (2018).

Our volume-limited sample also contains 27 L and T dwarfs that are companions to hotter objects (corrected 8.3% ± 1.7%). These L and T dwarfs were identified as resolved (typically >10") common proper motion companions mostly to main-sequence stars, but also include VHS J125601.92−125723.9 b (hereinafter VHS J1256−1257b; Gauza et al. 2015), whose primary is a young M7 binary with component masses near the stellar/substellar boundary (Stone et al. 2016; Dupuy et al. 2020), and the wide sdL7+(sd)T7.5 pair SDSS J141624.08+134826.7 and ULAS J141623.94+134836.3. Three of the companions — Gl 337CD (Wilson et al. 2001; Burgasser et al. 2005a), Gl 417BC (Kirkpatrick et al. 2000; Bouy et al. 2003), and Gl 564BC (Potter et al. 2002) — are themselves close binaries and are included in the preceding discussion of binaries. Figure 2 shows the positions of our non-binary companions in the M_J versus $J-K$ CMD. The companions include a smaller fraction of early-L dwarfs and a larger fraction of late-T dwarfs than the full volume-limited sample, but otherwise appear to follow the same sequence on the CMD as the single L and T dwarfs.

Unresolved binaries blend the light of two objects and therefore do not accurately represent the evolution of individual objects on a CMD. The components of binaries and the resolved companions, on the other hand, are as much individual ultracool dwarfs as the isolated ones. However, these components and companions may have different distributions of masses from the single objects, in which case they could be distributed differently along the L and T dwarf sequence in Figure 2. The overabundance of late-T type companions, for example, is suggestive of a different underlying distribution. Previous efforts to constrain the mass distribution of companions have found results consistent with most substellar initial mass function (IMF) constraints (within large error bars; e.g., Brandt et al. 2014; Bowler 2016; Baron et al. 2019; Nielsen et al. 2019). However, those studies have primarily focused on planetary-mass companions found by adaptive optics surveys, and have not encompassed the full range of brown dwarf masses and separations that characterize the mostly wide companions in our volume-limited sample. There is also evidence that the mass distribution of the components of binaries is different from single objects. The mass ratio distribution of brown dwarf binaries skews strongly toward equal masses (Burgasser et al. 2006b), whereas the IMF for brown dwarfs is thought to be roughly flat: for a power-law IMF of the form ($\frac{dN}{dM} \propto M^{-\alpha}$), most studies have found $-0.5 \lesssim \alpha \lesssim 0.5$ (e.g., Allen et al. 2005; Metchev et al. 2008; Day-Jones et al. 2013; K19). In addition, to the extent that selection effects are present in our sample, they may be different for companions and binaries as a result of different goals and methods used for past searches (compared with field objects). In short, since the singles, companions, and components of close binaries in our sample may all have different mass distributions, it is appropriate to consider those groups separately, especially when studying their population properties. Therefore, we have removed the known binaries and companions from our volume-limited sample for the remainder of this paper. This allows us to present a clean picture of the NIR photometric evolution of *single* brown dwarfs, uncluttered by the blended photometry of unresolved binaries and free of any bias from possible differences in the mass distributions of binary components or companions.

3. A GAP IN THE L/T TRANSITION

Figure 5 shows the M_J versus $J-K$ (MKO) CMD for our volume-limited sample of 301 single objects after removing the 44 binaries and 27 companions (three of which are themselves binaries; Section 2.7). Figure 5 highlights the sources of the parallaxes that define our sample. The CMD reveals a significant gap at $(J-K)_{\rm MKO} \approx 0.9$–$1.4$ mag, early in the evolution of L/T transition dwarfs from redder to bluer colors, implying a phase of rapid atmospheric evolution as brown dwarfs cool through $T_{\rm eff} \approx 1300$ K (e.g., Dupuy & Liu 2017). The gap was not identifiable in CMDs using previous samples requiring parallaxes because those samples (e.g., DL12) contained too few L/T transition dwarfs to securely identify trends in the population. The Best20 parallaxes now allow us to present a volume-limited CMD that reveals this L/T transition gap for the first time.

Figure 5 also shows the M_J versus $J-K$ CMD as a density map, obtained by Monte Carlo sampling of the objects (to account for observational uncertainties), binning into 0.2×0.2 mag cells, and smoothing by a two-dimensional Gaussian of FWHM 1.5 cells. The smoothed cells contain 0–5 objects. The gap in the L/T transition seen in Figure 5 stands out clearly as the most prominent underdensity in the brown dwarf sequence through mid-T dwarfs ($M_{J_{\rm MKO}} \lesssim 15.5$ mag, after which our sample becomes less complete).

The $J-K$ color of L/T transition spectral subtypes varies as much as the width of the gap (Best et al. 2018), and the spectral types in our sample have not been ho-

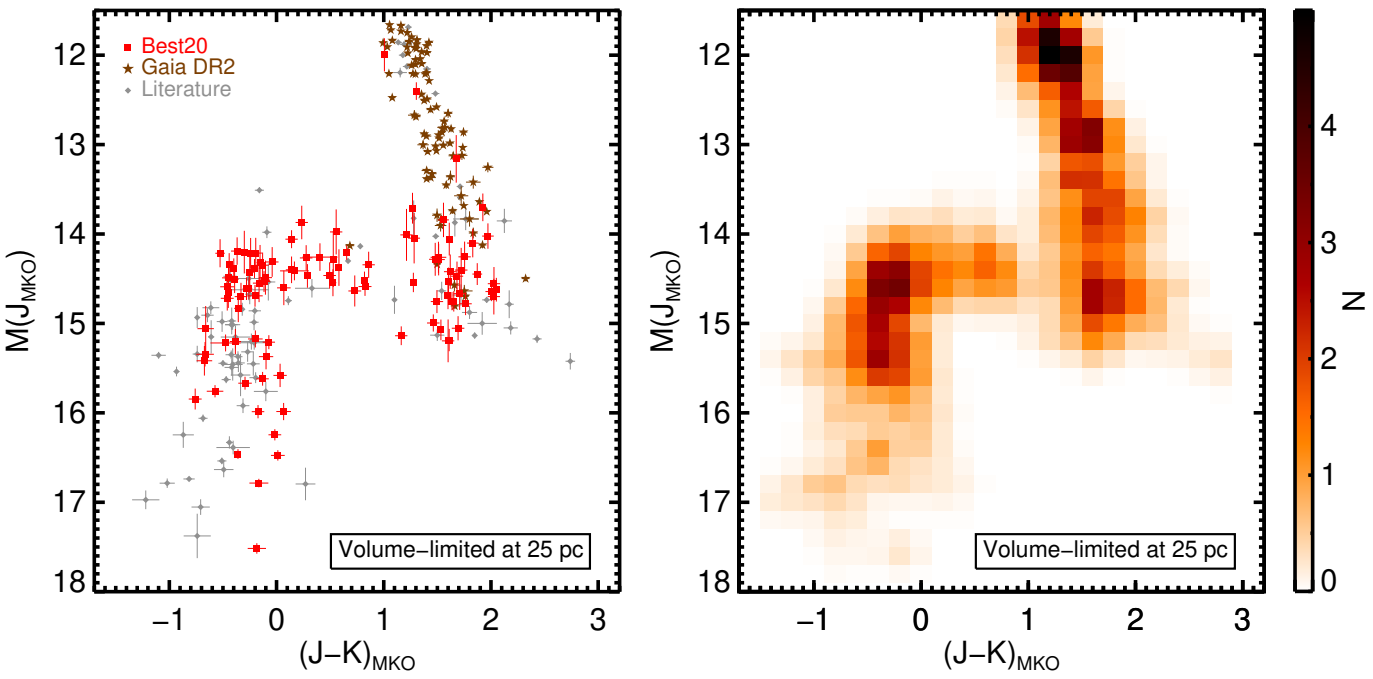

Figure 5. Left: M_J vs. $J-K$ (MKO) color-magnitude diagram for our volume-limited sample of 301 single objects (binaries and companions removed). Symbols indicate the source of the parallax measurement: Gaia DR2 (brown stars), literature sources (gray diamonds), and Best20 (red squares). For objects with more than one parallax measurement, we use the most precise one. Right: density map of the same CMD, obtained by smoothing the mean number of objects in 0.2×0.2 mag cells from Monte Carlo trials. The color bar at right indicates the number of objects in the smoothed cells. The large gap (underdensity) at $J-K \approx 1$ mag, $M_J \approx 14.5$ mag is clearly identified for the first time by our volume-limited sample. The gap occurs early in the L/T transition and implies a phase of rapid atmospheric evolution as brown dwarfs cool through $T_{\rm eff} \approx 1300$ K (e.g., Dupuy & Liu 2017).

mogeneously assigned, so we cannot claim that the gap occurs at a specific spectral type. For reference, however, we show spectral type as a function of $(J-K)_{\rm MKO}$ for our sample in Figure 6, and note that the gap occurs in the vicinity of spectral types ≈T0–T3. We note also that Figure 3 shows our sample to be ≈100% complete for T0–T4 dwarfs, the spectral type range that likely encompasses the gap, so the gap is not an incompleteness artifact.

Figure 7 shows the $J-K$ color distribution of single L/T transition dwarfs in our volume-limited sample. We used Monte Carlo trials to incorporate the uncertainties in the colors. To account for random variations due to the limited size and incomplete sky coverage of our sample, we calculated uncertainties from the binomial distribution (Appendix B, Equation B5) and added these in quadrature. To select L/T transition objects in an objective fashion, we chose objects with $13.5 \leq M_{H_{\rm MKO}} \leq 15.0$ mag, using $M_{H_{\rm MKO}}$ because it is essentially constant across the L/T transition (DL12). This selection includes 104 objects. The gap seen in the CMD stands out clearly in the color distribution.

How significant is this gap in the L/T transition? We assessed this in two stages. We first addressed the statistical significance of our measurement of a gap by evaluating its depth. The normalized histogram in Figure 7 shows a sudden drop in probability from the 0.2 mag wide bin centered at $J-K = 0.7$ mag to the bin centered at 0.9 mag. Adding the uncertainties for these bins in quadrature, we found the difference between these bins to be 3.1 times the combined uncertainty, i.e., a 3.1σ measurement. At the red edge of the gap, the rise from the 1.3 mag bin to the 1.5 mag bin is a 2.3σ measurement. Treating the gap as a single 0.6 mag wide bin centered at $J-K = 1.1$ mag, in comparison to adjacent 0.6 mag wide bins centered at 0.5 and 1.7 mag, the gap's significance is more pronounced: the drop at the blue side is 4.6σ, while the rise at the red side is 6.6σ. Clearly the gap is a statistically significant feature in our sample.

We then considered the possibility that the gap is simply a random fluctuation in the color distribution of L/T transition dwarfs of our particular volume-limited sample. Without prior knowledge of the true $(J-K)_{\rm MKO}$

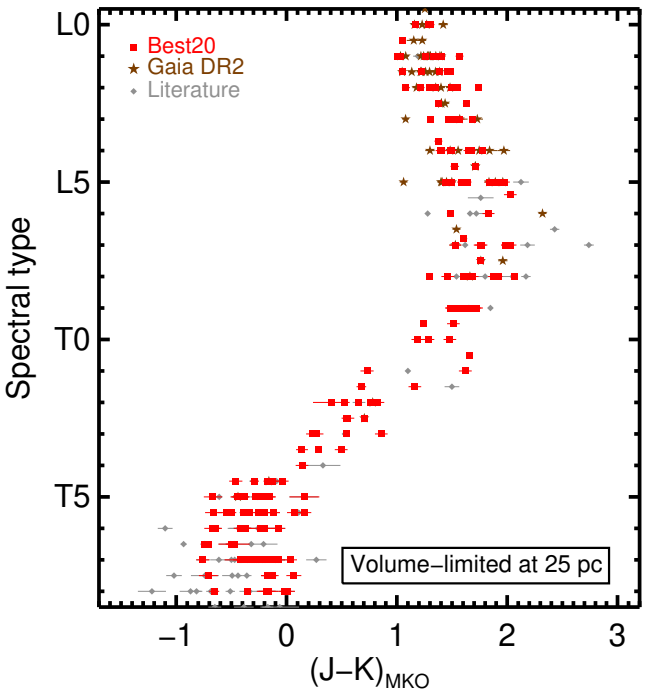

Figure 6. Spectral type as a function of $(J-K)_{\rm MKO}$ color for the single objects in our volume-limited sample. The gap occurs at $J-K \approx 0.9-1.4$ mag, in the vicinity of spectral types ≈T0–T3.

distribution of L/T transition dwarfs, one cannot directly determine the extent to which the gap is a deviation from a specific physical scenario. We can, however, estimate the likelihood of a gap like the one in our volume-limited sample randomly appearing when the underlying distribution has no gaps. Again referring to Figure 7 and considering the gap as one 0.6 mag wide bin centered at $J-K = 1.1$ mag, that gap contains on average 4.99 objects in our Monte Carlo trials, out of a total of 104 objects. The 0.6 mag bin centered at $J-K = 0.5$ mag (adjacent to the gap) contains an average of 19.94 objects, 14.95 more than the gap does. For comparison, we drew random samples of 104 objects with $(J-K)_{\rm MKO}$ colors between −0.5 and 2.1 mag from a uniform distribution. In these draws, a 0.6 mag wide bin anywhere in the interval with both adjacent bins having at least 15 more objects occurs 1.9% of the time. In our volume-limited sample, the 0.6 mag wide bin to the red side of the gap is even taller than the bin on the blue side, so a gap like ours is actually less likely to occur. In addition, a 0.6 mag wide bin with five or fewer objects anywhere in the interval occurred less than 0.001% of the time in our random draws, i.e., it is a $>4.4\sigma$ event. We therefore conclude that the gap is extremely unlikely to occur if the true $J-K$ distribution across the L/T transition is uniform.

Could our removal of binaries and companions have biased our sample in such a way as to create the gap? Figure 2 shows there are no binaries or companions in the gap, partly answering the question. We must also consider that the individual components of a binary can have different photometry than the binary's integrated-light photometry, and thus a resolved component could lie in the gap even when the blended light of the unresolved binary does not. For the addition of binary components to change the appearance of the CMD, such components would need to be highly concentrated in the gap, which seems implausible given that binaries account for only 10% of our entire sample, spanning all spectral types. More generally, binary components (as well as resolved companions) are themselves ultracool dwarfs with the same spectral and evolutionary properties as single objects, so it is extremely unlikely that the components would preferentially congregate in the single-object gap (e.g., given the previous paragraph's estimate of a <0.001% chance of a uniform color distribution across the L/T transition). In other words, removing binary components cannot create a phase of evolution that is not seen in single objects.

Using a much smaller sample of 36 objects defined by parallaxes but not volume-limited, DL12 tentatively identified a gap at a bluer $(J-K)_{\rm MKO} \approx 0.1$–$0.5$ mag color, along with a pileup at $(J-K)_{\rm MKO} \approx 0.5$–$0.8$ mag, similar to the predictions of the "hybrid" evolutionary models of SM08 (see the discussion in Section 4.3). Best et al. (2015) found further evidence for this bluer gap in a sample of 70 objects, volume-limited at 25 pc but incomplete and selected in part using photometric distances. Our parallax-defined 25 pc sample now reveals this tentative gap to in fact be a minor underdensity (Figure 7), possibly another phase of mildly accelerated evolution. The samples of DL12 and Best et al. (2015) do show hints of the gap we now clearly identify at $(J-K)_{\rm MKO} \approx 1$ mag, but its significance is unapparent without the large number of early-T dwarf parallaxes now provided by Best20. These discrepancies with previous tentative results and models demonstrate how essential a complete volume-limited sample is for accurate population analysis.

4. DISCUSSION

4.1. *L/T Transition Colors in Multiple Bands*

L/T transition dwarfs simultaneously brighten in the J band while dimming in the K band as they cool through the transition (e.g., Tinney et al. 2003; DL12). This behavior is thought to be caused by a depletion

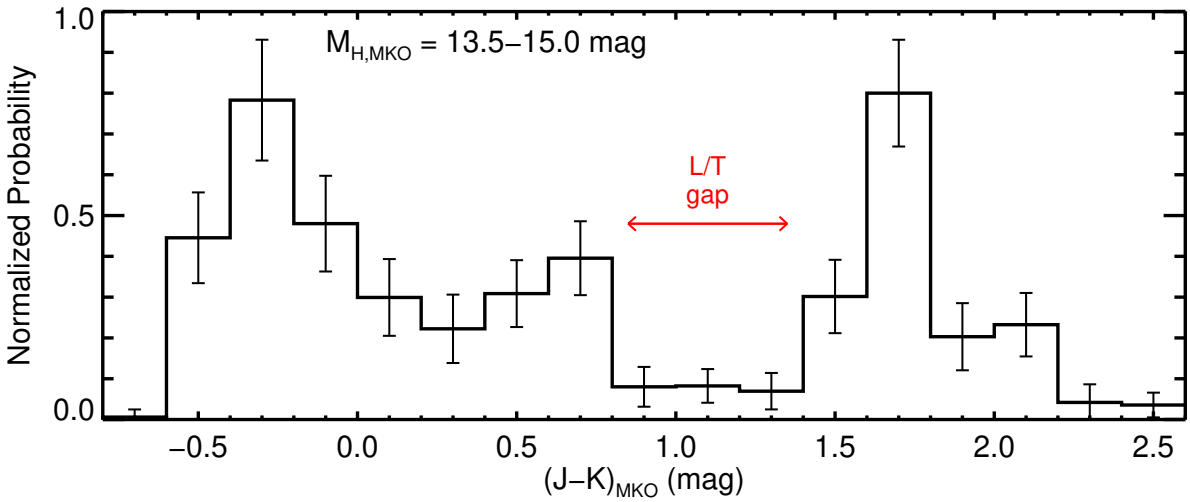

Figure 7. Distribution of $(J-K)_{\rm MKO}$ colors for single L/T transition dwarfs in our volume-limited sample. We computed the histogram from objects having $13.5 \leq M_{H_{\rm MKO}} \leq 15.0$ mag (we used $M_{H_{\rm MKO}}$ because it is essentially constant across the L/T transition; DL12), sampling their color uncertainties in a Monte Carlo fashion. The error bars are the RMS for each color bin from our Monte Carlo trials added in quadrature to the binomial uncertainties for a sample covering 68.3% of the sky. The gap seen in Figure 5 is labeled in red. A gap seen previously at $(J-K)_{\rm MKO} \approx 0.0-0.5$ mag in smaller, less complete samples by DL12 and Best et al. (2015) appears as a shallow deficit in our volume-limited sample, suggesting another slightly accelerated evolutionary phase.

of condensate clouds (e.g., Ackerman & Marley 2001; Burrows et al. 2006) or the evolution of thermochemical instabilities (Tremblin et al. 2016, cf. Leconte 2018). The gap we identify suggests that the distinctive blueward evolution of the L/T transition is occurring much more quickly at $(J-K)_{\rm MKO} \approx 1$ mag than in subsequent parts of the transition.

In Figure 8 we present CMDs of single objects in our volume-limited sample using eight different colors spanning Pan-STARRS1 $y_{\rm P1}$ (0.96 μm) to WISE $W2$ (4.6 μm). We highlight the objects inside, above, and at the edges of the $(J-K)_{\rm MKO}$ L/T transition gap to illustrate the location (or lack) of the gap in other colors. The gap appears widest in $(J-K)_{\rm MKO}$, but is also clearly visible in $(J-H)_{\rm MKO}$ and $J_{\rm MKO}-W1$, underscoring the importance of J-band flux in the L/T transition evolution. The gap is also apparent in similar colors that replace $J_{\rm MKO}$ with $y_{\rm P1}$ including $y_{\rm P1}-K_{\rm MKO}$ and $y_{\rm P1}-W1$, and is also visible (although narrower) in $y_{\rm P1}-J_{\rm MKO}$. The gap is not visible at all in $J_{\rm MKO}-W2$ and $W1-W2$, indicating a more gradual evolution in these colors.

4.2. *Objects in or near the L/T Transition Gap*

Assuming the L/T transition gap represents a rapid phase of brown dwarf evolution, single objects with gap photometry ($J-K \approx 1$ mag, $M_J \approx 14.5$ mag) should be relatively rare. The gap in Figure 5 is not completely empty, featuring three objects within the gap and four directly above it (highlighted in the first panel of Figure 8 and labeled in Figure 9), suggesting that L/T transition objects may have gap colors for a brief but observable period of time.

However, another type of object could appear in or directly above the gap: an unresolved binary with components that individually sit on either side of the gap but whose blended color overlaps the gap. To assess the possibility that the seven objects in and above the gap are unrecognized binaries, we performed spectral decomposition (e.g., Burgasser et al. 2005b, 2010a, hereinafter B10; Liu et al. 2006) of these objects following the method described in DL12. Briefly, we used the library of 178 IRTF/SpeX prism spectra from B10 — for which they determined uniform NIR spectral types and removed binaries, young objects, and other unusual spectra — as templates to create blended spectra. For each template pairing we determined the scale factor needed to minimize the χ^2 of the difference with the spectrum of a gap object. We then examined the resulting best pairing to determine the component spectral types, taking into account spectral type uncertainties in the best-match templates. We estimated the flux ratios for the template pairings in standard NIR bandpasses and $J-K$ colors using our χ^2 values and the weighting scheme described in B10. For the $J-K$ colors, we added 0.05 mag in quadrature to the uncertainties to account for systematic uncertainties we have previ-

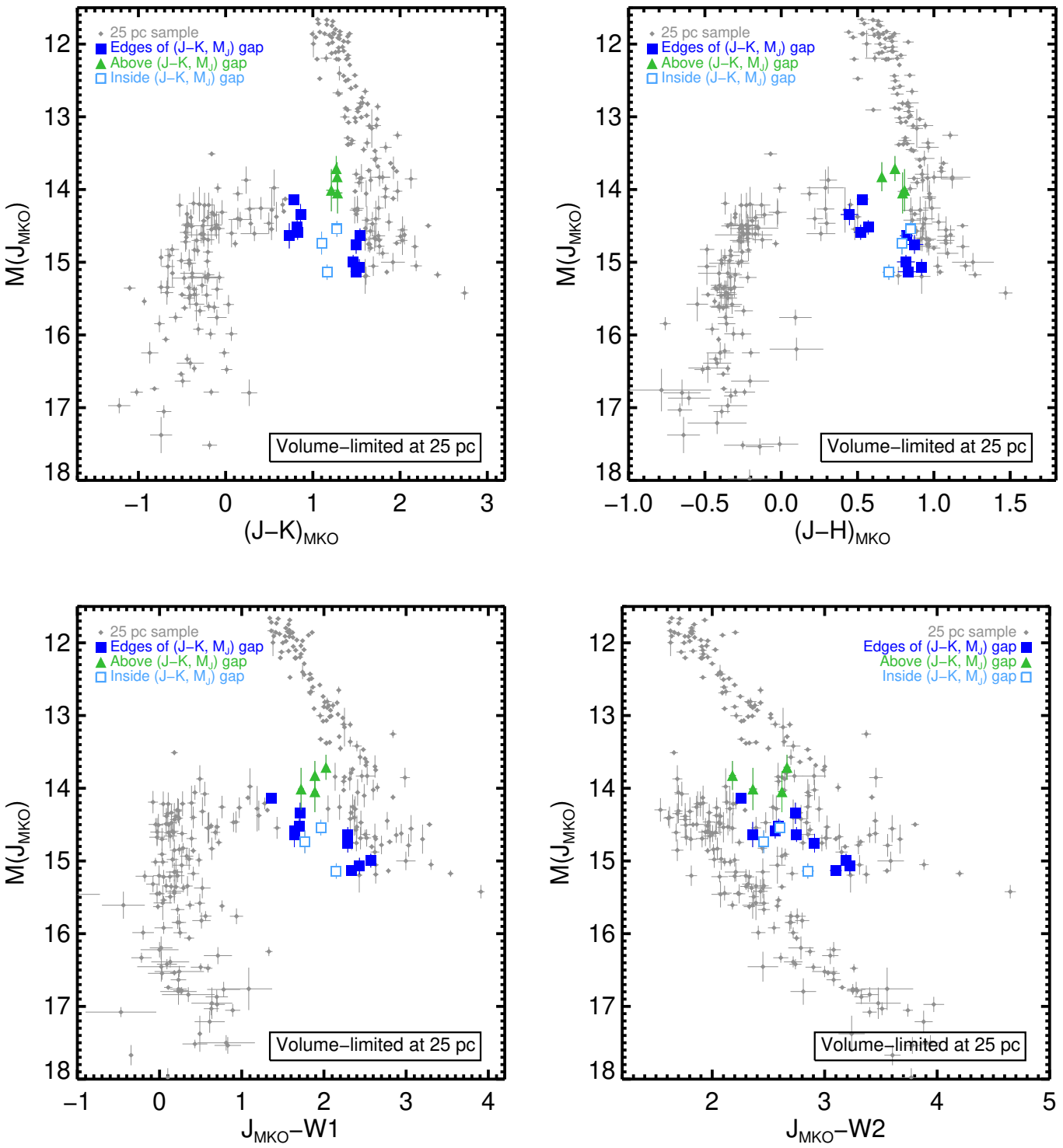

Figure 8. CMDs for single objects in our volume-limited sample, tracing objects in or near the $(J-K)_{\rm MKO}$ L/T transition gap through eight different colors. The top left CMD reproduces Figure 5 but highlights only objects inside the M_J vs. $J-K$ (MKO) gap (light blue open squares), on the edges of the gap (dark blue filled squares), or directly above the gap (green triangles). The same objects are highlighted in the same colors in the other diagrams. The gap remains a prominent feature in $(J-H)_{\rm MKO}$ (top right) and $J_{\rm MKO}-W1$ (bottom left) but is not visible in $J_{\rm MKO}-W2$ (bottom right).

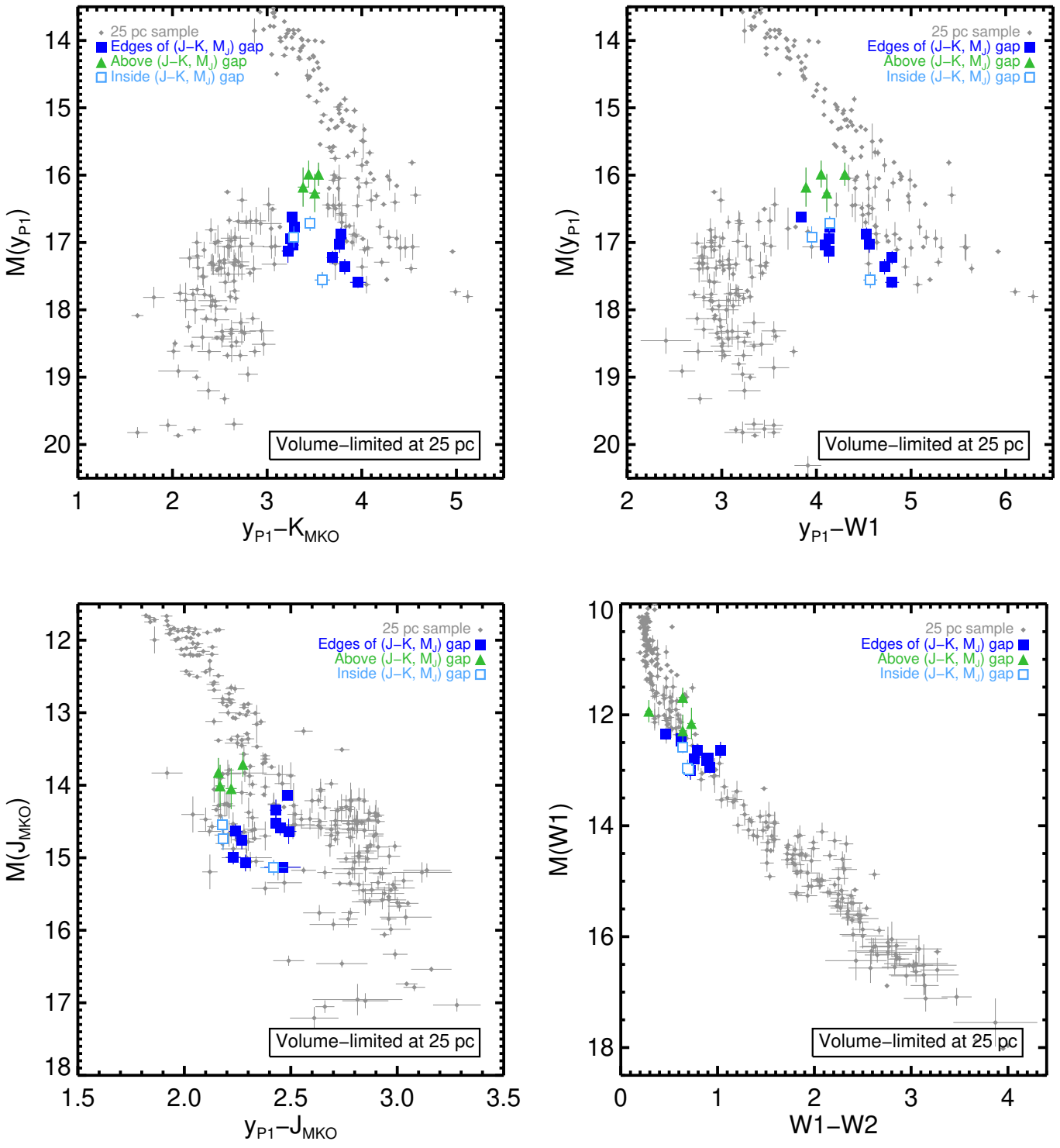

Figure 8. continued. The L/T transition gap is clearly visible in $y_{\rm P1} - K_{\rm MKO}$ (top left) and $y_{\rm P1} - W1$ (top right), but is contaminated with other objects in $y_{\rm P1} - J_{\rm MKO}$ (bottom left) and not at all present in $W1 - W2$ (bottom right).

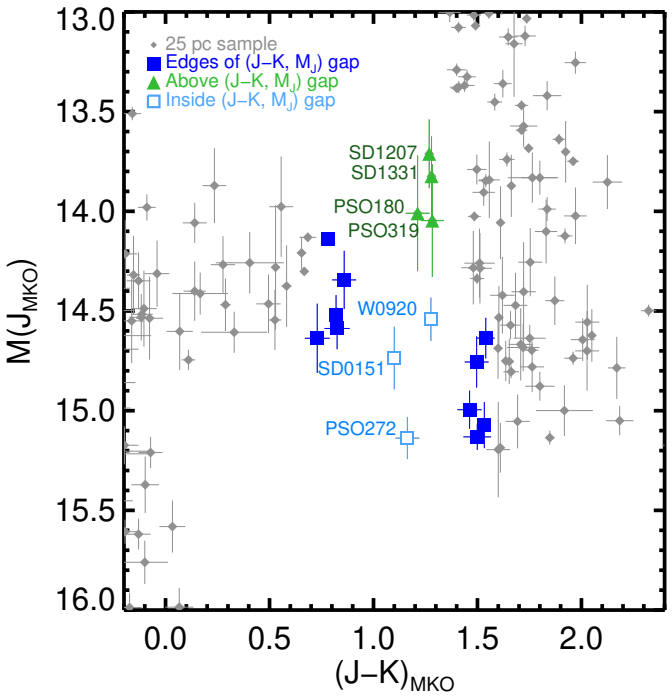

Figure 9. M_J vs. $J-K$ (MKO) color-magnitude diagram for single objects in our volume-limited sample, using the same color scheme as Figure 8 but showing only the central portion of the first panel of Figure 8 in order to highlight the objects above and inside the L/T transition gap. These objects are labeled here and discussed in Section 4.2.

ously found in colors derived from low-resolution NIR spectra (DL12). The best template pairings for the gap objects are listed in Table 3, placed on the M_J versus $J-K$ color-magnitude diagram in Figure 10, presented in Figures 11 and 12, and discussed below. Unlike the approach used by B10, our analysis does not make any prior assumptions about the flux ratios of the components (e.g., based on spectral types), nor does it assess whether pairs of templates are better matches to our observed spectra than single-object templates.

We note that four of our seven decompositions identified the L7.5 dwarf SDSS J152039.82+354619.8 (Chiu et al. 2006) as the primary component template. This brown dwarf has inconsistent NIR spectral types in the literature — T0 ± 1 from Chiu et al. (2006) and L7.5 from B10, and visually matches well the NIR L9 standard DENIS-P J025503.3−470049 (Martín et al. 1999b; Kirkpatrick et al. 2010) — but otherwise has no unusual features. In the end, only one of the decompositions using SDSS J152039.82+354619.8 as the primary template (for PSO J319.3102−29.6682) is plausible, as discussed below.

Table 3. Spectral decomposition of objects in or above the L/T transition gap

Object	Primary	Secondary	MKO Photometry							
			M_J (combined)	$J-K$ (primary)	$J-K$ (secondary)	ΔJ	ΔH	ΔCH_4short	ΔK
	(SpT)	(SpT)	(mag)	(mag)	(mag)	(mag)	(mag)	(mag)	(mag)
SDSS J015141.69+124429.6	L7.5 ± 2	T2 ± 1	14.74 ± 0.16	1.45 ± 0.06	0.48 ± 0.07	−0.07 ± 0.25	0.34 ± 0.23	0.21 ± 0.24	0.89 ± 0.22
WISE J092055.40+453856.3	L7.5 ± 1	T2 ± 2	14.54 ± 0.11	1.45 ± 0.05	0.73 ± 0.12	1.22 ± 0.91	1.45 ± 0.69	1.39 ± 0.75	1.66 ± 0.50
PSO J180.1475−28.6160	L7.5 ± 1	T2 ± 1	14.01 ± 0.29	1.44 ± 0.11	0.58 ± 0.32	0.43 ± 0.52	0.79 ± 0.70	0.67 ± 0.66	1.29 ± 0.78
SDSS J120747.17+024424.8	L6 ± 1	T2 ± 1	13.72 ± 0.17	1.40 ± 0.05	0.86 ± 0.06	0.28 ± 0.05	0.50 ± 0.06	0.39 ± 0.06	0.82 ± 0.06
SDSS J133148.92−011651.4	L6.5 ± 1	T5 ± 1	13.82 ± 0.20	1.34 ± 0.05	−0.30 ± 0.31	1.97 ± 0.18	2.86 ± 0.37	2.55 ± 0.31	3.61 ± 0.48
PSO J272.0887−04.9943	L9 ± 1	T3 ± 1	15.14 ± 0.11	1.10 ± 0.33	1.43 ± 0.51	1.09 ± 1.22	0.93 ± 0.83	0.98 ± 0.94	0.76 ± 0.46
PSO J319.3102−29.6682	L7.5 ± 1	T3 ± 1	14.05 ± 0.28	1.45 ± 0.06	0.35 ± 0.40	1.13 ± 0.49	1.66 ± 0.75	1.51 ± 0.68	2.23 ± 0.85

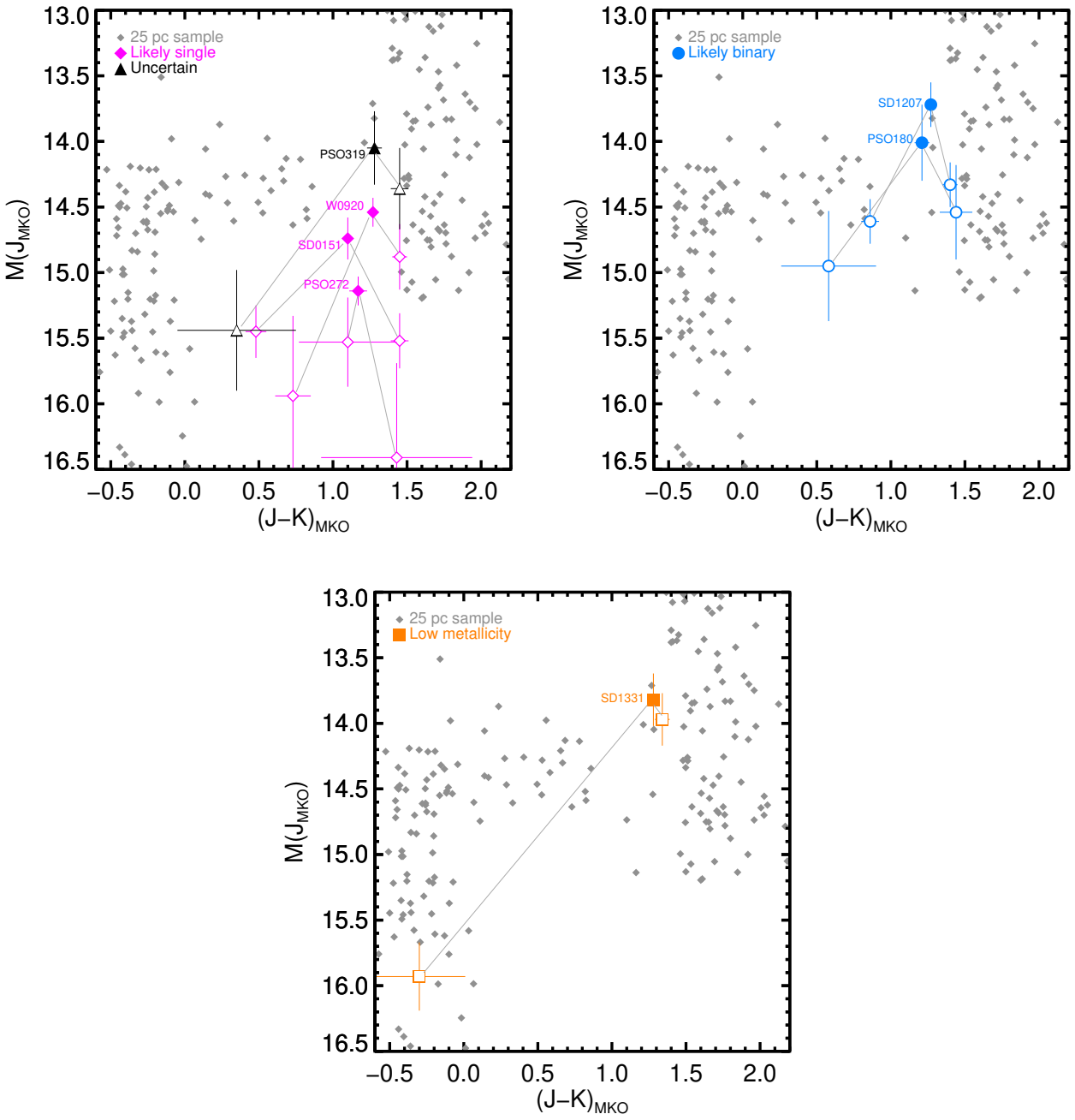

Figure 10. M_J vs. $J-K$ (MKO) CMDs for our volume-limited sample, enlarging a portion centered on the L/T transition. All three panels show the same portion of the CMD; we use three separate panels for clarity. The filled colored symbols show the objects in and above the L/T transition gap that are labeled in Figure 9, connected by light gray lines to the best-fit components from our binary template matching (open symbols). Other (single) objects in the sample are plotted as light gray diamonds. Top left: for all three objects in the gap (SDSS J0151+1244, WISE J0920+4538, and PSO J272.0−04.9; pink diamonds) as well as PSO J319.3−29.6 (black triangles), at least one of the best-fit binary components is implausibly faint for its color and spectral type, suggesting that the objects are single. Top right: PSO J180.1−28.6 and SDSS J1207+0244 (blue circles) have plausible binary decompositions. Bottom: SDSS J1331−0116 (orange square) is most likely a low-metallicity mid-L dwarf (Knapp et al. 2004; Marocco et al. 2013).

4.2.1. *Objects inside the Gap*

The T1 dwarf SDSS J015141.69+124429.6 (hereinafter SDSS J0151+1244; Geballe et al. 2002) appears single at a resolution of 40 mas (Burgasser et al. 2006b) and has no previous spectral indication of binarity (B10). Our spectral decomposition does find a good match to an L7.5 + T2 blend, and plausible matches for blends of spectral types L8 ± 2 with T2 ± 1. For the most likely match, the difference in $J_{\rm MKO}$ between the two components is −0.07 ± 0.25 mag, consistent with equal-brightness components. In this case, both components would be ≈0.75 mag fainter than the combined absolute magnitude of 14.74 mag (Figure 10). At $M_{J_{\rm MKO}} = 15.5$ mag, both components would be implausibly faint in J-band — fainter than any known object with spectral type earlier than T7. SDSS J0151+1244 thus appears to be a single T1 dwarf.

The L9.5 dwarf WISE J092055.40+453856.3 (hereinafter WISE J0920+4538; Mace et al. 2013a; Best et al. 2013) was characterized as a weak binary candidate with L7.5 ± 1.5 and T1.5 ± 1.5 components by Mace et al. (2013a). Laser guide star adaptive optics imaging of this object using Keck II/NIRC2 with an angular resolution of 95 mas has detected no sign of a companion (W. Best et al, in preparation). Our spectral decomposition identifies a possible blend combination of L7.5 + T2, but the difference in J-band luminosity for the two components would be >1 mag, inconsistent with an expected difference of ≈0.3 mag in $J_{\rm MKO}$ (DL12). We therefore find it unlikely that WISE J0920+4538 is a binary.

The T1.5 pec dwarf PSO J272.0887−04.9943 (hereinafter PSO J272.0−04.9; Best et al. 2015), which sits at the bottom of the gap (Figure 9), is a candidate binary (Best et al. 2015) based on the appearance of its NIR spectrum and the spectral indices defined by B10. However, PSO J272.0−04.9 is already the faintest early-T dwarf in our sample, and its position at the bottom of the L/T transition sequence would require potential binary components to be an unusually faint late-L dwarf and a much fainter late-T dwarf. Our spectral decomposition does not support this pairing, finding instead an L9 + T3 pairing whose components are both ≈1.5 mag fainter than expected for those spectral types (Figure 10). In addition, laser guide star adaptive optics imaging of this object using Keck II/NIRC2 with an angular resolution of 80 mas has detected no sign of a companion (W. Best et al, in preparation). PSO J272.0−04.9 therefore appears to be a single object, and an unusually faint one for its spectral type.

SDSS J0151+1244, WISE J0920+4538, and PSO J272.0−04.9 thus all appear to be single brown

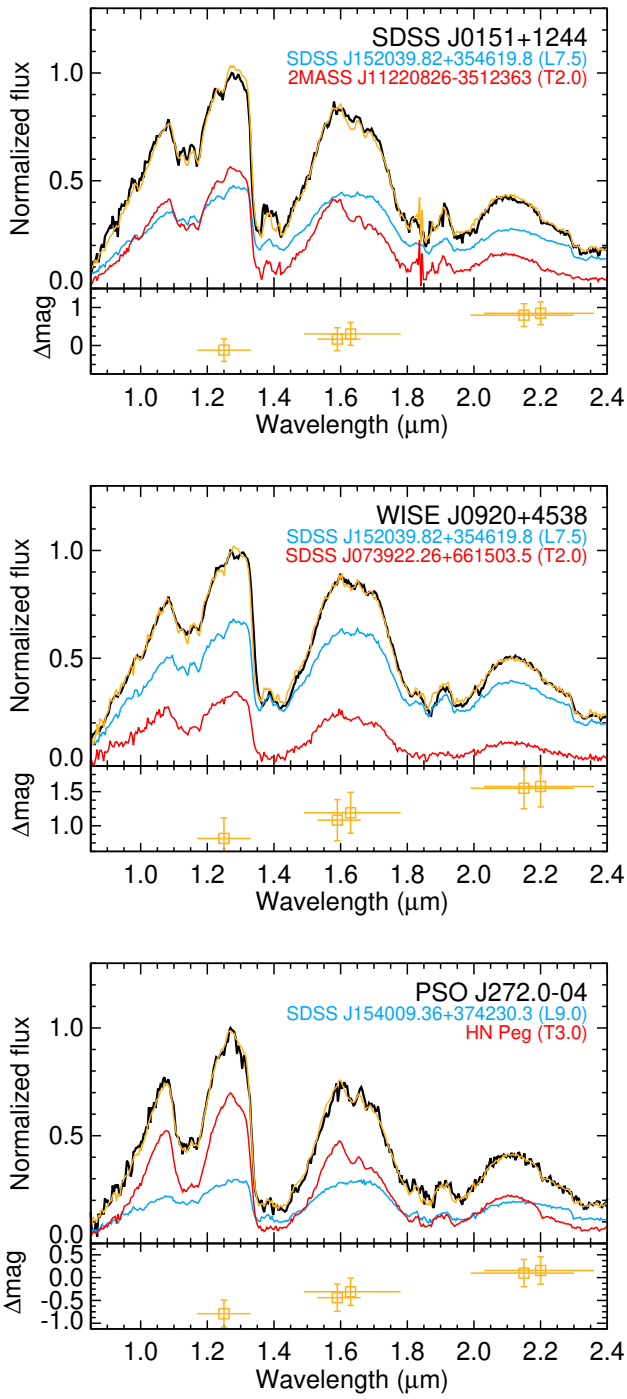

Figure 11. Best-matching template pairings for the three objects that lie inside the L/T transition gap (Figures 9 and 10). Observed spectra are shown in black, individual component templates in blue and red, and convolved templates (i.e., template blended spectra) in orange. The lower subpanels show the resulting flux ratios over standard NIR bandpasses computed from the best-matching template pairs (open orange squares) which are listed in Table 3. The convolved templates provide good matches to the observed spectra but often require unrealistic flux ratios; see the object descriptions in Section 4.2 for details.

dwarfs caught crossing the L/T transition gap. This indicates that $(J-K)_{\rm MKO} \approx 0.9$–$1.4$ mag colors are rare (≈5% of L/T transition dwarfs) but not forbidden.

4.2.2. *Objects above the Gap*

Unresolved binaries that combine the light of two objects will be brighter than single objects with the same effective temperature. We therefore expect to find binaries sitting higher on a CMD than either of the single components. Four objects sit directly above the gap in Figure 9.

The T0 dwarf PSO J180.1475−28.6160 (hereinafter PSO J180.1−28.6; Best et al. 2015) is a candidate binary based on its spectral features. Laser guide star adaptive optics imaging of this object using Keck II/NIRC2 with an angular resolution of 110 mas has detected no sign of a companion (W. Best et al, in preparation). However, our spectral decomposition finds a best match for types L7.5 + T2 with reasonable differences in component fluxes, along with other plausible matches for L5/L6 + T1/T2 dwarfs. At $M_{J_{\rm MKO}} = 14.01 \pm 0.29$ mag, PSO J180.1−28.6 could plausibly be either a bright single T0 dwarf or a late-L + early-T blend.

SDSS J120747.17+024424.8 (SDSS J1207+0244; Hawley et al. 2002) is the NIR T0 spectral standard (Burgasser et al. 2006a), but has also been identified as a candidate L6 + T3 spectral blend (B10). It has not been observed with high-resolution imaging. SDSS J1207+0244 has $M_{J_{\rm MKO}} = 13.72 \pm 0.17$ mag, which would make it the brightest T dwarf in our sample if it is in fact single, almost a full magnitude above the center of the gap. On the other hand, our spectral decomposition finds a good match for L6 + T2, similar to that of B10. We therefore regard SDSS J1207+0244 as a likely binary.

SDSS J133148.92−011651.4 (SDSS J1331−0116) was discovered and assigned a spectral type of L6 by Hawley et al. (2002) based on an optical spectrum. Subsequent analyses of NIR photometry and spectra have noted the object's unusually blue color and atypical spectral features, finding spectral types of L8 ± 2.5 (Knapp et al. 2004), L1 pec (Marocco et al. 2013), L6.5 (Bardalez Gagliuffi et al. 2014), and L6 (Marocco et al. 2015). While this degree of spectral-type discrepancy often points to a blend of binary components with different spectral types, Knapp et al. (2004) and Marocco et al. (2013) explain the spectral features as indicative of low metallicity, consistent with the object's blue colors. SDSS J1331−0116's position on the CMD in Figure 9 is also consistent with that of an unusually blue mid-L dwarf. Our spectral decomposition finds a best pairing of L6 + T5 with $\Delta J = 1.97 \pm 0.18$ mag, much larger than expected from the observed absolute magnitudes of these spectral types ($\Delta J \approx 0.6$ mag; DL12; Filippazzo et al. 2015), adding evidence that this object is not a spectral binary. SDSS J1331−0116 has not been observed with high-resolution imaging.

The T0 dwarf PSO J319.3102−29.6682 (hereinafter PSO J319.3−29.6) is a candidate spectral blend (Best et al. 2015) as well as a candidate member of the β Pictoris Moving Group (Best et al. 2015, 2020). The best pair found by our spectral decomposition is L7.5 + T3, but for this particular blend the T3 dwarf would need to be implausibly fainter (<1 mag) in the J and H bands than the L dwarf. The $M_{J_{\rm MKO}} = 14.05$ mag of PSO J319.3−29.6 is nevertheless consistent with the combined flux from ≈L8 and ≈T2 dwarfs, as well as with the fluxes from brighter single early-T dwarfs. Laser guide star adaptive optics imaging of this object using Keck II/NIRC2 with an angular resolution of 60 mas has detected no sign of a companion (W. Best et al, in preparation). We draw no conclusion about whether PSO J319.3−29.6 is a tighter unresolved binary.

4.2.3. *No Suggestion of Binarity in the Astrometric Solutions*

Astrometric solutions derived from observations of binaries can have larger residuals and/or less accurate results if there is significant photocenter motion due to the binary's orbital motion or if the binary is partially resolved. For five of the seven objects with gap colors described above, the parallaxes come from the Best20 sample. We examined the χ^2_ν for their astrometric solutions for indications of larger residuals and/or poor solutions. For the five objects WISE J0920+4538, PSO J180.1−28.6, SDSS J1207+0244, PSO J272.0−04.9, and PSO J319.3−29.6, the χ^2/degrees of freedom are 22.4/19, 3.6/7, 18.2/23, 12.9/17, and 8.9/11, respectively, all within the range of typical values for the Best20 solutions. We see no indication of χ^2_ν much greater than 1 or widely disparate values that could indicate problems with the solutions due to partially resolved binaries. We also visually examined the solutions for these fits and found no structure in the residuals. The other two gap-color objects (SDSS J0151+1244 and SDSS J1331−0116) do not have published χ^2_ν for their astrometric solutions (Vrba et al. 2004; Smart et al. 2018).

4.2.4. *Objects outside the Volume-limited Sample*

Figure 13 shows the density map of the 25 pc volume-limited sample from Figure 5 overlaid with the L0–T8 objects having published parallaxes that are not part of our volume-limited sample, including apparently sin-

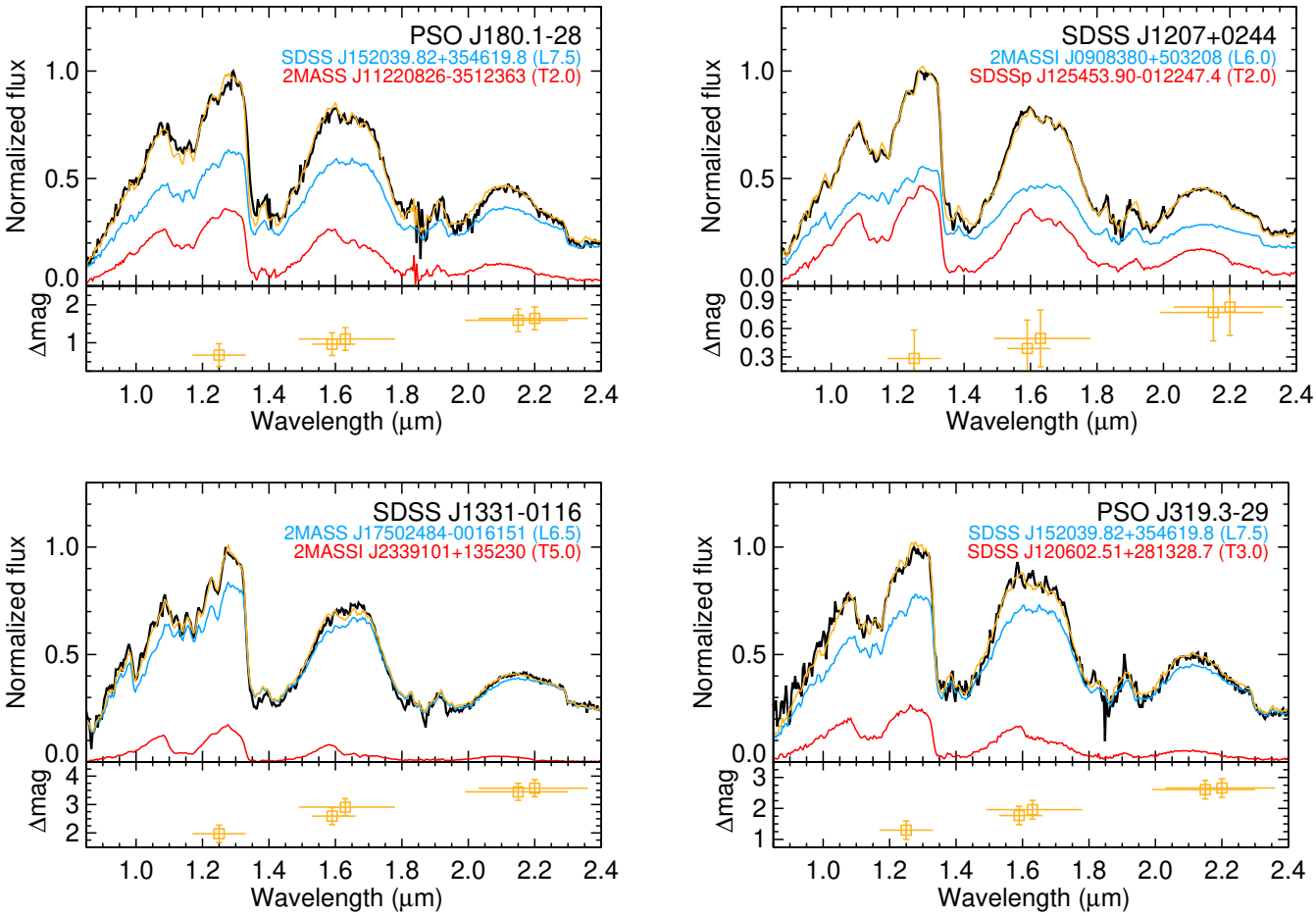

Figure 12. Same as Figure 11, but for objects lying above the L/T transition gap in Figures 9 and 10.

gle objects beyond 25 pc and known binaries at any distance. The known binaries are clearly ≈0.5 − 0.7 brighter as a population than the single objects, indicating that the brightest putatively single objects in the L/T transition may indeed be unrecognized binaries. Most of the objects directly above the gap are known binaries, suggesting that their apparent colors may be a blend of two components on either side of the gap similar to our decompositions for PSO J180.1−28.6 and SDSS J1207+0244. We note there are also several known binaries in our full volume-limited sample (included in Figure 2 and excluded from Figure 5) that lie in the same region directly above the gap.

4.3. *Do Models Predict the L/T Transition Gap?*

The "hybrid" models of SM08 are the only models that agree with the mass-luminosity relationship of L/T transition dwarfs (Dupuy et al. 2015; Dupuy & Liu 2017). Briefly, the hybrid models are a set of evolutionary models coupled to cloudy atmospheres for objects with $T_{\rm eff} > 1400$ K (essentially L dwarfs), clear atmospheres for objects with $T_{\rm eff} \leq 1200$ K (mid-T and later dwarfs), and a linear interpolation between the two for $1200 < T_{\rm eff} \leq 1400$ K (the L/T transition), interpolating the surface boundary condition in $T_{\rm eff}$ for each value of gravity. We note that this modeling of the L/T transition was developed to explore the ramifications of cloud clearing in a notional sense and does not invoke a specific physical explanation for the cloud clearing. The starting and ending $T_{\rm eff}$ for the transition were chosen to approximate the NIR colors of the ultracool dwarf sequence.

We compare the volume-limited synthetic population of L and T dwarfs generated by SM08 from their hybrid models to our volume-limited sample of single objects in Figure 14. The hybrid models generally reproduce the overall shape of the L and T dwarf evolutionary sequence, but predict $(J-K)_{\rm MKO}$ colors that are too blue for early-L and late-T dwarfs and too red for late-L dwarfs. As described in SM08, this synthetic population did not attempt to fully capture the observed scatter within the sequence, which is likely due to vari-

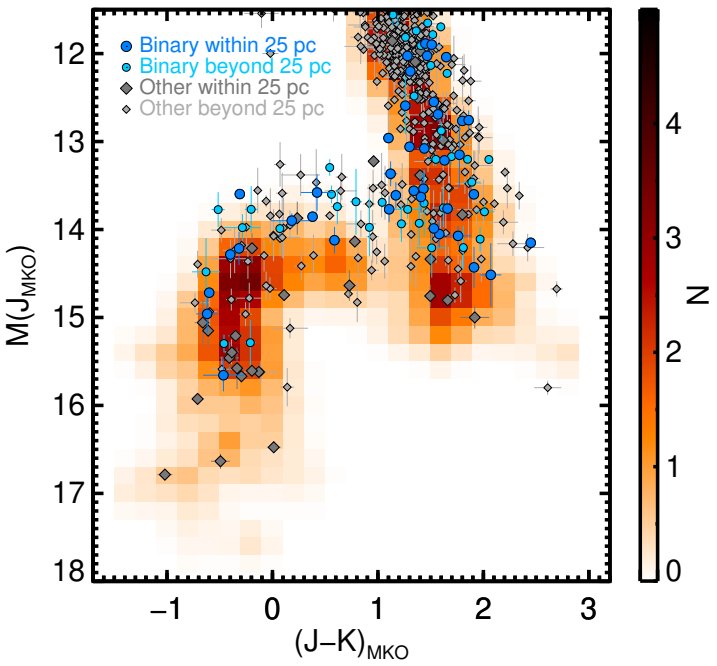

Figure 13. Density map of the CMD from Figure 5, overlaid with objects having parallaxes but excluded from our volume-limited sample of single objects, i.e., known binaries within 25 pc (larger dark blue circles) and beyond 25 pc (smaller light blue circles), and other apparently single objects (including companions) within 25 pc (larger dark gray diamonds) and beyond 25 pc (smaller light gray diamonds). The known binaries are clearly brighter as a population than the single objects, and the brightest apparently single objects in the L/T transition may actually be unrecognized binaries.

ations in gravity, cloud properties, and/or metallicity, but SM08 also generated alternative populations based on different assumptions to explore the effects of these variations. The original synthetic population shown in Figure 14 assumes a 0–10 Gyr uniform age distribution, and the visible scatter in luminosities originates from this spread of ages, as younger brown dwarfs have larger radii (lower gravity) and are therefore more luminous. We note that this uniform age distribution is not consistent with the expected younger age distribution of our sample (Section 2.6).

For comparison, SM08 generated a younger population (0-5 Gyr) that spreads the population somewhat toward brighter absolute magnitudes (lower gravity), better matching the scatter in our volume-limited sample. SM08 also generated an old-skewing population (exponential decline in star-formation rate with characteristic time 5 Gyr) which makes their sequence thinner and clearly a worse match to our volume-limited sample, especially along the L dwarf sequence where the color offset is exaggerated for this population.

The SM08 synthetic population in Figure 14 also assumes a power-law IMF of the form ($\frac{dN}{dM} \propto M^{-\alpha}$) with $\alpha = 1$; we note that while α is poorly constrained by observations, most estimates have found $-0.5 \lesssim \alpha \lesssim 0.5$ (e.g., Allen et al. 2005; Metchev et al. 2008; Burningham et al. 2013; K19). Using a log-normal IMF, SM08 also generated a population with fewer low-mass (and thus low-gravity and low-$T_{\rm eff}$) objects, so this synthetic sequence is narrower toward the cooler end, which is again a poorer match to our volume-limited sample, supporting their initial assumption of a bottom-heavy IMF. Finally, SM08 use cloudless models (appropriate for later-T dwarfs) with a moderate range of metallicities ($-0.9 \leq [M/H] \leq 0.3$) to generate a synthetic population that displays considerably more scatter in its CMD sequence, suggesting that metallicity contributes significantly to the scatter for the T dwarfs in our volume-limited sample.

In the L/T transition, the SM08 hybrid models approximately replicate the slopes of each of the NIR CMDs (Figure 14), and show an uneven distribution of objects across the $J-K$ colors (Figure 15) that is reminiscent of the gap and clumps in our volume-limited sample. However, the peaks of the model color distribution are inconsistent with our sample; in particular, the models predict a "pileup" of objects at the $J-K \approx 1$ mag location of our gap, as well as a clear paucity of objects at $J-K \approx 0.3$–0.5 mag where our volume-limited sample shows only a marginal underdensity. Our volume-limited sample instead has clumps of objects at the beginning ($J-K \approx 1.5$ mag) and end ($J-K \approx -0.5$ mag) of the L/T transition. To quantitatively assess the degree of consistency of these $J-K$ distributions, we performed a two-sided Kolmogorov-Smirnov test and found a probability of 0.06 that the two sets of L/T transition colors are drawn from the same population.

SM08 attributed their pileup to a slowdown in the cooling of L/T transition dwarfs, as heat trapped by L-dwarf clouds takes time to radiate away when the clouds begin to clear. Figure 16 demonstrates that this pileup in $J-K$ corresponds directly to a maximum in the $T_{\rm eff}$ distribution at ≈1300 K. This suggests that the disagreement in color distribution with our volume-limited sample could be mitigated by adjusting the SM08 temperature prescription for the L/T transition to move their pileup to ≈0.5 mag bluer colors (Figure 15).

5. SUMMARY

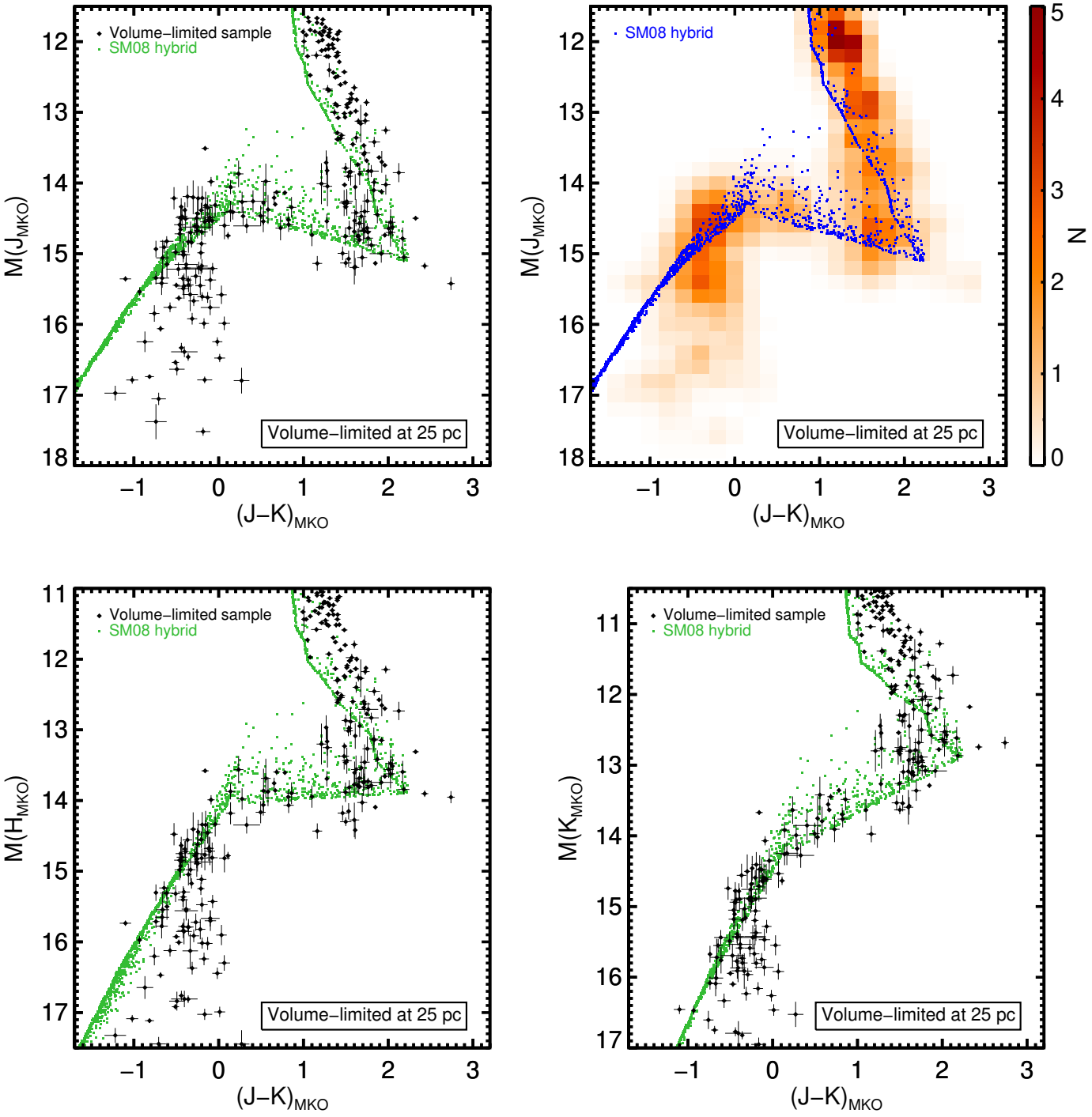

Figure 14. M_J, M_H, and M_K vs. $J-K$ (MKO) color-magnitude diagrams for single objects in our volume-limited sample (black), overlaid on the synthetic population derived by SM08 from their "hybrid" model (green, except in the top right panel where we use blue for visual clarity). The top two panels reproduce the objects and density map from Figure 5. The bottom right panel updates Figure 14 from SM08 with our much larger and volume-limited sample. The hybrid models generally reproduce the shape of the L and T dwarf evolutionary sequence, but predict significantly different $(J-K)_{\rm MKO}$ colors for most L dwarfs and late-T dwarfs. In the L/T transition, the models show an uneven distribution of objects across the $J-K$ colors, but predict an overdensity of objects at the $J-K$ colors of our gap.

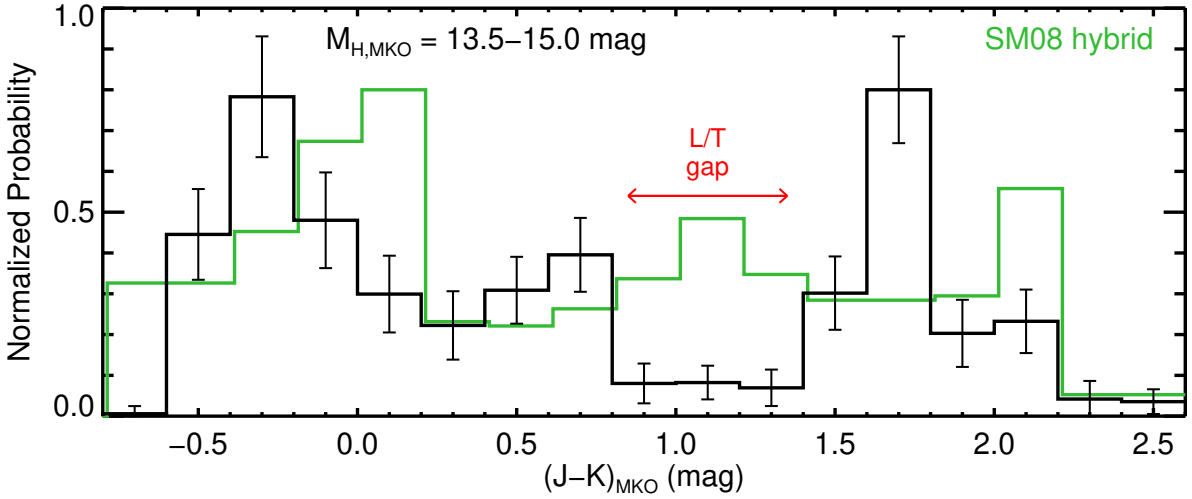

Figure 15. Same as Figure 7, but also including the distribution of $(J-K)_{\rm MKO}$ colors for the synthetic population generated by SM08 from their hybrid model (green, slightly offset horizontally for clarity). As with the volume-limited sample, we computed the SM08 histogram for objects having $13.5 \leq M_{H_{\rm MKO}} \leq 15.0$ mag. The relative pileup of the synthetic population at the colors of our gap (labeled in red) is evident. Shifting the synthetic colors blueward by ≈0.5 mag would appear to improve the agreement with our volume-limited sample (although without a significant gap), highlighting the need for a model that explains the cloud processes that lead to the L/T transition color changes.

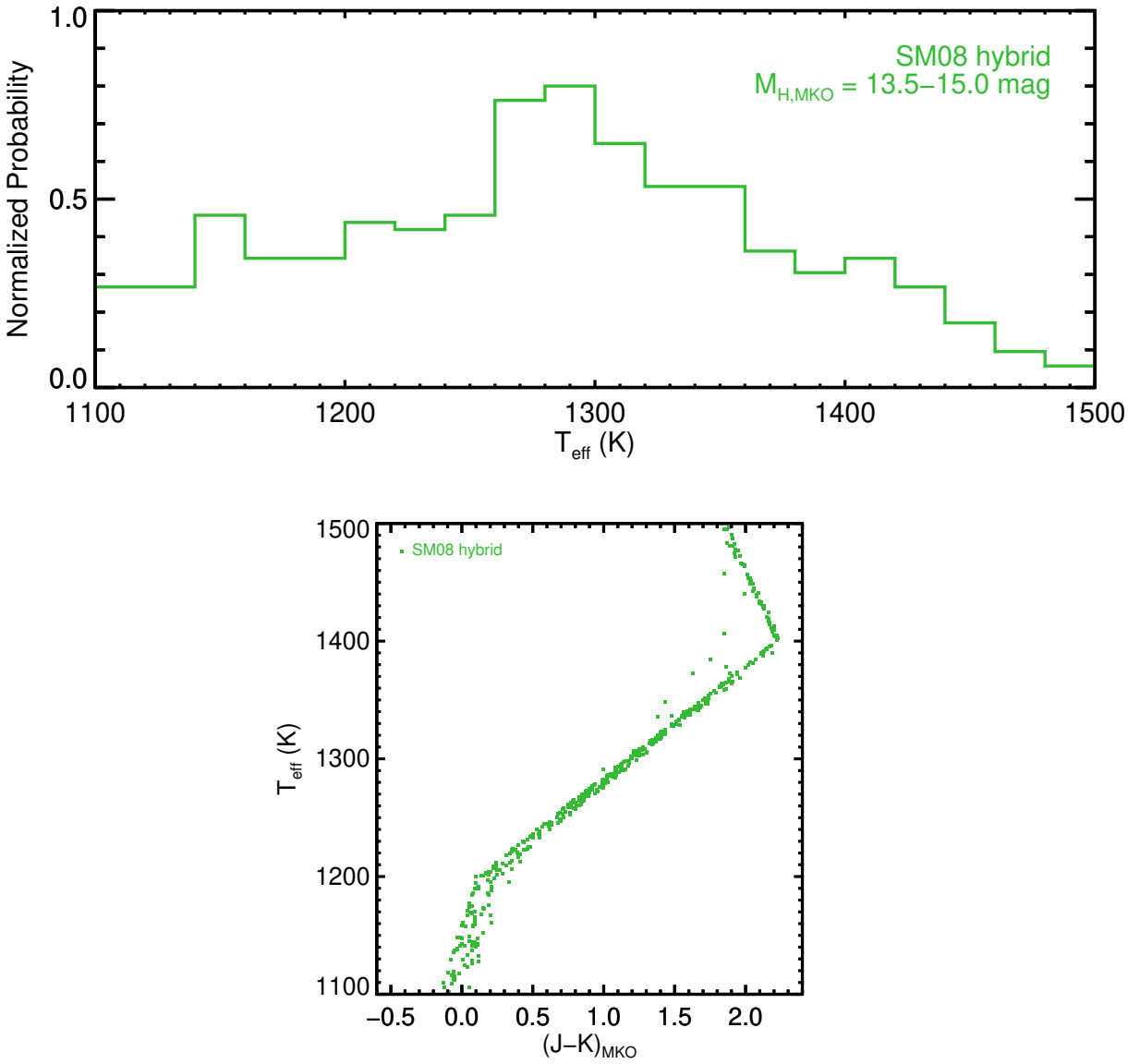

Figure 16. Top: distribution of model-derived $T_{\rm eff}$ for the same synthetic population of single L/T transition dwarfs from the SM08 hybrid model shown in Figure 14. Bottom: $T_{\rm eff}$ vs. $J-K$ (MKO) for this synthetic population. The peak in the $T_{\rm eff}$ distribution near 1300 K corresponds to the pileup at $J-K \approx 1$ mag in Figure 15. Changing the hybrid model's $T_{\rm eff}$ prescription for the L/T transition could shift the $J-K$ color of the pileup and improve agreement with the color distribution of our volume-limited sample.

We present a volume-limited sample of 369 L0–T8 dwarfs chosen entirely by parallaxes, twice as large as any previous parallax-defined ultracool dwarf sample and more than 10 times larger than the last sample covering our full spectral type range. Our sample spans 68.3% of the sky ($\delta = -30°$ to $+60°$), extends out to 25 pc, and combines parallaxes from Best20, Gaia DR2, and the literature. Using the $\langle V/V_{\rm max}\rangle$ statistic, we determine that our sample is 83%±5% complete. Breaking our sample into spectral type bins, we find it is complete for T0–T4.5 dwarfs, 90% ± 8% complete for L dwarfs, and 69% ± 8% complete for T5–T8 dwarfs, making ours the first volume-limited sample to provide an unbiased picture of the L/T transition (spectral types ≈L8–T4). We find a completeness-corrected binary fraction of 9.9%±1.6% for our sample, and another 8.3%±1.7% are companions to main-sequence stars (except for one wide pair of brown dwarfs, SDSS J141624.08+134826.7 and ULAS J141623.94+134836.3). 5.5% ± 1.2% of our sample is young objects ($\lesssim$200 Myr) but only 2.6% ± 1.6% is subdwarfs, implying that the local brown dwarf population is younger than the standard assumption of a

0–10 Gyr age distribution, in agreement with other recent studies.

Our volume-limited sample reveals a previously unidentified gap at $(J-K)_{\rm MKO} \approx 0.9$–$1.4$ mag (spectral types ≈T0–T3; $T_{\rm eff} \approx 1300$ K) in the L/T transition. The gap's existence implies a rapid blueward evolution in color resulting from changes in the atmospheres of these cooling brown dwarfs. The gap is apparent in several other NIR colors spanning y through K bands, but is not present in the MIR $W1-W2$ color. Two objects that sit directly above the gap on the M_J versus $J-K$ CMD are good candidate binaries whose unresolved blends give them gap-like $J-K$ colors. On the other hand, the three objects that lie within the gap all appear to be single objects in the process of crossing the gap.

The evolutionary and atmospheric models that to date have most accurately matched the observed luminosities of L/T transition dwarfs – the "hybrid" models of SM08 – also predict an L/T transition with an uneven distribution of colors, reminiscent of the gap and comparative overdensities in our volume-limited sample. However, our gap is located at $J-K$ colors where the hybrid models predict a pileup of objects, suggesting that a different temperature prescription for the L/T transition is needed.

Our volume-limited sample is ideally suited for unbiased population studies of local L and T dwarfs, including atmospheric characteristics, properties of binaries and companions, space densities, the luminosity function, and assessment of the IMF and birth history underlying the formation of nearby ultracool dwarfs, topics that will be addressed in upcoming papers. Our sample also provides a stepping stone to the expanded volume-limited samples that the upcoming Rubin Observatory Legacy Survey of Space and Time (LSST) will provide.

We thank Didier Saumon and Mark Marley for providing the synthetic population data used in SM08 and for helpful comments on the manuscript. This research has benefitted from the SpeX Prism Library and the SpeX Prism Library Analysis Toolkit, maintained by Adam Burgasser at http://www.browndwarfs.org/spexprism. This work has made use of data from the European Space Agency (ESA) mission Gaia (http://www.cosmos.esa.int/gaia), processed by the Gaia Data Processing and Analysis Consortium (DPAC, http://www.cosmos.esa.int/web/gaia/dpac/consortium). Funding for the DPAC has been provided by national institutions, in particular the institutions participating in the Gaia Multilateral Agreement. This publication makes use of data products from the Two Micron All Sky Survey (2MASS), which is a joint project of the University of Massachusetts and the Infrared Processing and Analysis Center/California Institute of Technology, funded by the National Aeronautics and Space Administration and the National Science Foundation. This research has made use of NASA's Astrophysical Data System and the SIMBAD and Vizier databases operated at CDS, Strasbourg, France. W.M.J.B. received support from NSF grant AST09-09222, and grant HST-GO-15238 provided by STScI and AURA. W.M.J.B., M.C.L., and E.A.M. received support from NSF grant AST-1313455. T.J.D. acknowledges research support from Gemini Observatory. Finally, the authors wish to recognize and acknowledge the very significant cultural role and reverence that the summit of Maunakea has always held within the indigenous Hawaiian community. We are most fortunate to have the opportunity to conduct observations from this mountain.

Software: TOPCAT (Taylor 2005).

APPENDIX

A. CALCULATION OF UNCERTAINTIES FOR $\langle V/V_{\rm max}\rangle$

To estimate the uncertainties on $\langle V/V_{\rm max}\rangle$ for a volume-limited sample or any of its subsets, we need to account for two contributing sources: the parallax uncertainties for the objects that comprise our sample, and the fact that our sample and its subsets have limited sizes and are therefore subject to statistical variations. We calculated the uncertainty on $\langle V/V_{\rm max}\rangle$ due to the individual parallax uncertainties using Monte Carlo resampling.

To assess the impact of these small-number statistical variations on the precision of $\langle V/V_{\rm max}\rangle$, we used an approach motivated by that of K19. They determined 68% confidence limits for a quantized binomial distribution of N measurements of $V/V_{\rm max}$ centered on 0.5 by treating each $V/V_{\rm max}$ measurement as having an equal probability (i.e., $\frac{1}{2}$) of being less than 0.5 or more than 0.5. They then compared their computed $\langle V/V_{\rm max}\rangle$ values to these confidence intervals to assess the distances at which their sample was consistent with completeness. Here, we also rely on binomial statistics, but rather than comparing each of our $\langle V/V_{\rm max}\rangle$ values to the expected dispersion of an assumed

uniform distribution, we directly determine the uncertainty for each $\langle V/V_{\rm max}\rangle$ regardless of the underlying distribution of objects. We calculate the uncertainty on each $\langle V/V_{\rm max}\rangle$, for a sample of N objects, as the standard deviation of a binomial distribution for N trials and probability $p = \langle V/V_{\rm max}\rangle$. The variance for such a binomial distribution is $\sigma^2 = Np(1-p)$, so the standard deviation takes the form

$$\sigma_N = \sqrt{N \times \langle V/V_{\rm max}\rangle \times (1 - \langle V/V_{\rm max}\rangle)}. \tag{A1}$$

We normalized this standard deviation to the $[0, 1]$ range of $\langle V/V_{\rm max}\rangle$ by dividing by N, giving us the uncertainty for $\langle V/V_{\rm max}\rangle$:

$$\sigma(\langle V/V_{\rm max}\rangle)_N = \sqrt{\frac{\langle V/V_{\rm max}\rangle \times (1 - \langle V/V_{\rm max}\rangle)}{N}}. \tag{A2}$$

In practice, we incorporated our calculation of this binomial uncertainty into the same Monte Carlo trials we used to assess the impact of the parallax uncertainties, replacing the $\langle V/V_{\rm max}\rangle$ value calculated for each trial with a random value drawn from a binomial distribution for N events and probability $p = \langle V/V_{\rm max}\rangle$, divided by N. We then took the mean and standard deviation of the $\langle V/V_{\rm max}\rangle$ values from the Monte Carlo trials as our final $\langle V/V_{\rm max}\rangle$ and uncertainty, respectively. For a sufficient number of Monte Carlo trials, this produces the same result as adding the uncertainty due to the parallax errors in quadrature with $\sigma(\langle V/V_{\rm max}\rangle)_N$ from Equation A2.

We note that Avni & Bahcall (1980) determined that for a homogeneously distributed sample of N objects subject to Poisson statistics, $\langle V/V_{\rm max}\rangle$ has dispersion

$$\sigma(\langle V/V_{\rm max}\rangle)_N = \sqrt{\frac{1}{12N}}. \tag{A3}$$

However, as we did not know a priori if our sample and its subsets were homogenously distributed, we adopted our approach (Equation A2), which directly estimates the uncertainty for each of our subsets without requiring them to be uniformly distributed — as indeed they cannot be if $\langle V/V_{\rm max}\rangle < 0.5$. The uncertainties we calculated using our approach were typically a little less than twice as large as those estimated using the method of Avni & Bahcall (1980).

B. CALCULATION OF POISSON AND BINOMIAL UNCERTAINTIES FOR SPACE DENSITY

As in Appendix A, to estimate the uncertainties on our space density calculations for our volume-limited sample, we needed to account for (1) the parallax uncertainties of the individual objects that comprise our sample and (2) the statistical fluctuations due to our finite sample. The latter can be assessed in more than one way depending on the statement we wish to make based on our volume-limited sample.

As a volume-limited sample corrected for incompleteness, our sample is representative of L0–T8 in our neighborhood of the Galaxy (in the Galactic midplane, excluding clusters and star-forming regions). Even in this limited neighborhood, however, our sample contains only a fraction of the total population of L0–T8 dwarfs. A collection of samples with the same volume as ours from around this neighborhood would therefore be expected to show variation in numbers of objects, described by Poisson statistics. So, to make a statement about the space density of L0–T8 dwarfs in the local Galaxy based on our sample, we needed to incorporate Poisson errors into our uncertainties, i.e., $\sigma_N = \sqrt{N}$ for a sample of size N. For the resulting space density uncertainty, we thus have

$$\sigma_{\rm Poisson} = \frac{\sqrt{N}}{V}, \tag{B4}$$

where V is the volume of our sample.

However, if we want to make a statement about the space density of L0–T8 dwarfs specifically within 25 pc of the Sun, we need a different assessment. Our sample does not cover the entire 25 pc volume, so Poisson-like statistical variations are possible, but because our sample covers a substantial fraction of the sky, such variations will be smaller than predicted by Poisson theory. In this context, binomial statistics accounting for the fraction of sky covered by our sample (68.3%) provide a more appropriate estimate of the space density uncertainty. For a set of $N_{\rm full}$ objects drawn from the full sky, each object will be either inside or outside of our sample volume (these are the only two options), and the probability of finding a given object inside our sample area is the same ($p = 0.683$) for every object. Given this situation, the binomial distribution describes the statistics of our sample. The expectation value for the number

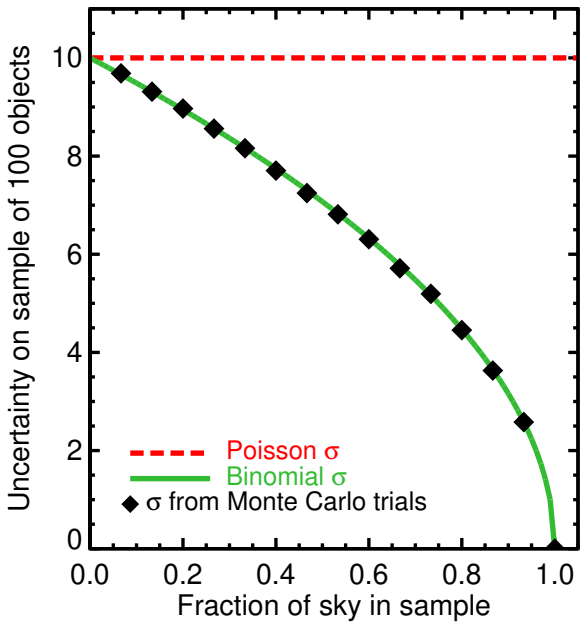

Figure 17. Uncertainties on the number of objects in a sample of 100 objects due to statistical fluctuations, for a range of coverage fractions of the sky, calculated using Monte Carlo trials (black diamonds). The green curve shows the uncertainties derived from the binomial distribution, which clearly match the Monte Carlo results. The red dashed line marks the Poisson uncertainty of $\sqrt{100}$, which is accurate only when the sample is a small fraction of the whole population. Our sample covers 68.3% of the sky, so our estimate of the space density in the full 25 pc volume has an uncertainty 0.56 times the Poisson uncertainty.

of objects in our sample area is $pN_{\rm full}$, with standard deviation $\sqrt{p(1-p)N_{\rm full}}$. Thus, for our observed sample of N objects drawn from a fraction p of the sky, we would expect that $N = pN_{\rm full}$ with uncertainty

$$\sigma_N = \sqrt{N(1-p)}. \tag{B5}$$

This gives us an uncertainty for the space density of

$$\sigma_{\rm binomial} = \frac{\sqrt{N(1-p)}}{V}, \tag{B6}$$

where V is again the volume of our sample.

To demonstrate this approach, we ran Monte Carlo trials to determine the scatter among the sizes of samples covering different fractions of the sky when the mean sample size is 100. Figure 17 shows that the scatter values are predicted by the binomial distribution, i.e., $\sigma_N = \sqrt{N(1-p)}$. Figure 17 also compares these binomial uncertainties to the fixed Poisson uncertainty for a sample of 100 objects. The Poisson distribution approximates the binomial distribution when N is large and p is small (the Poisson limit theorem; Poisson 1837), i.e., when the sample in question is a small fraction of a large full population. As p increases, the binomial uncertainty falls steadily below the Poisson value and reaches zero when the sample covers the whole sky (i.e., a volume-complete sample has no uncertainty for determining the number of objects in that specific volume). For our volume-limited sample with $p = 0.683$, the binomial uncertainty is 0.56 times the Poisson uncertainty.

As with our $\langle V/V_{\rm max}\rangle$ uncertainty calculations in Appendix A, we incorporated our calculation of the Poisson and binomial space density uncertainties into Monte Carlo trials along with the parallax uncertainties. To incorporate the Poisson uncertainties into our calculations, we replaced the number of objects N in each Monte Carlo trial with a random number drawn from a Poisson distribution having mean value $N + 0.5$ (this more accurately accounts for Poissonian likelihoods when N is small; Metchev et al. 2008). To incorporate the binomial errors into our calculations, we replaced the number of objects N in each Monte Carlo trial with a random number drawn from a binomial

distribution for N/p events and sky fraction p. We then computed the mean and standard deviation of the Monte Carlo trials and divided by our sample volume to obtain the final space density uncertainties.

Binomial uncertainties are also the appropriate choice for comparing the space densities of two samples that cover the same volume of space. For example, to compare our volume-limited sample, which covers 68.3% of the full 25 pc volume, to a sample that covers a different (possibly overlapping) portion of the full 25 pc volume, binomial uncertainties should be used for the completeness-corrected space densities of both samples. To compare the space density of our sample with that of a volume-limited sample that covered the entire 25 pc volume, one would use the binomial uncertainties for our sample and no uncertainties for the full-volume sample.

In summary, we have described two distinct ways to estimate the uncertainty on the space density of our volume-limited sample, each appropriate for different uses for our sample. To describe how well our sample represents L and T dwarfs in our general neighborhood of the Galaxy, of which our sample is a small portion, Poisson uncertainties ($\sigma_{\rm Poisson}$, Equation B4) are appropriate. When we narrow our context to the 25 pc volume around the Sun, of which our sample covers a much larger portion, binomial uncertainties ($\sigma_{\rm binomial}$, Equation B6) should be used to describe how precisely our volume-limited sample represents the full 25 pc volume. Binomial uncertainties are also the appropriate uncertainties to use when comparing space densities for two different samples that represent the same volume of space.

C. ADDITIONAL MKO PHOTOMETRY

In Table 4 we list NIR $Y_{\rm MKO}$, $J_{\rm MKO}$, $H_{\rm MKO}$, and $K_{\rm MKO}$ photometry for 934 objects, compiled during the development of our volume-limited sample. Table 4 contains a mixture of new and previously published photometry, but for each of these objects the photometry is new in at least one band. This table includes all of the new photometry presented for 238 L0–T8 dwarfs in our volume-limited sample (Table 1), along with photometry for an additional 696 M, L, and T dwarfs. Most of the new photometry we present here is either synthetic or converted from 2MASS using the methods described in Section 2.5. In addition, we present new $Y_{\rm MKO}$ photometry for 26 objects, $J_{\rm MKO}$ photometry for 2 objects, and $H_{\rm MKO}$ photometry for 3 objects from observations on multiple nights in 2010–2013 using WFCAM (Casali et al. 2007) on the 3.8-meter United Kingdom InfraRed Telescope (UKIRT). The observations were conducted and data were reduced in standard fashion as described in Best et al. (2015).

Table 4. New MKO Photometry

Object	Spectral Type[a] (Optical/NIR)	Y_{MKO} (mag)	J_{MKO} (mag)	H_{MKO} (mag)	K_{MKO} (mag)	References (Disc; SpT; Phot)
WISEA J000131.93−084126.9	.../L1pec	[16.65 ± 0.07]	[15.65 ± 0.05]	[15.12 ± 0.09]	[14.67 ± 0.09]	154; 154; 1
SDSS J000250.98+245413.8	.../L5.5	[18.34 ± 0.23]	[17.09 ± 0.22]	[16.14 ± 0.22]	[15.64 ± 0.22]	43; 43; 1
WISEA J000430.66−260402.3	.../T2 (blue)	[17.28 ± 0.06]	16.18 ± 0.02	[15.83 ± 0.06]	[15.57 ± 0.05]	99; 99; 1,16
2MASS J00054844−2157196	M9/...	[14.07 ± 0.06]	[13.24 ± 0.03]	[12.68 ± 0.02]	[12.18 ± 0.03]	191; 189; 1
2MASSI J0006205−172051	L2.5/L3.0	[16.87 ± 0.08]	[15.61 ± 0.06]	[14.72 ± 0.05]	[13.99 ± 0.05]	108; 108,7; 1
WISEA J000622.67−131955.2	.../L5pec	[17.64 ± 0.14]	[16.59 ± 0.13]	[15.63 ± 0.13]	[15.11 ± 0.13]	154; 154; 1
SDSS J000649.16−085246.3	M9/...	[14.98 ± 0.06]	[14.10 ± 0.03]	[13.61 ± 0.04]	[13.11 ± 0.04]	226; 226; 1
2MASS J00070787−2458042	M7/...	[13.94 ± 0.05]	[13.09 ± 0.02]	[12.50 ± 0.02]	[12.04 ± 0.02]	191; 47; 1
2MASS J00100009−2031122	L0/M8.8:	[15.04 ± 0.05]	[14.10 ± 0.02]	[13.42 ± 0.03]	[12.86 ± 0.03]	47; 47,7; 1
2MASS J00132229−1143006	.../T3pec	...	16.05 ± 0.02	[[15.74 ± 0.22]]	[[15.76 ± 0.22]]	107; 107; 16,1,51
2MASSI J0013578−223520	L4/L5.7	[17.00 ± 0.08]	[15.70 ± 0.06]	[14.68 ± 0.05]	[14.02 ± 0.05]	108; 108,7; 1
2MASS J00135882−1816462	L1/L5pec	[17.69 ± 0.15]	[16.45 ± 0.14]	[15.97 ± 0.13]	[15.02 ± 0.13]	8; 8,14; 1
WISEA J001450.17−083823.4	sdL0/sdM9	[15.10 ± 0.06]	[14.43 ± 0.03]	[13.99 ± 0.05]	[13.75 ± 0.05]	121; 121,154; 1
2MASS J00145575−4844171	L2.5pec/L2.5	[15.20 ± 0.06]	[13.98 ± 0.04]	[13.18 ± 0.03]	[12.70 ± 0.03]	118,164; 118,164; 1
2MASS J00150206+2959323	L7/L7.5pec	[17.26 ± 0.06]	16.15 ± 0.02	15.22 ± 0.03	[14.57 ± 0.05]	119; 119,119; 1,16,57
2MASSW J0015447+351603	L2/L1.0	[14.95 ± 0.05]	13.74 ± 0.02	[12.96 ± 0.02]	[12.25 ± 0.02]	116; 116,7; 1,16
SDSS J001637.62−103911.2	L0/M8.9	[16.35 ± 0.07]	[15.42 ± 0.05]	[14.84 ± 0.10]	[14.51 ± 0.10]	226; 226,7; 1
PSO J004.1834+23.0741	.../T0	[17.60 ± 0.05]	16.50 ± 0.02	15.72 ± 0.02	[15.19 ± 0.05]	14; 14; 1,16,14
2MASS J00165953−4056541	L3.5/L4.5:	[16.59 ± 0.08]	[15.25 ± 0.06]	[14.29 ± 0.04]	[13.41 ± 0.04]	118; 118,37; 1
PSO J004.7148+51.8918	.../L7	[18.04 ± 0.07]	16.70 ± 0.05	[15.53 ± 0.07]	[14.51 ± 0.07]	14; 14; 1,14
SDSS J001911.65+003017.8	L1/L0.4	16.008 ± 0.007	14.843 ± 0.004	[14.25 ± 0.03]	[13.55 ± 0.03]	102; 102,7; 126,1
2MASS J00192626+4614078	M8/M8: INT-G	[13.31 ± 0.05]	[12.55 ± 0.02]	[11.980 ± 0.014]	[11.470 ± 0.014]	45; 45,6; 1
NLTT 1011B	.../L2	[16.67 ± 0.08]	[15.48 ± 0.06]	[15.00 ± 0.07]	[14.30 ± 0.07]	57; 57; 1
2MASS J00193927−3724392	L3:/L2.2 INT-G	[16.74 ± 0.08]	[15.47 ± 0.06]	[14.55 ± 0.06]	[13.67 ± 0.06]	37; 37,76; 1
Koenigstuhl 1B	M9.5/M9.8 FLD-G	[14.48 ± 0.06]	[13.47 ± 0.03]	[12.88 ± 0.03]	[12.28 ± 0.03]	224; 9,76; 1
SDSS J002209.31−011040.2	L0/M8.9	[16.65 ± 0.08]	[15.78 ± 0.07]	[15.15 ± 0.10]	[14.67 ± 0.10]	226; 226,7; 1
PSO J005.6302−06.8669	.../T3	[17.25 ± 0.05]	16.10 ± 0.02	[15.69 ± 0.05]	[15.15 ± 0.05]	16; 16; 1,16
BRI 0021−0214	M9.5/M9.5	[12.81 ± 0.05]	11.754 ± 0.007	11.082 ± 0.011	10.500 ± 0.008	105; 113,79; 1,129
LHS 1074	sdM6/M8	[15.20 ± 0.07]	[14.67 ± 0.04]	[14.27 ± 0.06]	[13.86 ± 0.06]	187; 187,7; 1
2MASS J00282091+2249050	.../L7:	[16.82 ± 0.05]	15.49 ± 0.02	[14.55 ± 0.06]	[13.77 ± 0.06]	37; 37; 1,16
2MASS J00285545−1927165	L0:/L0.7	[15.25 ± 0.06]	[14.14 ± 0.03]	[13.40 ± 0.03]	[12.82 ± 0.03]	189; 189,7; 1
HIP 2397B	.../L0.5	[15.58 ± 0.05]	14.552 ± 0.012	13.912 ± 0.011	[13.37 ± 0.05]	57; 57; 1,57
2MASSW J0030438+313932	L2/L3.2	[16.59 ± 0.07]	[15.42 ± 0.05]	[14.69 ± 0.05]	[14.00 ± 0.05]	115; 115,7; 1
WISE J003110.04+574936.3	.../L9	[15.92 ± 0.05]	14.796 ± 0.012	13.862 ± 0.014	[13.21 ± 0.03]	219; 13; 1,13
DENIS J0031192−384035	L2.5/L2pec	[15.16 ± 0.06]	[14.04 ± 0.03]	[13.47 ± 0.03]	[12.90 ± 0.03]	164,120; 164,120; 1
PSO J007.9194+33.5961	.../L9	[17.48 ± 0.06]	16.38 ± 0.02	[15.46 ± 0.05]	[14.67 ± 0.05]	14; 14; 1,16
2MASSI J0032431−223727	L1/M9.7	[16.35 ± 0.07]	[15.35 ± 0.05]	[14.57 ± 0.05]	[13.94 ± 0.05]	108; 108,7; 1

Table 4 continued

Table 4 *(continued)*

Object	Spectral Type[a] (Optical/NIR)	Y_{MKO} (mag)	J_{MKO} (mag)	H_{MKO} (mag)	K_{MKO} (mag)	References (Disc; SpT; Phot)
EROS−MP J0032−4405	L0 γ/L0: VL-G	[15.81 ± 0.06]	14.68 ± 0.04	13.89 ± 0.03	13.23 ± 0.04	63; 48,6; 1,67
2MASS J00332386−1521309	L4 β/L1: FLD-G	[16.38 ± 0.08]	[15.22 ± 0.06]	[14.26 ± 0.04]	[13.39 ± 0.04]	90; 48,6; 1
2MASSI J0034568−070601	L3/L4.3	[16.74 ± 0.08]	[15.46 ± 0.06]	[14.65 ± 0.06]	[13.92 ± 0.06]	108; 108,7; 1
SDSS J003609.26+241343.3	.../L5.5	[18.28 ± 0.22]	[16.96 ± 0.20]	[16.19 ± 0.19]	[15.64 ± 0.19]	43; 43; 1
HD 3651B	.../T7.5	[17.12 ± 0.06]	16.16 ± 0.03	16.68 ± 0.04	16.87 ± 0.05	173; 150; 1,150
2MASS J00412179+3547133	sdM9/d/sdM9	[16.79 ± 0.10]	[15.89 ± 0.08]	[15.79 ± 0.12]	[15.14 ± 0.12]	27; 27,27; 1
LHS 1135	M6.5/M7	[14.50 ± 0.06]	[13.92 ± 0.03]	[13.49 ± 0.04]	[13.12 ± 0.04]	85; 187,7; 1
2MASSW J0045214+163445	L2 β/L2: VL-G	[14.22 ± 0.05]	[12.98 ± 0.02]	[12.12 ± 0.02]	[11.33 ± 0.02]	228; 48,6; 1
WISE J004542.56+361139.1	.../T5	[16.81 ± 0.05]	15.91 ± 0.02	[16.13 ± 0.05]	[16.07 ± 0.05]	156; 156; 1,16
WISEP J004701.06+680352.1	L7pec/L7 INT-G	[16.80 ± 0.09]	[15.48 ± 0.07]	[14.04 ± 0.03]	[13.01 ± 0.03]	93; 95,95; 1
WISE J004945.61+215120.0	.../T8.5	[17.29 ± 0.17]	[16.44 ± 0.16]	16.72 ± 0.02	[16.80 ± 0.17]	156; 156; 1,122
SIPS J0050−1538	L1:/L0.5	[14.68 ± 0.05]	13.69 ± 0.02	[13.15 ± 0.03]	[12.62 ± 0.03]	53; 47,7; 1,16
2MASSW J0051107−154417	L3.5/L5:	[16.51 ± 0.05]	15.16 ± 0.02	[14.25 ± 0.04]	[13.44 ± 0.04]	116; 116,37; 1,16
RG 0050−2722	M8/...	[14.47 ± 0.06]	[13.58 ± 0.03]	[13.05 ± 0.03]	[12.51 ± 0.03]	184; 113; 1
2MASS J00531899−3631102	L3.5/L4:	[15.62 ± 0.06]	[14.38 ± 0.03]	[13.56 ± 0.03]	[12.92 ± 0.03]	118; 118,160; 1
LHS 1166	sdM6.5/M7	[14.79 ± 0.06]	[14.23 ± 0.03]	[13.82 ± 0.04]	[13.55 ± 0.04]	187; 187,7; 1
SDSS J005705.55−084624.2	L0/M9.3	[16.62 ± 0.08]	[15.66 ± 0.06]	[14.98 ± 0.08]	[14.33 ± 0.08]	226; 226,7; 1
WISEA J005757.64+201304.0	sdL7/sdL7	[17.32 ± 0.11]	[16.20 ± 0.09]	[15.53 ± 0.13]	[14.96 ± 0.13]	121; 121,121; 1
2MASSW J0058425−065123	L0/L0.6 INT-G	[15.34 ± 0.06]	[14.25 ± 0.03]	[13.49 ± 0.03]	[12.87 ± 0.03]	116; 116,76; 1
LHS 132	M8/M8.1	[11.89 ± 0.05]	[11.10 ± 0.02]	[10.54 ± 0.02]	[10.05 ± 0.02]	205; 192,7; 1
2MASSI J0103320+193536	L6 β/L6: INT-G	[17.45 ± 0.09]	16.16 ± 0.08	14.94 ± 0.06	14.09 ± 0.06	116; 67,6; 1,67
2MASS J01071607−1517577	M7/...	[14.07 ± 0.05]	[13.31 ± 0.02]	[12.76 ± 0.02]	[12.26 ± 0.02]	47; 47; 1
2MASS J01165457−1357342	M9/...	[15.13 ± 0.06]	[14.18 ± 0.03]	[13.57 ± 0.03]	[12.95 ± 0.03]	189; 189; 1
SDSS J011912.22+240331.6	.../T2	[18.14 ± 0.05]	17.02 ± 0.02	[16.55 ± 0.05]	[16.21 ± 0.05]	43; 43; 1,16
WISEPA J012333.21+414203.9	.../T7	[18.10 ± 0.05]	16.99 ± 0.02	[17.25 ± 0.05]	[17.25 ± 0.05]	120; 120; 1,16
SSSPM J0124−4240	M8/M8.4	[13.98 ± 0.05]	[13.12 ± 0.02]	[12.53 ± 0.02]	[12.02 ± 0.02]	142; 189,7; 1
SERC 296A	M6/M6: VL-G	[13.32 ± 0.06]	[12.65 ± 0.03]	[12.16 ± 0.02]	[11.77 ± 0.02]	218; 218,6; 1
2MASSI J0125369−343505	L2/L1.2	16.646 ± 0.006	15.396 ± 0.003	14.574 ± 0.004	[13.88 ± 0.05]	108; 108,7; 64,1
CTI 012657.5+280202	M8.5/...	[14.89 ± 0.06]	[13.95 ± 0.03]	[13.42 ± 0.03]	[12.84 ± 0.03]	112; 113; 1
2MASSW J0129122+351758	L4/L3.0 FLD-G	[18.06 ± 0.17]	[16.72 ± 0.16]	[15.43 ± 0.08]	[14.68 ± 0.08]	115; 115,76; 1
2MASS J01303563−4445411	.../M9	[14.94 ± 0.06]	[14.02 ± 0.03]	[13.45 ± 0.03]	[12.85 ± 0.03]	189; 189; 1
2MASS J01311838+3801554	L4:/L1.5	[15.91 ± 0.05]	14.63 ± 0.02	[13.77 ± 0.03]	[13.03 ± 0.03]	47; 47,37; 1,16
LHS 1265	esdM9.5/M8.8	[15.76 ± 0.08]	[15.23 ± 0.06]	[14.84 ± 0.13]	[14.74 ± 0.13]	187; 161,7; 1
WISE J013525.64+171503.4	.../T6	[18.03 ± 0.06]	17.07 ± 0.02	[17.43 ± 0.06]	[17.74 ± 0.07]	156; 156; 1,16
PSO J024.1519+37.6443	.../M7	[18.97 ± 0.12]	18.23 ± 0.10	17.46 ± 0.10	[17.15 ± 0.12]	14; 14; 1,14
WISEPC J013836.59−032221.2	.../T3	[17.16 ± 0.05]	16.13 ± 0.02	[15.68 ± 0.05]	[15.27 ± 0.05]	120; 120; 1,16
2MASSW J0141032+180450	L1/L4.5	[15.01 ± 0.06]	[13.83 ± 0.03]	[13.10 ± 0.03]	[12.48 ± 0.03]	228; 47,228; 1
2MASS J01414839−1601196	.../L7:	[17.25 ± 0.06]	16.06 ± 0.02	[15.15 ± 0.05]	[14.34 ± 0.05]	119; 119; 1,16
2MASS J01415823−4633574	L0 γ/L0: VL-G	[16.00 ± 0.07]	[14.78 ± 0.04]	[13.96 ± 0.03]	[13.06 ± 0.03]	117; 48,6; 1

Table 4 continued

Table 4 *(continued)*

Object	Spectral Type[a] (Optical/NIR)	Y_{MKO} (mag)	J_{MKO} (mag)	H_{MKO} (mag)	K_{MKO} (mag)	References (Disc; SpT; Phot)
2MASS J01443536−0716142	L5/L5	[15.52 ± 0.05]	14.15 ± 0.02	[13.09 ± 0.02]	[12.26 ± 0.02]	135; 135,160; 1,16
2MASS J01460119−4545263	M9/...	[15.35 ± 0.06]	[14.37 ± 0.04]	[13.60 ± 0.03]	[13.01 ± 0.03]	189; 189; 1
2MASS J01472702+4731142	.../L1.5	[16.94 ± 0.10]	[15.80 ± 0.09]	[14.92 ± 0.06]	[14.26 ± 0.06]	119; 119; 1
2MASSW J0147334+345311	L0.5/L1.0	[15.98 ± 0.06]	[14.90 ± 0.04]	[14.24 ± 0.04]	[13.55 ± 0.04]	115; 115,7; 1
2MASSW J0149090+295613	M9.5/M9.7	[14.49 ± 0.05]	[13.41 ± 0.02]	[12.65 ± 0.02]	[11.96 ± 0.02]	115; 115,7; 1
WISEPA J015010.86+382724.3	.../T0	[17.05 ± 0.05]	15.93 ± 0.02	[15.11 ± 0.05]	[14.54 ± 0.05]	120; 120; 1,16
GD 280B	.../M9	[16.91 ± 0.10]	[16.01 ± 0.08]	[15.05 ± 0.08]	[14.52 ± 0.08]	57; 57; 1
2MASS J01550354+0950003	L5/L3.2 INT-G	16.109 ± 0.007	14.731 ± 0.004	13.884 ± 0.003	[13.11 ± 0.04]	189; 189,76; 126,1
HIP 9269B	.../L6	[17.30 ± 0.05]	16.13 ± 0.02	15.082 ± 0.014	14.30 ± 0.02	57; 57; 1,57
2MASS J02042212−3632308	M9/...	[14.05 ± 0.06]	[13.23 ± 0.03]	[12.66 ± 0.03]	[12.17 ± 0.03]	142; 142; 1
SDSS J020551.36−075925.0	L3/L2	[17.19 ± 0.09]	[15.97 ± 0.08]	[15.25 ± 0.08]	[14.33 ± 0.08]	198,119; 198,119; 1
SDSS J020608.97+223559.2	.../L4.5 blue	[17.66 ± 0.12]	[16.47 ± 0.11]	[15.61 ± 0.13]	[15.15 ± 0.13]	43; 201; 1
PSO J031.5651+20.9097	.../T5.5	[17.85 ± 0.06]	16.83 ± 0.02	17.02 ± 0.07	[16.85 ± 0.06]	14; 14; 1,16,14
WISEPA J020625.26+264023.6	.../L8 (red)	[17.60 ± 0.12]	[16.42 ± 0.11]	[15.16 ± 0.08]	[14.50 ± 0.08]	120; 139; 1
2MASSW J0208183+254253	L1/...	[15.06 ± 0.05]	13.91 ± 0.02	[13.18 ± 0.03]	[12.57 ± 0.03]	116; 116; 1,16
2MASSW J0208236+273740	L5/L5	[16.99 ± 0.05]	15.66 ± 0.02	[14.64 ± 0.05]	[13.86 ± 0.05]	116; 116,37; 1,16
2MASSW J0208549+250048	L5/L5.9	[17.42 ± 0.11]	[16.12 ± 0.09]	[15.06 ± 0.07]	[14.38 ± 0.07]	116; 116,7; 1
WISE J021010.25+400829.6	.../T4.5	[17.70 ± 0.20]	[16.58 ± 0.19]	[16.12 ± 0.18]	[16.61 ± 0.20]	156; 156; 1
2MASSI J0213288+444445	L1.5/...	...	13.41 ± 0.02	[[12.81 ± 0.02]]	[[12.19 ± 0.02]]	45; 45; 16,1,51
2MASSI J0218291−313322	L3/L5.5	15.802 ± 0.005	14.607 ± 0.002	13.770 ± 0.002	[13.13 ± 0.04]	45; 45,160; 64,1
SSSPM J0219−1939	L1/L1:	[15.14 ± 0.06]	[14.06 ± 0.03]	[13.41 ± 0.03]	[12.89 ± 0.03]	141; 142,160; 1
WISEPC J022322.39−293258.1	.../T7.5	[18.08 ± 0.07]	17.10 ± 0.05	17.30 ± 0.11	[17.59 ± 0.08]	120; 120; 1,120
HIP 11161B	.../L1.5	[17.55 ± 0.05]	16.51 ± 0.02	15.86 ± 0.02	15.25 ± 0.03	57; 57; 1,57
2MASSI J0224367+253704	L2/L2.3	[17.79 ± 0.12]	[16.53 ± 0.10]	[15.49 ± 0.08]	[14.67 ± 0.08]	116; 116,7; 1
CFBDS J022644.65−062522.0	.../T3	18.36 ± 0.02	17.575 ± 0.013	17.26 ± 0.02	[17.22 ± 0.06]	3; 3; 64,1
2MASS J02271036−1624479	L1/L0.5:	[14.66 ± 0.05]	13.53 ± 0.02	[12.70 ± 0.03]	[12.13 ± 0.03]	189; 189,160; 1,16
2MASSW J0228110+253738	L0:/L0	[14.84 ± 0.05]	13.76 ± 0.02	[13.06 ± 0.03]	[12.46 ± 0.03]	228; 45,228; 1,16
2MASS J02284243+1639329	L0:/M8.7	[14.05 ± 0.05]	13.09 ± 0.02	[12.38 ± 0.02]	[11.80 ± 0.02]	189; 189,7; 1,16
2MASS J02301551+2704061	L0:/M9.4	[15.27 ± 0.06]	[14.26 ± 0.03]	[13.54 ± 0.02]	[12.96 ± 0.02]	47; 47,7; 1
WISE J023038.90−022554.0	.../L8:pec	[18.00 ± 0.05]	16.86 ± 0.02	[15.88 ± 0.05]	[15.07 ± 0.05]	219; 219; 1,16
2MASS J02304442−3027275	.../L1	[16.85 ± 0.09]	[15.78 ± 0.08]	[15.29 ± 0.11]	[14.86 ± 0.11]	119; 119; 1
DENIS J0230450−095305	L0/L0.9	[15.90 ± 0.06]	[14.77 ± 0.03]	[13.98 ± 0.04]	[13.38 ± 0.04]	164; 164,7; 1
WISE J023318.05+303030.5	.../T6	[17.54 ± 0.05]	16.52 ± 0.02	16.79 ± 0.02	[17.03 ± 0.06]	156; 156; 1,16,122
NLTT 8245B	.../M7	[15.73 ± 0.07]	[14.89 ± 0.05]	[14.28 ± 0.06]	[13.79 ± 0.06]	57; 57; 1
SDSS J023547.56−084919.8	L2/L2	[16.62 ± 0.07]	[15.52 ± 0.05]	[14.88 ± 0.07]	[14.17 ± 0.07]	102; 102,7; 1
GJ 1048B	L1/L1	[13.82 ± 0.50]	12.66 ± 0.50	[12.80 ± 0.08]	12.17 ± 0.08	88; 88,88; 1,67
SDSSp J023617.93+004855.0	L6/L6.5	17.17 ± 0.02	[16.01 ± 0.08]	15.131 ± 0.008	14.550 ± 0.008	79; 102,123; 126,1
PSO J039.6352−21.7746	.../L2.6: INT-G	[15.69 ± 0.06]	14.73 ± 0.04	14.24 ± 0.05	13.68 ± 0.05	5; 5; 1,5
2MASSI J0239424−173547	L0/M9	[15.31 ± 0.06]	[14.25 ± 0.03]	[13.59 ± 0.03]	[13.02 ± 0.03]	45; 45,160; 1

Table 4 continued

Table 4 *(continued)*

Object	Spectral Type[a] (Optical/NIR)	Y_{MKO} (mag)	J_{MKO} (mag)	H_{MKO} (mag)	K_{MKO} (mag)	References (Disc; SpT; Phot)
2MASS J02411151−0326587	L0 γ/L1: VL-G	[16.90 ± 0.08]	[15.72 ± 0.06]	[14.87 ± 0.05]	[14.00 ± 0.05]	47; 48,6; 1
LSPM J0241+2553B	.../L1	[18.11 ± 0.19]	[16.99 ± 0.18]	[16.10 ± 0.15]	[15.30 ± 0.15]	57; 57; 1
2MASSI J0241536−124106	L2:/L1.9	[16.74 ± 0.09]	[15.56 ± 0.07]	[14.72 ± 0.06]	[13.91 ± 0.06]	45; 45,7; 1
2MASSW J0242435+160739	L1.5/L1.7	[16.82 ± 0.07]	[15.72 ± 0.05]	[15.07 ± 0.06]	[14.32 ± 0.06]	115; 115,7; 1
SDSS J024256.98+212319.6	.../L4	[18.15 ± 0.20]	[16.90 ± 0.19]	[16.01 ± 0.23]	[15.43 ± 0.23]	43; 43; 1
WISE J024512.62−345047.8	.../T8	[18.65 ± 0.10]	17.77 ± 0.09	[18.27 ± 0.10]	[18.05 ± 0.11]	156; 156; 1,156
SDSS J024749.90−163112.6	.../T2:	[18.17 ± 0.19]	[17.03 ± 0.18]	[16.25 ± 0.19]	[15.63 ± 0.19]	43; 43; 1
BR B0246-1703	M8/...	[13.35 ± 0.06]	12.50 ± 0.03	11.81 ± 0.03	11.45 ± 0.03	223; 114; 1,127
TVLM 831-154910	.../M7.3 VL-G	[13.54 ± 0.06]	[12.86 ± 0.03]	[12.33 ± 0.02]	[11.88 ± 0.02]	220; 76; 1
2MASSI J0251148−035245	L3/L1	...	12.94 ± 0.02	[[12.30 ± 0.02]]	[[11.64 ± 0.02]]	45; 45,228; 16,1,51
DENIS-P J025503.3−470049	L8/L9	[14.28 ± 0.07]	13.14 ± 0.05	12.22 ± 0.05	11.56 ± 0.05	163; 118,28; 1,67
HIP 13589B	.../M7.5	[15.61 ± 0.06]	14.79 ± 0.03	14.226 ± 0.012	[13.82 ± 0.05]	4,57; 57; 1,57
2MASS J02572581−3105523	L8/L8:	15.660 ± 0.004	[14.59 ± 0.04]	[13.60 ± 0.03]	[12.87 ± 0.03]	118; 118,160; 64,1
2MASS J03001631+2130205	.../L6pec	[17.05 ± 0.09]	[15.81 ± 0.08]	[14.81 ± 0.06]	[14.30 ± 0.06]	119; 119; 1
WISEA J030119.39−231921.1	.../T1 (sl. blue)	[17.72 ± 0.05]	16.63 ± 0.02	[15.89 ± 0.05]	[15.42 ± 0.05]	99; 99; 1,16
2MASSI J0302012+135814	L3/L2.7:	[17.77 ± 0.13]	[16.48 ± 0.12]	[15.52 ± 0.08]	[14.60 ± 0.08]	116; 116,7; 1
WISEA J030601.66−033059.0	sdL0/sdL0	[15.16 ± 0.06]	[14.40 ± 0.03]	[14.10 ± 0.04]	[13.95 ± 0.05]	121; 121,121; 1
SSSPM J0306−3648	M8/M8.7	[12.49 ± 0.05]	[11.65 ± 0.02]	[11.13 ± 0.02]	[10.60 ± 0.02]	142; 142,7; 1
2MASSW J0306268+154514	L6:/L6.0:	[18.29 ± 0.19]	[17.03 ± 0.18]	[16.33 ± 0.14]	[15.11 ± 0.14]	116; 116,7; 1
WISEPA J030724.57+290447.6	.../T6.5	18.63 ± 0.06	17.34 ± 0.03	[17.75 ± 0.14]	18.08 ± 0.12	120; 120; 125,1,126
WISEA J030845.36+325923.1	.../L1pec	[16.68 ± 0.08]	[15.73 ± 0.06]	[15.27 ± 0.07]	[14.69 ± 0.07]	154; 154; 1
2MASSW J0309088−194938	L4.5/L4.9	[17.01 ± 0.08]	[15.68 ± 0.06]	[14.74 ± 0.06]	[14.04 ± 0.06]	116; 116,7; 1
2MASS J03101401−2756452	L5/L6.5	[17.10 ± 0.09]	[15.72 ± 0.07]	[14.75 ± 0.06]	[13.94 ± 0.06]	47; 47,7; 1
2MASSW J0310599+164816	L8/L9	[17.06 ± 0.10]	[15.92 ± 0.08]	[15.02 ± 0.07]	[14.30 ± 0.07]	116; 116,28; 1
2MASS J03140344+1603056	L0/L0: FLD-G	[13.51 ± 0.05]	[12.47 ± 0.02]	[11.87 ± 0.02]	[11.21 ± 0.02]	189; 189,6; 1
PSO J048.9806+07.5414	.../L6: (blue)	[18.09 ± 0.07]	16.95 ± 0.04	16.19 ± 0.04	[15.65 ± 0.06]	14; 14; 1,14
PSO J049.1124+17.0885	.../L9.5	[18.16 ± 0.06]	17.06 ± 0.04	16.43 ± 0.04	[15.93 ± 0.06]	14; 14; 1,14
PSO J049.1159+26.8409	.../T2.5	[17.17 ± 0.05]	16.11 ± 0.02	15.82 ± 0.02	[15.50 ± 0.05]	14; 14; 1,14
2MASSI J0316451−284852	L0:/L1.7 INT-G	[15.67 ± 0.06]	[14.53 ± 0.04]	[13.85 ± 0.04]	[13.09 ± 0.04]	45; 45,76; 1
2MASS J03201720−1026124	M8/...	[14.66 ± 0.06]	[13.85 ± 0.03]	[13.15 ± 0.03]	[12.67 ± 0.03]	47; 47; 1
2MASSW J0320284−044636	M8/L0.5	[14.13 ± 0.05]	13.18 ± 0.02	[12.59 ± 0.03]	[12.11 ± 0.03]	228; 45,228; 1,16
LP 412-31	M8/...	[12.59 ± 0.05]	[11.73 ± 0.02]	[11.12 ± 0.02]	[10.62 ± 0.02]	113; 113; 1
WISEA J032301.86+562558.0	.../L7	[17.06 ± 0.05]	15.78 ± 0.02	[14.70 ± 0.05]	[13.75 ± 0.05]	154; 154; 1,16
2MASS J03231002−4631237	L0 γ/M9.4 VL-G	[16.64 ± 0.09]	[15.35 ± 0.07]	[14.41 ± 0.05]	[13.67 ± 0.05]	189; 48,69; 1
2MASS J03250136+2253039	L3/L3.3	[16.64 ± 0.07]	[15.37 ± 0.05]	[14.40 ± 0.05]	[13.75 ± 0.05]	47; 47,7; 1
WISE J032547.72+083118.2	.../T7	[17.14 ± 0.09]	[16.29 ± 0.07]	[16.19 ± 0.08]	[16.39 ± 0.09]	156; 156; 1
2MASSW J0326137+295015	L3.5/L4.6	[16.70 ± 0.05]	15.421 ± 0.004	14.545 ± 0.003	13.820 ± 0.004	115; 115,7; 1,148
2MASS J03264225−2102057	L5 β/L4.1 FLD-G	[17.55 ± 0.11]	[16.05 ± 0.09]	[14.89 ± 0.07]	[13.89 ± 0.07]	90; 69,76; 1
PSO J052.2746+13.3754	.../T3.5	[17.34 ± 0.05]	16.23 ± 0.02	[15.93 ± 0.05]	[15.73 ± 0.05]	16; 16; 1,16

Table 4 continued

Table 4 *(continued)*

Object	Spectral Type[a] (Optical/NIR)	Y_{MKO} (mag)	J_{MKO} (mag)	H_{MKO} (mag)	K_{MKO} (mag)	References (Disc; SpT; Phot)
LSPM J0330+3504	.../d/sdM7	[16.62 ± 0.12]	[15.98 ± 0.11]	[15.39 ± 0.15]	[15.29 ± 0.15]	7; 7; 1
LEHPM 1-3365	.../d/sdM7	[16.31 ± 0.09]	[15.78 ± 0.07]	[15.34 ± 0.14]	[14.91 ± 0.14]	7; 7; 1
PSO J052.7214−03.8409	.../L9:	[17.36 ± 0.05]	16.26 ± 0.02	15.24 ± 0.02	[14.58 ± 0.05]	14; 14; 1,14
2MASS J03320043−2317496	M8/...	[14.39 ± 0.06]	[13.58 ± 0.03]	[13.02 ± 0.03]	[12.48 ± 0.03]	189; 189; 1
LEHPM 3396	M9/M9.4	[12.14 ± 0.05]	11.31 ± 0.02	10.84 ± 0.03	10.36 ± 0.02	178; 178,7; 1,67
2MASS J03354535+0658058	M8/...	[14.25 ± 0.06]	[13.38 ± 0.03]	[12.78 ± 0.03]	[12.23 ± 0.02]	189; 189; 1
2MASSW J0337036−175807	L4.5/L4.3 FLD-G	[16.99 ± 0.05]	15.51 ± 0.02	[14.50 ± 0.04]	[13.56 ± 0.04]	116; 116,76; 1,16
WISE J033713.43+114824.5	.../M7	[15.62 ± 0.07]	[14.95 ± 0.05]	[14.61 ± 0.08]	[14.24 ± 0.08]	219; 219; 1
PSO J054.8149−11.7792	.../L3:	[18.01 ± 0.07]	16.71 ± 0.05	15.75 ± 0.03	[14.97 ± 0.07]	14; 14; 1,14
PSO J055.0493−21.1704	.../T2	[18.02 ± 0.07]	16.95 ± 0.05	16.29 ± 0.05	[16.12 ± 0.07]	14; 14; 1,14
PSO J057.2893+15.2433	.../L7 (red)	19.04 ± 0.19	17.29 ± 0.06	16.04 ± 0.05	14.90 ± 0.02	14; 14; 1,14
2MASS J03521086+0210479	M9/M8.6	[13.99 ± 0.06]	[13.05 ± 0.03]	[12.47 ± 0.02]	[11.94 ± 0.02]	110; 189,7; 1
SDSS J035308.54+103056.0	L1/L0.9	[16.53 ± 0.08]	[15.41 ± 0.06]	[14.72 ± 0.05]	[14.16 ± 0.05]	198; 198,7; 1
2MASS J03552337+1133437	L5 γ/L3: VL-G	[15.46 ± 0.06]	[13.95 ± 0.02]	[12.60 ± 0.02]	11.502 ± 0.001	188; 48,6; 1,125
DENIS-P J035726.9−441730	L0 β/L0 β	[15.41 ± 0.06]	[14.32 ± 0.03]	[13.61 ± 0.03]	[12.88 ± 0.03]	21; 48,69; 1
2MASS J04012977−4050448	L0:/L0.0	[15.52 ± 0.06]	[14.49 ± 0.04]	[13.79 ± 0.03]	[13.15 ± 0.03]	189; 189,7; 1
WISE J040137.21+284951.7	L3/L2.5	[14.61 ± 0.05]	13.34 ± 0.02	[12.50 ± 0.02]	[11.80 ± 0.02]	42; 42,42; 1,16
LSPM J0402+1730	.../sdM7	[16.11 ± 0.08]	[15.57 ± 0.06]	[15.12 ± 0.15]	14.836 ± 0.010	7; 7; 1,126
WISE J040418.01+412735.6	L2/L2pec	[15.37 ± 0.05]	14.08 ± 0.02	[13.17 ± 0.02]	12.343 ± 0.002	42; 42,42; 1,16,148
2MASS J04062677−3812102	L0 γ/L1: VL-G	[17.94 ± 0.14]	[16.72 ± 0.13]	[15.80 ± 0.12]	[15.08 ± 0.12]	119; 119,6; 1
2MASS J04070752+1546457	L3.5/L3: FLD-G	[16.86 ± 0.08]	[15.39 ± 0.06]	[14.41 ± 0.04]	13.588 ± 0.004	189; 189,6; 1,126
2MASS J04070885+1514565	.../T5	[16.88 ± 0.05]	15.67 ± 0.02	[15.84 ± 0.05]	15.88 ± 0.03	27; 28; 1,16,126
2MASS J04081032+0742494	M8/...	[14.40 ± 0.05]	[13.56 ± 0.02]	[12.95 ± 0.04]	12.398 ± 0.001	189; 189; 1,126
2MASSI J0408290−145033	L2/L4.5	[15.33 ± 0.05]	14.15 ± 0.02	[13.41 ± 0.02]	[12.80 ± 0.02]	228; 45,228; 1,16
2MASSI J0409095+210439	L3/L3.4	[16.66 ± 0.05]	15.373 ± 0.004	14.535 ± 0.004	13.822 ± 0.005	116; 116,7; 1,148
PSO J062.3459+11.1794	.../T3.5	...	16.17 ± 0.02	[[15.73 ± 0.15]]	15.88 ± 0.02	16; 16; 16,1,51,126
Hya03	L0.5/...	[16.82 ± 0.09]	[15.70 ± 0.07]	[14.85 ± 0.06]	14.226 ± 0.006	143; 143; 1,126
WISEPA J041054.48+141131.6	.../T6	[18.00 ± 0.11]	[16.93 ± 0.09]	[17.32 ± 0.12]	17.82 ± 0.20	120; 120; 1,126
2MASSI J0415195−093506	T8/T8	[16.39 ± 0.06]	15.32 ± 0.03	15.70 ± 0.03	15.83 ± 0.03	24; 25,28; 1,123
2MASS J04174743−2129191	M8/...	[14.76 ± 0.06]	[13.86 ± 0.03]	[13.21 ± 0.03]	[12.65 ± 0.03]	47; 47; 1
2MASS J04203904+2355502	L1/L1	[15.99 ± 0.06]	[14.85 ± 0.03]	[14.13 ± 0.03]	13.476 ± 0.003	149; 149,149; 1,126
2MASS J04221413+1530525	M6: γ/M6: VL-G	[13.64 ± 0.05]	12.65 ± 0.03	11.75 ± 0.05	11.24 ± 0.03	59; 67,6; 1,59
2MASS J04270723+0859027	M8/...	[13.77 ± 0.06]	[12.89 ± 0.03]	[12.25 ± 0.03]	11.726 ± 0.001	189; 189; 1,126
DENIS-P J04272708−1127143	M7/M7.9	[14.49 ± 0.06]	[13.71 ± 0.03]	[13.13 ± 0.03]	[12.65 ± 0.03]	164; 164,7; 1
2MASSI J0428510−225323	L0.5/M9.9	[14.60 ± 0.05]	[13.47 ± 0.02]	[12.73 ± 0.03]	[12.10 ± 0.03]	108; 108,7; 1
2MASS J04305157−0849007	M8/...	[13.74 ± 0.05]	[12.87 ± 0.02]	[12.26 ± 0.02]	[11.75 ± 0.02]	45; 45; 1
Cl* Melotte 25 DKJ 14784e	M9/...	[16.38 ± 0.06]	15.45 ± 0.03	14.82 ± 0.07	14.18 ± 0.02	59; 59; 1,59
2MASS J04351455−1414468	M8 γ/M7: VL-G	[13.04 ± 0.06]	[11.81 ± 0.03]	[10.68 ± 0.02]	[9.90 ± 0.02]	45; 69,6; 1
LP 775-031	M7/M8.0	[11.12 ± 0.06]	[10.36 ± 0.03]	[9.83 ± 0.03]	[9.33 ± 0.02]	166; 197,7; 1

Table 4 continued

Table 4 *(continued)*

Object	Spectral Type[a] (Optical/NIR)	Y_{MKO} (mag)	J_{MKO} (mag)	H_{MKO} (mag)	K_{MKO} (mag)	References (Disc; SpT; Phot)
WISEA J043535.82+211508.9	sdL0/sdL0	[15.76 ± 0.05]	14.995 ± 0.003	14.750 ± 0.003	14.575 ± 0.009	121; 121,121; 1,148
Hya12	L3.5/L6: (red)	[18.24 ± 0.06]	16.89 ± 0.03	15.80 ± 0.02	14.987 ± 0.014	143; 143,14; 1,14
2MASS J04362054−4218523	L0:/L0.4	[15.57 ± 0.06]	[14.44 ± 0.04]	[13.73 ± 0.04]	[13.12 ± 0.04]	189; 189,7; 1
2MASS J04362788−4114465	M8 β/M9: VL-G	[13.85 ± 0.06]	[13.05 ± 0.03]	[12.49 ± 0.03]	[12.02 ± 0.03]	45; 69,6; 1
2MASS J04373705+2331080	L0/L1:	[18.47 ± 0.06]	17.24 ± 0.02	16.162 ± 0.011	15.20 ± 0.02	151; 151,15; 1,148,126
2MASSI J0439010−235308	L6.5/L6	[15.51 ± 0.06]	14.31 ± 0.03	13.44 ± 0.03	12.77 ± 0.02	45; 45,37; 1,67
PSO J070.3773+04.7333	.../T4.5	[17.57 ± 0.06]	16.33 ± 0.02	16.46 ± 0.04	[16.33 ± 0.06]	14; 14; 1,16,14
Hya04	M9.5/...	[16.59 ± 0.08]	[15.56 ± 0.06]	[15.03 ± 0.07]	14.255 ± 0.006	143; 143; 1,126
2MASSI J0443058−320209	L5/L6.4:	[16.42 ± 0.07]	[15.19 ± 0.05]	[14.43 ± 0.06]	[13.86 ± 0.06]	108; 108,7; 1
2MASS J04433761+0002051	M9 γ/L0: VL-G	[13.40 ± 0.06]	[12.45 ± 0.03]	[11.86 ± 0.02]	[11.18 ± 0.02]	102; 69,6; 1
2MASS J04441479+0543573	M8/...	[14.47 ± 0.05]	[13.64 ± 0.02]	[13.03 ± 0.03]	[12.50 ± 0.03]	189; 189; 1
PSO J071.4708+36.4930	.../L6:	[17.84 ± 0.06]	16.72 ± 0.03	15.79 ± 0.02	[14.98 ± 0.06]	14; 14; 1,14
2MASSI J0445538−304820	L2/...	[14.45 ± 0.06]	13.31 ± 0.03	12.61 ± 0.02	11.94 ± 0.02	45; 45; 1,67
WISE J044633.45−242956.8	.../L6 (blue)	17.40 ± 0.03	16.29 ± 0.02	15.58 ± 0.02	15.13 ± 0.02	219; 14; 1,14
Hya09	L2/...	[17.91 ± 0.13]	[16.61 ± 0.12]	[15.36 ± 0.09]	14.604 ± 0.007	143; 143; 1,126
PSO J071.8769−12.2713	.../T2:	[17.76 ± 0.06]	16.69 ± 0.02	16.08 ± 0.04	[15.65 ± 0.06]	14; 14; 1,16,14
2MASS J04474307−1936045	L5:/L4:	[17.26 ± 0.05]	15.91 ± 0.02	[14.87 ± 0.05]	[13.99 ± 0.05]	37; 37,37; 1,16
WISEPA J044853.29−193548.5	.../T5pec	[17.51 ± 0.06]	16.63 ± 0.02	[16.94 ± 0.06]	[17.30 ± 0.08]	120; 120; 1,16
2MASSI J0451009−340214	L0.5/L0.6	[14.60 ± 0.05]	[13.50 ± 0.02]	[12.90 ± 0.03]	[12.27 ± 0.03]	45; 45,7; 1
LEHPM 2-59	esdM8/...	[16.00 ± 0.07]	[15.50 ± 0.05]	[15.26 ± 0.08]	[14.74 ± 0.11]	29; 32; 1
2MASSI J0453264−175154	L3:/L2.5 INT-G	[16.26 ± 0.05]	14.99 ± 0.02	[14.14 ± 0.04]	[13.44 ± 0.04]	45; 45,76; 1,16
WISEPA J045853.89+643452.9	.../T8.5	[18.02 ± 0.09]	17.13 ± 0.07	17.45 ± 0.11	[17.74 ± 0.10]	157; 120; 1,81
WISEA J045921.21+154059.2	.../sdL0	[15.61 ± 0.06]	[14.91 ± 0.03]	[14.65 ± 0.06]	14.247 ± 0.006	121; 121; 1,126
WISEPA J050003.05−122343.2	.../T8	[18.69 ± 0.06]	17.88 ± 0.02	18.13 ± 0.12	[18.06 ± 0.08]	120; 120; 1,16,120
2MASS J05002100+0330501	L4/L4.2 FLD-G	[14.93 ± 0.05]	[13.60 ± 0.02]	[12.76 ± 0.02]	[12.04 ± 0.02]	189; 189,76; 1
2MASS J05012406−0010452	L4 γ/L3: VL-G	[16.26 ± 0.06]	[14.89 ± 0.04]	[13.78 ± 0.04]	[12.92 ± 0.04]	189; 48,6; 1
2MASSI J0502134+144236	L0/M8.9	[15.20 ± 0.06]	[14.24 ± 0.03]	[13.45 ± 0.03]	12.944 ± 0.002	198; 198,7; 1,126
PSO J076.7092+52.6087	.../T4.5	[16.61 ± 0.05]	15.44 ± 0.02	15.47 ± 0.02	15.60 ± 0.03	14; 14; 1,14
PSO J077.1034+24.3810	.../L2: VL-G	[18.08 ± 0.06]	17.06 ± 0.04	16.31 ± 0.04	15.59 ± 0.03	15; 15; 1,14
LSR J0510+2713	M8/...	[11.477 ± 0.055]	[10.640 ± 0.020]	[9.994 ± 0.018]	9.537 ± 0.019	186; 133; 1
2MASS J05103520−4208140	.../T5	[17.25 ± 0.10]	[16.02 ± 0.09]	[16.29 ± 0.28]	[16.10 ± 0.28]	144; 144; 1
2MASSI J0512063−294954	L5 γ/L3.8 INT-G	[16.86 ± 0.08]	[15.38 ± 0.06]	[14.26 ± 0.04]	[13.25 ± 0.04]	45; 69,76; 1
WISEPA J051317.28+060814.7	.../T6.5	...	[[15.97 ± 0.06]]	[[16.19 ± 0.08]]	[[16.17 ± 0.11]]	120; 120; 1,120
PSO J078.9904+31.0171	.../L1.5 VL-G	[17.67 ± 0.06]	16.67 ± 0.03	15.96 ± 0.03	15.30 ± 0.03	14; 14; 1,14
2MASS J05161597−3332046	L3:/L4.5:	[17.16 ± 0.08]	[15.82 ± 0.06]	[14.89 ± 0.05]	[13.96 ± 0.05]	37; 37,37; 1
2MASS J05170548−4154413	M9/...	[14.36 ± 0.05]	[13.42 ± 0.02]	[12.79 ± 0.03]	[12.25 ± 0.02]	189; 189; 1
2MASS J05173766−3349027	M8/...	[12.89 ± 0.05]	[11.96 ± 0.02]	[11.38 ± 0.02]	[10.81 ± 0.02]	155; 45; 1
2MASS J05184616−2756457	L1 γ/L1: VL-G	[16.43 ± 0.07]	[15.19 ± 0.04]	[14.36 ± 0.04]	[13.57 ± 0.04]	47; 68,6; 1
2MASS J05185995−2828372	L7/T1pec	[17.12 ± 0.11]	15.87 ± 0.10	14.86 ± 0.07	14.11 ± 0.07	46; 118,28; 1,67

Table 4 continued

Table 4 *(continued)*

Object	Spectral Type[a] (Optical/NIR)	Y_{MKO} (mag)	J_{MKO} (mag)	H_{MKO} (mag)	K_{MKO} (mag)	References (Disc; SpT; Phot)
WISE J052126.29+102528.4	.../T7.5	[15.71 ± 0.05]	14.87 ± 0.02	[15.27 ± 0.05]	[15.00 ± 0.05]	18; 18; 1,16
2MASSI J0523382−140302	L2.5/L5	···	[[13.02 ± 0.03]]	[[12.27 ± 0.03]]	[[11.62 ± 0.03]]	45; 45,228; 1,51
WISEPA J052536.33+673952.3	.../T6pec	[18.49 ± 0.06]	17.49 ± 0.04	17.87 ± 0.05	[18.36 ± 0.08]	120; 120; 1,120
2MASS J05264348−4455455	M9.5/L1	[15.08 ± 0.06]	[14.04 ± 0.03]	[13.37 ± 0.03]	[12.68 ± 0.03]	110; 118,110; 1
WISE J052857.68+090104.4	.../L1 VL-G	[17.18 ± 0.12]	[16.21 ± 0.11]	[15.52 ± 0.12]	[14.93 ± 0.11]	219; 39; 1
2MASS J05301261+6253254	L1/L1.1	[15.09 ± 0.06]	[14.00 ± 0.03]	[13.34 ± 0.03]	[12.69 ± 0.03]	189; 189,7; 1
2MASS J05341594−0631397	M8 γ/M8: VL-G	[16.78 ± 0.09]	[16.02 ± 0.08]	[15.44 ± 0.10]	[14.90 ± 0.10]	119; 119,6; 1
2MASS J05345844−1511439	M9/...	[14.12 ± 0.06]	[13.16 ± 0.03]	[12.57 ± 0.03]	[11.95 ± 0.02]	47; 47; 1
2MASS J05361998−1920396	L2 γ/L2: VL-G	[17.10 ± 0.09]	[15.68 ± 0.08]	[14.76 ± 0.06]	[13.81 ± 0.06]	47; 68,6; 1
HIP 26653B	.../L1.5	[15.81 ± 0.05]	14.67 ± 0.02	[13.98 ± 0.03]	[13.30 ± 0.03]	57; 57; 1,16
2MASS J05402325−0906326	.../M8.0 INT-G	[15.44 ± 0.06]	[14.51 ± 0.04]	[13.89 ± 0.05]	[13.37 ± 0.05]	76; 76; 1
WISEPA J054231.26−162829.1	.../T6.5	···	16.28 ± 0.02	[[16.63 ± 0.10]]	[[16.76 ± 0.14]]	120; 120; 16,1,120
2MASS J05431887+6422528	L1/L1.9 INT-G	[14.64 ± 0.06]	[13.51 ± 0.03]	[12.74 ± 0.02]	[12.03 ± 0.02]	189; 189,76; 1
2MASS J05441150−2433018	M8/...	[13.32 ± 0.05]	[12.51 ± 0.02]	[11.93 ± 0.03]	[11.44 ± 0.02]	47; 47; 1
WISE J054601.19−095947.5	.../T5	[17.04 ± 0.05]	15.98 ± 0.02	[16.24 ± 0.05]	[16.43 ± 0.06]	156; 156; 1,16
WISEA J055007.94+161051.9	.../L2	[15.64 ± 0.05]	14.36 ± 0.02	[13.56 ± 0.03]	[12.81 ± 0.03]	121; 121; 1,16
PSO J087.7749−12.6537	.../L8	[17.67 ± 0.06]	16.55 ± 0.02	15.52 ± 0.03	[14.75 ± 0.05]	14; 14; 1,16,14
PSO J088.0452+43.2123	.../L4pec	[17.55 ± 0.06]	16.29 ± 0.03	15.52 ± 0.02	14.80 ± 0.03	14; 14; 1,14
PSO J088.3324−24.4439	.../L1:	[17.74 ± 0.11]	16.84 ± 0.09	16.48 ± 0.12	[15.61 ± 0.11]	14; 14; 1,14
PSO J088.5709−00.1430	.../T4.5	[17.28 ± 0.05]	16.08 ± 0.02	[16.06 ± 0.05]	[15.99 ± 0.05]	16; 16; 1,16
PSO J089.1751−09.4513	.../T5.5	[17.66 ± 0.06]	16.46 ± 0.02	[16.58 ± 0.06]	[16.66 ± 0.07]	16; 16; 1,16
2MASS J05575096−1359503	M7/M7: VL-G	[13.61 ± 0.05]	[12.82 ± 0.02]	[12.19 ± 0.02]	[11.69 ± 0.02]	47,216; 216,6; 1
APMPM J0559−2903	esdM7/...	[15.42 ± 0.06]	[14.88 ± 0.04]	[14.48 ± 0.04]	[14.44 ± 0.07]	214; 214; 1
2MASS J06020638+4043588	.../T4.5	[16.38 ± 0.05]	15.28 ± 0.02	[15.39 ± 0.05]	[15.41 ± 0.05]	144; 144; 1,16
2MASS J06022216+6336391	L1:/L1.7 FLD-G	[15.41 ± 0.06]	[14.22 ± 0.03]	[13.43 ± 0.02]	[12.66 ± 0.02]	189; 189,76; 1
LSR J0602+3910	L1/L2: INT-G	[13.35 ± 0.05]	[12.23 ± 0.02]	[11.51 ± 0.02]	[10.83 ± 0.02]	196; 196,6; 1
2MASS J06050196−2342270	L0:/M9.8	[15.52 ± 0.06]	[14.47 ± 0.04]	[13.80 ± 0.03]	[13.12 ± 0.03]	47; 47,7; 1
WISEP J060738.65+242953.4	L8/L9	[15.35 ± 0.06]	[14.12 ± 0.03]	[13.12 ± 0.03]	[12.46 ± 0.02]	41; 42,42; 1
WISEA J060742.13+455037.0	.../L2.5	[16.15 ± 0.05]	14.91 ± 0.02	[14.11 ± 0.03]	[13.31 ± 0.03]	121; 121; 1,16
2MASS J06085283−2753583	M8.5 γ/L0: VL-G	[14.46 ± 0.06]	[13.53 ± 0.03]	[12.95 ± 0.03]	[12.33 ± 0.03]	45; 193,6; 1
HD 253662B	.../L0.5	16.511 ± 0.009	15.653 ± 0.007	[14.91 ± 0.05]	[14.29 ± 0.05]	57; 57; 57,1
WISEPA J061407.49+391236.4	.../T6	···	[[16.70 ± 0.16]]	[[16.42 ± 0.25]]	···	120; 120; 1,120
SIPS J0614−2019	.../L2	[15.89 ± 0.06]	[14.74 ± 0.03]	[13.97 ± 0.04]	[13.36 ± 0.04]	54; 160; 1
WISE J061437.73+095135.0	.../T7	[17.54 ± 0.05]	16.44 ± 0.02	[16.66 ± 0.05]	[16.51 ± 0.05]	156; 156; 1,16
2MASS J06143818+3950357	.../L9:	[17.63 ± 0.05]	16.54 ± 0.02	[15.67 ± 0.05]	[15.04 ± 0.05]	174; 174; 1,16
DENIS-P J0615493−010041	L2:/L1.0	[14.75 ± 0.06]	[13.70 ± 0.03]	[13.05 ± 0.03]	[12.52 ± 0.03]	179; 179,7; 1
2MASS J06195260−2903592	M6/M6: VL-G	[16.01 ± 0.06]	[15.08 ± 0.04]	[14.24 ± 0.05]	[13.41 ± 0.05]	45; 45,139; 1
WISEPA J062309.94−045624.6	.../T8	[18.04 ± 0.06]	17.10 ± 0.02	[17.34 ± 0.07]	[17.26 ± 0.09]	120; 120; 1,16
WISE J062442.37+662625.6	L1/L1	[14.46 ± 0.07]	[13.36 ± 0.05]	[12.84 ± 0.03]	[12.25 ± 0.03]	42; 42,42; 1

Table 4 continued

Table 4 *(continued)*

Object	Spectral Type[a] (Optical/NIR)	Y_{MKO} (mag)	J_{MKO} (mag)	H_{MKO} (mag)	K_{MKO} (mag)	References (Disc; SpT; Phot)
2MASS J06244595−4521548	L5:/L6	[15.67 ± 0.06]	14.36 ± 0.03	13.38 ± 0.03	12.55 ± 0.03	189; 189,160; 1,67
WISEPA J062542.21+564625.5	.../T6	···	16.73 ± 0.02	[[16.96 ± 0.10]]	[[16.96 ± 0.15]]	120; 120; 16,1,120
SDSS J062621.22+002934.2	L1/L0.3	[16.87 ± 0.11]	[15.87 ± 0.09]	[15.27 ± 0.12]	[14.84 ± 0.12]	102; 102,7; 1
WISEPA J062720.07−111428.8	.../T6	[16.37 ± 0.07]	[15.25 ± 0.05]	[15.50 ± 0.18]	[15.51 ± 0.18]	120; 120; 1
WISE J062905.13+241804.9	.../T2	[17.45 ± 0.05]	16.34 ± 0.02	[15.72 ± 0.05]	[15.12 ± 0.05]	156; 156; 1,16
LSPM J0632+5053B	.../L1.5	[17.74 ± 0.06]	16.61 ± 0.03	15.86 ± 0.02	[15.17 ± 0.06]	57; 57; 1,57
2MASS J06411840−4322329	L1.5/L2.4:	[14.79 ± 0.06]	13.67 ± 0.03	12.96 ± 0.03	12.42 ± 0.03	189; 189,7; 1,67
WISE J064205.58+410155.5	.../L9 (red)	[17.30 ± 0.05]	16.15 ± 0.02	15.113 ± 0.014	14.306 ± 0.012	156; 14; 1,14
2MASS J06431685−1843375	.../M8	[13.92 ± 0.06]	[12.97 ± 0.02]	[12.34 ± 0.02]	[11.78 ± 0.02]	72; 72; 1
WISE J064336.71−022315.4	.../L8	···	[[15.35 ± 0.05]]	[[14.44 ± 0.05]]	[[13.60 ± 0.06]]	158; 158; 1,51
PSO J101.8428+39.7462	.../M9.5	[17.74 ± 0.06]	16.83 ± 0.03	16.20 ± 0.04	15.61 ± 0.02	14; 14; 1,14
WISEA J064750.85−154616.4	.../L9.5	···	15.15 ± 0.02	[[14.35 ± 0.06]]	[[13.72 ± 0.06]]	213; 213; 16,1,51
HIP 32728B	.../M6.5	[15.28 ± 0.06]	[14.48 ± 0.03]	[13.98 ± 0.04]	[13.49 ± 0.04]	57; 57; 1
DENIS-P J0652197−253450	L0/M9.2	[13.67 ± 0.05]	[12.72 ± 0.02]	[12.09 ± 0.02]	[11.49 ± 0.02]	179; 179,7; 1
PSO J103.0927+41.4601	.../T0	[16.47 ± 0.05]	15.361 ± 0.014	14.51 ± 0.03	13.95 ± 0.03	13; 13; 1,13
2MASSI J0652307+471034	L4.5/L6.5	[14.74 ± 0.05]	13.38 ± 0.02	[12.47 ± 0.02]	[11.67 ± 0.02]	45; 45,37; 1,16
SDSS J065405.63+652805.4	.../L6:	[17.32 ± 0.10]	[16.08 ± 0.09]	[15.27 ± 0.08]	[14.58 ± 0.08]	43; 43; 1
WISEPA J065609.60+420531.0	T2/T3	[16.19 ± 0.05]	15.27 ± 0.02	[14.98 ± 0.05]	[14.99 ± 0.05]	120; 180,120; 1,16
WISEA J065958.55+171710.9	.../L2	···	14.74 ± 0.02	[[13.82 ± 0.03]]	[[13.00 ± 0.03]]	121; 121; 16,1,51
WISE J070159.79+632129.2	.../T2.5	[16.70 ± 0.08]	[15.63 ± 0.06]	[15.15 ± 0.11]	[14.88 ± 0.11]	156; 14; 1
ESO 207-61	M9/M8.5	[14.04 ± 0.06]	[13.19 ± 0.03]	[12.60 ± 0.03]	[12.09 ± 0.03]	194; 194,120; 1
2MASSW J0708213+295035	L5/L5.4:	[17.86 ± 0.13]	[16.64 ± 0.12]	[15.65 ± 0.09]	[14.74 ± 0.09]	116; 116,7; 1
PSO J108.4590+38.2086	.../L7	[17.94 ± 0.06]	16.68 ± 0.03	15.66 ± 0.02	14.84 ± 0.01	14; 14; 1,14
WISEA J071552.38−114532.9	.../L4pec	[15.41 ± 0.05]	14.18 ± 0.02	[13.58 ± 0.05]	[12.78 ± 0.04]	121; 121; 1,16
DENIS-P J0716478−063037	L1:/L1.1	[14.85 ± 0.05]	13.799 ± 0.002	13.131 ± 0.001	12.556 ± 0.002	179; 179,7; 1,148
2MASSW J0717163+570543	L3/L6.5	[15.92 ± 0.06]	[14.57 ± 0.03]	[13.68 ± 0.03]	[12.92 ± 0.03]	228; 189,228; 1
PSO J109.4864+46.5278	.../T0	[18.20 ± 0.07]	17.06 ± 0.04	16.45 ± 0.04	15.86 ± 0.03	14; 14; 1,14
2MASS J07231462+5727081	L1/L0.2	[15.05 ± 0.05]	13.92 ± 0.02	[13.23 ± 0.03]	[12.59 ± 0.03]	189; 189,7; 1,16
2MASS J07290002−3954043	.../T8pec	[16.60 ± 0.09]	[15.66 ± 0.08]	[16.05 ± 0.09]	[16.50 ± 0.10]	144; 144; 1
SDSS J073519.59+410850.4	L0/M8.9	[16.54 ± 0.09]	[15.73 ± 0.07]	[15.32 ± 0.10]	[14.82 ± 0.10]	226; 226,7; 1
SDSS J073922.26+661503.5	.../T1.5:	[17.78 ± 0.14]	[16.69 ± 0.13]	[16.09 ± 0.18]	[15.87 ± 0.18]	43; 43; 1
2MASSW J0740096+321203	L4.5/L4.0	[17.43 ± 0.10]	[16.12 ± 0.09]	[14.95 ± 0.06]	[14.20 ± 0.06]	116; 116,7; 1
PSO J115.0659+59.0473	.../M9.5	17.77 ± 0.07	16.76 ± 0.04	16.13 ± 0.04	15.56 ± 0.03	14; 14; 1,14
2MASS J07410404−0359495	L0/...	···	14.240 ± 0.003	[13.72 ± 0.04]	[13.18 ± 0.03]	124; 124; 168,1
2MASS J07415784+0531568	.../L1.5	[15.44 ± 0.05]	14.33 ± 0.02	[13.69 ± 0.03]	[13.10 ± 0.03]	119; 119; 1,16
SDSS J074201.41+205520.5	.../T5	[16.98 ± 0.06]	15.60 ± 0.03	15.95 ± 0.03	16.06 ± 0.03	123; 28; 1,123
WISEPA J074457.15+562821.8	.../T8	···	17.27 ± 0.02	[[17.65 ± 0.12]]	[[17.70 ± 0.20]]	120; 120; 16,1,120
SDSS J074756.31+394732.9	L0/M8.3	[16.02 ± 0.06]	[15.05 ± 0.04]	[14.22 ± 0.05]	[13.70 ± 0.05]	102; 102,7; 1
PSO J117.0600−01.6779	.../T5.5	[17.50 ± 0.05]	16.34 ± 0.02	[16.57 ± 0.06]	[16.44 ± 0.06]	16; 16; 1,16

Table 4 continued

Table 4 *(continued)*

Object	Spectral Type[a] (Optical/NIR)	Y_{MKO} (mag)	J_{MKO} (mag)	H_{MKO} (mag)	K_{MKO} (mag)	References (Disc; SpT; Phot)
SDSS J074838.61+174332.9	.../L5 FLD-G	[17.41 ± 0.05]	16.16 ± 0.02	15.26 ± 0.02	14.502 ± 0.013	7; 14; 1,14
SDSS J075054.74+445418.7	L0/M8pec	[15.89 ± 0.08]	[15.08 ± 0.06]	[14.52 ± 0.07]	[14.22 ± 0.07]	226; 226,219; 1
DENIS-P J0751164−253043	L1.5/L1.1	[14.15 ± 0.05]	[13.10 ± 0.02]	[12.57 ± 0.02]	[11.97 ± 0.02]	179; 179,7; 1
NLTT 18587B	.../M7.5	[17.71 ± 0.20]	[16.85 ± 0.20]	[15.99 ± 0.22]	[15.87 ± 0.20]	57; 57; 1
SDSS J075752.70+091410.0	.../L3.7:	[17.09 ± 0.10]	[15.80 ± 0.08]	[14.91 ± 0.06]	[14.07 ± 0.06]	7; 7; 1
HIP 38939B	.../T4.5	[16.84 ± 0.05]	15.78 ± 0.02	[15.87 ± 0.05]	[15.98 ± 0.05]	56; 56; 1,16
SDSS J075840.33+324723.4	T3/T2	[15.82 ± 0.05]	14.73 ± 0.02	14.21 ± 0.04	[13.90 ± 0.06]	123; 180,28; 1,16,176
SDSS J080048.13+465825.5	L2/L1.3	[16.60 ± 0.09]	[15.47 ± 0.07]	[14.62 ± 0.08]	[14.29 ± 0.08]	102; 102,7; 1
2MASSW J0801405+462850	L6.5/L5.5	[17.32 ± 0.14]	[16.20 ± 0.13]	[15.53 ± 0.10]	[14.52 ± 0.10]	116; 116,37; 1
2MASS J08041429+0330474	M8.5/...	[14.62 ± 0.06]	[13.65 ± 0.03]	[13.03 ± 0.03]	[12.41 ± 0.02]	189; 189; 1
SDSS J080531.84+481233.0	L4/L9:	[15.81 ± 0.06]	14.61 ± 0.03	14.01 ± 0.03	13.51 ± 0.03	102; 102,123; 1,123
WISE J080700.23+413026.8	.../L8pec	[17.08 ± 0.05]	15.93 ± 0.02	[15.00 ± 0.05]	[14.25 ± 0.05]	219; 219; 1,16
SDSS J080959.01+443422.2	.../L5.4 INT-G	[17.69 ± 0.05]	16.42 ± 0.02	[15.34 ± 0.05]	[14.39 ± 0.05]	123; 76; 1,16
NLTT 19109B	.../M8.5	[17.33 ± 0.05]	16.51 ± 0.02	[16.04 ± 0.05]	15.68 ± 0.03	57; 57; 1,57
DENIS-P J0812316−244442	L2.5:/L0.9	[14.94 ± 0.06]	[13.78 ± 0.03]	[13.00 ± 0.02]	[12.38 ± 0.02]	179; 179,7; 1
SDSS J081757.49+182405.0	L1/L2.0	[16.11 ± 0.06]	[15.05 ± 0.04]	[14.36 ± 0.04]	[13.80 ± 0.04]	198; 198,7; 1
SDSS J081812.28+331048.2	L0/L1.3	[17.02 ± 0.10]	[15.92 ± 0.09]	[15.44 ± 0.14]	[15.04 ± 0.14]	198; 198,7; 1
2MASS J08194602+1658539	M9/...	[14.65 ± 0.05]	[13.76 ± 0.02]	[13.16 ± 0.03]	[12.60 ± 0.02]	45; 45; 1
WISEPA J081958.05−033529.0	T4/T4	[15.94 ± 0.05]	14.78 ± 0.02	[14.60 ± 0.05]	[14.64 ± 0.05]	120; 180,120; 1,16
2MASSW J0820299+450031	L5/L4.5::	[17.64 ± 0.06]	16.24 ± 0.02	[15.13 ± 0.05]	[14.24 ± 0.05]	116; 116,37; 1,16
SDSS J082030.12+103737.0	.../L9.5::	[17.99 ± 0.19]	[16.87 ± 0.19]	[16.17 ± 0.19]	[15.53 ± 0.19]	43; 43; 1
WISEPA J082131.63+144319.3	.../T5.5	[17.49 ± 0.06]	16.40 ± 0.02	[16.61 ± 0.05]	[16.33 ± 0.06]	120; 120; 1,16
DENIS-P J0823031−491201	L1.5/L1.5	[14.65 ± 0.06]	[13.49 ± 0.03]	[12.71 ± 0.02]	[12.04 ± 0.02]	179; 179,195; 1
2MASS J08230838+6125208	L2:/L2.5	[16.01 ± 0.06]	[14.77 ± 0.04]	[13.89 ± 0.03]	[13.18 ± 0.03]	189; 189,7; 1
WISEA J082640.45−164031.8	.../L9	···	15.60 ± 0.02	[[14.66 ± 0.07]]	[[14.09 ± 0.07]]	121; 121; 16,1,51
SDSS J082642.65+193922.0	L0/M9.2	[15.68 ± 0.06]	[14.74 ± 0.03]	[14.07 ± 0.03]	[13.56 ± 0.03]	226; 226,7; 1
SSSPM J0829−1309	L2/L2:	[13.91 ± 0.06]	[12.76 ± 0.03]	[11.92 ± 0.02]	[11.28 ± 0.02]	207; 142,160; 1
2MASSW J0829066+145622	L2/L1.0	[15.92 ± 0.05]	14.70 ± 0.02	[13.87 ± 0.03]	[13.15 ± 0.03]	116; 116,7; 1,16
LHS 248	M6.5/...	[8.92 ± 0.05]	[8.21 ± 0.02]	[7.67 ± 0.02]	[7.24 ± 0.02]	20; 111; 1
PSO J127.4696+10.5777	.../L4	18.38 ± 0.06	17.07 ± 0.03	16.11 ± 0.03	15.25 ± 0.02	14; 14; 1,14
PSO J127.5648−11.1861	.../T3	[16.89 ± 0.05]	15.71 ± 0.02	[15.40 ± 0.05]	[15.48 ± 0.05]	16; 16; 1,16
LHS 2021	M7.5/...	[12.72 ± 0.05]	[11.86 ± 0.02]	[11.22 ± 0.02]	[10.73 ± 0.02]	103; 103; 1
2MASS J08315598+1025417	M9/...	[14.47 ± 0.06]	[13.59 ± 0.03]	[13.03 ± 0.02]	[12.42 ± 0.03]	189; 189; 1
2MASSW J0832045−012835	L1.5/L1:	[15.24 ± 0.05]	14.08 ± 0.02	[13.39 ± 0.03]	[12.69 ± 0.03]	116; 116,160; 1,16
WISE J083450.79+642526.8	.../M8	[16.43 ± 0.08]	[15.59 ± 0.07]	[15.19 ± 0.09]	[14.54 ± 0.09]	219; 219; 1
2MASS J08352366+1029318	M7/...	[13.94 ± 0.05]	[13.11 ± 0.02]	[12.54 ± 0.03]	[12.02 ± 0.02]	189; 189; 1
2MASSI J0835425−081923	L5/L4pec	[14.37 ± 0.05]	13.04 ± 0.02	11.99 ± 0.02	11.08 ± 0.02	45; 45,76; 1,67
SDSS J083621.98+494931.5	M9/M9.3:	[16.31 ± 0.08]	[15.38 ± 0.06]	[14.70 ± 0.12]	[14.51 ± 0.12]	226; 226,7; 1
WISEPC J083641.12−185947.2	.../T8pec	···	[[18.71 ± 0.22]]	19.49 ± 0.24	···	120; 120; 1,156,11

Table 4 continued

Table 4 *(continued)*

Object	Spectral Type[a] (Optical/NIR)	Y_{MKO} (mag)	J_{MKO} (mag)	H_{MKO} (mag)	K_{MKO} (mag)	References (Disc; SpT; Phot)
2MASS J08381155+1511155	.../T3.5	[17.51 ± 0.17]	[16.47 ± 0.16]	[16.24 ± 0.17]	[16.20 ± 0.17]	182; 182; 1
2MASS J08391608+1253543	M9/...	[14.60 ± 0.05]	[13.71 ± 0.02]	[13.15 ± 0.03]	[12.56 ± 0.02]	45; 45; 1
SDSS J084016.42+543002.1	L1/...	[17.31 ± 0.13]	[16.36 ± 0.12]	[15.58 ± 0.15]	[15.33 ± 0.15]	229; 229; 1
LHS 2034	M6/M7.0	11.722 ± 0.001	11.106 ± 0.001	[10.47 ± 0.02]	[10.02 ± 0.02]	12; 112,7; 126,1
SDSS J084106.85+603506.3	L4/L1.5	[17.09 ± 0.11]	[15.90 ± 0.09]	[15.11 ± 0.09]	[14.67 ± 0.09]	198; 198,7; 1
SDSS J084307.95+314129.2	L3/L2.5	[17.15 ± 0.11]	[15.93 ± 0.10]	[15.30 ± 0.11]	[14.62 ± 0.11]	198; 198,7; 1
2MASSI J0847287−153237	L2/...	[14.62 ± 0.06]	13.42 ± 0.03	12.66 ± 0.03	12.02 ± 0.02	45; 45; 1,67
WISEA J085224.36+513925.5	.../M7	[14.65 ± 0.06]	[13.96 ± 0.03]	[13.51 ± 0.02]	[13.09 ± 0.02]	121; 121; 1
SDSS J085234.90+472035.0	.../L9.5:	[17.23 ± 0.05]	16.16 ± 0.02	[15.31 ± 0.05]	[14.65 ± 0.05]	123; 123; 1,16
LHS 2065	M9/M9	[12.17 ± 0.07]	11.18 ± 0.05	10.48 ± 0.05	9.91 ± 0.05	12; 111,79; 1,130
PSO J133.8016−02.5658	.../T0pec	[17.16 ± 0.05]	16.00 ± 0.02	15.29 ± 0.02	[14.74 ± 0.05]	14; 14; 1,14
PSO J133.8302+06.0160	.../M9 FLD-G	17.40 ± 0.02	16.342 ± 0.011	[15.68 ± 0.05]	15.140 ± 0.013	14; 14; 126,1,125
2MASSI J0856479+223518	L3:/...	[16.92 ± 0.08]	[15.62 ± 0.06]	[14.63 ± 0.05]	[13.92 ± 0.05]	45; 45; 1
SDSSp J085758.45+570851.4	L8/L8:	[16.09 ± 0.05]	14.86 ± 0.02	[13.89 ± 0.03]	[12.94 ± 0.03]	79; 118,79; 1,16
SDSS J085834.42+325627.7	.../T1	[17.42 ± 0.06]	16.36 ± 0.02	[15.50 ± 0.05]	[14.74 ± 0.05]	43; 43; 1,16
2MASSI J0859254−194926	L6::/L8	[16.66 ± 0.07]	15.42 ± 0.05	14.47 ± 0.04	13.70 ± 0.06	45; 45,219; 1,67
2MASS J08593854+6341355	L0/M8.6	[14.69 ± 0.06]	[13.67 ± 0.03]	[12.95 ± 0.03]	[12.37 ± 0.03]	189; 189,7; 1
2MASS J08594029+1145325	M8/...	[13.65 ± 0.06]	[12.71 ± 0.03]	[12.09 ± 0.03]	[11.47 ± 0.02]	189; 189; 1
PSO J135.0395+32.0845	.../L1.5 FLD-G	[16.86 ± 0.05]	15.76 ± 0.02	15.035 ± 0.014	14.41 ± 0.03	14; 14; 1,14
LP 368-128	M6/M7.3	[10.13 ± 0.05]	[9.41 ± 0.02]	[8.89 ± 0.02]	[8.41 ± 0.02]	206; 104,7; 1
SDSS J090023.68+253934.3	L6/L6.7	[17.50 ± 0.13]	[16.34 ± 0.12]	[15.50 ± 0.08]	[14.64 ± 0.08]	198; 229,7; 1
WISEA J090258.99+670833.1	.../L7 (sl. red)	[18.38 ± 0.25]	[16.86 ± 0.25]	[15.15 ± 0.11]	[14.31 ± 0.11]	204; 204; 1
PSO J135.7840+16.9932	.../T0pec	17.64 ± 0.05	16.41 ± 0.02	15.80 ± 0.02	15.26 ± 0.02	14; 14; 1,14
2MASS J09054654+5623117	L5/L6	[16.67 ± 0.06]	15.33 ± 0.02	[14.37 ± 0.04]	[13.71 ± 0.04]	189; 189,37; 1,16
PSO J136.5380−14.3267	.../T3.5	[17.47 ± 0.05]	16.43 ± 0.02	[16.18 ± 0.05]	[16.04 ± 0.06]	16; 16; 1,16
PSO J136.5494−06.1944	.../L2pec	[15.88 ± 0.05]	14.75 ± 0.02	14.19 ± 0.03	13.70 ± 0.02	14; 14; 1,14
WISEPA J090649.36+473538.6	.../T8	···	[[17.87 ± 0.16]]	[[17.87 ± 0.16]]	[[18.67 ± 0.34]]	120; 120; 1,120
2MASSI J0908380+503208	L5/L9:	[15.52 ± 0.05]	14.43 ± 0.02	[13.56 ± 0.03]	[12.93 ± 0.03]	45; 45,123; 1,16
SDSS J090900.73+652527.2	.../T1.5	[17.00 ± 0.10]	[15.91 ± 0.09]	[15.30 ± 0.15]	[15.20 ± 0.15]	43; 43; 1
SDSS J090948.13+194043.9	L1/M9.9	[15.74 ± 0.06]	[14.70 ± 0.03]	[13.99 ± 0.03]	[13.42 ± 0.03]	198; 198,7; 1
DENIS-P J090957.1−065806	L0/L0:	[14.90 ± 0.05]	13.81 ± 0.02	13.12 ± 0.02	12.50 ± 0.03	58; 118,160; 1,67
Gl 337CD	L8/T0	[16.68 ± 0.05]	15.53 ± 0.02	14.65 ± 0.08	14.00 ± 0.06	227; 227,28; 1,16,67
2MASS J09161504+2139512	M9/...	[14.12 ± 0.05]	[13.18 ± 0.02]	[12.58 ± 0.03]	[12.05 ± 0.03]	45; 45; 1
WISEA J091657.18−112104.7	.../M9	[15.01 ± 0.06]	[14.06 ± 0.03]	[13.53 ± 0.03]	[12.98 ± 0.03]	121; 121; 1
2MASS J09175418+6028065	.../L5	[18.60 ± 0.28]	[17.08 ± 0.27]	[16.05 ± 0.13]	[15.40 ± 0.16]	80; 80; 1
2MASSW J0918382+213406	L2.5/L2.7	[16.87 ± 0.08]	[15.60 ± 0.06]	[14.66 ± 0.04]	[13.88 ± 0.04]	115; 115,7; 1
2MASSW J0920122+351742	L6.5/T0pec	[16.72 ± 0.08]	[15.52 ± 0.06]	[14.75 ± 0.06]	[13.97 ± 0.06]	116; 116,28; 1
WISE J092055.40+453856.3	.../L9.5	[16.14 ± 0.05]	15.04 ± 0.01	14.19 ± 0.02	13.766 ± 0.011	156; 13; 1,13
2MASS J09211410−2104446	L1.5/L4:	[13.77 ± 0.05]	12.71 ± 0.02	[12.23 ± 0.02]	[11.66 ± 0.02]	189; 189,34; 1,16

Table 4 continued

Table 4 *(continued)*

Object	Spectral Type[a] (Optical/NIR)	Y_{MKO} (mag)	J_{MKO} (mag)	H_{MKO} (mag)	K_{MKO} (mag)	References (Disc; SpT; Phot)
SDSS J092308.70+234013.7	L1/L2.3	[14.82 ± 0.05]	13.79 ± 0.02	[13.23 ± 0.02]	[12.78 ± 0.02]	198; 198,7; 1,16
2MASS J09240328+3653444	.../...	···	17.04 ± 0.02	···	···	107; –; 1
SDSSp J092615.38+584720.9	T5/T4.5	[16.90 ± 0.08]	[15.71 ± 0.06]	[15.38 ± 0.19]	[15.53 ± 0.19]	79; 180,28; 1
2MASSW J0928397−160312	L2/L2:	[16.53 ± 0.07]	[15.27 ± 0.04]	[14.37 ± 0.05]	[13.60 ± 0.05]	116; 116,160; 1
SDSS J093113.23+280227.1	L3/L2.5:	[16.05 ± 0.06]	[14.91 ± 0.04]	[14.33 ± 0.04]	[13.71 ± 0.04]	198; 198,7; 1
SDSS J093237.47+672514.5	L0/M9.4	[16.80 ± 0.10]	[15.87 ± 0.09]	[15.44 ± 0.12]	[14.96 ± 0.12]	198; 198,7; 1
NLTT 22073B	.../M7.5	[15.45 ± 0.06]	[14.64 ± 0.04]	[14.14 ± 0.05]	[13.67 ± 0.05]	57; 57; 1
PSO J143.6774−29.8356	.../L1	17.54 ± 0.04	16.47 ± 0.03	15.87 ± 0.02	15.33 ± 0.02	14; 14; 1,14
2MASS J09352803−2934596	L0/L0.3	[14.99 ± 0.06]	[13.99 ± 0.03]	[13.38 ± 0.03]	[12.80 ± 0.03]	189; 189,7; 1
2MASS J09384022−2748184	M8/...	[13.77 ± 0.06]	[12.97 ± 0.03]	[12.41 ± 0.03]	[11.91 ± 0.02]	189; 189; 1
SDSS J094047.88+294653.0	L1/L0.4	[16.40 ± 0.09]	[15.25 ± 0.07]	[14.41 ± 0.05]	[13.91 ± 0.05]	198; 198,7; 1
TVLM 262-111511	M8/...	[14.99 ± 0.06]	[14.16 ± 0.03]	[13.57 ± 0.04]	[13.07 ± 0.04]	220; 226; 1
2MASS J09490860−1545485	.../T2	[17.09 ± 0.05]	15.82 ± 0.02	15.22 ± 0.11	[15.16 ± 0.05]	225; 28; 1,16,67
PSO J147.5092−27.6337	.../L0.5	[17.88 ± 0.19]	[16.84 ± 0.18]	[16.29 ± 0.19]	[15.43 ± 0.19]	14; 14; 1
TVLM 262-70502	.../M6.5	[14.90 ± 0.06]	[14.15 ± 0.03]	[13.52 ± 0.03]	[13.07 ± 0.03]	220; 120; 1
WISEPC J095259.29+195507.3	.../T6	[17.88 ± 0.08]	[16.89 ± 0.06]	[17.28 ± 0.10]	[17.51 ± 0.08]	120; 120; 1
2MASS J09532126−1014205	L0/M9.7 VL-G	[14.46 ± 0.06]	[13.43 ± 0.03]	[12.72 ± 0.02]	[12.12 ± 0.02]	47; 47,69; 1
PSO J149.0341−14.7857	.../L9	17.18 ± 0.05	15.99 ± 0.02	15.073 ± 0.013	14.46 ± 0.02	14; 14; 1,14
PSO J149.1907−19.1730	.../L5pec	[16.33 ± 0.05]	15.13 ± 0.01	14.43 ± 0.02	13.899 ± 0.011	14; 14; 1,14
WISEA J095729.41+462413.5	.../L5pec	[17.51 ± 0.12]	[16.20 ± 0.11]	[15.46 ± 0.09]	[14.43 ± 0.09]	154; 154; 1
2MASS J09593276+4523309	.../L3 γ	[17.34 ± 0.05]	15.84 ± 0.02	[14.86 ± 0.04]	[13.64 ± 0.04]	69; 69; 1,16
G 196-3B	L3 β/L3: VL-G	[16.23 ± 0.07]	[14.73 ± 0.05]	[13.72 ± 0.03]	[12.73 ± 0.03]	183; 48,6; 1
2MASSW J1004392−333518	L4/L5:	[15.69 ± 0.06]	14.38 ± 0.04	13.52 ± 0.04	12.88 ± 0.02	89; 89,160; 1,67
DENIS J1004403−131818	.../L1:	···	[[14.62 ± 0.04]]	[[13.93 ± 0.04]]	[[13.34 ± 0.04]]	164; 160; 1,51
SDSS J100711.74+193056.2	.../L8:	[17.78 ± 0.06]	16.70 ± 0.02	[15.88 ± 0.05]	[15.24 ± 0.05]	43; 43; 1,16
2MASS J10073369−4555147	.../T5	[16.84 ± 0.09]	15.65 ± 0.07	15.68 ± 0.12	15.56 ± 0.23	144; 144; 1,67
PSO J152.2977+15.9912	.../L1.5	[17.69 ± 0.06]	16.68 ± 0.04	16.14 ± 0.04	[15.53 ± 0.06]	14; 14; 1,14
WISE J100926.40+354137.5	.../M8	[15.93 ± 0.06]	[15.07 ± 0.04]	[14.53 ± 0.07]	[14.10 ± 0.07]	219; 219; 1
2MASSI J1010148−040649	L6/L6	[16.67 ± 0.05]	15.40 ± 0.02	14.43 ± 0.04	13.57 ± 0.05	45; 45,119; 1,16,67
TVLM 263-71765	M8/...	[14.17 ± 0.06]	[13.34 ± 0.03]	[12.78 ± 0.02]	[12.29 ± 0.02]	220; 226; 1
2MASS J10163470+2751497	M8/...	[12.73 ± 0.05]	[11.96 ± 0.02]	[11.38 ± 0.02]	[10.93 ± 0.02]	162; 162; 1
SDSS J101742.51+431057.9	L1/L0.9	[16.60 ± 0.09]	[15.49 ± 0.07]	[14.96 ± 0.10]	[14.49 ± 0.10]	198; 198,7; 1
2MASSW J1018588−290953	L1/L0.3	[15.21 ± 0.06]	14.13 ± 0.03	13.46 ± 0.02	12.76 ± 0.02	89; 89,7; 1,67
WISEPA J101905.63+652954.2	T7/T6	[17.40 ± 0.08]	[16.34 ± 0.05]	[16.58 ± 0.12]	[16.50 ± 0.18]	120; 120,120; 1
DENIS J1019245−270717	L0.5/M9.5	[14.42 ± 0.05]	13.50 ± 0.02	[12.97 ± 0.02]	[12.45 ± 0.02]	164; 164,110; 1,16
TVLM 213-2005	M7/...	[14.19 ± 0.06]	[13.37 ± 0.02]	[12.79 ± 0.02]	[12.23 ± 0.02]	221; 66; 1
2MASS J10213232−2044069	M9/...	[14.05 ± 0.05]	[13.16 ± 0.02]	[12.55 ± 0.02]	[12.05 ± 0.03]	178; 178; 1
2MASS J10224821+5825453	L1 β/L1: FLD-G	[14.55 ± 0.06]	[13.43 ± 0.03]	[12.69 ± 0.03]	[12.13 ± 0.03]	189; 48,6; 1
WISEA J102304.04+155616.4	.../M8pec	[14.70 ± 0.06]	[13.89 ± 0.03]	[13.46 ± 0.03]	[12.94 ± 0.03]	121; 121; 1

Table 4 continued

Table 4 *(continued)*

Object	Spectral Type[a] (Optical/NIR)	Y_{MKO} (mag)	J_{MKO} (mag)	H_{MKO} (mag)	K_{MKO} (mag)	References (Disc; SpT; Phot)
SDSS J102552.43+321234.0	.../L7: FLD-G	[18.03 ± 0.07]	16.89 ± 0.05	15.98 ± 0.03	15.16 ± 0.03	43; 139; 1,43
2MASSI J1029216+162652	L2.5/L2.8	[15.52 ± 0.05]	14.23 ± 0.02	[13.41 ± 0.02]	[12.60 ± 0.02]	116; 116,7; 1,16
SDSS J102947.68+483412.2	L0/...	[17.72 ± 0.20]	[16.73 ± 0.19]	[16.09 ± 0.24]	[15.58 ± 0.24]	229; 229; 1
2MASS J10315064+3349595	.../L2	[17.30 ± 0.10]	[16.04 ± 0.09]	[15.09 ± 0.06]	[14.31 ± 0.06]	119; 119; 1
SDSS J103321.92+400549.5	.../L6	[17.81 ± 0.17]	[16.56 ± 0.16]	[15.84 ± 0.17]	[15.29 ± 0.17]	43; 43; 1
2MASSW J1035245+250745	L1/L1.1	[15.85 ± 0.06]	[14.71 ± 0.03]	[13.98 ± 0.03]	[13.26 ± 0.03]	116; 116,7; 1
HIP 51877B	.../M9.5	[16.17 ± 0.08]	[15.16 ± 0.06]	[14.57 ± 0.05]	[13.97 ± 0.05]	57; 57; 1
PSO J159.0433−27.6357	.../L2	[17.11 ± 0.06]	16.02 ± 0.02	15.361 ± 0.014	[14.72 ± 0.06]	14; 14; 1,14
2MASSW J1036530−344138	L6/L6.5	[16.67 ± 0.07]	15.51 ± 0.05	14.48 ± 0.04	13.75 ± 0.04	89; 89,37; 1,67
PSO J159.2399−26.3885	.../T1.5	17.77 ± 0.07	16.61 ± 0.02	16.03 ± 0.03	15.51 ± 0.03	14; 14; 1,16,14
WISE J103907.73−160002.9	.../T7.5	18.19 ± 0.03	16.89 ± 0.02	17.19 ± 0.04	[17.09 ± 0.07]	156; 156; 168,1
SDSS J103931.35+325625.5	.../T1	[17.28 ± 0.05]	16.10 ± 0.02	[15.42 ± 0.05]	[14.87 ± 0.05]	43; 43; 1,16
PSO J160.0416−21.3281	.../T2pec	[17.64 ± 0.05]	16.49 ± 0.02	16.01 ± 0.03	[15.51 ± 0.05]	14; 14; 1,14
2MASS J10430758+2225236	L8/L9:	[17.03 ± 0.06]	15.85 ± 0.02	[14.82 ± 0.04]	[13.98 ± 0.04]	47; 47,37; 1,16
2MASS J10461875+4441149	.../L5pec	[16.81 ± 0.08]	[15.55 ± 0.06]	[14.73 ± 0.05]	[14.11 ± 0.05]	119; 119; 1
LP 213-68	M8/M8.2	[13.27 ± 0.05]	[12.41 ± 0.02]	[11.75 ± 0.02]	[11.23 ± 0.02]	86; 185,7; 1
DENIS-P J104731.1−181558	L2.5/L0: FLD-G	[15.20 ± 0.06]	[14.14 ± 0.03]	[13.47 ± 0.03]	[12.87 ± 0.03]	163; 163,6; 1
Luhman 16	.../L7.5+T0.5	[11.91 ± 0.06]	10.61 ± 0.03	9.63 ± 0.03	[8.82 ± 0.02]	153; 38; 1,38
2MASS J10511900+5613086	L2/L0.8	[14.31 ± 0.05]	13.18 ± 0.02	[12.49 ± 0.02]	[11.88 ± 0.02]	189; 189,7; 1,16
SDSS J105213.51+442255.7	L7.5/T0.5:	[17.03 ± 0.11]	[15.85 ± 0.10]	[15.24 ± 0.09]	[14.57 ± 0.09]	43; 180,43; 1
WISE J105257.95−194250.2	.../T7.5	[17.72 ± 0.05]	16.83 ± 0.02	[17.08 ± 0.05]	[17.00 ± 0.05]	219; 219; 1,16
2MASSI J1059513−211308	L1/L2	[15.62 ± 0.06]	[14.50 ± 0.04]	[13.82 ± 0.03]	[13.19 ± 0.03]	45; 45,160; 1
2MASS J10595185+3042059	.../T4	[17.18 ± 0.05]	16.02 ± 0.02	[15.93 ± 0.05]	[15.85 ± 0.05]	215; 215; 1,16
2MASS J11000965+4957470	L3.5/L3	[16.49 ± 0.05]	15.17 ± 0.02	[14.27 ± 0.03]	[13.45 ± 0.03]	189; 189,37; 1,16
SSSPM J1102−3431	M8.5 γ/M9: VL-G	[13.83 ± 0.05]	[12.97 ± 0.02]	[12.41 ± 0.02]	[11.85 ± 0.02]	210; 67,6; 1
2MASSI J1104012+195921	L4/L5.5	[15.64 ± 0.05]	14.34 ± 0.02	[13.56 ± 0.03]	[12.93 ± 0.03]	45; 45,37; 1,16
2MASS J11061197+2754225	.../T2.5	[16.10 ± 0.06]	14.96 ± 0.04	14.20 ± 0.05	13.84 ± 0.05	144; 144; 1,159
Gl 417BC	L4.5/L5: FLD-G	[15.83 ± 0.05]	14.47 ± 0.02	13.55 ± 0.03	12.67 ± 0.03	116; 116,6; 1,16,67
PSO J168.1800−27.2264	.../T2.5	18.38 ± 0.04	17.12 ± 0.03	16.75 ± 0.03	[16.65 ± 0.06]	14; 14; 168,1
SDSS J111320.16+343057.9	.../L3	[17.97 ± 0.21]	[16.69 ± 0.20]	[15.88 ± 0.26]	[15.49 ± 0.26]	43; 43; 1
2MASS J11181292−0856106	L6/L6pec	[16.85 ± 0.10]	[15.65 ± 0.09]	[14.85 ± 0.08]	[14.16 ± 0.08]	119; 119,119; 1
SDSS J112118.57+433246.5	.../L7.5	[18.03 ± 0.20]	[16.91 ± 0.20]	[16.31 ± 0.21]	[15.55 ± 0.21]	43; 43; 1
LHS 2397a	M8/M8.5	[12.71 ± 0.05]	11.792 ± 0.005	11.173 ± 0.010	10.639 ± 0.009	111; 113,7; 1,129
2MASS J11220826−3512363	.../T2	[16.00 ± 0.06]	[14.88 ± 0.04]	[14.43 ± 0.07]	[14.43 ± 0.07]	225; 28; 1
2MASSW J1122362−391605	L3/L3.7::	[16.91 ± 0.08]	[15.63 ± 0.06]	[14.77 ± 0.05]	[13.86 ± 0.05]	89; 89,7; 1
WISEPC J112254.73+255021.5	.../T6	[17.29 ± 0.06]	16.29 ± 0.02	[16.67 ± 0.06]	[16.67 ± 0.06]	120; 120; 1,16
2MASS J11240487+3808054	M8.5/...	[13.57 ± 0.05]	[12.67 ± 0.02]	[12.08 ± 0.03]	[11.54 ± 0.03]	45; 45; 1
WISE J112438.12−042149.7	.../T7	[17.35 ± 0.05]	16.37 ± 0.02	[16.77 ± 0.05]	[16.64 ± 0.06]	156; 156; 1,16
2MASS J11263991−5003550	L4.5/L6.5::pec	[15.14 ± 0.06]	[13.91 ± 0.03]	[13.37 ± 0.04]	[12.81 ± 0.03]	71; 34,34; 1

Table 4 continued

Table 4 *(continued)*

Object	Spectral Type[a] (Optical/NIR)	Y_{MKO} (mag)	J_{MKO} (mag)	H_{MKO} (mag)	K_{MKO} (mag)	References (Disc; SpT; Phot)
SDSS J112647.03+581632.2	L3/L1.3	[16.82 ± 0.09]	[15.78 ± 0.08]	[15.19 ± 0.08]	[14.52 ± 0.08]	198; 198,7; 1
NLTT 27966B	.../L4	17.31 ± 0.04	16.11 ± 0.02	15.28 ± 0.02	[14.67 ± 0.05]	57; 57; 57,1
PSO J174.6630−18.6530	.../M9	[17.23 ± 0.07]	16.29 ± 0.05	15.67 ± 0.04	[15.13 ± 0.07]	14; 14; 1,14
TWA 26	M9 γ/M9: VL-G	[13.49 ± 0.06]	[12.62 ± 0.03]	[12.05 ± 0.02]	[11.46 ± 0.02]	89; 67,6; 1
2MASS J11414406−2232156	M7.5/...	[13.46 ± 0.05]	[12.60 ± 0.02]	[12.05 ± 0.02]	[11.55 ± 0.02]	45; 45; 1
PSO J175.8169−20.4072	.../T2	[17.75 ± 0.18]	16.74 ± 0.17	16.30 ± 0.04	[15.99 ± 0.18]	14; 14; 1,14
2MASSW J1146345+223053	L3/...	[15.35 ± 0.06]	14.07 ± 0.03	13.21 ± 0.03	12.55 ± 0.03	115; 115; 1,67
WISEA J114724.10−204021.3	.../L7: red	[18.87 ± 0.06]	17.44 ± 0.02	16.12 ± 0.06	[14.74 ± 0.05]	203; 203; 1,16
2MASS J11533966+5032092	L1:/L0.3	[15.10 ± 0.05]	14.04 ± 0.02	[13.37 ± 0.03]	[12.83 ± 0.03]	189; 189,7; 1,16
LHS 2471	M6.5/M7.0	[11.913 ± 0.055]	[11.200 ± 0.022]	[10.688 ± 0.022]	[10.233 ± 0.022]	12; 52,7; 1
2MASS J11544223−3400390	L0 β/L0.8 INT-G	[15.28 ± 0.06]	[14.15 ± 0.03]	[13.41 ± 0.03]	[12.82 ± 0.03]	21; 69,76; 1
2MASSW J1155395−372735	L2/L2.3	[13.91 ± 0.05]	12.73 ± 0.02	12.07 ± 0.03	11.43 ± 0.02	89; 89,7; 1,67
LP 851-346	M7.5/M7.7	[11.69 ± 0.05]	[10.91 ± 0.02]	[10.35 ± 0.02]	[9.86 ± 0.02]	44; 44,7; 1
DENIS-P J1157480−484442	L0.5:/M9.4	[14.96 ± 0.06]	[13.97 ± 0.03]	[13.39 ± 0.03]	[12.77 ± 0.03]	179; 179,7; 1
SDSS J115940.72+540938.6	L2/L0.9	[16.34 ± 0.07]	[15.17 ± 0.04]	[14.41 ± 0.04]	[13.73 ± 0.04]	198; 198,7; 1
PSO J180.1475−28.6160	.../T0	[17.06 ± 0.05]	15.96 ± 0.02	15.15 ± 0.01	[14.75 ± 0.05]	14; 14; 1,14
2MASS J12022564−0629026	M9/...	[14.62 ± 0.06]	[13.70 ± 0.03]	[13.08 ± 0.03]	[12.57 ± 0.03]	45; 45; 1
NLTT 29395B	.../M8	[16.51 ± 0.09]	[15.75 ± 0.08]	[15.19 ± 0.09]	[14.75 ± 0.09]	57; 57; 1
2MASSI J1204303+321259	L0/M9	[14.84 ± 0.05]	13.80 ± 0.02	[13.16 ± 0.03]	[12.49 ± 0.03]	45; 45,228; 1,16
HIP 58918B	.../M7	[15.16 ± 0.06]	[14.44 ± 0.03]	[13.95 ± 0.02]	[13.50 ± 0.02]	57; 57; 1
SDSS J120610.49+624257.2	L1/L2.1	[16.73 ± 0.09]	[15.59 ± 0.07]	[14.82 ± 0.07]	[13.93 ± 0.07]	198; 198,7; 1
DENIS J1206501−393725	L2/L1.9	[15.34 ± 0.06]	[14.26 ± 0.03]	[13.67 ± 0.03]	[13.07 ± 0.03]	164; 164,7; 1
2MASS J12070374−3151298	L3:/L2.5	[17.06 ± 0.08]	[15.80 ± 0.07]	[14.80 ± 0.06]	[13.98 ± 0.06]	189; 189,37; 1
2MASSW J1207334−393254	M8 γ/M8: VL-G	[13.72 ± 0.06]	[12.94 ± 0.03]	[12.44 ± 0.03]	[11.91 ± 0.03]	89; 69,6; 1
2MASS J12073804−3909050	L2:/L0.9	[15.77 ± 0.06]	[14.64 ± 0.04]	[13.89 ± 0.04]	[13.22 ± 0.04]	189; 189,7; 1
2MASS J12074836−3900043	L0 γ/L1: VL-G	[15.68 ± 0.08]	[15.51 ± 0.06]	[14.68 ± 0.06]	[14.03 ± 0.06]	75; 75,75; 1
HIP 59310B	.../M7	[14.43 ± 0.06]	[13.67 ± 0.03]	[13.10 ± 0.02]	[12.68 ± 0.02]	57; 57; 1
PSO J182.6569−26.6197	.../L2	[17.82 ± 0.07]	16.72 ± 0.05	16.11 ± 0.06	[15.27 ± 0.07]	14; 14; 1,14
2MASSI J1213033−043243	L5/L4.2	[15.85 ± 0.05]	14.58 ± 0.02	[13.73 ± 0.03]	[13.00 ± 0.03]	45; 45,7; 1,16
PSO J183.4547+40.7901	.../T4	[18.21 ± 0.06]	17.05 ± 0.04	16.86 ± 0.05	[16.75 ± 0.07]	14; 14; 1,14
SDSS J121440.95+631643.4	.../T3.5:	[17.50 ± 0.13]	[16.39 ± 0.12]	[15.88 ± 0.23]	[15.94 ± 0.23]	43; 43; 1
PSO J183.9318−09.7914	.../L0	17.53 ± 0.02	16.313 ± 0.011	15.566 ± 0.011	[14.95 ± 0.05]	14; 14; 168,1
2MASS J12154432−3420591	.../T4.5	[17.54 ± 0.14]	16.24 ± 0.13	15.71 ± 0.19	[16.08 ± 0.14]	144; 144; 1,67
2MASS J12172372−0237369	.../L4	18.29 ± 0.02	16.839 ± 0.007	15.938 ± 0.008	[15.18 ± 0.05]	80; 80; 64,1
WISE J122152.28−313600.8	.../T6.5	[17.24 ± 0.14]	[16.13 ± 0.13]	[16.50 ± 0.14]	[16.18 ± 0.14]	156; 156; 1
NLTT 30510B	.../M9.5	[16.90 ± 0.09]	[15.92 ± 0.08]	[15.35 ± 0.09]	[14.83 ± 0.09]	57; 57; 1
BRI B1222−1222	M9/...	[13.44 ± 0.05]	[12.54 ± 0.02]	[11.88 ± 0.03]	[11.33 ± 0.03]	113; 113; 1
WISE J122558.86−101345.0	.../T6	17.33 ± 0.02	16.120 ± 0.009	16.49 ± 0.03	[16.49 ± 0.06]	156; 156; 168,1
2MASS J12312141+4959234	L2/L3.4	[15.77 ± 0.05]	14.52 ± 0.02	[13.79 ± 0.03]	[13.11 ± 0.03]	47; 47,7; 1,16

Table 4 continued

Table 4 *(continued)*

Object	Spectral Type[a] (Optical/NIR)	Y_{MKO} (mag)	J_{MKO} (mag)	H_{MKO} (mag)	K_{MKO} (mag)	References (Disc; SpT; Phot)
2MASS J12321827−0951502	L0/M9.5	[14.73 ± 0.05]	13.72 ± 0.02	[13.14 ± 0.03]	[12.53 ± 0.03]	189; 189,7; 1,16
NLTT 31450B	.../L6	[17.28 ± 0.05]	15.97 ± 0.02	15.08 ± 0.02	[14.30 ± 0.05]	57; 57; 1,16,57
TWA 29	M9.5 γ/L0: VL-G	[15.36 ± 0.06]	[14.45 ± 0.03]	[13.86 ± 0.04]	[13.32 ± 0.04]	145; 69,6; 1
SDSS J124555.66+490210.9	L1/M7.8:	[16.66 ± 0.09]	[15.92 ± 0.08]	[15.41 ± 0.14]	[15.18 ± 0.14]	198; 198,7; 1
2MASSW J1246467+402715	L4/L4.0	[16.29 ± 0.05]	14.90 ± 0.02	[14.04 ± 0.04]	[13.25 ± 0.04]	116; 116,7; 1,16
2MASS J12474428−3816464	.../M9 VL-G	[15.64 ± 0.06]	[14.75 ± 0.03]	[14.16 ± 0.04]	[13.54 ± 0.04]	75; 75; 1
2MASS J12474944−1117551	.../L0:	[16.88 ± 0.09]	[15.94 ± 0.07]	[15.16 ± 0.10]	[14.70 ± 0.10]	119; 119; 1
SDSS J124908.66+415728.6	L0/M9	[16.35 ± 0.07]	[15.40 ± 0.05]	[14.76 ± 0.05]	[14.27 ± 0.05]	226; 226,119; 1
SDSS J125011.65+392553.9	.../T4	...	16.14 ± 0.02	[[16.24 ± 0.25]]	[[16.18 ± 0.25]]	43; 43; 16,1,51
PSO J192.6717−21.8250	.../T2.5	[17.87 ± 0.06]	16.84 ± 0.04	16.30 ± 0.04	[16.22 ± 0.06]	14; 14; 1,14
WISE J125448.52−072828.4	.../T7	[18.41 ± 0.05]	17.300 ± 0.010	17.63 ± 0.03	[17.40 ± 0.07]	219; 219; 1,219
VHS J125601.92−125723.9 b	L8::/L7:: VL-G	18.56 ± 0.05	17.14 ± 0.02	15.78 ± 0.02	[[14.55 ± 0.12]]	77; 77,77; 168,1,51
WISE J125715.90+400854.2	.../T7	[18.14 ± 0.06]	16.89 ± 0.02	[17.14 ± 0.06]	[17.18 ± 0.06]	156; 156; 1,16
2MASSW J1300425+191235	L1/L3	[13.65 ± 0.05]	12.63 ± 0.02	[12.16 ± 0.02]	[11.60 ± 0.02]	87; 87,34; 1,16
HIP 63506C	.../L1	[16.15 ± 0.06]	[15.11 ± 0.04]	[14.49 ± 0.05]	[13.98 ± 0.05]	57; 57; 1
2MASS J13015465−1510223	L1/M9.6 FLD-G	[15.61 ± 0.06]	[14.50 ± 0.04]	[13.73 ± 0.03]	[13.08 ± 0.03]	189; 189,76; 1
2MASS J13023811+5650212	L2/L3:pec	[17.48 ± 0.13]	[16.29 ± 0.12]	[15.53 ± 0.12]	[14.95 ± 0.12]	119; 119,119; 1
2MASSI J1305410+204639	L5/L6.5	[16.45 ± 0.07]	[15.12 ± 0.05]	[14.13 ± 0.04]	[13.35 ± 0.04]	45; 98,7; 1
2MASS J13061727+3820296	L0/L0.6	[15.73 ± 0.06]	[14.59 ± 0.03]	[13.87 ± 0.04]	[13.19 ± 0.04]	189; 189,7; 1
WISEA J130729.56−055815.4	.../L8 (sl. blue)	[17.96 ± 0.17]	[16.84 ± 0.16]	[15.51 ± 0.09]	[14.80 ± 0.14]	202; 202; 1
2MASS J13081228+6103486	.../L2	[17.80 ± 0.15]	[16.62 ± 0.15]	[15.86 ± 0.15]	[15.17 ± 0.15]	80; 80; 1
WISEP J131141.91+362925.2	.../L5pec	[16.71 ± 0.07]	[15.46 ± 0.05]	[14.83 ± 0.05]	[14.13 ± 0.05]	120; 120; 1
2MASS J13120707+3937445	L0:/M8.8	[15.08 ± 0.06]	[14.13 ± 0.03]	[13.47 ± 0.02]	[12.92 ± 0.02]	47; 47,7; 1
HD 114762B	.../d/sdM9:	[14.62 ± 0.11]	13.67 ± 0.10	13.44 ± 0.10	12.99 ± 0.10	175; 22; 1,60
2MASSI J1315309−264951	L5.5/L6.7	[16.28 ± 0.07]	[15.11 ± 0.05]	[14.14 ± 0.04]	[13.45 ± 0.04]	100; 118,7; 1
WISE J131833.98−175826.5	.../T8	...	[[18.15 ± 0.19]]	[[17.76 ± 0.23]]	...	156; 165; 1,156
2MASS J13184794+1736117	.../L5.5	[17.57 ± 0.11]	[16.28 ± 0.10]	[15.31 ± 0.06]	[14.51 ± 0.06]	119; 119; 1
WISEPC J132004.16+603426.2	.../T6.5	[17.33 ± 0.10]	[16.23 ± 0.09]	[16.74 ± 0.15]	[16.48 ± 0.21]	120; 120; 1
WISEPA J132233.66−234017.1	.../T8	[17.74 ± 0.12]	[16.75 ± 0.10]	[16.65 ± 0.14]	[17.02 ± 0.40]	120; 120; 1
DENIS-P J1323−1806	L0/L0.0	[15.94 ± 0.06]	[14.87 ± 0.04]	[14.26 ± 0.05]	[13.64 ± 0.05]	163; 163,7; 1
PSO J201.0320+19.1072	.../T3.5	[16.58 ± 0.05]	15.63 ± 0.02	[15.62 ± 0.05]	[15.56 ± 0.05]	55; 55; 1,16
2MASS J13243553+6358281	.../T2.5pec	[16.52 ± 0.08]	[15.44 ± 0.07]	[14.68 ± 0.06]	[14.08 ± 0.06]	144; 119; 1
2MASSW J1326201−272937	L5/L6.6:	[17.02 ± 0.05]	15.74 ± 0.02	[14.83 ± 0.05]	[13.83 ± 0.05]	89; 89,7; 1,16
PSO J202.1635−03.7660	.../T4.5	[17.92 ± 0.06]	16.91 ± 0.02	16.69 ± 0.04	[16.64 ± 0.06]	14; 14; 1,16,14
2MASSW J1328550+211449	L5/L4.1	[17.44 ± 0.11]	16.07 ± 0.10	15.04 ± 0.08	14.21 ± 0.08	115; 115,7; 1,67
2MASS J13364062+3743230	L1/L0.4	[15.48 ± 0.06]	[14.37 ± 0.03]	[13.70 ± 0.02]	[13.08 ± 0.02]	47; 47,7; 1
2MASS J13373116+4938367	L0/M8.9	[14.66 ± 0.05]	13.73 ± 0.02	[13.10 ± 0.03]	[12.55 ± 0.03]	47; 47,7; 1,16
2MASSW J1338261+414034	L2.5/L2.4	[15.33 ± 0.05]	14.13 ± 0.02	[13.38 ± 0.02]	[12.75 ± 0.02]	116; 116,7; 1,16
2MASS J13411160−3052505	L2::/L2.7:	[15.72 ± 0.06]	[14.56 ± 0.03]	[13.79 ± 0.03]	[13.07 ± 0.03]	189; 189,7; 1

Table 4 continued

Table 4 *(continued)*

Object	Spectral Type[a] (Optical/NIR)	Y_{MKO} (mag)	J_{MKO} (mag)	H_{MKO} (mag)	K_{MKO} (mag)	References (Disc; SpT; Phot)
WISEA J134310.44−121628.8	.../L6.5::pec	[17.38 ± 0.11]	[16.19 ± 0.10]	[15.56 ± 0.17]	[15.20 ± 0.17]	154; 154; 1
2MASSW J1343167+394508	L5/L5	[17.35 ± 0.05]	15.95 ± 0.02	[14.95 ± 0.05]	[14.12 ± 0.05]	116; 116,106; 1,16
SDSS J134525.57+521634.0	.../L3.5	[18.18 ± 0.19]	[16.88 ± 0.18]	[16.33 ± 0.14]	[15.34 ± 0.14]	43; 43; 1
WISEPC J134806.99+660327.8	.../L9	[18.05 ± 0.20]	[16.87 ± 0.19]	[16.01 ± 0.15]	[15.25 ± 0.15]	120; 120; 1
PM I13518+4157B	.../L1.5	[15.11 ± 0.08]	[15.02 ± 0.03]	[14.42 ± 0.04]	[13.84 ± 0.04]	57; 57; 1
WISE J135307.51−085712.0	.../L0	...	...	[14.70 ± 0.08]	[14.16 ± 0.08]	219; 219; 1
2MASS J13571497−1438529	M7/...	[13.68 ± 0.06]	[12.84 ± 0.03]	[12.26 ± 0.03]	[11.71 ± 0.03]	177; 178; 1
SDSS J135852.68+374711.9	.../T4.5:	[17.32 ± 0.05]	16.24 ± 0.02	[16.50 ± 0.05]	[16.70 ± 0.06]	43; 43; 1,16
2MASS J13595510−4034582	L1/L3.1:	[14.59 ± 0.06]	13.58 ± 0.03	13.06 ± 0.03	12.54 ± 0.03	189; 189,7; 1,67
SDSS J140023.12+433822.3	.../L7:	[17.33 ± 0.05]	16.20 ± 0.02	[15.21 ± 0.05]	[14.45 ± 0.05]	43; 43; 1,16
WISE J140035.40−385013.5	.../T4	[16.87 ± 0.11]	[15.87 ± 0.10]	[15.68 ± 0.11]	[15.87 ± 0.11]	156; 156; 1
2MASS J14044495+4634297	L0:/M9.7	[15.31 ± 0.06]	[14.30 ± 0.03]	[13.60 ± 0.03]	[13.03 ± 0.03]	47; 47,7; 1
2MASS J14044941−3159329	T0/T2.5	[16.59 ± 0.08]	15.51 ± 0.06	14.97 ± 0.07	[14.70 ± 0.08]	144; 147,144; 1,67
SDSS J140601.47+524931.0	L0/M9.8	[16.54 ± 0.07]	[15.52 ± 0.05]	[15.03 ± 0.10]	[14.54 ± 0.10]	226; 226,7; 1
2MASS J14090310−3357565	L2/L1.3	[15.31 ± 0.06]	[14.19 ± 0.03]	[13.49 ± 0.03]	[12.85 ± 0.03]	118; 118,7; 1
2MASSW J1411175+393636	L1.5/L1.5	[15.65 ± 0.05]	14.55 ± 0.02	[13.85 ± 0.04]	[13.22 ± 0.04]	116; 116,7; 1,16
2MASSI J1411213−211950	M9 β/M8: INT-G	[13.22 ± 0.05]	[12.40 ± 0.02]	[11.89 ± 0.02]	[11.30 ± 0.02]	45; 69,6; 1
WISE J141144.13−140300.5	.../M8pec	[15.71 ± 0.06]	[14.87 ± 0.04]	[14.48 ± 0.06]	[13.94 ± 0.06]	219; 219; 1
2MASS J14122268+2354108	M9/...	[14.53 ± 0.06]	[13.70 ± 0.03]	[13.14 ± 0.03]	[12.63 ± 0.02]	47; 47; 1
2MASSW J1412244+163312	L0.5/...	[14.92 ± 0.05]	13.85 ± 0.02	[13.22 ± 0.03]	[12.50 ± 0.03]	116; 116; 1,16
SDSS J141530.05+572428.7	.../T3:	[17.67 ± 0.05]	16.54 ± 0.02	[16.09 ± 0.05]	[15.47 ± 0.05]	43; 43; 1,16
ULAS J141623.94+134836.3	.../(sd)T7.5	18.16 ± 0.03	17.26 ± 0.02	17.58 ± 0.03	[18.42 ± 0.09]	211,40; 36; 126,1
2MASS J14182962−3538060	.../L1.5	[16.29 ± 0.07]	[15.12 ± 0.05]	[14.33 ± 0.05]	[13.67 ± 0.05]	119; 119; 1
SDSS J141858.92+600018.8	L0/M9	[16.12 ± 0.06]	[15.21 ± 0.04]	[14.54 ± 0.05]	[13.90 ± 0.05]	226; 226,119; 1
2MASS J14192618+5919047	.../L1:	[17.65 ± 0.14]	[16.44 ± 0.13]	[15.76 ± 0.16]	[15.26 ± 0.16]	119; 119; 1
SDSS J142058.30+213156.6	L1/L0.0:	[16.08 ± 0.07]	[15.07 ± 0.04]	[14.59 ± 0.06]	[14.03 ± 0.06]	198; 198,7; 1
2MASSW J1421314+182740	L0/M8.9	[14.16 ± 0.05]	13.14 ± 0.02	[12.49 ± 0.02]	[11.92 ± 0.02]	87; 189,7; 1,16
SDSS J142227.25+221557.1	.../L6.5::	[18.16 ± 0.19]	[16.98 ± 0.18]	[16.11 ± 0.17]	[15.63 ± 0.17]	43; 43; 1
2MASS J14232186+6154005	.../L4	[17.81 ± 0.16]	[16.56 ± 0.15]	[16.03 ± 0.15]	[15.26 ± 0.13]	80; 80; 1
DENIS-P J142527.97−365023.4	L3:/L3.1 INT-G	[15.04 ± 0.06]	[13.67 ± 0.03]	[12.67 ± 0.03]	[11.77 ± 0.03]	109; 189,76; 1
SDSS J142612.86+313039.4	.../L4.0::	[17.80 ± 0.17]	[16.55 ± 0.16]	[15.68 ± 0.09]	[14.70 ± 0.09]	7; 7; 1
2MASS J14283132+5923354	L4/L4.4	[16.03 ± 0.05]	14.73 ± 0.02	[13.95 ± 0.03]	[13.25 ± 0.03]	189; 189,7; 1,16
2MASSI J1430435+291540	L2/L0.5	[15.43 ± 0.06]	[14.22 ± 0.03]	[13.51 ± 0.03]	[12.75 ± 0.03]	228; 45,228; 1
2MASS J14313097+1436539	L2/L3.5:	[16.06 ± 0.06]	[15.08 ± 0.04]	[14.58 ± 0.06]	[14.10 ± 0.06]	215; 229,215; 1
SDSS J143242.10+345142.7	L1/L1.2	[16.76 ± 0.12]	[15.70 ± 0.11]	[15.12 ± 0.10]	[14.74 ± 0.10]	198; 198,7; 1
PSO J218.4532+50.7231	.../T2.5	[17.97 ± 0.06]	16.91 ± 0.03	16.54 ± 0.04	[16.21 ± 0.06]	14; 14; 1,14
PSO J218.5616−27.8952	.../L6	[17.68 ± 0.06]	16.32 ± 0.03	15.43 ± 0.02	[14.59 ± 0.06]	14; 14; 1,14
2MASS J14343616+2202463	.../sdM9	[15.35 ± 0.06]	[14.46 ± 0.04]	[13.90 ± 0.04]	[13.52 ± 0.04]	215; 215; 1
2MASS J14351087−2333025	.../M8	[14.32 ± 0.06]	[13.52 ± 0.03]	[12.99 ± 0.03]	[12.49 ± 0.03]	152; 152; 1

Table 4 continued

Table 4 *(continued)*

Object	Spectral Type[a] (Optical/NIR)	Y_{MKO} (mag)	J_{MKO} (mag)	H_{MKO} (mag)	K_{MKO} (mag)	References (Disc; SpT; Phot)
2MASSI J1438082+640836	M9.5/L0.2	[13.96 ± 0.05]	[12.95 ± 0.02]	[12.22 ± 0.02]	[11.63 ± 0.02]	45; 45,7; 1
SDSS J143832.63+572216.9	L5/L4.6	[17.20 ± 0.09]	[15.89 ± 0.07]	[15.18 ± 0.06]	[14.35 ± 0.06]	229; 229,7; 1
2MASSW J1438549−130910	L3:/L3:	[16.71 ± 0.08]	[15.43 ± 0.06]	[14.58 ± 0.05]	[13.84 ± 0.05]	116; 116,160; 1
SDSS J143945.86+304220.6	.../T2.5	[18.08 ± 0.06]	16.97 ± 0.03	16.53 ± 0.03	16.34 ± 0.05	43; 43; 1,43
2MASS J14403186−1303263	L1/L1pec	[16.32 ± 0.07]	[15.34 ± 0.05]	[14.79 ± 0.06]	[14.23 ± 0.06]	119; 119,119; 1
2MASS J14410457+2719323	M7/...	[13.70 ± 0.05]	[12.97 ± 0.02]	[12.42 ± 0.02]	[11.96 ± 0.02]	47; 47; 1
WISE J144127.48−515807.6	.../M7	[15.02 ± 0.06]	[14.31 ± 0.03]	[13.96 ± 0.02]	[13.46 ± 0.04]	219; 219; 1
DENIS-P J144137.2−094558	L0.5/L1: FLD-G	[15.04 ± 0.06]	13.94 ± 0.03	13.22 ± 0.03	12.62 ± 0.03	163; 118,139; 1,67
G 239-25B	.../L0:	[12.16 ± 0.06]	11.44 ± 0.03	10.86 ± 0.03	10.30 ± 0.07	97,73; 73; 1,67
SSSPM J1444−2019	d/sdM9/d/sdM7	[13.33 ± 0.06]	12.56 ± 0.03	12.14 ± 0.03	11.93 ± 0.03	209; 32,7; 1,67
NLTT 38489B	.../M9	[17.60 ± 0.06]	16.72 ± 0.03	16.15 ± 0.04	[15.61 ± 0.06]	57; 57; 1,57
2MASSW J1449378+235537	L0/M9.5	[16.75 ± 0.09]	[15.78 ± 0.08]	[15.07 ± 0.09]	[14.28 ± 0.09]	116; 116,7; 1
SDSS J145255.58+272324.4	L0/L0.2:	[15.77 ± 0.06]	[14.87 ± 0.04]	[14.43 ± 0.06]	[14.06 ± 0.06]	198; 198,7; 1
SDSS J145325.89+142041.8	L1/L1	[16.18 ± 0.06]	[15.02 ± 0.04]	[14.47 ± 0.04]	[13.88 ± 0.04]	198,119; 198,119; 1
2MASSI J1456014−274735	M9/M9	[14.11 ± 0.06]	[13.20 ± 0.03]	[12.72 ± 0.02]	[12.16 ± 0.02]	45; 45,109; 1
LHS 3003	M7/M7	[10.72 ± 0.07]	9.94 ± 0.05	9.43 ± 0.05	8.93 ± 0.05	12; 113,79; 1,128
WISEPC J145715.03+581510.2	T8/T7	[17.81 ± 0.05]	16.79 ± 0.02	[17.14 ± 0.06]	[17.21 ± 0.06]	120; 120,120; 1,16
PSO J224.3820+47.4057	.../T7	[18.01 ± 0.05]	17.11 ± 0.02	17.43 ± 0.06	[17.08 ± 0.06]	14; 14; 1,16,14
2MASS J14582453+2839580	M8/...	[13.96 ± 0.05]	[13.05 ± 0.02]	[12.37 ± 0.02]	[11.83 ± 0.02]	189; 189; 1
2MASS J15004572+4219448	M9/...	[14.64 ± 0.06]	[13.75 ± 0.03]	[13.17 ± 0.04]	[12.63 ± 0.02]	189; 189; 1
TVLM 513-46546	M8.5/M8.5	[12.74 ± 0.07]	11.76 ± 0.05	11.18 ± 0.05	10.69 ± 0.05	222; 113,79; 1,128
TVLM 513-42404A	.../M7	[14.98 ± 0.07]	14.31 ± 0.05	13.75 ± 0.03	13.47 ± 0.03	220; 17; 1,127
TVLM 513-42404B	.../M9	[16.29 ± 0.07]	15.35 ± 0.05	14.67 ± 0.05	14.25 ± 0.05	220; 17; 1,127
WISE J150406.66−455223.9	.../L8	[17.56 ± 0.12]	[16.48 ± 0.11]	[15.51 ± 0.09]	[14.81 ± 0.09]	219; 219; 1
PSO J226.2599−28.8959	.../T1.5	[16.84 ± 0.05]	15.75 ± 0.02	[15.13 ± 0.05]	[14.73 ± 0.05]	55; 55; 1,16
NLTT 39312B	.../M8	[16.95 ± 0.06]	16.28 ± 0.04	16.01 ± 0.05	[15.45 ± 0.06]	57; 57; 1,57
2MASSW J1506544+132106	L3/L4	[14.52 ± 0.05]	13.23 ± 0.02	[12.46 ± 0.02]	[11.72 ± 0.02]	87; 87,37; 1,16
SDSS J151110.91+434036.3	.../L5.8	[17.83 ± 0.16]	[16.52 ± 0.15]	[15.56 ± 0.13]	[14.69 ± 0.13]	7; 7; 1
SDSS J151240.67+340350.1	L3/L0.7	[16.18 ± 0.05]	14.97 ± 0.02	[14.12 ± 0.04]	[13.40 ± 0.04]	198; 198,7; 1,16
WISE J151314.61+401935.6	.../L8	[18.11 ± 0.10]	[16.98 ± 0.09]	[16.24 ± 0.07]	[15.20 ± 0.10]	219; 219; 1
PSO J228.6775−29.7088	.../L1:	[17.72 ± 0.07]	16.72 ± 0.05	16.18 ± 0.05	[15.37 ± 0.07]	15; 15; 1,14
2MASSW J1515008+484742	L6/L6	[15.14 ± 0.05]	13.97 ± 0.02	[13.18 ± 0.02]	[12.48 ± 0.02]	228; 47,228; 1,16
SDSS J151506.11+443648.3	.../L7.5:	[17.85 ± 0.05]	16.61 ± 0.02	[15.59 ± 0.05]	[14.75 ± 0.05]	43; 43; 1,16
PSO J229.2354−26.6737	.../L0:	[17.92 ± 0.06]	16.75 ± 0.03	15.85 ± 0.02	[15.14 ± 0.06]	15; 15; 1,14
2MASS J15200224−4422419	L1/L2.5	[14.42 ± 0.06]	[13.18 ± 0.03]	[12.44 ± 0.03]	[11.88 ± 0.03]	110; 179,31; 1
SDSS J152039.82+354619.8	.../T0:	[16.61 ± 0.05]	15.49 ± 0.02	14.58 ± 0.05	[14.01 ± 0.05]	43; 43; 1,16,176
2MASS J15230657−2347526	.../L2.5	[15.05 ± 0.05]	14.06 ± 0.02	[13.49 ± 0.03]	[12.88 ± 0.03]	110; 110; 1,16
2MASSI J1526140+204341	L7/L5.5	[16.57 ± 0.05]	15.41 ± 0.02	14.52 ± 0.04	13.88 ± 0.05	116; 116,37; 1,16,67
PSO J231.7900−26.4494	.../L0: VL-G	[16.99 ± 0.05]	15.98 ± 0.02	15.25 ± 0.03	[14.65 ± 0.05]	15; 15; 1,14

Table 4 continued

Table 4 *(continued)*

Object	Spectral Type[a] (Optical/NIR)	Y_{MKO} (mag)	J_{MKO} (mag)	H_{MKO} (mag)	K_{MKO} (mag)	References (Disc; SpT; Phot)
PSO J231.8943−29.0599	.../L0: VL-G	[16.75 ± 0.11]	[15.72 ± 0.09]	[14.91 ± 0.08]	[14.29 ± 0.08]	15; 15; 1
2MASS J15293306+6730215	.../L0:	[17.30 ± 0.13]	[16.29 ± 0.12]	[15.40 ± 0.10]	[14.70 ± 0.10]	119; 119; 1
SDSS J153012.87+514717.1	L0/...	[15.93 ± 0.06]	[15.02 ± 0.04]	[14.37 ± 0.05]	[13.71 ± 0.05]	226; 226; 1
2MASSI J1534498−295227	T6/T5.5	[15.68 ± 0.06]	14.60 ± 0.03	14.74 ± 0.03	14.91 ± 0.03	24; 25,28; 1,123
SDSS J153453.33+121949.2	.../L4:	[16.56 ± 0.06]	15.30 ± 0.02	[14.38 ± 0.04]	[13.80 ± 0.04]	43; 43; 1,16
2MASS J15345704−1418486	M7/...	[12.22 ± 0.05]	[11.35 ± 0.02]	[10.79 ± 0.02]	[10.28 ± 0.02]	89; 89; 1
2MASS J15382417−1953116	L4 γ/L3.5 VL-G	[17.23 ± 0.08]	[15.86 ± 0.06]	[14.95 ± 0.06]	[13.97 ± 0.05]	189; 69,69; 1
DENIS-P J153941.96−052042.4	L4:/L2	[15.11 ± 0.06]	13.84 ± 0.03	13.08 ± 0.03	12.54 ± 0.03	109; 118,109; 1,67
SDSS J154009.36+374230.3	.../L9:	[17.44 ± 0.06]	16.35 ± 0.02	[15.40 ± 0.05]	[14.63 ± 0.05]	43; 43; 1,16
2MASS J15412408+5425598	.../d/sdM7.5	···	[15.90 ± 0.10]	[15.74 ± 0.18]	[15.30 ± 0.18]	27; 7; 1
WISE J154459.27+584204.5	.../T7.5	···	18.09 ± 0.02	[[18.39 ± 0.29]]	···	156; 156; 16,1,156
2MASS J15461461+4932114	.../T2.5:	[16.78 ± 0.05]	15.64 ± 0.02	15.35 ± 0.12	[15.08 ± 0.05]	170; 170; 1,16,176
2MASSI J1546291−332511	.../T5.5	[16.77 ± 0.07]	15.62 ± 0.05	15.42 ± 0.09	15.48 ± 0.18	24; 28; 1,67
SDSS J154849.02+172235.4	.../L5	···	[16.02 ± 0.11]	[15.23 ± 0.08]	[14.44 ± 0.08]	43; 43; 1
2MASS J15485834−1636018	.../L2:	[14.78 ± 0.05]	13.83 ± 0.02	[13.16 ± 0.03]	[12.61 ± 0.03]	110; 110; 1,16
2MASS J15500845+1455180	L3/...	[15.98 ± 0.05]	14.74 ± 0.02	[13.87 ± 0.04]	[13.24 ± 0.04]	47; 35; 1,16
SDSS J155120.86+432930.3	L3/L3.1	[16.10 ± 0.05]	14.93 ± 0.02	[14.28 ± 0.04]	[13.60 ± 0.04]	198; 198,7; 1,16
2MASS J15515237+0941148	L4 γ/L4: VL-G	[17.57 ± 0.12]	[16.22 ± 0.11]	[15.19 ± 0.06]	[14.26 ± 0.06]	189; 68,6; 1
SDSS J155252.32−003501.9	L0/M9.6:	[16.70 ± 0.05]	15.922 ± 0.008	15.552 ± 0.011	15.091 ± 0.014	226; 226,7; 1,126
WISE J155254.84+503307.6	.../L9:pec	[18.51 ± 0.11]	[17.39 ± 0.10]	[16.16 ± 0.13]	[15.52 ± 0.13]	219; 219; 1
2MASSW J1552591+294849	L0 β/L0: INT-G	[14.55 ± 0.06]	[13.41 ± 0.03]	[12.66 ± 0.03]	[11.98 ± 0.03]	228; 48,6; 1
2MASSW J1553214+210907	L5.5/L6.6:	[17.96 ± 0.17]	[16.63 ± 0.16]	[15.43 ± 0.11]	[14.65 ± 0.11]	115; 115,7; 1
2MASSW J1555157−095605	L1/L1.6	[13.55 ± 0.05]	[12.50 ± 0.02]	[12.06 ± 0.02]	[11.42 ± 0.02]	89; 89,7; 1
SDSS J155644.35+172308.9	L0/L0.7	[15.75 ± 0.06]	[14.62 ± 0.03]	[13.94 ± 0.04]	[13.32 ± 0.04]	198; 198,7; 1
2MASS J15575011−2952431	M9 δ/L1: VL-G	[17.25 ± 0.13]	[16.26 ± 0.12]	15.481 ± 0.011	14.861 ± 0.009	119; 119,6; 1,126
WISE J155755.29+591425.3	.../M9	[15.19 ± 0.05]	14.25 ± 0.02	13.61 ± 0.04	13.09 ± 0.03	219; 219; 1,57
2MASSI J1600054+170832	L1.5/L1.8	[17.12 ± 0.10]	[15.99 ± 0.09]	[15.18 ± 0.11]	[14.65 ± 0.11]	116; 116,7; 1
PSO J241.1376+39.0369	.../T2	[18.73 ± 0.14]	17.71 ± 0.13	[17.10 ± 0.13]	16.72 ± 0.07	14; 14; 1,14
HIP 78916B	.../M8	[15.84 ± 0.05]	15.15 ± 0.02	14.60 ± 0.03	[14.17 ± 0.05]	57; 57; 1,57
HIP 78923B	.../M8	[14.90 ± 0.05]	14.136 ± 0.011	13.62 ± 0.11	[13.26 ± 0.04]	57; 57; 1,57
LSR J1610−0040	d/sdM6/d/sdM6	[13.53 ± 0.05]	12.82 ± 0.02	12.31 ± 0.03	11.98 ± 0.03	132; 190,49; 1,67
PSO J242.9129+02.4856	.../T1	[18.19 ± 0.14]	17.11 ± 0.13	16.40 ± 0.09	[16.07 ± 0.14]	14; 14; 1,14
SDSS J161459.98+400435.1	.../L2	[17.67 ± 0.13]	[16.50 ± 0.12]	[15.92 ± 0.12]	[14.98 ± 0.12]	229; 219; 1
2MASS J16150413+1340079	.../T6	[17.35 ± 0.10]	16.32 ± 0.09	[16.73 ± 0.10]	[16.70 ± 0.10]	144; 144; 1,67
2MASS J16154255+4953211	L4 γ/L3: VL-G	[18.16 ± 0.15]	[16.68 ± 0.14]	[15.40 ± 0.07]	[14.26 ± 0.07]	47; 68,6; 1
2MASSW J1615441+355900	L3/L3.6	[15.73 ± 0.05]	14.43 ± 0.02	[13.60 ± 0.03]	[12.91 ± 0.03]	116; 116,7; 1,16
SDSS J161611.36+521328.0	L0/...	[16.36 ± 0.07]	[15.36 ± 0.04]	[14.70 ± 0.07]	[14.15 ± 0.07]	226; 226; 1
PSO J244.1180+06.3598	.../L9 (red)	[18.64 ± 0.08]	17.51 ± 0.06	16.35 ± 0.04	[15.50 ± 0.08]	14; 14; 1,14
SDSS J161731.65+401859.7	.../L4	[18.11 ± 0.16]	[16.67 ± 0.15]	[15.69 ± 0.10]	[14.74 ± 0.10]	43; 43; 1

Table 4 continued

Table 4 *(continued)*

Object	Spectral Type[a] (Optical/NIR)	Y_{MKO} (mag)	J_{MKO} (mag)	H_{MKO} (mag)	K_{MKO} (mag)	References (Disc; SpT; Phot)
PSO J244.6801+08.7185	.../T4.5	[18.01 ± 0.06]	16.83 ± 0.03	16.80 ± 0.03	[16.79 ± 0.06]	14; 14; 1,14
2MASS J16184503−1321297	L0:/M9.3	[15.24 ± 0.05]	[14.21 ± 0.02]	[13.47 ± 0.03]	[12.90 ± 0.03]	118; 118,7; 1
SDSS J161928.31+005011.9	L2/L1.3	[15.49 ± 0.05]	14.35 ± 0.02	[13.73 ± 0.04]	[13.17 ± 0.04]	102; 102,7; 1,16
GJ 618.1B	L2.5/L2.4	[16.42 ± 0.07]	15.18 ± 0.05	14.40 ± 0.04	13.55 ± 0.04	227; 227,7; 1,67
WISEPA J162208.94−095934.6	.../T6	[17.28 ± 0.05]	16.194 ± 0.011	[16.46 ± 0.05]	[16.51 ± 0.05]	120; 120; 1,168
SDSS J162255.27+115924.1	.../L6:	[17.91 ± 0.19]	[16.80 ± 0.18]	[16.24 ± 0.20]	[15.53 ± 0.20]	43; 43; 1
WISE J162359.70−050811.4	.../L1	[15.97 ± 0.06]	[14.89 ± 0.04]	[14.14 ± 0.04]	[13.54 ± 0.04]	219; 219; 1
SDSS J162603.03+211313.0	L3/L4.7:	[16.72 ± 0.07]	[15.41 ± 0.05]	[14.68 ± 0.05]	[13.90 ± 0.05]	198; 198,7; 1
2MASS J16262034+3925190	esdL4/sdL	[15.08 ± 0.06]	14.44 ± 0.03	14.52 ± 0.05	14.46 ± 0.07	26; 230,26; 1,67
LSPM J1627+3328B	.../M9	[15.62 ± 0.05]	14.730 ± 0.012	14.052 ± 0.011	[13.39 ± 0.05]	57; 57; 1,57
WISEPA J162725.64+325525.5	.../T6	[17.33 ± 0.05]	16.23 ± 0.02	[16.56 ± 0.05]	[16.87 ± 0.05]	120; 120; 1,16
SDSS J163030.53+434404.0	.../L7:	[17.66 ± 0.05]	16.53 ± 0.02	[15.56 ± 0.05]	[14.77 ± 0.05]	123; 123; 1,16
2MASS J16304139+0938446	L0::/L0.4:	[15.97 ± 0.06]	[14.83 ± 0.03]	[14.02 ± 0.04]	[13.27 ± 0.04]	189; 189,7; 1
WISE J163236.47+032927.3	.../T5	[17.48 ± 0.05]	16.43 ± 0.02	[16.58 ± 0.05]	[16.51 ± 0.06]	156; 156; 1,16
SDSS J163239.34+415004.3	.../T1:	[18.04 ± 0.07]	16.87 ± 0.05	16.42 ± 0.08	16.19 ± 0.08	123; 28; 1,123
SDSS J163256.13+350507.2	L1/L0.7	[15.69 ± 0.06]	[14.61 ± 0.03]	[13.94 ± 0.03]	[13.27 ± 0.03]	199; 199,7; 1
SDSS J163359.23−064056.5	.../L6	[17.15 ± 0.10]	[16.06 ± 0.09]	[15.24 ± 0.09]	[14.53 ± 0.09]	43; 43; 1
2MASS J16351919+4223053	M8/...	[13.70 ± 0.06]	[12.84 ± 0.03]	[12.29 ± 0.02]	[11.76 ± 0.02]	87; 87; 1
SDSSp J163600.79−003452.6	L0/M9.0	[15.50 ± 0.07]	[14.55 ± 0.04]	[13.97 ± 0.04]	[13.39 ± 0.04]	70; 70,7; 1
WISE J163645.56−074325.1	.../T4.5	[17.60 ± 0.05]	16.42 ± 0.02	[16.28 ± 0.05]	[16.32 ± 0.05]	156; 156; 1,16
2MASS J16382073+1327354	.../L2	[17.53 ± 0.12]	[16.40 ± 0.10]	[15.52 ± 0.11]	[14.95 ± 0.11]	119; 119; 1
2MASS J16403197+1231068	d/sdM9/...	...	[16.17 ± 0.48]	...	...	27; 32; 1
HIP 81910B	.../M6	[13.05 ± 0.05]	12.400 ± 0.010	11.858 ± 0.010	[11.51 ± 0.03]	57; 57; 1,57
2MASSW J1645221−131951	L1.5/...	[13.47 ± 0.06]	12.37 ± 0.03	11.71 ± 0.03	11.11 ± 0.03	89; 89; 1,67
WISEPA J164715.59+563208.2	L7/L9pec	[17.71 ± 0.05]	16.49 ± 0.02	[15.41 ± 0.05]	[14.48 ± 0.05]	120; 180,120; 1,16
2MASS J16490419+0444571	M8/...	[13.75 ± 0.06]	[12.93 ± 0.03]	[12.39 ± 0.03]	[11.86 ± 0.02]	189; 189; 1
SDSS J164916.89+464340.0	.../L5	[18.25 ± 0.07]	17.09 ± 0.03	16.33 ± 0.03	15.74 ± 0.03	43; 43; 1,43
WISEPA J165311.05+444423.9	T8/T8	[18.11 ± 0.06]	17.08 ± 0.02	[17.59 ± 0.05]	[17.07 ± 0.06]	120; 120,120; 1,16
SDSS J165329.69+623136.5	L3/L1	[16.21 ± 0.07]	[15.04 ± 0.05]	[14.34 ± 0.07]	[13.73 ± 0.07]	102; 102,37; 1
SDSS J165450.79+374714.6	L2/L0.7	[16.08 ± 0.06]	[14.97 ± 0.04]	[14.25 ± 0.04]	[13.64 ± 0.04]	198; 198,7; 1
2MASS J16573454+1054233	L2/L1.4	[15.23 ± 0.05]	14.09 ± 0.02	[13.40 ± 0.03]	[12.78 ± 0.03]	189; 189,7; 1,16
WISE J165842.56+510335.0	.../L6pec	[16.19 ± 0.05]	14.98 ± 0.02	[14.26 ± 0.04]	[13.64 ± 0.04]	219; 219; 1,16
SDSS J165850.26+182000.6	L0/L0.9	[16.41 ± 0.08]	[15.43 ± 0.06]	[14.98 ± 0.09]	[14.55 ± 0.09]	226; 226,7; 1
SDSS J170316.71+190636.0	L0/M8.9	[15.83 ± 0.06]	[14.87 ± 0.04]	[14.16 ± 0.05]	[13.63 ± 0.05]	226; 226,7; 1
DENIS-P J170548.38−051645.7	L0.5/L1: FLD-G	[14.32 ± 0.06]	[13.24 ± 0.03]	[12.60 ± 0.02]	[12.00 ± 0.02]	109; 189,6; 1
2MASS J17065487−1314396	.../L5.0 FLD-G	...	[[14.44 ± 0.04]]	[[13.68 ± 0.03]]	[[13.08 ± 0.03]]	76; 76; 1,51
2MASS J17072343−0558249	M9/L1	[12.99 ± 0.05]	[12.01 ± 0.02]	[11.32 ± 0.02]	[10.69 ± 0.02]	89; 89,167; 1
DENIS J1707252−013809	L0.5/L1.0	[15.32 ± 0.06]	[14.23 ± 0.03]	[13.63 ± 0.03]	[13.05 ± 0.03]	164; 164,7; 1
WISEA J170726.69+545109.3	.../L1 (blue)	...	15.91 ± 0.02	...	...	202; 202; 1

Table 4 continued

Table 4 *(continued)*

Object	Spectral Type[a] (Optical/NIR)	Y_{MKO} (mag)	J_{MKO} (mag)	H_{MKO} (mag)	K_{MKO} (mag)	References (Disc; SpT; Phot)
2MASSI J1707333+430130	L0.5/M9: FLD-G	[14.94 ± 0.06]	[13.92 ± 0.03]	[13.23 ± 0.03]	[12.60 ± 0.03]	45; 45,6; 1
SDSS J171049.35+332325.2	L0/M9.4	[15.98 ± 0.06]	[15.09 ± 0.04]	[14.61 ± 0.05]	[14.06 ± 0.05]	226; 226,7; 1
WISEPA J171104.60+350036.8	.../T8	[18.55 ± 0.14]	[17.63 ± 0.13]	[18.06 ± 0.14]	[18.09 ± 0.14]	120; 120; 1
2MASS J17111353+2326333	L0 γ/L1: INT-G	[15.65 ± 0.06]	[14.42 ± 0.03]	[13.73 ± 0.03]	[13.03 ± 0.03]	47; 69,6; 1
2MASS J17114559+4028578	.../L5.0	[16.17 ± 0.05]	14.96 ± 0.02	[14.38 ± 0.05]	[13.78 ± 0.05]	181; 7; 1,16
2MASSI J1711457+223204	L6.5/L9::	[18.13 ± 0.19]	16.94 ± 0.18	15.88 ± 0.11	14.67 ± 0.10	116; 116,37; 1,67
NLTT 44368B	.../L1.5	[15.67 ± 0.05]	14.637 ± 0.013	13.993 ± 0.012	[13.44 ± 0.05]	57; 57; 1,57
GJ 660.1B	.../d/sdM7 FLD-G	[13.47 ± 0.07]	[13.04 ± 0.05]	[12.60 ± 0.02]	[12.21 ± 0.03]	200; 2; 1
PSO J258.2413+06.7612	.../T0pec	[17.22 ± 0.06]	16.03 ± 0.02	15.42 ± 0.02	14.76 ± 0.02	14; 14; 1,14
2MASS J17164260+2945536	.../L3	[18.28 ± 0.20]	[17.00 ± 0.20]	[16.54 ± 0.27]	[15.89 ± 0.27]	80; 80; 1
SDSS J171714.10+652622.2	L4/L6.2	[16.13 ± 0.06]	[14.86 ± 0.04]	[13.93 ± 0.03]	[13.17 ± 0.03]	102; 102,7; 1
LSPM J1717+5925B	.../M9	[17.47 ± 0.05]	16.51 ± 0.02	[15.79 ± 0.05]	[15.19 ± 0.05]	57; 57; 1,57
2MASSI J1721039+334415	L3/L5:	[14.63 ± 0.05]	[13.54 ± 0.02]	[13.03 ± 0.03]	[12.46 ± 0.02]	45; 45,34; 1
PSO J260.3363+46.6739	.../L9	[17.86 ± 0.06]	16.79 ± 0.02	15.84 ± 0.02	[15.24 ± 0.06]	14; 14; 1,14
WISE J172134.46+111739.4	.../T6	[17.45 ± 0.06]	16.42 ± 0.02	[16.69 ± 0.06]	[16.50 ± 0.06]	156; 156; 1,16
SDSS J172244.32+632946.8	L0/L0.7	[16.34 ± 0.07]	[15.31 ± 0.05]	[14.62 ± 0.07]	[14.05 ± 0.07]	102; 102,7; 1
PSO J261.2881+22.9269	.../T5	[18.02 ± 0.06]	16.83 ± 0.03	16.89 ± 0.04	[16.84 ± 0.06]	14; 14; 1,14
SDSS J172543.84+532534.9	L1/M8.0	[15.90 ± 0.07]	[15.14 ± 0.05]	[14.67 ± 0.08]	[14.19 ± 0.08]	198; 198,7; 1
2MASSI J1726000+153819	L3.5 γ/L3: INT-G	[16.92 ± 0.08]	[15.58 ± 0.06]	[14.53 ± 0.05]	[13.62 ± 0.05]	116; 69,6; 1
HIP 85365B	.../L5.5	[17.41 ± 0.05]	16.184 ± 0.010	[15.30 ± 0.05]	14.718 ± 0.010	57; 57; 1,57
VVV BD001	.../L5: blue	14.290 ± 0.012	13.200 ± 0.010	12.670 ± 0.010	[[12.21 ± 0.03]]	10; 10; 217,1,51
2MASSW J1728114+394859	L7/...	[17.10 ± 0.09]	15.86 ± 0.08	14.81 ± 0.07	13.85 ± 0.05	116; 116; 1,67
WISEPA J172844.93+571643.6	.../T6	[18.54 ± 0.06]	17.42 ± 0.02	[17.68 ± 0.06]	[17.81 ± 0.06]	120; 120; 1,16
WISE J173035.99+420742.5	.../T0	[18.02 ± 0.19]	[16.82 ± 0.18]	[16.07 ± 0.19]	[15.76 ± 0.19]	156; 156; 1
SDSS J173101.41+531047.9	.../L6:	[17.59 ± 0.12]	[16.29 ± 0.11]	[15.57 ± 0.14]	[14.83 ± 0.14]	43; 43; 1
2MASS J17312974+2721233	L0/L0: FLD-G	[13.06 ± 0.06]	[12.05 ± 0.03]	[11.45 ± 0.02]	[10.89 ± 0.02]	189; 189,6; 1
2MASS J17320014+2656228	.../L1	[17.01 ± 0.10]	[15.89 ± 0.08]	[15.09 ± 0.05]	[14.44 ± 0.05]	119; 119; 1
WISE J173332.50+314458.3	.../L2pec	[17.05 ± 0.08]	[15.81 ± 0.07]	[14.97 ± 0.06]	[14.28 ± 0.06]	219; 219; 1
DENIS-P J1733423−165449	L0.5:/L0.9	[14.59 ± 0.07]	[13.48 ± 0.05]	[12.87 ± 0.03]	[12.33 ± 0.03]	179; 179,7; 1
WISE J173421.02+502349.9	.../T4	[17.36 ± 0.05]	16.11 ± 0.02	[16.07 ± 0.05]	[16.04 ± 0.05]	156; 156; 1,16
2MASS J17343053−1151388	.../M8.5	[13.99 ± 0.06]	[13.08 ± 0.03]	[12.43 ± 0.02]	[11.86 ± 0.02]	119; 119; 1
2MASS J17373467+5953434	.../L5pec	[18.91 ± 0.09]	[17.65 ± 0.08]	[17.04 ± 0.07]	[16.51 ± 0.07]	80; 106; 1
WISE J173859.27+614242.1	.../extremely red	[18.99 ± 0.14]	[17.72 ± 0.13]	[16.44 ± 0.08]	[15.24 ± 0.10]	156; 156; 1
2MASS J17392515+2454421	.../L4	[16.92 ± 0.09]	[15.73 ± 0.07]	[14.73 ± 0.05]	[13.93 ± 0.05]	119; 119; 1
PSO J265.0759+11.4855	.../T0.5	[18.55 ± 0.10]	17.49 ± 0.09	16.59 ± 0.06	[16.33 ± 0.10]	14; 14; 1,14
WISE J174102.78−464225.5	.../L7::	[17.19 ± 0.09]	[15.69 ± 0.08]	[14.64 ± 0.04]	[13.39 ± 0.04]	201; 201; 1
WISE J174113.12+132711.9	.../T5	[17.96 ± 0.06]	16.90 ± 0.02	[17.11 ± 0.06]	[17.15 ± 0.06]	156; 156; 1,16
WISEPA J174124.26+255319.5	T9/T9	[17.09 ± 0.05]	16.18 ± 0.02	16.31 ± 0.04	17.02 ± 0.20	120,212; 120,120; 1,61
WISE J174303.71+421150.0	.../T4.5	[16.82 ± 0.05]	15.62 ± 0.02	[15.64 ± 0.05]	[15.66 ± 0.06]	156; 156; 1,16

Table 4 continued

Table 4 *(continued)*

Object	Spectral Type[a] (Optical/NIR)	Y_{MKO} (mag)	J_{MKO} (mag)	H_{MKO} (mag)	K_{MKO} (mag)	References (Disc; SpT; Phot)
WISEA J174336.62+154901.3	.../L1pec	[15.40 ± 0.06]	[14.41 ± 0.03]	[13.85 ± 0.04]	[13.48 ± 0.04]	154; 154; 1
2MASSW J1743415+212707	L2.5/L2.4	[17.03 ± 0.10]	[15.78 ± 0.09]	[14.86 ± 0.10]	[14.31 ± 0.10]	116; 116,7; 1
DENIS-P J1745346−164053	L1.5:/L1.3	[14.63 ± 0.06]	[13.59 ± 0.03]	[12.95 ± 0.02]	[12.38 ± 0.02]	179; 179,7; 1
2MASS J17461199+5034036	L5/L5.7	[16.23 ± 0.05]	14.95 ± 0.02	[14.12 ± 0.04]	[13.51 ± 0.04]	189; 189,7; 1,16
2MASSW J1750129+442404	M7.5/M8	[13.60 ± 0.05]	12.75 ± 0.02	12.20 ± 0.02	11.74 ± 0.02	87; 87,60; 1,60
SDSS J175024.01+422237.8	.../T2	[17.36 ± 0.05]	16.17 ± 0.02	[15.61 ± 0.05]	[15.25 ± 0.05]	123; 28; 1,16
2MASS J17502484−0016151	L5/L5.5	[14.40 ± 0.05]	13.21 ± 0.02	12.44 ± 0.02	11.81 ± 0.02	110; 180,110; 1,67
2MASS J17545447+1649196	T5/T5.5	[16.53 ± 0.05]	15.49 ± 0.02	15.64 ± 0.13	[15.61 ± 0.05]	67,33; 180,67; 1,16,67
WISE J175510.28+180320.2	.../T2.5	[16.87 ± 0.05]	15.82 ± 0.02	15.32 ± 0.02	15.24 ± 0.02	156; 14; 1,14
2MASS J17561080+2815238	sdL1/L1pec	[15.60 ± 0.06]	[14.65 ± 0.03]	[14.20 ± 0.04]	[13.78 ± 0.04]	119; 119,119; 1
2MASS J18000116−1559235	.../L4.3	[14.67 ± 0.05]	13.34 ± 0.02	[12.60 ± 0.03]	[11.96 ± 0.03]	7; 7; 1,16
WISEP J180026.60+013453.1	L7.5/L7.5	[15.30 ± 0.05]	14.17 ± 0.02	[13.20 ± 0.03]	[12.41 ± 0.03]	92; 96,92; 1,16
2MASSI J1807159+501531	L1.5/L1	[14.02 ± 0.06]	[12.88 ± 0.02]	[12.20 ± 0.03]	[11.58 ± 0.03]	45; 45,228; 1
PSO J272.0887−04.9943	.../T1.5pec	[17.99 ± 0.05]	16.98 ± 0.02	16.27 ± 0.04	[15.82 ± 0.05]	14; 14; 1,16,14
WISE J180901.07+383805.4	.../T7.5	[18.23 ± 0.06]	17.39 ± 0.02	[17.70 ± 0.06]	[17.32 ± 0.06]	152; 156; 1,16
WISE J180952.53−044812.5	.../T1	[16.21 ± 0.05]	15.147 ± 0.007	[14.44 ± 0.05]	13.977 ± 0.006	156; 13; 1,13
2MASS J18131803+5101246	.../L5	[17.02 ± 0.10]	[15.84 ± 0.08]	[15.19 ± 0.11]	[14.41 ± 0.11]	119; 119; 1
WISE J181329.40+283533.3	.../T8	[17.86 ± 0.05]	16.91 ± 0.02	[17.11 ± 0.05]	[16.93 ± 0.06]	156; 156; 1,16
PSO J274.0908+30.5470	.../T3	[18.54 ± 0.08]	17.53 ± 0.06	16.93 ± 0.06	[17.30 ± 0.09]	14; 14; 1,14
2MASS J18212815+1414010	L4.5pec/L5: FLD-G	[14.63 ± 0.06]	[13.33 ± 0.02]	[12.46 ± 0.02]	[11.62 ± 0.02]	146; 146,139; 1
LSR J1826+3014	M8.5/d/sdM8.5	...	[11.52 ± 0.08]	[11.28 ± 0.08]	[10.82 ± 0.11]	131; 131,7; 1
PSO J276.8234+22.4380	.../L9	[17.70 ± 0.06]	16.53 ± 0.02	15.62 ± 0.02	[14.86 ± 0.05]	14; 14; 1,16,14
2MASS J18283572−4849046	.../T5.5	[16.17 ± 0.08]	15.17 ± 0.06	14.85 ± 0.07	15.18 ± 0.14	27; 28; 1,67
WISEPA J183058.57+454257.9	.../L9	18.28 ± 0.06	17.22 ± 0.04	16.23 ± 0.03	[15.55 ± 0.06]	120; 120; 1,14
PSO J280.2973+63.2600	.../L9.5	[17.10 ± 0.11]	[16.02 ± 0.10]	[15.43 ± 0.12]	[14.82 ± 0.12]	14; 14; 1
PSO J282.5878+34.7691	.../L1	18.24 ± 0.05	17.10 ± 0.04	16.28 ± 0.03	[15.68 ± 0.06]	14; 14; 1,14
WISE J185101.83+593508.6	.../L9	[16.04 ± 0.05]	14.846 ± 0.013	14.03 ± 0.02	[13.45 ± 0.05]	219; 14; 1,13
WISEPA J185215.78+353716.3	.../T7	[17.41 ± 0.05]	16.32 ± 0.02	[16.73 ± 0.05]	[16.51 ± 0.05]	120; 120; 1,16
PSO J284.7214+39.3189	.../T4	18.47 ± 0.06	17.41 ± 0.04	17.17 ± 0.06	[17.03 ± 0.07]	14; 14; 1,14
2MASS J19010601+4718136	.../T5	[16.58 ± 0.05]	15.53 ± 0.02	[15.66 ± 0.05]	[15.72 ± 0.05]	27; 28; 1,16
WISEPA J190624.75+450808.2	.../T6	17.03 ± 0.05	15.98 ± 0.02	16.37 ± 0.08	[16.40 ± 0.05]	120; 120; 1,16
WISEP J190648.47+401106.8	L1/L1	[14.13 ± 0.05]	[13.04 ± 0.02]	[12.33 ± 0.02]	[11.75 ± 0.02]	91; 94,91; 1
DENIS-P J1909081−193748	L1:/...	...	14.46 ± 0.02	[[13.59 ± 0.03]]	[[12.90 ± 0.03]]	179; 179; 16,1,51
2MASS J19163888−3700026	.../L1	[16.62 ± 0.07]	[15.63 ± 0.05]	[14.94 ± 0.08]	[14.36 ± 0.08]	119; 119; 1
WISE J191915.54+304558.4	.../L9	[16.68 ± 0.05]	15.52 ± 0.02	14.557 ± 0.014	[13.96 ± 0.05]	219; 14; 1,14
PSO J291.2688+68.5310	.../T1	[17.58 ± 0.16]	[16.52 ± 0.16]	[16.19 ± 0.23]	[15.52 ± 0.23]	14; 14; 1
WISE J192841.35+235604.9	.../T6	[15.09 ± 0.05]	13.98 ± 0.02	[14.24 ± 0.05]	[14.18 ± 0.05]	156; 156; 1,16
2MASS J19285196−4356256	L4/L4pec	[16.45 ± 0.07]	[15.13 ± 0.04]	[14.21 ± 0.04]	[13.44 ± 0.04]	189; 189,160; 1
2MASS J19355595−2846343	M9 γ/M9: VL-G	[14.89 ± 0.06]	[13.89 ± 0.03]	[13.23 ± 0.03]	[12.67 ± 0.03]	189; 69,6; 1

Table 4 continued

Table 4 *(continued)*

Object	Spectral Type[a] (Optical/NIR)	Y_{MKO} (mag)	J_{MKO} (mag)	H_{MKO} (mag)	K_{MKO} (mag)	References (Disc; SpT; Phot)
WISEA J194128.98−342335.8	M8.5V/M8pec	[15.18 ± 0.06]	[14.45 ± 0.04]	[14.03 ± 0.05]	[13.66 ± 0.05]	154; 154,154; 1
2MASS J19415458+6826021	.../L2	[17.47 ± 0.12]	[16.26 ± 0.10]	[15.30 ± 0.08]	[14.54 ± 0.08]	119; 119; 1
2MASS J19495702+6222440	L2pec/L2pec	[17.59 ± 0.13]	[16.33 ± 0.12]	[15.55 ± 0.11]	[14.73 ± 0.11]	119; 119,119; 1
WISE J195113.62−331116.7	.../L1pec	[16.75 ± 0.08]	[15.65 ± 0.06]	[15.10 ± 0.07]	[14.48 ± 0.07]	219; 219; 1
WISEA J195311.04−022954.7	.../L2pec	[16.65 ± 0.07]	[15.59 ± 0.05]	[14.94 ± 0.08]	[14.43 ± 0.08]	154; 154; 1
2MASS J19561542−1754252	M8/M8.5	[14.56 ± 0.06]	[13.71 ± 0.03]	[13.17 ± 0.03]	[12.62 ± 0.03]	110; 189,7; 1
WISEPA J195905.66−333833.7	.../T8	[17.67 ± 0.09]	16.71 ± 0.07	17.18 ± 0.05	[16.92 ± 0.09]	120; 120; 1,120
WISE J200050.19+362950.1	.../T8	[16.31 ± 0.05]	15.440 ± 0.010	15.850 ± 0.010	16.13 ± 0.04	50; 50; 1,50,148
2MASS J20025073−0521524	L5 β/L7	[16.52 ± 0.05]	15.22 ± 0.02	[14.38 ± 0.04]	[13.39 ± 0.04]	47; 69,160; 1,16
HR 7672B	.../L4.5:	...	...	[[14.10 ± 0.14]]	[[13.02 ± 0.10]]	137; 137; 1,19
WISE J200804.71−083428.5	.../T5.5	[17.16 ± 0.05]	16.03 ± 0.02	[16.31 ± 0.05]	[16.36 ± 0.05]	156; 156; 1,16
DENIS J2013108−124244	L1.5/L0.7	[15.75 ± 0.06]	[14.63 ± 0.04]	[13.95 ± 0.03]	[13.28 ± 0.03]	164; 164,7; 1
2MASS J20135152−2806020	M9 γ/L0: VL-G	[15.20 ± 0.06]	[14.18 ± 0.03]	[13.52 ± 0.03]	[12.90 ± 0.03]	189; 69,6; 1
WISE J201404.13+042408.5	.../T6.5pec	...	18.01 ± 0.02	[[18.71 ± 0.30]]	[[17.97 ± 0.29]]	156; 156; 16,1,156
PSO J304.7573−07.2350	.../M9	17.83 ± 0.03	16.77 ± 0.03	16.24 ± 0.03	[15.70 ± 0.06]	14; 14; 1,14
2MASS J20261584−2943124	L1:/...	[15.89 ± 0.06]	[14.75 ± 0.03]	[14.01 ± 0.03]	[13.35 ± 0.03]	47; 47; 1
SDSS J202820.32+005226.5	L3/L2	[15.38 ± 0.05]	14.18 ± 0.02	[13.45 ± 0.03]	[12.77 ± 0.03]	102; 102,37; 1,16
WISE J203042.79+074934.7	.../T1.5	15.220 ± 0.012	14.046 ± 0.011	[13.51 ± 0.04]	[13.36 ± 0.04]	156; 156; 1,13
2MASS J20343769+0827009	L1/L0.5	[15.57 ± 0.06]	[14.42 ± 0.03]	[13.66 ± 0.03]	[13.06 ± 0.03]	189; 201,37; 1
PSO J308.9834−09.7312	.../L4.5	18.89 ± 0.08	17.67 ± 0.08	16.86 ± 0.06	[16.33 ± 0.09]	14; 14; 1,14
2MASS J20360316+1051295	L3/L3.5	[15.12 ± 0.06]	[13.89 ± 0.03]	[13.09 ± 0.03]	[12.42 ± 0.03]	189; 189,37; 1
WISEA J204027.30+695924.1	sdL0/sdM9	[14.39 ± 0.09]	[13.69 ± 0.07]	[13.35 ± 0.07]	[13.10 ± 0.05]	121; 121,154; 1
2MASS J20414283−3506442	L2:/L0.7 FLD-G	[16.06 ± 0.06]	[14.83 ± 0.03]	[14.06 ± 0.04]	[13.38 ± 0.04]	47; 47,76; 1
SDSS J204317.69−155103.4	.../L9	[17.60 ± 0.17]	[16.52 ± 0.16]	[16.14 ± 0.21]	[15.40 ± 0.21]	43; 43; 1
WISE J204356.42+622048.9	.../T1.5	[16.49 ± 0.09]	[15.46 ± 0.07]	[14.78 ± 0.08]	[14.44 ± 0.08]	156; 156; 1
SDSS J204749.61−071818.3	.../T0:	[17.78 ± 0.06]	16.70 ± 0.03	15.88 ± 0.03	15.34 ± 0.03	123; 28; 1,123
2MASS J20491972−1944324	M7.5/...	[13.60 ± 0.05]	[12.82 ± 0.02]	[12.28 ± 0.02]	[11.76 ± 0.02]	87; 87; 1
PSO J313.1577−26.0050	.../L1	18.45 ± 0.06	17.24 ± 0.05	16.49 ± 0.05	[15.92 ± 0.08]	14; 14; 1,14
2MASSI J2054358+151904	L1:/L0.3	[17.45 ± 0.14]	[16.34 ± 0.13]	[15.49 ± 0.14]	[14.97 ± 0.14]	116; 116,7; 1
2MASSI J2057153+171515	L1.5/M9.9	[17.04 ± 0.10]	[15.93 ± 0.09]	[15.26 ± 0.08]	[14.48 ± 0.08]	116; 116,7; 1
2MASSI J2057540−025230	L1.5/L2: FLD-G	[14.19 ± 0.05]	[13.05 ± 0.02]	[12.32 ± 0.03]	[11.69 ± 0.03]	45; 45,6; 1
2MASSI J2104149−103736	L2.5/L2	[14.99 ± 0.06]	[13.78 ± 0.03]	[13.05 ± 0.02]	[12.35 ± 0.02]	45; 118,37; 1
PSO J316.5156+04.1173	.../L6 (blue) FLD-G	18.27 ± 0.05	17.00 ± 0.04	16.09 ± 0.03	[15.49 ± 0.06]	14; 14; 1,14
2MASSI J2107316−030733	L0/...	[15.14 ± 0.05]	14.13 ± 0.02	[13.51 ± 0.03]	[12.86 ± 0.03]	45; 45; 1,16
2MASS J21075409−4544064	L0:/L2.6	[16.10 ± 0.06]	[14.87 ± 0.03]	[14.03 ± 0.03]	[13.36 ± 0.03]	189; 189,7; 1
PSO J318.4243+35.1277	.../L0.9: INT-G	[15.37 ± 0.05]	14.23 ± 0.02	13.47 ± 0.02	12.77 ± 0.02	5; 5; 1,5
WISEA J211543.59−322540.4	.../M6:	[14.52 ± 0.06]	[13.77 ± 0.03]	[13.18 ± 0.03]	[12.72 ± 0.03]	121; 121; 1
2MASS J21163374−0729200	.../L6	[18.53 ± 0.22]	[17.13 ± 0.21]	[16.29 ± 0.13]	[14.96 ± 0.13]	80; 80; 1
PSO J319.3102−29.6682	.../T0:	16.59 ± 0.02	15.45 ± 0.02	14.655 ± 0.012	[14.17 ± 0.05]	14; 14; 1,14

Table 4 continued

Table 4 *(continued)*

Object	Spectral Type[a] (Optical/NIR)	Y_{MKO} (mag)	J_{MKO} (mag)	H_{MKO} (mag)	K_{MKO} (mag)	References (Disc; SpT; Phot)
WISEA J211807.07−321713.5	.../L1.5	[16.48 ± 0.07]	[15.38 ± 0.05]	[14.63 ± 0.06]	[14.07 ± 0.06]	154; 154; 1
[HB88] M18	M8.5/M8.6	[14.22 ± 0.06]	[13.39 ± 0.03]	[12.83 ± 0.03]	[12.34 ± 0.03]	101; 142,7; 1
HD 203030B	.../L7.5	[20.03 ± 0.09]	18.77 ± 0.08	17.57 ± 0.08	16.16 ± 0.10	169; 169; 1,172,67
WISE J212321.92−261405.1	.../T5.5	[18.07 ± 0.06]	17.03 ± 0.02	[17.52 ± 0.06]	[17.69 ± 0.07]	156; 156; 1,16
WISEA J212354.78−365223.4	.../L1.5	[16.48 ± 0.07]	[15.32 ± 0.05]	[14.62 ± 0.06]	[13.97 ± 0.06]	154; 154; 1
PSO J321.1619+18.8243	.../L9	18.23 ± 0.04	16.99 ± 0.03	16.10 ± 0.03	[15.62 ± 0.06]	14; 14; 1,14
[HB88] M19	M7.5/M8.5 FLD-G	[14.18 ± 0.05]	[13.29 ± 0.02]	[12.73 ± 0.02]	[12.17 ± 0.02]	101; 189,76; 1
[HB88] M20	.../M8.2	[15.12 ± 0.06]	[14.28 ± 0.03]	[13.66 ± 0.03]	[13.14 ± 0.03]	101,120; 7; 1
2MASSW J2130446−084520	L1.5/M8.3	[15.16 ± 0.05]	14.07 ± 0.02	[13.40 ± 0.03]	[12.80 ± 0.03]	118; 118,7; 1,16
SDSS J213154.43−011939.3	L9:/L9	[18.40 ± 0.27]	17.23 ± 0.01	16.42 ± 0.02	[15.55 ± 0.21]	43; 78,43; 1,78
2MASS J21321145+1341584	L6/L5	[16.93 ± 0.08]	15.68 ± 0.06	14.65 ± 0.05	13.79 ± 0.06	47; 47,37; 1,67
PSO J323.1320+29.5308	.../T4.5	[17.30 ± 0.05]	16.17 ± 0.02	[16.22 ± 0.05]	[16.37 ± 0.06]	16; 16; 1,16
SDSS J213240.36+102949.4	.../L2.0 FLD-G	[17.87 ± 0.15]	[16.52 ± 0.14]	[15.46 ± 0.10]	[14.60 ± 0.10]	43; 76; 1
SDSS J213352.72+101841.0	.../L5:	[18.04 ± 0.18]	[16.81 ± 0.17]	[15.91 ± 0.17]	[15.22 ± 0.17]	43; 43; 1
2MASS J21371044+1450475	L2/L0.8	[15.21 ± 0.05]	14.07 ± 0.02	[13.37 ± 0.03]	[12.80 ± 0.03]	189; 189,7; 1,16
2MASS J21373742+0808463	L5:/L5	...	14.64 ± 0.02	[[13.67 ± 0.03]]	[[13.00 ± 0.03]]	189; 189,37; 16,1,51
DENIS J2139136−352950	L0/L2.1:	[15.57 ± 0.06]	[14.52 ± 0.04]	[13.83 ± 0.03]	[13.29 ± 0.03]	164; 164,7; 1
2MASS J21392676+0220226	T2/T1.5	[16.23 ± 0.07]	[15.10 ± 0.05]	[14.27 ± 0.05]	[13.60 ± 0.05]	189,30; 180,28; 1
2MASS J21403907+3655563	.../M8pec	[16.32 ± 0.08]	[15.55 ± 0.07]	[15.11 ± 0.08]	[14.64 ± 0.11]	119; 139; 1
2MASS J21420580−3101162	L3/L1.5 FLD-G	[17.06 ± 0.09]	[15.80 ± 0.07]	[14.84 ± 0.05]	[13.95 ± 0.05]	136; 136,76; 1
HN Peg B	.../T2.5	[16.91 ± 0.06]	15.86 ± 0.03	15.40 ± 0.03	15.12 ± 0.03	150; 150; 1,150
2MASS J21481628+4003593	L6/L6 FLD-G	[15.52 ± 0.06]	[14.04 ± 0.03]	[12.86 ± 0.02]	[11.72 ± 0.02]	146; 146,138; 1
2MASS J21495655+0603349	M9/...	[14.19 ± 0.06]	[13.31 ± 0.03]	[12.68 ± 0.03]	[12.15 ± 0.03]	189; 189; 1
NLTT 52268B	.../M9	[15.87 ± 0.05]	14.95 ± 0.02	14.30 ± 0.01	[13.82 ± 0.05]	57; 57; 1,57
2MASS J21512543−2441000	L3/L4pec	[17.07 ± 0.09]	[15.69 ± 0.08]	[14.66 ± 0.05]	[13.63 ± 0.05]	136; 47,76; 1
2MASS J21512797+3547206	M9/...	[14.39 ± 0.06]	[13.46 ± 0.03]	[12.86 ± 0.03]	[12.39 ± 0.02]	171; 171; 1
2MASS J21513839−4853542	.../T4	[16.94 ± 0.09]	15.71 ± 0.07	15.10 ± 0.10	15.42 ± 0.18	65; 28; 1,67
2MASS J21513979+3402444	.../L7pec	[17.86 ± 0.16]	[16.64 ± 0.15]	[15.87 ± 0.11]	[14.97 ± 0.11]	119; 119; 1
2MASS J21522609+0937575	L6:/...	...	15.09 ± 0.02	[[14.13 ± 0.03]]	[[13.32 ± 0.03]]	188; 189; 16,1,51
LSPM J2153+1157B	.../M7	[15.24 ± 0.05]	14.450 ± 0.011	13.834 ± 0.011	13.368 ± 0.011	57; 57; 1,57
2MASS J21542494−1023022	.../T4.5	[17.41 ± 0.13]	[16.24 ± 0.12]	[16.21 ± 0.13]	[16.14 ± 0.13]	144; 144; 1
2MASS J21543318+5942187	.../T5	[16.54 ± 0.09]	[15.44 ± 0.07]	[15.70 ± 0.09]	[15.70 ± 0.09]	144; 144; 1
SIMP J21543454−1055308	L4 β/L4 INT-G	[17.74 ± 0.13]	[16.34 ± 0.12]	[15.14 ± 0.07]	[14.16 ± 0.07]	74; 69,74; 1
2MASS J21555848+2345307	.../L2	[17.20 ± 0.10]	[15.93 ± 0.08]	[15.02 ± 0.07]	[14.25 ± 0.07]	119; 119; 1
WISEPC J215751.38+265931.4	.../T7	[18.00 ± 0.05]	17.04 ± 0.02	[17.49 ± 0.04]	[17.35 ± 0.06]	120; 120; 1,16
2MASS J21580457−1550098	L4:/L5	[16.13 ± 0.05]	14.84 ± 0.02	[13.95 ± 0.04]	[13.16 ± 0.04]	118; 118,160; 1,16
DENIS-P J220002.05−303832.9	M9 + L0/M9: FLD-G+ L0: FLD-G	[14.38 ± 0.06]	[13.41 ± 0.03]	[12.72 ± 0.03]	[12.18 ± 0.03]	109; 189,139; 1
PSO J330.3214+32.3686	.../T2.5	[17.24 ± 0.05]	16.20 ± 0.02	15.63 ± 0.04	[15.41 ± 0.05]	14; 14; 1,16,14
PSO J331.6058+33.0207	.../T1.5	17.83 ± 0.03	16.66 ± 0.03	16.08 ± 0.03	[15.75 ± 0.06]	14; 14; 1,14

Table 4 continued

Table 4 *(continued)*

Object	Spectral Type[a] (Optical/NIR)	Y_{MKO} (mag)	J_{MKO} (mag)	H_{MKO} (mag)	K_{MKO} (mag)	References (Disc; SpT; Phot)
2MASSW J2206450−421721	L4 γ/L3.3 INT-G	[16.88 ± 0.08]	[15.50 ± 0.07]	[14.54 ± 0.05]	[13.58 ± 0.05]	116; 69,69; 1
PSO J331.9397−07.0570	.../L7	[18.85 ± 0.07]	17.54 ± 0.05	16.45 ± 0.03	[15.50 ± 0.07]	14; 14; 1,14
2MASSW J2208136+292121	L3 γ/L3: VL-G	[17.20 ± 0.05]	15.859 ± 0.009	[14.98 ± 0.05]	[14.12 ± 0.05]	116; 48,6; 1,62
2MASS J22092183−2711329	.../T2.5	...	15.53 ± 0.02	[[15.20 ± 0.15]]	[[15.11 ± 0.15]]	160; 160; 16,1,51
WISEPC J220922.10−273439.5	.../T7	[17.53 ± 0.05]	16.55 ± 0.02	[16.91 ± 0.05]	[17.31 ± 0.06]	120; 120; 1,16
GRH 2208-20	M7.5/M8.8	[14.64 ± 0.06]	[13.95 ± 0.03]	[13.56 ± 0.04]	[13.12 ± 0.04]	84; 52,7; 1
PM I22118-1005B	.../L1.5	[16.34 ± 0.07]	[15.21 ± 0.05]	[14.76 ± 0.05]	[14.03 ± 0.05]	57; 57; 1
2MASS J22114470+6856262	.../L2	[16.82 ± 0.08]	[15.66 ± 0.07]	[14.89 ± 0.07]	[14.17 ± 0.07]	119; 119; 1
2MASS J22120703+3430351	L5:/L6	[17.52 ± 0.11]	[16.24 ± 0.10]	[15.27 ± 0.07]	[14.35 ± 0.07]	189; 189,119; 1
2MASS J22134491−2136079	L0 γ/L0: VL-G	[16.51 ± 0.06]	[15.31 ± 0.04]	[14.47 ± 0.04]	[13.72 ± 0.04]	47; 48,6; 1
WISEPC J221354.69+091139.4	.../T7	[17.81 ± 0.05]	16.76 ± 0.02	[17.11 ± 0.05]	[17.12 ± 0.06]	120; 120; 1,16
2MASS J22153705+2110554	.../T1pec	...	15.90 ± 0.02	[[15.51 ± 0.06]]	[[15.17 ± 0.06]]	106; 106; 16,1,106
PSO J334.1193+19.8800	.../T3	[17.59 ± 0.08]	16.59 ± 0.06	16.41 ± 0.07	[16.28 ± 0.08]	14; 14; 1,14
PSO J334.2624+28.9438	.../L3.5: INT-G	[18.14 ± 0.18]	[16.78 ± 0.17]	[15.99 ± 0.20]	[15.05 ± 0.16]	5; 5; 1
PSO J334.8034+11.2278	.../L5	17.88 ± 0.04	16.58 ± 0.02	15.61 ± 0.02	[14.90 ± 0.06]	14; 14; 1,14
WISE J222219.93+302601.4	.../L9	[17.65 ± 0.05]	16.58 ± 0.02	[15.67 ± 0.05]	[14.99 ± 0.05]	219; 219; 1,16
WISEA J222409.64−185242.1	.../M8	[15.26 ± 0.06]	[14.49 ± 0.04]	[13.98 ± 0.05]	[13.49 ± 0.05]	154; 154; 1
PSO J336.9036−18.9148	.../L6:: (red) VL-G	[18.83 ± 0.07]	17.37 ± 0.05	16.10 ± 0.02	[15.14 ± 0.07]	14; 14; 1,14
LHS 523	M6.5/M7.7	[11.44 ± 0.05]	[10.74 ± 0.02]	[10.27 ± 0.02]	[9.80 ± 0.02]	134; 82,7; 1
PSO J337.4317+16.4213	.../M9	18.03 ± 0.04	17.02 ± 0.03	16.46 ± 0.05	[15.85 ± 0.06]	14; 14; 1,14
PSO J338.8587+31.4729	.../L2pec	18.30 ± 0.05	17.05 ± 0.03	16.19 ± 0.03	[15.75 ± 0.06]	14; 14; 1,14
WISE J223617.59+510551.9	.../T5	15.655 ± 0.014	14.457 ± 0.011	14.61 ± 0.02	[14.57 ± 0.05]	156; 13; 1,13
WISEPC J223729.53−061434.2	.../T5	[18.23 ± 0.05]	17.21 ± 0.02	[17.48 ± 0.06]	[17.81 ± 0.06]	120; 120; 1,16
2MASSI J2238074+435317	L1.5/L0.6	[14.64 ± 0.06]	[13.81 ± 0.03]	[13.12 ± 0.03]	[12.53 ± 0.03]	45; 45,7; 1
WISEPC J223937.55+161716.2	.../T3	[17.00 ± 0.05]	15.96 ± 0.02	[15.57 ± 0.05]	[15.37 ± 0.05]	120; 120; 1,16
2MASS J22425317+2542573	L3/...	[16.03 ± 0.06]	[14.76 ± 0.04]	[13.82 ± 0.03]	[13.03 ± 0.03]	90; 47; 1
HIP 112422B	.../L1.5	[17.25 ± 0.05]	16.02 ± 0.02	15.25 ± 0.01	[14.62 ± 0.05]	57; 57; 1,57
PSO J341.7509−15.1075	.../L5 FLD-G	[17.73 ± 0.05]	16.43 ± 0.02	15.55 ± 0.02	[14.78 ± 0.05]	14; 14; 1,14
2MASS J22490917+3205489	L5/...	...	15.54 ± 0.02	[[14.41 ± 0.05]]	[[13.57 ± 0.05]]	47; 47; 16,1,51
PSO J342.3797−16.4665	.../L5:	[17.27 ± 0.05]	16.08 ± 0.02	15.37 ± 0.02	[14.83 ± 0.05]	14; 14; 1,14
2MASSI J2254188+312349	T5/T4	[16.54 ± 0.07]	15.32 ± 0.05	15.06 ± 0.08	14.99 ± 0.15	24; 180,28; 1,159
NLTT 55219B	.../L5.5	[17.72 ± 0.06]	16.61 ± 0.03	15.77 ± 0.02	[15.29 ± 0.06]	57; 57; 1,57
2MASSI J2254519−284025	L0.5/L0.5	[15.11 ± 0.05]	[14.09 ± 0.02]	[13.50 ± 0.02]	[12.94 ± 0.02]	45; 45,109; 1
WISEPC J225540.74−311841.8	.../T8	18.38 ± 0.02	17.334 ± 0.011	17.66 ± 0.03	[17.42 ± 0.05]	120; 120; 64,1
SDSS J225913.88−005158.2	L2/L1.6	17.50 ± 0.02	[16.31 ± 0.10]	15.394 ± 0.009	14.697 ± 0.008	102; 102,7; 126,1
PSO J344.8146+20.1917	.../L2.5 INT-G	[18.06 ± 0.06]	16.76 ± 0.03	15.76 ± 0.03	[15.00 ± 0.06]	14; 14; 1,14
WISEA J230329.45+315022.7	.../T2 (blue)	...	15.92 ± 0.02	[[15.53 ± 0.16]]	[[15.52 ± 0.16]]	202; 202; 16,1,51
WISE J230356.79+191432.9	.../T4:	[17.67 ± 0.16]	[16.68 ± 0.16]	[16.69 ± 0.16]	[16.79 ± 0.17]	156; 156; 1
PSO J346.3203−11.1654	.../L8.5	[18.29 ± 0.06]	17.14 ± 0.03	16.24 ± 0.03	[15.51 ± 0.06]	14; 14; 1,14

Table 4 continued

Table 4 *(continued)*

Object	Spectral Type[a] (Optical/NIR)	Y_{MKO} (mag)	J_{MKO} (mag)	H_{MKO} (mag)	K_{MKO} (mag)	References (Disc; SpT; Phot)
PSO J346.5281−15.9406	.../L7	[17.90 ± 0.06]	16.56 ± 0.02	15.50 ± 0.02	[14.63 ± 0.06]	14; 14; 1,14
2MASS J23062928−0502285	M7.5/M8	[12.10 ± 0.05]	[11.32 ± 0.02]	[10.77 ± 0.02]	[10.27 ± 0.02]	87; 87,83; 1
DENIS J2308113−272200	L1.5/L1.4	[15.69 ± 0.06]	[14.61 ± 0.03]	[13.91 ± 0.04]	[13.31 ± 0.04]	164; 164,7; 1
SSSPM J2310−1759	L0:/L1:	[15.33 ± 0.05]	14.29 ± 0.02	[13.65 ± 0.03]	[12.95 ± 0.03]	141; 47,160; 1,16
2MASS J23174712−4838501	L4/L6.5pec	[16.48 ± 0.06]	[15.06 ± 0.04]	[14.02 ± 0.03]	[13.15 ± 0.03]	189; 189,119; 1
2MASS J23185497−1301106	.../T5	...	15.30 ± 0.02	[[15.30 ± 0.13]]	[[15.13 ± 0.13]]	160; 160; 16,1,51
WISEPC J231939.13−184404.3	.../T7.5	[18.56 ± 0.06]	17.56 ± 0.02	17.95 ± 0.05	[18.27 ± 0.08]	120; 120; 1,120
2MASS J2320292+412341	.../M9.8	[15.58 ± 0.06]	[14.55 ± 0.04]	[13.83 ± 0.04]	[13.17 ± 0.04]	7; 7; 1
2MASS J23211254−1326282	.../L1	[15.60 ± 0.06]	[14.46 ± 0.03]	[13.65 ± 0.03]	[13.12 ± 0.03]	110; 110; 1
PSO J350.4673−19.0783	.../L4.5	[18.07 ± 0.06]	16.86 ± 0.03	15.93 ± 0.02	[15.31 ± 0.06]	14; 14; 1,14
WISEA J232219.45−140726.2	.../L1pec	[16.81 ± 0.08]	[15.91 ± 0.07]	[15.60 ± 0.14]	[15.07 ± 0.14]	154; 154; 1
2MASS J23231347−0244360	M8.5/M7.7 INT-G	[14.37 ± 0.06]	[13.55 ± 0.03]	[12.98 ± 0.03]	[12.45 ± 0.03]	47; 47,76; 1
2MASS J23254530+4251488	L8/L7.5:	[16.58 ± 0.05]	15.42 ± 0.02	[14.53 ± 0.05]	[13.76 ± 0.05]	47; 47,37; 1,16
2MASS J23255604−0259508	L3:/L1.3 INT-G	[17.15 ± 0.09]	[15.89 ± 0.08]	[15.02 ± 0.06]	[14.09 ± 0.06]	37; 37,76; 1
WISEPC J232728.75−273056.5	.../L9	[17.58 ± 0.05]	16.47 ± 0.02	[15.55 ± 0.05]	[14.87 ± 0.05]	120; 120; 1,16
SDSS J232804.58−103845.7	.../L3.5	[18.22 ± 0.18]	[16.95 ± 0.17]	[15.92 ± 0.13]	[15.07 ± 0.13]	43; 43; 1
2MASS J23302258−0347189	L1:/L0.5	[15.52 ± 0.06]	[14.44 ± 0.03]	[13.81 ± 0.03]	[13.10 ± 0.03]	47; 47,7; 1
LSPM J2331+4607N	.../d/sdM7	[16.48 ± 0.20]	[15.89 ± 0.19]	[15.62 ± 0.14]	[15.15 ± 0.14]	7; 7; 1
2MASS J23312378−4718274	.../T5	[16.62 ± 0.09]	[15.45 ± 0.07]	[15.58 ± 0.20]	[15.48 ± 0.20]	27; 28; 1
PSO J353.0517−29.8947	.../L1:	18.51 ± 0.02	17.236 ± 0.008	16.676 ± 0.010	[16.01 ± 0.05]	14; 14; 64,1
WISE J233527.07+451140.9	.../L7pec	[18.02 ± 0.06]	16.83 ± 0.03	15.63 ± 0.02	14.65 ± 0.06	219; 139; 1,14
2MASS J23392527+3507165	L3.5/L3.0 FLD-G	[16.63 ± 0.05]	15.26 ± 0.02	[14.43 ± 0.04]	[13.56 ± 0.04]	189; 189,76; 1,16
WISEPC J234026.62−074507.2	T7/T7	[17.20 ± 0.06]	16.08 ± 0.03	16.41 ± 0.04	[16.51 ± 0.06]	120; 120,120; 1
2MASS J23440624−0733282	L4.5/L6.0	[16.01 ± 0.05]	14.74 ± 0.02	[13.93 ± 0.03]	[13.22 ± 0.03]	118; 118,7; 1,16
APMPM J2347−3154	M8/...	[14.10 ± 0.06]	[13.25 ± 0.02]	[12.74 ± 0.03]	[12.17 ± 0.03]	53; 142; 1
WISEPC J234841.10−102844.4	.../T7	[17.69 ± 0.05]	16.62 ± 0.02	[16.99 ± 0.05]	[16.84 ± 0.06]	120; 120; 1,16
PM I23492+3458B	.../L9	[17.43 ± 0.05]	16.33 ± 0.02	15.47 ± 0.02	[14.81 ± 0.05]	57; 57; 1,16,57
PSO J357.8314+49.6330	.../T0 (blue)	17.67 ± 0.03	16.48 ± 0.02	15.91 ± 0.04	15.50 ± 0.04	14; 14; 1,14
2MASS J23512200+3010540	L5.5/L5: FLD-G	[17.05 ± 0.11]	[15.76 ± 0.10]	[14.64 ± 0.06]	[13.99 ± 0.06]	119; 119,139; 1
1RXS J235133.3+312720 B	.../L0::	[16.17 ± 0.11]	[15.33 ± 0.10]	[14.64 ± 0.05]	13.93 ± 0.05	23; 23; 1,23
2MASS J23515044−2537367	M8/M8	[13.36 ± 0.06]	[12.43 ± 0.03]	[11.79 ± 0.03]	[11.25 ± 0.03]	142; 47,33; 1
2MASS J23520507−1100435	M7/M7.6 INT-G	[13.60 ± 0.05]	[12.81 ± 0.02]	[12.22 ± 0.02]	[11.72 ± 0.02]	47; 47,76; 1
2MASS J23535946−0833311	M8.5/...	[13.87 ± 0.06]	[13.00 ± 0.03]	[12.43 ± 0.02]	[11.91 ± 0.03]	177; 178; 1
LHS 4039C	M8.5/M8	[13.89 ± 0.05]	13.00 ± 0.02	12.41 ± 0.03	11.86 ± 0.02	208; 208,33; 1,60
WISEA J235422.31−081129.7	.../L5 (red)	18.58 ± 0.03	17.08 ± 0.01	15.90 ± 0.02	[14.92 ± 0.05]	204; 204; 168,1
DENIS J2354599−185221	L2/L2.6:	[15.22 ± 0.05]	14.10 ± 0.02	[13.51 ± 0.03]	[13.02 ± 0.03]	164; 164,7; 1,16
SSSPM J2356−3426	M9/L0.5	13.740 ± 0.001	12.908 ± 0.001	12.424 ± 0.001	[11.94 ± 0.02]	142; 142,142; 64,1
PSO J359.8867−01.8651	.../T1	18.19 ± 0.04	17.05 ± 0.03	16.36 ± 0.04	[15.97 ± 0.06]	14; 14; 1,14
SSSPM J2400−2008	M9.5/L1	[15.21 ± 0.06]	[14.34 ± 0.03]	[13.69 ± 0.04]	[13.22 ± 0.04]	140; 142,142; 1

Table 4 continued

Table 4 *(continued)*

Object	Spectral Type[a]	$Y_{\rm MKO}$	$J_{\rm MKO}$	$H_{\rm MKO}$	$K_{\rm MKO}$	References
	(Optical/NIR)	(mag)	(mag)	(mag)	(mag)	(Disc; SpT; Phot)

NOTE—This table presents NIR MKO photometry for all 934 M, L, and T dwarfs for which we acquired new observed, synthetic, or converted photometry in at least one band during the development of our volume-limited sample. This table includes new photometry for 238 objects in our volume-limited sample (Table 1) and 696 additional M, L, and T dwarfs. Photometry enclosed in single brackets indicates synthetic photometry; double brackets indicates photometry converted from 2MASS into the MKO system using $M_{Ks,2{\rm MASS}}$ and the polynomials of Dupuy & Liu (2017); no brackets indicates photometry observed with UKIRT/WFCAM.

References—(1) This work, (2) Aganze et al. (2016), (3) Albert et al. (2011), (4) Allen et al. (2012), (5) Aller et al. (2016), (6) Allers & Liu (2013), (7) Bardalez Gagliuffi et al. (2014), (8) Baron et al. (2015), (9) Basri et al. (2000), (10) Beamín et al. (2013), (11) Beichman et al. (2014), (12) Bessell (1991), (13) Best et al. (2013), (14) Best et al. (2015), (15) Best et al. (2017), (16) Best et al. (2020), (17) W. Best et al. (in prep), (18) Bihain et al. (2013), (19) Boccaletti et al. (2003), (20) Boeshaar (1976), (21) Bouy et al. (2003), (22) Bowler et al. (2009), (23) Bowler et al. (2015), (24) Burgasser et al. (2002), (25) Burgasser et al. (2003a), (26) Burgasser (2004), (27) Burgasser et al. (2004), (28) Burgasser et al. (2006a), (29) Burgasser & Kirkpatrick (2006), (30) Burgasser & McElwain (2006), (31) Burgasser et al. (2007b), (32) Burgasser et al. (2007a), (33) Burgasser et al. (2008a), (34) Burgasser et al. (2008b), (35) Burgasser et al. (2009), (36) Burgasser et al. (2010b), (37) Burgasser et al. (2010a), (38) Burgasser et al. (2013), (39) Burgasser et al. (2016), (40) Burningham et al. (2010b), (41) Castro & Gizis (2012), (42) Castro et al. (2013), (43) Chiu et al. (2006), (44) Crifo et al. (2005), (45) Cruz et al. (2003), (46) Cruz et al. (2004), (47) Cruz et al. (2007), (48) Cruz et al. (2009), (49) Cushing & Vacca (2006), (50) Cushing et al. (2014), (51) Cutri et al. (2003), (52) Dahn et al. (2002), (53) Deacon et al. (2005), (54) Deacon & Hambly (2007), (55) Deacon et al. (2011), (56) Deacon et al. (2012a), (57) Deacon et al. (2014), (58) Delfosse et al. (1999), (59) Dobbie et al. (2002), (60) Dupuy & Liu (2012), (61) Dupuy & Kraus (2013), (62) Dye et al. (2018), (63) EROS Collaboration et al. (1999), (64) Edge et al. (2016), (65) Ellis et al. (2005), (66) Faherty et al. (2009), (67) Faherty et al. (2012), (68) Faherty et al. (2013), (69) Faherty et al. (2016), (70) Fan et al. (2000), (71) Folkes et al. (2007), (72) Folkes et al. (2012), (73) Forveille et al. (2004), (74) Gagné et al. (2014b), (75) Gagné et al. (2014a), (76) Gagné et al. (2015b), (77) Gauza et al. (2015), (78) Gauza et al. (2019), (79) Geballe et al. (2002), (80) Geißler et al. (2011), (81) Gelino et al. (2011), (82) Giampapa & Liebert (1986), (83) Gillon et al. (2016), (84) Gilmore et al. (1985), (85) Gizis & Reid (1997), (86) Gizis et al. (2000a), (87) Gizis et al. (2000b), (88) Gizis et al. (2001), (89) Gizis (2002), (90) Gizis et al. (2003), (91) Gizis et al. (2011b), (92) Gizis et al. (2011a), (93) Gizis et al. (2012), (94) Gizis et al. (2013), (95) Gizis et al. (2015a), (96) Gizis et al. (2015b), (97) Golimowski et al. (2004), (98) Gomes et al. (2013), (99) Greco et al. (2019), (100) Hall (2002b), (101) Hawkins & Bessell (1988), (102) Hawley et al. (2002), (103) Henry et al. (2004), (104) Henry et al. (2006), (105) Irwin et al. (1991), (106) Kellogg et al. (2015), (107) Kellogg et al. (2017), (108) Kendall et al. (2003), (109) Kendall et al. (2004), (110) Kendall et al. (2007), (111) Kirkpatrick et al. (1991), (112) Kirkpatrick et al. (1994), (113) Kirkpatrick et al. (1995), (114) Kirkpatrick et al. (1997), (115) Kirkpatrick et al. (1999), (116) Kirkpatrick et al. (2000), (117) Kirkpatrick et al. (2006), (118) Kirkpatrick et al. (2008), (119) Kirkpatrick et al. (2010), (120) Kirkpatrick et al. (2011), (121) Kirkpatrick et al. (2014), (122) Kirkpatrick et al. (2019), (123) Knapp et al. (2004), (124) Koen et al. (2017), (125) Lawrence et al. (2007), (126) Lawrence et al. (2012), (127) Leggett et al. (1998), (128) Leggett et al. (2002b), (129) Leggett et al. (2006), (130) Leggett et al. (2010), (131) Lépine et al. (2002), (132) Lépine et al. (2003), (133) Lépine et al. (2009), (134) Liebert et al. (1979), (135) Liebert et al. (2003), (136) Liebert & Gizis (2006), (137) Liu et al. (2002), (138) Liu et al. (2013), (139) Liu et al. (2016), (140) M. Liu et al. (in prep), (141) Lodieu et al. (2002), (142) Lodieu et al. (2005), (143) Lodieu et al. (2014), (144) Looper et al. (2007b), (145) Looper et al. (2007a), (146) Looper et al. (2008b), (147) Looper et al. (2008a), (148) Lucas et al. (2012), (149) Luhman (2006), (150) Luhman et al. (2007), (151) Luhman et al. (2009), (152) Luhman et al. (2012), (153) Luhman (2013), (154) Luhman & Sheppard (2014), (155) Luyten (1979), (156) Mace et al. (2013a), (157) Mainzer et al. (2011), (158) Mamajek et al. (2018), (159) Manjavacas et al. (2013), (160) Marocco et al. (2013), (161) Marshall (2008), (162) Martín et al. (1994), (163) Martín et al. (1999b), (164) Martín et al. (2010), (165) Martin et al. (2018), (166) McCaughrean et al. (2002), (167) McElwain & Burgasser (2006), (168) McMahon et al. (2013), (169) Metchev & Hillenbrand (2006), (170) Metchev et al. (2008), (171) Metodieva et al. (2015), (172) Miles-Páez et al. (2017), (173) Mugrauer et al. (2006), (174) Muzic et al. (2012), (175) Patience et al. (2002), (176) Peña Ramírez et al. (2015), (177) Phan-Bao et al. (2001), (178) Phan-Bao et al. (2006), (179) Phan-Bao et al. (2008), (180) Pineda et al. (2016), (181) Radigan et al. (2008), (182) Radigan et al. (2013), (183) Rebolo et al. (1998), (184) Reid & Gilmore (1981), (185) Reid et al. (2002), (186) Reid et al. (2004), (187) Reid & Gizis (2005), (188) Reid et al. (2006a), (189) Reid et al. (2008b), (190) Reiners & Basri (2006), (191) Reylé & Robin (2004), (192) Reylé et al. (2006), (193) Rice et al. (2010), (194) Ruiz et al. (1991), (195) Sahlmann et al. (2015), (196) Salim et al. (2003), (197) Schmidt et al. (2007), (198) Schmidt et al. (2010b), (199) Schmidt et al. (2015), (200) Schneider et al. (2011), (201) Schneider et al. (2014), (202) Schneider et al. (2016a), (203) Schneider et al. (2016b), (204) Schneider et al. (2017), (205) Scholz et al. (2000), (206) Scholz et al. (2001), (207) Scholz & Meusinger (2002), (208) Scholz et al. (2004a), (209) Scholz et al. (2004b), (210) Scholz et al. (2005), (211) Scholz (2010b), (212) Scholz et al. (2011), (213) Scholz et al. (2014), (214) Schweitzer et al. (1999), (215) Sheppard & Cushing (2009), (216) Shkolnik et al. (2009), (217) Smith et al. (2018), (218) Thackrah et al. (1997), (219) Thompson et al. (2013), (220) Tinney (1993a), (221) Tinney (1993b), (222) Tinney et al. (1993), (223) Tinney (1996), (224) Tinney et al. (1998), (225) Tinney et al. (2005), (226) West et al. (2008), (227) Wilson et al. (2001), (228) Wilson et al. (2003), (229) Zhang et al. (2009), (230) Zhang et al. (2013).

REFERENCES

Ackerman, A. S., & Marley, M. S. 2001, ApJ, 556, 872

Aganze, C., Burgasser, A. J., Faherty, J. K., et al. 2016, AJ, 151, 46

Albert, L., Artigau, E., Delorme, P., et al. 2011, AJ, 141, 203

Allen, P. R., Burgasser, A. J., Faherty, J. K., & Kirkpatrick, J. D. 2012, AJ, 144, 62

Allen, P. R., Koerner, D. W., Reid, I. N., & Trilling, D. E. 2005, ApJ, 625, 385

Aller, K. M., Liu, M. C., Magnier, E. A., et al. 2016, ApJ, 821, 120

Allers, K. N., & Liu, M. C. 2013, ApJ, 772, 79

Artigau, E., Doyon, R., Lafreniere, D., et al. 2006, ApJL, 651, L57

Avni, Y., & Bahcall, J. N. 1980, ApJ, 235, 694

Bardalez Gagliuffi, D. C., Gelino, C. R., & Burgasser, A. J. 2015, AJ, 150, 163

Bardalez Gagliuffi, D. C., Burgasser, A. J., Gelino, C. R., et al. 2014, ApJ, 794, 143

Bardalez Gagliuffi, D. C., Burgasser, A. J., Schmidt, S. J., et al. 2019, ApJ, 883, 205

Barman, T. S., Macintosh, B., Konopacky, Q. M., & Marois, C. 2011, ApJ, 733, 65

Baron, F., Lafreniere, D., Artigau, E., et al. 2019, AJ, 158, 187

—. 2015, ApJ, 802, 37

Basri, G., Mohanty, S., Allard, F., et al. 2000, ApJ, 538, 363

Beamín, J. C., Minniti, D., Gromadzki, M., et al. 2013, A&A, 557, L8

Beichman, C., Gelino, C. R., Kirkpatrick, J. D., et al. 2014, ApJ, 783, 68

Bell, C. P. M., Mamajek, E. E., & Naylor, T. 2015, MNRAS, 454, 593

Bernat, D., Bouchez, A. H., Ireland, M., et al. 2010, ApJ, 715, 724

Bessell, M. S. 1991, AJ, 101, 662

Best, W. M. J., Liu, M. C., Magnier, E. A., & Dupuy, T. J. 2020, AJ, 159, 257

Best, W. M. J., Liu, M. C., Magnier, E. A., et al. 2013, ApJ, 777, 84

—. 2015, ApJ, 814, 118

—. 2017, ApJ, 837, 95

Best, W. M. J., Magnier, E. A., Liu, M. C., et al. 2018, ApJS, 234, 1

Bihain, G., & Scholz, R.-D. 2016, A&A, 589, A26

Bihain, G., Scholz, R.-D., Storm, J., & Schnurr, O. 2013, A&A, 557, 43

Blake, C. H., Charbonneau, D., White, R. J., et al. 2008, ApJL, 678, L125

Boccaletti, A., Chauvin, G., Lagrange, A. M., & Marchis, F. 2003, A&A, 410, 283

Boeshaar, P. C. 1976, PhD thesis, Ph.D. thesis, Ohio State University, Ohio State University, Columbus.

Bouy, H., Brandner, W., Martín, E. L., et al. 2003, AJ, 126, 1526

Bouy, H., Martín, E. L., Brandner, W., & Bouvier, J. 2005, AJ, 129, 511

Bowler, B. P. 2016, PASP, 128, 102001

Bowler, B. P., Liu, M. C., & Cushing, M. C. 2009, ApJ, 706, 1114

Bowler, B. P., Liu, M. C., & Dupuy, T. J. 2010a, ApJ, 710, 45

Bowler, B. P., Liu, M. C., Dupuy, T. J., & Cushing, M. C. 2010b, ApJ, 723, 850

Bowler, B. P., Liu, M. C., Shkolnik, E. L., & Tamura, M. 2015, ApJS, 216, 7

Brandt, T. D., McElwain, M. W., Turner, E. L., et al. 2014, ApJ, 794, 159

Burgasser, A. J. 2004, ApJL, 614, L73

—. 2007a, ApJ, 659, 655

—. 2007b, AJ, 134, 1330

Burgasser, A. J., Cruz, K. L., Cushing, M. C., et al. 2010a, ApJ, 710, 1142

Burgasser, A. J., Cruz, K. L., & Kirkpatrick, J. D. 2007a, ApJ, 657, 494

Burgasser, A. J., Dhital, S., & West, A. A. 2009, AJ, 138, 1563

Burgasser, A. J., Geballe, T. R., Leggett, S. K., Kirkpatrick, J. D., & Golimowski, D. A. 2006a, ApJ, 637, 1067

Burgasser, A. J., & Kirkpatrick, J. D. 2006, ApJ, 645, 1485

Burgasser, A. J., Kirkpatrick, J. D., Cruz, K. L., et al. 2006b, ApJS, 166, 585

Burgasser, A. J., Kirkpatrick, J. D., Liebert, J., & Burrows, A. S. 2003a, ApJ, 594, 510

Burgasser, A. J., Kirkpatrick, J. D., & Lowrance, P. J. 2005a, AJ, 129, 2849

Burgasser, A. J., Kirkpatrick, J. D., McElwain, M. W., et al. 2003b, AJ, 125, 850

Burgasser, A. J., Kirkpatrick, J. D., Reid, I. N., et al. 2003c, ApJ, 586, 512

Burgasser, A. J., Liu, M. C., Ireland, M. J., Cruz, K. L., & Dupuy, T. J. 2008a, ApJ, 681, 579

Burgasser, A. J., Looper, D. L., Kirkpatrick, J. D., Cruz, K. L., & Swift, B. J. 2008b, ApJ, 674, 451

Burgasser, A. J., Looper, D. L., Kirkpatrick, J. D., & Liu, M. C. 2007b, ApJ, 658, 557

Burgasser, A. J., Looper, D. L., & Rayner, J. T. 2010b, AJ, 139, 2448
Burgasser, A. J., & McElwain, M. W. 2006, AJ, 131, 1007
Burgasser, A. J., McElwain, M. W., & Kirkpatrick, J. D. 2003d, AJ, 126, 2487
Burgasser, A. J., McElwain, M. W., Kirkpatrick, J. D., et al. 2004, AJ, 127, 2856
Burgasser, A. J., Melis, C., Todd, J., et al. 2015, AJ, 150, 180
Burgasser, A. J., Reid, I. N., Leggett, S. K., et al. 2005b, ApJL, 634, L177
Burgasser, A. J., Sheppard, S. S., & Luhman, K. L. 2013, ApJ, 772, 129
Burgasser, A. J., Sitarski, B. N., Gelino, C. R., Logsdon, S. E., & Perrin, M. D. 2011, ApJ, 739, 49
Burgasser, A. J., Tinney, C. G., Cushing, M. C., et al. 2008c, ApJL, 689, L53
Burgasser, A. J., Kirkpatrick, J. D., Brown, M. E., et al. 1999, ApJ, 522, L65
Burgasser, A. J., Kirkpatrick, J. D., Cutri, R. M., et al. 2000a, ApJ, 531, L57
Burgasser, A. J., Wilson, J. C., Kirkpatrick, J. D., et al. 2000b, AJ, 120, 1100
Burgasser, A. J., Kirkpatrick, J. D., Brown, M. E., et al. 2002, ApJ, 564, 421
Burgasser, A. J., Gillon, M., Faherty, J. K., et al. 2014, ApJ, 785, 48
Burgasser, A. J., Lopez, M. A., Mamajek, E. E., et al. 2016, ApJ, 820, 32
Burningham, B., Pinfield, D. J., Lucas, P. W., et al. 2010a, MNRAS, 406, 1885
Burningham, B., Leggett, S. K., Lucas, P. W., et al. 2010b, MNRAS, 404, 1952
Burningham, B., Cardoso, C. V., Smith, L., et al. 2013, MNRAS, 433, 457
Burrows, A. S., Sudarsky, D., & Hubeny, I. 2006, ApJ, 640, 1063
Casali, M., Adamson, A., Alves de Oliveira, C., et al. 2007, A&A, 467, 777
Castro, P. J., & Gizis, J. E. 2012, ApJ, 746, 3
Castro, P. J., Gizis, J. E., Harris, H. C., et al. 2013, ApJ, 776, 126
Chabrier, G., Baraffe, I., Allard, F., & Hauschildt, P. 2000, ApJ, 542, 464
Chambers, K. C., Magnier, E. A., Metcalfe, N., et al. 2020, ApJS, in press, arXiv:1612.05560
Charnay, B., Bézard, B., Baudino, J. L., et al. 2018, ApJ, 854, 172
Chiu, K., Fan, X., Leggett, S. K., et al. 2006, AJ, 131, 2722
Crifo, F., Phan-Bao, N., Delfosse, X., et al. 2005, A&A, 441, 653
Cruz, K. L., Burgasser, A. J., Reid, I. N., & Liebert, J. 2004, ApJL, 604, L61
Cruz, K. L., Kirkpatrick, J. D., & Burgasser, A. J. 2009, AJ, 137, 3345
Cruz, K. L., Núñez, A., Burgasser, A. J., et al. 2018, AJ, 155, 34
Cruz, K. L., Reid, I. N., Liebert, J., Kirkpatrick, J. D., & Lowrance, P. J. 2003, AJ, 126, 2421
Cruz, K. L., Reid, I. N., Kirkpatrick, J. D., et al. 2007, AJ, 133, 439
Cushing, M. C., Kirkpatrick, J. D., Gelino, C. R., et al. 2014, AJ, 147, 113
Cushing, M. C., & Vacca, W. D. 2006, AJ, 131, 1797
Cushing, M. C., Marley, M. S., Saumon, D., et al. 2008, ApJ, 678, 1372
Cushing, M. C., Kirkpatrick, J. D., Gelino, C. R., et al. 2011, ApJ, 743, 50
Cutri, R. M., Skrutskie, M. F., Van Dyk, S., et al. 2003, yCat, II/246, 0
Cutri, R. M., Wright, E. L., Conrow, T., et al. 2014, yCat, II/328, 0
Dahn, C. C., Harris, H. C., Vrba, F. J., et al. 2002, AJ, 124, 1170
Dahn, C. C., Harris, H. C., Subasavage, J. P., et al. 2017, AJ, 154, 147
Day-Jones, A. C., Marocco, F., Pinfield, D. J., et al. 2013, MNRAS, 430, 1171
Deacon, N. R., & Hambly, N. C. 2007, A&A, 468, 163
Deacon, N. R., Hambly, N. C., & Cooke, J. A. 2005, A&A, 435, 363
Deacon, N. R., Liu, M. C., Magnier, E. A., et al. 2011, AJ, 142, 77
—. 2012a, ApJ, 755, 94
—. 2012b, ApJ, 757, 100
—. 2014, ApJ, 792, 119
Deacon, N. R., Magnier, E. A., Liu, M. C., et al. 2017a, MNRAS, 467, 1126
Deacon, N. R., Magnier, E. A., Best, W. M. J., et al. 2017b, MNRAS, 468, 3499
Delfosse, X., Tinney, C. G., Forveille, T., et al. 1999, A&AS, 135, 41
—. 1997, A&A, 327, L25
Dobbie, P. D., Kenyon, F., Jameson, R. F., et al. 2002, MNRAS, 329, 543
Dupuy, T. J., & Kraus, A. L. 2013, Science, 341, 1492
Dupuy, T. J., & Liu, M. C. 2012, ApJS, 201, 19
—. 2017, ApJS, 231, 15

Dupuy, T. J., Liu, M. C., & Ireland, M. J. 2009a, ApJ, 699, 168
—. 2009b, ApJ, 692, 729
Dupuy, T. J., Liu, M. C., Leggett, S. K., et al. 2015, ApJ, 805, 56
Dupuy, T. J., Liu, M. C., Magnier, E. A., et al. 2020, RNAAS, 4, 54
Dye, S., Lawrence, A., Read, M. A., et al. 2018, MNRAS, 473, 5113
Edge, A., Sutherland, W., & Team, V. 2016, yCat, II/343, 0
Ellis, S. C., Tinney, C. G., Burgasser, A. J., Kirkpatrick, J. D., & McElwain, M. W. 2005, AJ, 130, 2347
EROS Collaboration, Goldman, B., Delfosse, X., et al. 1999, A&A, 351, L5
Faherty, J. K., Burgasser, A. J., Cruz, K. L., et al. 2009, AJ, 137, 1
Faherty, J. K., Burgasser, A. J., West, A. A., et al. 2010, AJ, 139, 176
Faherty, J. K., Rice, E. L., Cruz, K. L., Mamajek, E. E., & Núñez, A. 2013, AJ, 145, 2
Faherty, J. K., Burgasser, A. J., Walter, F. M., et al. 2012, ApJ, 752, 56
Faherty, J. K., Riedel, A. R., Cruz, K. L., et al. 2016, ApJS, 225, 10
Fan, X., Knapp, G. R., Strauss, M. A., et al. 2000, AJ, 119, 928
Filippazzo, J. C., Rice, E. L., Faherty, J., et al. 2015, ApJ, 810, 158
Folkes, S. L., Pinfield, D. J., Kendall, T. R., & Jones, H. R. A. 2007, MNRAS, 378, 901
Folkes, S. L., Pinfield, D. J., Jones, H. R. A., et al. 2012, MNRAS, 427, 3280
Fontanive, C., Biller, B. A., Bonavita, M., & Allers, K. N. 2018, MNRAS, 479, 2702
Forveille, T., Ségransan, D., Delorme, P., et al. 2004, A&A, 427, L1
Freed, M., Close, L. M., & Siegler, N. 2003, ApJ, 584, 453
Gagné, J., Burgasser, A. J., Faherty, J. K., et al. 2015a, ApJL, 808, L20
Gagné, J., & Faherty, J. K. 2018, ApJ, 862, 138
Gagné, J., Faherty, J. K., Cruz, K. L., et al. 2014a, ApJL, 785, L14
Gagné, J., Lafreniere, D., Doyon, R., et al. 2014b, ApJL, 792, L17
Gagné, J., Faherty, J. K., Cruz, K. L., et al. 2015b, ApJS, 219, 33
Gagné, J., Faherty, J. K., Burgasser, A. J., et al. 2017, ApJL, 841, L1
Gaia Collaboration, Brown, A. G. A., Vallenari, A., et al. 2018, A&A, 616, A1
Gauza, B., Bejar, V. J. S., Pérez Garrido, A., et al. 2015, ApJ, 804, 96
Gauza, B., Béjar, V. J. S., Pérez Garrido, A., et al. 2019, MNRAS, 487, 1149
Geballe, T. R., Knapp, G. R., Leggett, S. K., et al. 2002, ApJ, 564, 466
Geißler, K., Metchev, S. A., Kirkpatrick, J. D., Berriman, G. B., & Looper, D. L. 2011, ApJ, 732, 56
Gelino, C. R., Kirkpatrick, J. D., Cushing, M. C., et al. 2011, AJ, 142, 57
Gelino, C. R., Smart, R. L., Marocco, F., et al. 2014, AJ, 148, 6
Giampapa, M. S., & Liebert, J. 1986, ApJ, 305, 784
Gillon, M., Jehin, E., Lederer, S. M., et al. 2016, Nature, 533, 221
Gilmore, G., Reid, I. N., & Hewett, P. 1985, MNRAS, 213, 257
Gizis, J. E. 2002, ApJ, 575, 484
Gizis, J. E., Allers, K. N., Liu, M. C., et al. 2015a, ApJ, 799, 203
Gizis, J. E., Burgasser, A. J., Berger, E., et al. 2013, ApJ, 779, 172
Gizis, J. E., Burgasser, A. J., Faherty, J. K., Castro, P. J., & Shara, M. M. 2011a, AJ, 142, 171
Gizis, J. E., Burgasser, A. J., & Vrba, F. J. 2015b, AJ, 150, 179
Gizis, J. E., Kirkpatrick, J. D., & Wilson, J. C. 2001, AJ, 121, 2185
Gizis, J. E., Monet, D. G., Reid, I. N., Kirkpatrick, J. D., & Burgasser, A. J. 2000a, MNRAS, 311, 385
Gizis, J. E., Monet, D. G., Reid, I. N., et al. 2000b, AJ, 120, 1085
Gizis, J. E., & Reid, I. N. 1997, PASP, 109, 849
Gizis, J. E., Reid, I. N., Knapp, G. R., et al. 2003, AJ, 125, 3302
Gizis, J. E., Troup, N. W., & Burgasser, A. J. 2011b, ApJL, 736, L34
Gizis, J. E., Faherty, J. K., Liu, M. C., et al. 2012, AJ, 144, 94
Goldman, B., Marsat, S., Henning, T., Clemens, C., & Greiner, J. 2010, MNRAS, 405, 1140
Golimowski, D. A., Henry, T. J., Krist, J. E., et al. 2004, AJ, 128, 1733
Gomes, J. I., Pinfield, D. J., Marocco, F., et al. 2013, MNRAS, 431, 2745
Goto, M., Kobayashi, N., Terada, H., et al. 2002, ApJL, 567, L59
Greco, J. J., Schneider, A. C., Cushing, M. C., Kirkpatrick, J. D., & Burgasser, A. J. 2019, AJ, 158, 182
Hall, P. B. 2002a, ApJL, 580, L77

—. 2002b, ApJL, 564, L89
Harris, H. C., Dahn, C. C., & Dupuy, T. J. 2015, in 18th Cambridge Workshop on Cool Stars, Stellar System, and the Sun, ed. G. T. van Belle & H. C. Harris (Flagstaff, AZ: Lowell Observatory), 413
Hawkins, M. R. S., & Bessell, M. S. 1988, MNRAS, 234, 177
Hawley, S. L., Covey, K. R., Knapp, G. R., et al. 2002, AJ, 123, 3409
Henry, T. J., Jao, W.-C., Subasavage, J. P., et al. 2006, AJ, 132, 2360
Henry, T. J., Subasavage, J. P., Brown, M. A., et al. 2004, AJ, 128, 2460
Irwin, M. J., McMahon, R. G., & Reid, I. N. 1991, MNRAS, 252, 61P
Kellogg, K., Metchev, S. A., Geißler, K., et al. 2015, AJ, 150, 182
Kellogg, K., Metchev, S. A., Miles-Páez, P. A., & Tannock, M. E. 2017, AJ, 154, 112
Kendall, T. R., Delfosse, X., Martín, E. L., & Forveille, T. 2004, A&A, 416, L17
Kendall, T. R., Jones, H. R. A., Pinfield, D. J., et al. 2007, MNRAS, 374, 445
Kendall, T. R., Mauron, N., Azzopardi, M., & Gigoyan, K. 2003, A&A, 403, 929
King, R. R., McCaughrean, M. J., Homeier, D., et al. 2010, A&A, 510, A99
Kirkpatrick, J. D. 2005, ARA&A, 43, 195
Kirkpatrick, J. D., Barman, T. S., Burgasser, A. J., et al. 2006, ApJ, 639, 1120
Kirkpatrick, J. D., Dahn, C. C., Monet, D. G., et al. 2001, AJ, 121, 3235
Kirkpatrick, J. D., Henry, T. J., & Irwin, M. J. 1997, AJ, 113, 1421
Kirkpatrick, J. D., Henry, T. J., & McCarthy, D. W. J. 1991, ApJS, 77, 417
Kirkpatrick, J. D., Henry, T. J., & Simons, D. A. 1995, AJ, 109, 797
Kirkpatrick, J. D., McGraw, J. T., Hess, T. R., Liebert, J., & McCarthy, D. W. J. 1994, ApJS, 94, 749
Kirkpatrick, J. D., Reid, I. N., Liebert, J., et al. 1999, ApJ, 519, 802
—. 2000, AJ, 120, 447
Kirkpatrick, J. D., Cruz, K. L., Barman, T. S., et al. 2008, ApJ, 689, 1295
Kirkpatrick, J. D., Looper, D. L., Burgasser, A. J., et al. 2010, ApJS, 190, 100
Kirkpatrick, J. D., Cushing, M. C., Gelino, C. R., et al. 2011, ApJS, 197, 19
Kirkpatrick, J. D., Gelino, C. R., Cushing, M. C., et al. 2012, ApJ, 753, 156
Kirkpatrick, J. D., Schneider, A. C., Fajardo-Acosta, S., et al. 2014, ApJ, 783, 122
Kirkpatrick, J. D., Martin, E. C., Smart, R. L., et al. 2019, ApJS, 240, 19
Knapp, G. R., Leggett, S. K., Fan, X., et al. 2004, AJ, 127, 3553
Koen, C., Miszalski, B., Vaisanen, P., & Koen, T. 2017, MNRAS, 465, 4723
Koerner, D. W., Kirkpatrick, J. D., McElwain, M. W., & Bonaventura, N. R. 1999, ApJL, 526, L25
Law, N. M., Hodgkin, S. T., & Mackay, C. D. 2006, MNRAS, 368, 1917
Lawrence, A., Warren, S. J., Almaini, O., et al. 2007, MNRAS, 379, 1599
—. 2012, yCat, II/314, 0
Leconte, J. 2018, ApJL, 853, L30
Leggett, S. K., Allard, F., & Hauschildt, P. H. 1998, ApJ, 509, 836
Leggett, S. K., Hauschildt, P. H., Allard, F., Geballe, T. R., & Baron, E. 2002a, MNRAS, 332, 78
Leggett, S. K., Geballe, T. R., Fan, X., et al. 2000, ApJL, 536, L35
Leggett, S. K., Golimowski, D. A., Fan, X., et al. 2002b, ApJ, 564, 452
Leggett, S. K., Currie, M. J., Varricatt, W. P., et al. 2006, MNRAS, 373, 781
Leggett, S. K., Saumon, D., Albert, L., et al. 2008, ApJ, 682, 1256
Leggett, S. K., Cushing, M. C., Saumon, D., et al. 2009, ApJ, 695, 1517
Leggett, S. K., Burningham, B., Saumon, D., et al. 2010, ApJ, 710, 1627
Leinert, C., Weitzel, N., Richichi, A., Eckart, A., & Tacconi-Garman, L. E. 1994, A&A, 291, L47
Lépine, S., Rich, R. M., Neill, J. D., Caulet, A., & Shara, M. M. 2002, ApJL, 581, L47
Lépine, S., Rich, R. M., & Shara, M. M. 2003, ApJL, 591, L49
Lépine, S., Thorstensen, J. R., Shara, M. M., & Rich, R. M. 2009, AJ, 137, 4109
Liebert, J., Dahn, C. C., Gresham, M., & Strittmatter, P. A. 1979, ApJ, 233, 226
Liebert, J., & Gizis, J. E. 2006, PASP, 118, 659
Liebert, J., Kirkpatrick, J. D., Cruz, K. L., et al. 2003, AJ, 125, 343
Liu, M. C., Dupuy, T. J., & Allers, K. N. 2016, ApJ, 833, 96
Liu, M. C., Dupuy, T. J., Bowler, B. P., Leggett, S. K., & Best, W. M. J. 2012, ApJ, 758, 57
Liu, M. C., Dupuy, T. J., & Leggett, S. K. 2010, ApJ, 722, 311

Liu, M. C., Fischer, D. A., Graham, J. R., et al. 2002, ApJ, 571, 519
Liu, M. C., & Leggett, S. K. 2005, ApJ, 634, 616
Liu, M. C., Leggett, S. K., Golimowski, D. A., et al. 2006, ApJ, 647, 1393
Liu, M. C., Deacon, N. R., Magnier, E. A., et al. 2011, ApJL, 740, L32
Liu, M. C., Magnier, E. A., Deacon, N. R., et al. 2013, ApJL, 777, L20
Lodieu, N., Boudreault, S., & Béjar, V. J. S. 2014, MNRAS, 445, 3908
Lodieu, N., Scholz, R.-D., & McCaughrean, M. J. 2002, A&A, 389, L20
Lodieu, N., Scholz, R.-D., McCaughrean, M. J., et al. 2005, A&A, 440, 1061
Lodieu, N., Pinfield, D. J., Leggett, S. K., et al. 2007, MNRAS, 379, 1423
Lodieu, N., Burningham, B., Day-Jones, A. C., et al. 2012, A&A, 548, 53
Looper, D. L., Burgasser, A. J., Kirkpatrick, J. D., & Swift, B. J. 2007a, ApJL, 669, L97
Looper, D. L., Gelino, C. R., Burgasser, A. J., & Kirkpatrick, J. D. 2008a, ApJ, 685, 1183
Looper, D. L., Kirkpatrick, J. D., & Burgasser, A. J. 2007b, AJ, 134, 1162
Looper, D. L., Kirkpatrick, J. D., Cutri, R. M., et al. 2008b, ApJ, 686, 528
Lucas, P. W., Hoare, M. G., Longmore, A., et al. 2012, yCat, II/316, 0
Luhman, K. L. 2006, ApJ, 645, 676
—. 2013, ApJL, 767, L1
Luhman, K. L., Mamajek, E. E., Allen, P. R., & Cruz, K. L. 2009, ApJ, 703, 399
Luhman, K. L., & Sheppard, S. S. 2014, ApJ, 787, 126
Luhman, K. L., Patten, B. M., Marengo, M., et al. 2007, ApJ, 654, 570
Luhman, K. L., Loutrel, N. P., McCurdy, N. S., et al. 2012, ApJ, 760, 152
Luyten, W. J. 1979, A Catalogue of Stars with Proper Motions Exceeding 0.2" Annually (NLTT Catalogue) (Minneapolis: Univ. Minnesota)
Mace, G. N., Kirkpatrick, J. D., Cushing, M. C., et al. 2013a, ApJS, 205, 6
—. 2013b, ApJ, 777, 36
Mainzer, A., Cushing, M. C., Skrutskie, M., et al. 2011, ApJ, 726, 30
Mamajek, E. E., Marocco, F., Rees, J. M., et al. 2018, RNAAS, 2, 205
Manjavacas, E., Goldman, B., Reffert, S., & Henning, T. 2013, A&A, 560, 52
Marley, M. S., Saumon, D., & Goldblatt, C. 2010, ApJL, 723, L117
Marocco, F., Smart, R. L., Jones, H. R. A., et al. 2010, A&A, 524, 38
Marocco, F., Andrei, A. H., Smart, R. L., et al. 2013, AJ, 146, 161
Marocco, F., Jones, H. R. A., Day-Jones, A. C., et al. 2015, MNRAS, 449, 3651
Marshall, J. L. 2008, AJ, 135, 1000
Martin, E. C., Kirkpatrick, J. D., Beichman, C. A., et al. 2018, ApJ, 867, 109
Martín, E. L., Brandner, W., & Basri, G. 1999a, Science, 283, 1718
Martín, E. L., Delfosse, X., Basri, G., et al. 1999b, AJ, 118, 2466
Martín, E. L., Rebolo, R., & Magazzu, A. 1994, ApJ, 436, 262
Martín, E. L., Phan-Bao, N., Bessell, M., et al. 2010, A&A, 517, 53
McCaughrean, M. J., Scholz, R.-D., & Lodieu, N. 2002, A&A, 390, L27
McElwain, M. W., & Burgasser, A. J. 2006, AJ, 132, 2074
McMahon, R. G., Banerji, M., Gonzalez, E., et al. 2013, The Messenger, 154, 35
Metchev, S. A., & Hillenbrand, L. A. 2006, ApJ, 651, 1166
Metchev, S. A., Kirkpatrick, J. D., Berriman, G. B., & Looper, D. L. 2008, ApJ, 676, 1281
Metodieva, Y., Antonova, A., Golev, V., et al. 2015, MNRAS, 446, 3878
Miles-Páez, P. A., Metchev, S. A., Luhman, K. L., Marengo, M., & Hulsebus, A. 2017, AJ, 154, 262
Mugrauer, M., Seifahrt, A., Neuhäuser, R., & Mazeh, T. 2006, MNRASL, 373, L31
Murray, D. N., Burningham, B., Jones, H. R. A., et al. 2011, MNRAS, 414, 575
Muzic, K., Radigan, J., Jayawardhana, R., et al. 2012, AJ, 144, 180
Nakajima, T., Oppenheimer, B. R., Kulkarni, S. R., et al. 1995, Nature, 378, 463
Naud, M.-E., Artigau, E., Malo, L., et al. 2014, ApJ, 787, 5
Nielsen, E. L., De Rosa, R. J., Macintosh, B., et al. 2019, AJ, 158, 13
Patience, J., White, R. J., Ghez, A. M., et al. 2002, ApJ, 581, 654
Peña Ramírez, K., Zapatero Osorio, M. R., & Béjar, V. J. S. 2015, A&A, 574, A118
Phan-Bao, N., Guibert, J., Crifo, F., et al. 2001, A&A, 380, 590
Phan-Bao, N., Bessell, M. S., Martín, E. L., et al. 2006, MNRASL, 366, L40

—. 2008, MNRAS, 383, 831
Pineda, J. S., Hallinan, G., Kirkpatrick, J. D., et al. 2016, ApJ, 826, 73
Pinfield, D. J., Burningham, B., Tamura, M., et al. 2008, MNRAS, 390, 304
Pinfield, D. J., Burningham, B., Lodieu, N., et al. 2012, MNRAS, 422, 1922
Poisson, S. D. 1837, Recherches sur la probabilité des jugements en matière criminelle et en matière civile: : Précédées des Règles générales du calcul des probabilités (Paris: Bachelier)
Pope, B., Martinache, F., & Tuthill, P. 2013, ApJ, 767, 110
Potter, D., Martín, E. L., Cushing, M. C., et al. 2002, ApJL, 567, L133
Radigan, J., Jayawardhana, R., Lafreniere, D., et al. 2013, ApJ, 778, 36
Radigan, J., Lafreniere, D., Jayawardhana, R., & Doyon, R. 2008, ApJ, 689, 471
Rajpurohit, A. S., Reylé, C., Schultheis, M., et al. 2012, A&A, 545, 85
Rayner, J. T., Toomey, D. W., Onaka, P. M., et al. 2003, PASP, 115, 362
Rebolo, R., Zapatero Osorio, M. R., Madruga, S., et al. 1998, Science, 282, 1309
Reid, I. N., Cruz, K. L., Burgasser, A. J., & Liu, M. C. 2008a, AJ, 135, 580
Reid, I. N., Cruz, K. L., Kirkpatrick, J. D., et al. 2008b, AJ, 136, 1290
Reid, I. N., & Gilmore, G. 1981, MNRAS, 196, 15P
Reid, I. N., & Gizis, J. E. 2005, PASP, 117, 676
Reid, I. N., Gizis, J. E., Kirkpatrick, J. D., & Koerner, D. W. 2001, AJ, 121, 489
Reid, I. N., Kirkpatrick, J. D., Gizis, J. E., et al. 2000, AJ, 119, 369
Reid, I. N., Kirkpatrick, J. D., Liebert, J., et al. 2002, AJ, 124, 519
Reid, I. N., Lewitus, E., Allen, P. R., Cruz, K. L., & Burgasser, A. J. 2006a, AJ, 132, 891
Reid, I. N., Lewitus, E., Burgasser, A. J., & Cruz, K. L. 2006b, ApJ, 639, 1114
Reid, I. N., Cruz, K. L., Allen, P., et al. 2004, AJ, 128, 463
Reiners, A., & Basri, G. 2006, AJ, 131, 1806
Reylé, C., & Robin, A. C. 2004, A&A, 421, 643
Reylé, C., Scholz, R.-D., Schultheis, M., Robin, A. C., & Irwin, M. J. 2006, MNRAS, 373, 705
Reylé, C., Delorme, P., Willott, C. J., et al. 2010, A&A, 522, A112
Reylé, C., Delorme, P., Artigau, E., et al. 2014, A&A, 561, 66
Rice, E. L., Faherty, J. K., & Cruz, K. L. 2010, ApJL, 715, L165
Ruiz, M. T., Leggett, S. K., & Allard, F. 1997, ApJL, 491, L107
Ruiz, M. T., Takamiya, M. Y., & Roth, M. 1991, ApJL, 367, L59
Sahlmann, J., Lazorenko, P. F., Bouy, H., et al. 2016, MNRAS, 455, 357
Sahlmann, J., Lazorenko, P. F., Ségransan, D., et al. 2014, A&A, 565, A20
Sahlmann, J., Burgasser, A. J., Martín, E. L., et al. 2015, A&A, 579, A61
Salim, S., Lépine, S., Rich, R. M., & Shara, M. M. 2003, ApJL, 586, L149
Saumon, D., & Marley, M. S. 2008, ApJ, 689, 1327
Schilbach, E., Röser, S., & Scholz, R.-D. 2009, A&A, 493, L27
Schmidt, M. 1968, ApJ, 151, 393
Schmidt, S. J., Cruz, K. L., Bongiorno, B. J., Liebert, J., & Reid, I. N. 2007, AJ, 133, 2258
Schmidt, S. J., Hawley, S. L., West, A. A., et al. 2015, AJ, 149, 158
Schmidt, S. J., West, A. A., Burgasser, A. J., Bochanski, J. J., & Hawley, S. L. 2010a, AJ, 139, 1045
Schmidt, S. J., West, A. A., Hawley, S. L., & Pineda, J. S. 2010b, AJ, 139, 1808
Schneider, A. C., Cushing, M. C., Kirkpatrick, J. D., et al. 2014, AJ, 147, 34
Schneider, A. C., Greco, J., Cushing, M. C., et al. 2016a, ApJ, 817, 112
Schneider, A. C., Melis, C., Song, I., & Zuckerman, B. 2011, ApJ, 743, 109
Schneider, A. C., Windsor, J., Cushing, M. C., Kirkpatrick, J. D., & Shkolnik, E. L. 2017, AJ, 153, 196
Schneider, A. C., Windsor, J., Cushing, M. C., Kirkpatrick, J. D., & Wright, E. L. 2016b, ApJL, 822, L1
Scholz, R.-D. 2010a, A&A, 515, 92
—. 2010b, A&A, 510, L8
Scholz, R.-D., Bihain, G., Schnurr, O., & Storm, J. 2011, A&A, 532, L5
—. 2012, A&A, 541, 163
Scholz, R.-D., Bihain, G., & Storm, J. 2014, A&A, 567, A43
Scholz, R.-D., Irwin, M. J., Ibata, R., Jahreiss, H., & Malkov, O. Y. 2000, A&A, 353, 958
Scholz, R.-D., Lehmann, I., Matute, I., & Zinnecker, H. 2004a, A&A, 425, 519
Scholz, R.-D., Lodieu, N., & McCaughrean, M. J. 2004b, A&A, 428, L25
Scholz, R.-D., McCaughrean, M. J., Zinnecker, H., & Lodieu, N. 2005, A&A, 430, L49

Scholz, R.-D., & Meusinger, H. 2002, MNRAS, 336, L49
Scholz, R.-D., Meusinger, H., & Jahreiss, H. 2001, A&A, 374, L12
Schweitzer, A., Scholz, R.-D., Stauffer, J., Irwin, M. J., & McCaughrean, M. J. 1999, A&A, 350, L62
Seifahrt, A., Reiners, A., Almaghrbi, K. A. M., & Basri, G. 2010, A&A, 512, A37
Sheppard, S. S., & Cushing, M. C. 2009, AJ, 137, 304
Shkolnik, E. L., Liu, M. C., & Reid, I. N. 2009, ApJ, 699, 649
Simons, D. A., & Tokunaga, A. T. 2002, PASP, 114, 169
Skrutskie, M. F., Cutri, R. M., Stiening, R., et al. 2006, AJ, 131, 1163
Smart, R. L., Tinney, C. G., Bucciarelli, B., et al. 2013, MNRAS, 433, 2054
Smart, R. L., Bucciarelli, B., Jones, H. R. A., et al. 2018, MNRAS, 481, 3548
Smith, L. C., Lucas, P. W., Kurtev, R., et al. 2018, MNRAS, 474, 1826
Stephens, D. C., Leggett, S. K., Cushing, M. C., et al. 2009, ApJ, 702, 154
Stone, J. M., Skemer, A. J., Kratter, K. M., et al. 2016, ApJL, 818, L12
Strauss, M. A., Fan, X., Gunn, J. E., et al. 1999, ApJL, 522, L61
Stumpf, M. B., Brandner, W., Köhler, R., Bouy, H., & Henning, T. 2009, in AIP Conf. Proc., 1094, 15th Cambridge Workshop on Cool Stars, Stellar Systems and the Sun, ed. E. Stempels (Melville, NY: AIP), 561
Taylor, M. B. 2005, in ASP Conf Ser, 351, Astronomical Data Analysis Software and Systems XV, ed. P. L. Shopbell, M. C. Britton, & R. Ebert (San Francisco, CA: ASP), 29
Thackrah, A., Jones, H., & Hawkins, M. 1997, MNRAS, 284, 507
Thompson, M. A., Kirkpatrick, J. D., Mace, G. N., et al. 2013, PASP, 125, 809
Thorstensen, J. R., & Kirkpatrick, J. D. 2003, PASP, 115, 1207
Tinney, C. G. 1993a, ApJ, 414, 279
—. 1993b, AJ, 105, 1169
—. 1996, MNRAS, 281, 644
Tinney, C. G., Burgasser, A. J., & Kirkpatrick, J. D. 2003, AJ, 126, 975
Tinney, C. G., Burgasser, A. J., Kirkpatrick, J. D., & McElwain, M. W. 2005, AJ, 130, 2326
Tinney, C. G., Delfosse, X., Forveille, T., & Allard, F. 1998, A&A, 338, 1066
Tinney, C. G., Mould, J. R., & Reid, I. N. 1993, AJ, 105, 1045
Tinney, C. G., Kirkpatrick, J. D., Faherty, J. K., et al. 2018, ApJS, 236, 28
Tokunaga, A. T., Simons, D. A., & Vacca, W. D. 2002, PASP, 114, 180
Tremblin, P., Amundsen, D. S., Chabrier, G., et al. 2016, ApJL, 817, L19
Tsvetanov, Z. I., Golimowski, D. A., Zheng, W., et al. 2000, ApJL, 531, L61
van Leeuwen, F. 2007, A&A, 474, 653
Vrba, F. J., Henden, A. A., Luginbuhl, C. B., et al. 2004, AJ, 127, 2948
West, A. A., Hawley, S. L., Bochanski, J. J., et al. 2008, AJ, 135, 785
Wilson, J. C., Kirkpatrick, J. D., Gizis, J. E., et al. 2001, AJ, 122, 1989
Wilson, J. C., Miller, N. A., Gizis, J. E., et al. 2003, in IAU Symp. 211, Brown Dwarfs, ed. E. L. Martín (San Francisco, CA: ASP), 197
Wright, E. L., Eisenhardt, P. R. M., Mainzer, A. K., et al. 2010, AJ, 140, 1868
York, D. G., Adelman, J., Anderson, J. E. J., et al. 2000, AJ, 120, 1579
Zapatero Osorio, M. R., Martín, E. L., Béjar, V. J. S., et al. 2007, ApJ, 666, 1205
Zhang, Z., Pokorny, R. S., Jones, H. R. A., et al. 2009, A&A, 497, 619
Zhang, Z., Pinfield, D. J., Burningham, B., et al. 2013, MNRAS, 434, 1005
Zhang, Z., Pinfield, D. J., Gálvez-Ortiz, M. C., et al. 2017, MNRAS, 464, 3040
Zhang, Z., Liu, M. C., Hermes, J. J., et al. 2020, ApJ, 891, 171
Zuckerman, B., Bessell, M. S., Song, I., & Kim, S. 2006, ApJ, 649, L115